Heat and Mass Transfer in Buildings

LECTURE NOTE OF COURSE 11122

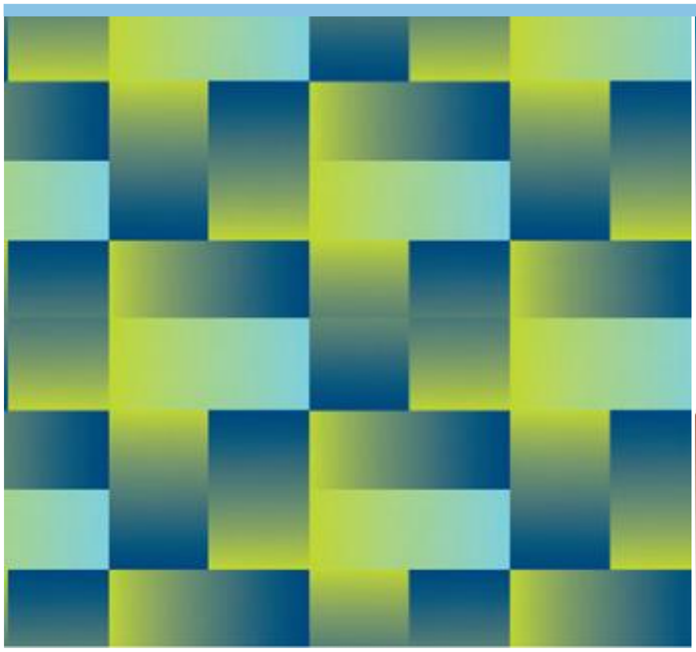

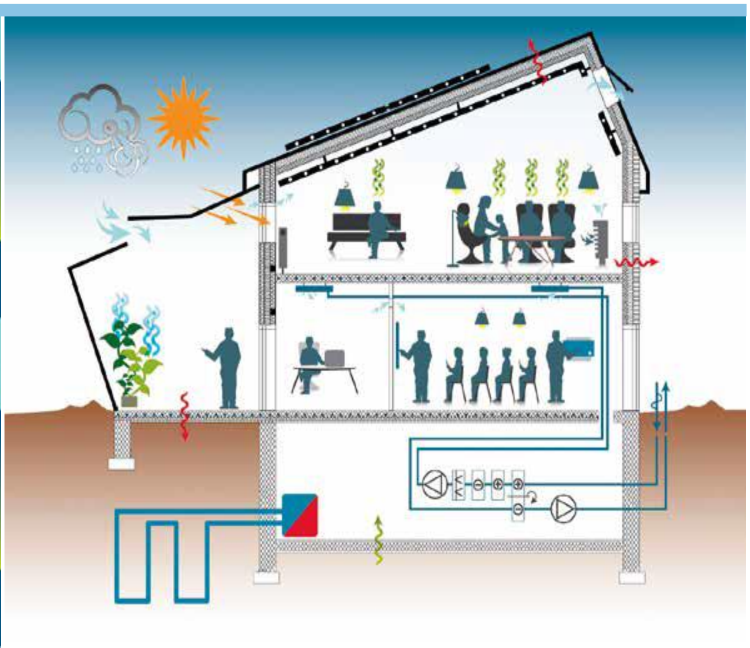

Written by
Carsten Rode, Menghao Qin and Ruut Peuhkuri
(September 2019)

DTU Civil Engineering
Department of Civil Engineering

CONTENTS

1 INTRODUCTION

Knowledge on theory of heat, air and mass transfer is essential for design of comfortable, healthy, durable and energy efficient buildings. This course concentrates on introducing the central theory of heat, air and mass transfer, which is also called "Hygrothermal Building Physics". However, general heat transfer theory is assumed known for the reader. The focus in this course is therefore on mass transfer and on combined and coupled effects of heat and mass transfer.

Combined heat and mass transfer – as well as the different forms of mass transfer – is a very complex field and the theory can partly be very challenging and requires advanced mathematics. In this course material, the theory is presented, however, in a relatively simple form in order to make the student able to use the knowledge in building engineering applications.

Building performance criteria – a short intro

Building performance is related to heat, air and moisture states of a building and in its components. Performance criteria can be divided into health, comfort, durability and sustainability criteria. Here are some examples on these criteria and which states of the building and its components plays a role

Health: is about optimising building occupant welfare (and productivity)

- VOC emission and release of other chemicals from building materials pollutes the interior living environment. VOC emission depends of **temperature and humidity**
- Radon is a radio-active gas present in soils and causes lung cancer. Distribution and concentration of radon in a house is related to **air flows**

Comfort: is about optimising building occupant welfare (and productivity)

- Air quality acceptability is how the indoor air quality is judged by the occupants. It depends on **air temperature and humidity**
- Draft experience is air flows experienced as uncomfortable to humans. It depends on the **air flow velocity and temperature**

Durability: is about maximising building service life (and avoiding damage)

- surface mold growth develops if the material and the surface is susceptible to mold growth and certain **humidity and temperature conditions** are present
- wood rot may develop in wood if kept wet for a long time. Rot initiation and development depend on **moisture content** in the wood
- thermal expansion and shrinking happen due to **temperature changes** and lead to cracks
- hygric expansion and shrinking happens due to **moisture content** changes and lead to cracks
- lower material strength and stiffness due to high **moisture content** lead to loss of structural capacity

- increased thermal conductivity due to high **moisture contents** in material lead to higher heat losses
- moss formation due to high **moisture content in material**
- corrosion due to **moisture on material**
- frost cracking due to high **moisture content** and low **temperature in material**
- efflorescence due to **moisture in material**

Sustainability: is about minimising consumption of fossil fuels and materials via optimal building design and solutions

- minimal heat losses and maximal solar gains are essential for energy consumption (winter) while control of sun and ventilation air are essential for comfort (summer). Energy use and comfort depend on **heat and air flows** that again depend on e.g. geometry, orientation and U-values
- performance of sustainable constructions (with low U-values) depends **on heat, moisture and air flows**
- active facades try capturing heat flows from interior and heat gains from sun and the performance depends on **heat and air flow**
- green roofs provide cooling (summer) and inertia (winter) and are important buffer for rain runoff. The performance depends on **heat and moisture flow**

More detailed performance criteria are found in lecture note *8. Hygrothermal assessment methods*.

Why is hygrothermal building physics important?

Traditional building design has evolved slowly through generations and the solutions are mostly performing well and as expected, due to the long experience with the solutions. In current building design, the solutions and materials change rapidly, and solutions are often unique. Due to the lacking long term experience, there is a need to be able to predict the building and component performance. This requires good knowledge on heat and mass transfer theory.

Ensuring good building performance in new buildings and especially with new solutions with new materials is one of the application fields for hygrothermal building physics.

There will be even more focus on and demand for comfortable, healthy, durable and sustainable buildings in the future. The challenge is not only for the future buildings to be designed but even more the refurbishment of existing buildings and constructions. Refurbishment is a highly relevant current and future application field for hygrothermal building physics.

The theory can be applied as well for **design** of well-performing new buildings and solutions as for **diagnosis** of failing performance: why there is mold growth or why is the indoor air too hot. A diagnosis will then require a solution, which again is found by applying hygrothermal building physics.

Focus on balances and flows

Heat and mass states of the building and its components are governed by heat and mass flows within them – and vice versa. Heat and mass states are often referred to as **HAM-states** (temperature, air pressure, vapor pressure, liquid pressure, moisture content). Heat and mass flows are often referred to as **HAM-flows** (heat flow, air flow, vapor flow, liquid flow).

When applying the theory either as a part of design process or as a part of diagnosis, there are two main concepts for approaching the solution:

1. ***HAM-state should remain between limits***
    a. **design:** how to keep HAM-state between lower & upper limits ?
    b. **diagnosis:** why is HAM-state outside of lower & upper limits ?

2. ***HAM-state results from balance of HAM-flows***
    a. **design/diagnosis:** requires knowledge & control of HAM-flows

A central method to solve a hygrothermal building physical problem (e.g. to find the resulting air temperature in a room) is to set up and solve a **HAM balance** (e.g.for the room air). In this course, the focus is therefore on setting up HAM balances and solving them.

Learning objectives

The course learning objectives are summarized here. After the course you should be able to

- explain why air and moisture transfer are essential in hygrothermal design or diagnosis of building components and whole buildings;
- explain and apply the transport equations for heat, air, moisture in building components and zones; and formulate heat, air, moisture balances for the analysis of hygrothermal problems;
- apply mathematical methods and problem solving approaches for the solution of hygrothermal problems; and assess the reliability of obtained results;
- classify building materials concerning their hygrothermal properties; and evaluate their influence on the generic hygrothermal response of building components and whole buildings;
- design hygrothermally correct building components and whole buildings; and diagnose hygrothermally incorrect building components and whole buildings;
  + Carstens Storyline skema som viser strukturen I emnerne, som også henviser til forudsætninger

2 HEAT TRANSFER

A first definition of heat is found in thermodynamics. Thermodynamics divides the world into systems and environments. A system can be almost anything: a volume of material, a building part, a building construction, a part of the heating system, etc. We can even look at a city as a system. ‘Heat’ indicates the way energy is transferred between a system and its environment. While ‘work’ is purposeful and organized, heat is diffuse and unorganized. A second definition can be found in particle physics in which heat denotes the statistically distributed kinetic energy of atoms and free electrons. In both cases heat is the least noble form of energy, which means the most diffuse of all, to which according to the second law of thermodynamics each nobler form degrades.

The “quality” of heat is determined by its potential: temperature. Higher temperature indicates higher quality, standing for higher mechanical energy of atoms and free electrons and the possibility to convert more heat into power via a cyclic process. Lower temperatures give heat a lower quality, which implies less mechanical energy on the atomic scale. Higher temperatures are obtained by warming up the system, i.e. by adding heat, lower temperatures are obtained by cooling, i.e. removing heat from the system.

Heat and temperature cannot be measured directly. Yet, temperature can be sensed, and is indirectly measurable because a great deal of material properties depends on it:

- thermal expansion: for a mercury thermometer, we use the volume expansion of mercury as a measure for temperature;
- electrical resistance: for a Pt100 resistance thermometer, the electrical resistance of a platinum wire functions as a measure of the temperature;
- contact potential: this is the basis for thermocouple measurement of temperature.

The SI-system uses 2 scales for temperature:

- empirical: *degree Celsius* (symbol: ϑ [°C]). 0 °C is the triple point of water, 100 °C is the boiling point of water at 1 Atm or 101300 Pa.
- thermodynamic: *degree Kelvin* (symbol: T [K]). 0 K is the absolute zero, 273.15 K is the triple point of water.

Some Definitions:

Heat

Symbol: *E*

Units: Joule [J]

Quantity which indicates the thermal energy content. Heat is a scalar.

Heat flow

Symbol: *Q*

Units: Joule per second [J/s] = Watt [W]

The heat energy transferred per unit of time. Heat flow is a scalar.

2.1 Heat conservation

The law of conservation of energy is an empirical law of physics. It asserts that the total amount of energy in an isolated system remains constant over time. A consequence of this law is that energy can neither be created nor destroyed: it can only be transformed, from one state to another. The only thing that can happen to energy in a closed system is that it can change form: for instance chemical energy can become kinetic energy.

For an open system – a system that allows exchange of energy with the environment –, conservation of energy implies that the amount of energy stored in the system must be equal to the difference between the energy amount added to the system and the energy amount taken from the system. When applied to heat transfer, this can be expressed as:

$$E_{stored} = \sum E_{in} - \sum E_{out} \tag{2.1}$$

in which E_{in} and E_{out} [J] are the added and taken amount of heat respectively. Translation to a rate-formulation gives:

$$dE_{stored}/dt = \sum Q_{in} - \sum Q_{out} \tag{2.2}$$

in which t [s] is the time and Q_{in} and Q_{out} [W] are the heat in- and outflows. This expression forms the basis of all heat transfer analysis: if we can relate heat storage and transfer to temperatures, then we can investigate the 'heat responses' of building components and whole buildings.

In many cases, we can limit ourselves to a stationary – or 'time-independent' – situation, in which all amounts of stored and transported energy remain constant. In that case, the time derivative in Equation 2.2 becomes zero, and the standard heat balance equation is obtained:

$$\sum Q_{in} - \sum Q_{out} = 0 \qquad \text{or} \qquad \sum Q_{in} = \sum Q_{out} \tag{2.3}$$

2.2 Heat storage

Heat exists in sensible form, which means temperature-related, or in latent form, as heat of transformation. The sensible energy content of an object consists of the kinetic energy of its vibrating atoms and free electrons. This sensible heat is proportional to the object's temperature:

$$E_{sens} = V_{mat} r_{mat} c_{mat} T \tag{2.4}$$

in which V_{mat} [m³] is the volume of the object, ρ_{mat} [kg/m³] is the material density and c_{mat} [J/(kg·K)] is the specific thermal capacity of the material. Examples of specific thermal capacity values for different building materials can be found in the lecture presentation and in the 'thermal properties of materials' document.

The latent energy content is related to phase transformations, and we will limit it here to the evaporation of water. Since energy is needed to transform liquid water into water vapor, the resulting vapor must have a higher heat content than the liquid:

$$E_{lat} = V_v \rho_v L_v \tag{2.5}$$

in which $V_v \rho_v$ [kg] is the mass of vapor and L_v [J/kg] is the heat of vaporization of water. In many cases however, the latent heat itself is not considered, only latent heat transfer is taken into account in condensation and evaporation processes.

2.3 Heat transfer

Sensible heat can be transferred by advection, conduction, convection and radiation. Latent heat transfer is only considered for condensation and evaporation processes.

2.3.1 ADVECTION

Advection implies the heat transfer due to global mass transport: any transport of mass inherently transfers the internal heat of the mass concerned and thus gives the advective heat transfer.

The transport law for advection:

$$Q = G_{bulk} cT \tag{2.6}$$

in which G_{bulk} [kg/s] is the global mass flow.

2.3.2 CONDUCTION

Conduction indicates the energy transported when vibrating atoms collide and free electrons move collectively. Heat is transferred that way between solids at different temperature in contact with each other and between points at different temperature within the same solid. The mode also intervenes when heat is transferred in gases and liquids and in the contacts between gases and liquids at one side and solids at the other. Conduction always occurs from points at a higher temperature to points at a lower temperature (2nd law of thermodynamics). Conduction requires a medium, but no observable macroscopic movement is linked to it.

Figure 2.1 representation of Fourier's law for finite (left) and infinitesimal (right) thickness.

For a slab of material with surface area A [m²], thickness [d] and surface temperatures T_y and T_z [K] (as show in Figure 2.1 left), the heat flow is proportional to the temperature difference and surface area, and inversely proportional to the thickness. The proportionality constant is the thermal conductivity λ [W/(m·K)] of the slab material. This gives Fourier's law for heat conduction:

$$Q = A\lambda \frac{T_y - T_z}{d} = A\frac{T_y - T_z}{R} \quad \text{where} \quad R = \frac{d}{\lambda} \tag{2.7}$$

The quotient of the slab's thickness and conductivity results in the thermal resistance R [m²·K/W], comparable to an electrical resistance. Equation (2.7) is only valid however under stationary conditions, for one-dimensional flow, with constant properties and without heat generation inside the slab.

A differential equation for conduction heat transfer can be obtained by inserting the infinitesimal thickness and temperature difference (as shown in Figure 2.1 right):

$$Q = A\,\lambda\,\frac{T - \left(T + dT\right)}{dx} = -A\,\lambda\,\frac{dT}{dx} \tag{2.8}$$

in which x [m] is the space coordinate. Equation (2.7) thus implies that the heat flow at any point in a medium is proportional and opposite to the local temperature gradient.

2.3.3 CONVECTION

Convection heat transfer mode is comprised of two earlier mechanisms: heat advection and heat conduction, at the local scale of the interactions between a surface and a fluid.

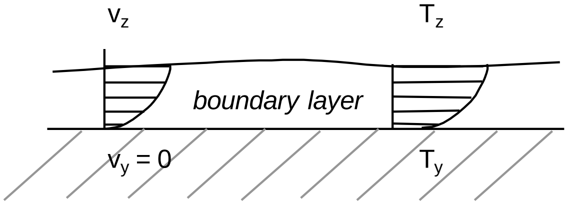

Figure 2.2 convection over a flat surface, with the velocity and thermal boundary layers.

Convection heat transfer occurs when a cool fluid flows past a warm surface (or vice versa) as depicted in Figure 2.2. The fluid adjacent to the surface forms a slowed down region called the boundary layer. The velocity of the fluid at the surface is reduced to zero due to the viscous action. Therefore, at this point the heat is transferred only by conduction. The moving fluid then carries the heat away. The temperature gradient at the surface of the body, and thus the overall heat exchange between body and fluid, depends on the rate at which the fluid carries the heat away.

Convection heat transfer may be classified according to the driving force of the fluid flow. Forced convection occurs when flow is caused by external means, such as fans or wind. An example is convection between exterior air and exterior building surfaces.

In contrast, in natural (or free) convection the airflow is induced by buoyancy forces, arising from density differences caused by temperature variations in the fluid. An example is convection heat transfer that occurs between interior air and interior building surfaces.

In such situation, the air that makes contact with the warm wall surface experiences an increase in temperature and therefore a reduction in density. Since the warm air is now lighter than the surrounding air, buoyancy forces induce a vertical motion and the hot air rising from the wall is replaced by the inflow of air at room temperature.

Another classification for convection heat transfer may be based on the nature of the flow in the boundary layer. Laminar flow occurs at lower values for v_z and is characterised as an orderly layered flow. As the mass exchange between different layers in the boundary layer is limited, laminar flow will give low convection heat transfer. Turbulent flow, on the hand, occurs at higher values for v_z and is characterised as a chaotic flow with lots of exchange between the different locations in the boundary layer. Turbulent flow hence typically yields high convection heat transfer.

While the combination of advection and conduction makes convection dependent on very many parameters, the transport law for convection is deceivingly simple:

$$Q = A\,h_{conv}\left(T_y - T_z\right) \tag{2.9}$$

In which h_{conv} [W/(m^2·K)] is the convective surface heat transfer coefficient. The h_{conv} value depends on many properties of the fluidum and the flow, but we will mainly work with the standard values:

interior environment:	*vertical surface*	*3.5* W/(m^{2}K)
	horizontal surface, heat flow upward	*5.5* W/(m^{2}K)
	horizontal surface, heat flow downward	*1.2* W/(m^{2}K)
exterior environment:	*all surface orientations*	*20* W/(m^{2}K)

Do however keep in mind that these are just accepted standard values, which may deviate strongly for specific applications. If your analysis is very sensitive to the value of the convective surface heat transfer coefficient, then more specific correlations are to be applied. That is however a subject of the 11121 'Thermal building physics' course.

2.3.4 RADIATION

All bodies emit energy by means of electromagnetic radiation. This electromagnetic radiation takes the form of photons moving in a random direction, with random phase and frequency. Electromagnetic radiation transferred as a result of a temperature difference is called thermal radiation. Radiation does not need a medium: on the contrary, it is least hampered in vacuum.

An ideal thermal radiator or a black body will emit energy at a rate proportional to the 4th power of its absolute temperature and its surface area:

$$Q_{emis} = A\sigma T_y^4 \tag{2.10}$$

in which σ [5.67 x 10^{-8} W/(m^2·K^4)] is the Stefan-Boltzmann constant. A non-ideal radiator will only emit a fraction of that energy:

$$Q_{emis} = A\varepsilon\sigma T_y^4 \tag{2.11}$$

in which ε [-] is the emissivity of the body, always between 0 and 1.

When the emitted radiation hits another body, fractions of the incoming radiation are absorbed, reflected and transmitted:

$$\begin{aligned} Q_{abs} &= A\alpha q_{in} = A\varepsilon q_{in} \\ Q_{refl} &= A\rho\, q_{in} \\ Q_{trans} &= A\tau\, q_{in} \end{aligned} \tag{2.12}$$

in which α, ρ, τ [-] are the absorptivity, reflectivity and transmissivity of the body, and q_{in} [W/m²] is the incoming radiation per m² of surface area. The equality in the first equation is Kirchov's Law, indicating that the absorptivity and emissivity are equal when considering radiation of a certain wavelength.

2.3.5 SHORT-WAVE AND LONG-WAVE RADIATION

All radiation properties – emissivity, absorptivity, reflectivity, transmissivity – depend on the wavelength of the radiation involved. This wavelength in turn depends on the radiation temperature of the radiator: the higher the temperatures, the shorter the wave lengths of the emitted radiation. In building physics, we distinguish only two radiation temperatures: the solar surface (at roughly 5800 K) and the normal environment (at around 300 K). The sun hence yields short-wave radiation, while the environment gives long-wave radiation. The absorptivity for short-wave radiation will hence be indicated with α_S, while the emissivity for long-wave radiation is given as e_L.

2.3.6 EXCHANGE OF LONG-WAVE RADIATION

The exchange of short-wave radiation is sufficiently described with Equation (2.12). The exchange of long-wave radiation between radiating bodies at different temperatures requires some further elaboration though. Leaving a lot of mathematics out, heat transfer by long-wave radiation can be described as:

$$Q = A_y \frac{\sigma\left(T_y^4 - T_z^4\right)}{\left(\frac{1-\varepsilon_{L1}}{\varepsilon_{L1}} + \frac{1}{F_{yz}} + \frac{(1-\varepsilon_{L2})A_y}{\varepsilon_{L2}A_z}\right)} = A_y F_{Ryz}\sigma\left(T_y^4 - T_z^4\right) \tag{2.13}$$

in which F_{yz} [-] is the view factor between surfaces A_y and A_z, and the term in blue makes up the radiation factor F_{Ryz} [-]. The view factor is determined by the geometry only, while the radiation factor also incorporates the radiation properties. The view factor gives the fraction of radiation emitted by A_y that is incident on A_z.

For two infinite parallel plates, or for a surface totally enclosed by the other surface, the view factor is 1: all radiation emitted by one surface is incident on the other surface. For these two cases, the radiation factor F_{Ryz} simplifies to:

$$\begin{aligned} &\text{Parallel plates:} && F_{Ryz} = 1\big/\left(1/\varepsilon_{Ly} + 1/\varepsilon_{Lz} - 1\right) \\ &\text{Enclosed surface:} && F_{Ryz} = \varepsilon_{Ly}\varepsilon_{Lz} \end{aligned} \tag{2.14}$$

For practical cases, Equation (2.13) is commonly simplified:

$$\begin{aligned} Q &= A_y F_{Ryz}\sigma\left(T_y^4 - T_z^4\right) \\ &= A_y F_{Ryz}\sigma\, 4T_{avg}^3\left(T_y - T_z\right) && T_{avg} = \left(T_y + T_z\right)\big/2 \\ &= A_y h_{rad}\left(T_y - T_z\right) && h_{rad} = F_{Ryz}\sigma\, 4T_{avg}^3 \end{aligned} \tag{2.15}$$

$$\begin{aligned} Q &= A_y F_{Ryz} \sigma \left(T_y^4 - T_z^4 \right) \\ &= A_y F_{Ryz} \sigma \left(T_y + T_z \right) \left(T_y{}^2 + T_z{}^2 \right) \left(T_y - T_z \right) \\ &= A_y F_{Ryz} \sigma \, 4 T_{avg}^3 \left(T_y - T_z \right) \\ &= A_y h_{rad} \left(T_y - T_z \right) \end{aligned}$$

$$\Rightarrow 4T_{avg}^3 = \left(T_y + T_z \right) \left(T_y{}^2 + T_z{}^2 \right)$$

$$\Rightarrow T_{avg} = \sqrt[3]{\frac{\left(T_y + T_z \right) \left(T_y{}^2 + T_z{}^2 \right)}{4}}$$

$$h_{rad} = F_{Ryz} \sigma \, 4 T_{avg}^3$$

in which h_{rad} [W/(m²·K)] is the radiative surface heat transfer coefficient, somewhat equivalent to its convective counterpart. As most building materials have emissivities of roughly 0.9, a standard value for h_{rad} can be obtained:

interior & exterior environment, all surface orientations	*4.5* W/(m²·K)

Do however keep in mind that this is just an accepted standard values, which may deviate strongly for specific applications. If your analysis is very sensitive to the value of the radiative surface heat transfer coefficient, then a more correct correlation is to be applied. That is however a subject of the 11121 'Thermal building physics' course.

2.3.7 LATENT HEAT TRANSFER

Latent heat moves along with a carrier, independent of temperature. Each time the carrier experiences a state change, related latent heat is converted into sensible heat or vice versa. For example, when water evaporates, it absorbs a quantity of sensible heat equal to its latent heat of evaporation. Water vapor diffuses (= transfer) to a cooler spot, where it may condense with reemission of the latent heat of evaporation as sensible heat. These conversions affect the temperature course as well as the flow of sensible heat in solid materials and building parts.

The transport law for latent heat:

$$Q = A \, g_{cond} \, L_v \tag{2.16}$$

in which g_{cond} [kg/m²] is the condensation flow per m² of surface area. Condensation will yield a heat gain for the surface, while evaporation will give a heat loss (can hence be included by use of a negative g_{cond}).

2.4 Steady-state one-dimensional heat transmission

While most heat transfer processes are essentially transient, in many cases the ratio of conductivity over capacity and the timescale involved allow making steady-state calculations. In such situations the energy content of the materials does not change in time, implying constant temperatures and heat flows.

2.4.1 SURFACE TRANSFER RESISTANCES

In many cases we will assume that latent heat transfer is insignificant, that no solar radiation is occurring and that the convective and radiative temperatures of the environment are equal to the air temperature (see Figure 2.3).

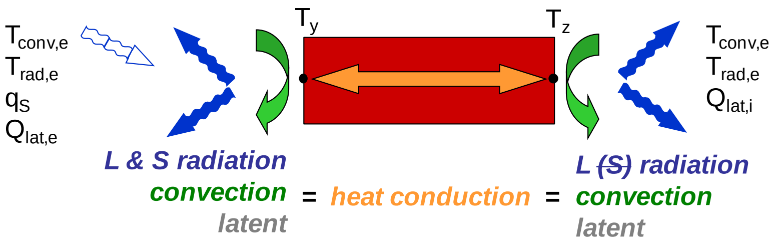

Figure 2.3 heat exchange between the exterior (left) and interior (right) environment and the surfaces of a building component.

This will allow simplifying the heat exchange between an environment and the surface of a building component significantly:

$$\begin{aligned} &Ah_{conv,e}\left(T_{conv,e}-T_y\right)+Ah_{rad,e}\left(T_{rad,e}-T_y\right)=Q_{wall} \\ &\quad\rightarrow\quad A\left(h_{conv,e}+h_{rad,e}\right)\left(T_e-T_y\right)=Q_{wall} \\ &\quad\rightarrow\quad Ah_e\left(T_e-T_y\right)=Q_{wall} \\ &\quad\rightarrow\quad A\frac{T_e-T_y}{R_{se}}=Q_{wall} \end{aligned} \tag{2.17}$$

$$\begin{aligned} &Q_{wall}=Ah_{conv,i}\left(T_z-T_{conv,i}\right)+Ah_{rad,i}\left(T_z-T_{rad,i}\right) \\ &\quad\rightarrow\quad Q_{wall}=Ah_i\left(T_z-T_i\right)=A\frac{T_z-T_i}{R_{si}} \end{aligned} \tag{2.18}$$

in which h_e and h_i [W/(m^2·K)] are the external and internal surface heat transfer coefficients, T_e and T_i [K] are the external and internal air temperatures, and R_{se} and R_{si} [m^2·K/W] are the external and internal surface resistances. This implies that, under the accepted conditions, the combined convection and radiation between an environment and a surface can be described as conduction.

Standard values for these surface transfer coefficients and resistances can be obtained by combining the earlier standard values for convection and radiation:

		h_i* or *h_e	***R_{si}* or *R_{se}***
interior environment:	*vertical surface*	*8* W/(m^{2}K)	*0.125* m^{2}K/W
	horizontal surface, flow up	*10* W/(m^{2}K)	*0.100* m^{2}K/W
	horizontal surface, flow down	*6* W/(m^{2}K)	*0.167* m^{2}K/W
exterior environment:	*all surface orientations*	*25* W/(m^{2}K)	*0.040* m^{2}K/W

2.4.2 'COMPOSITE' WALL

With the surface transfer resistances defined above, even single-layered walls are to be considered composite: a combination of the exterior surface resistance, the conduction resistances of the material layer(s) and the interior surface resistance. The elaboration below will not distinguish between material or surface resistances at first, so it is applicable to various configurations.

Example: 3-layer wall

In steady-state, without heat sources or sinks, the heat flow rate in each layer must be the same. If not, conservation of energy would yield temperature changes, rendering the regime time-dependent. Suppose a 3-layer wall, with a temperature T_y on the left wall surface, and T_z on the right wall surface (see Figure 2.4).

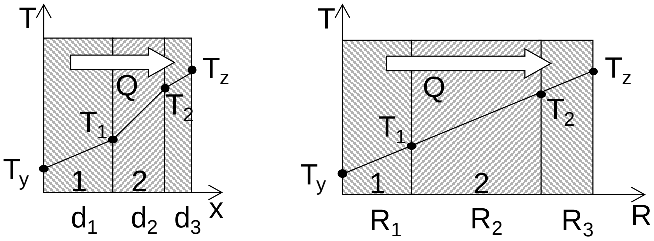

Figure 2.4 Temperature profile through a 3-layer wall, in function of the coordinate (left) and the resistance (right).

For the 3 layers we can write:

$$\begin{aligned} Q &= A\frac{T_y - T_1}{R_1} & \text{or} \quad T_y - T_1 &= Q\frac{R_1}{A} \\ Q &= A\frac{T_1 - T_2}{R_2} & \text{or} \quad T_1 - T_2 &= Q\frac{R_2}{A} \\ Q &= A\frac{T_2 - T_z}{R_3} & \text{or} \quad T_2 - T_z &= Q\frac{R_3}{A} \end{aligned} \tag{2.19}$$

After summation of the right-hand sides of equation (2.19), we obtain:

$$Q = A\frac{T_y - T_z}{R_1 + R_2 + R_3} \tag{2.20}$$

The higher the total thermal resistance of a wall, the lower its steady-state heat flow rate and the better the wall insulates. This is achieved by integrating a sufficiently thick insulation layer in the wall. Since the energy crisis (1973-1979) and global warming (1983-...) such thermal insulation of all components of the building envelope is seen as an efficient means to lower the energy consumption for heating of buildings.

An expression for the temperature profile in the 'composite' wall is obtained from the expressions for the temperature differences over the different layers. This temperature difference can, for example for the second layer in Figure 2.4, be obtained by inserting equation (2.20) into the second expression of equation (2.19):

$$T_2 - T_1 = \left(T_z - T_y\right)\frac{R_2}{R_1 + R_2 + R_3} \tag{2.21}$$

This indicates that the layer with the largest resistance (commonly the insulation layer in a real component) will experience the largest temperature difference. Summing Equation (2.21) with a similar equation for the first layer, and some rearranging, yields:

$$T_2 = T_y + \left(T_z - T_y\right)\frac{R_1 + R_2}{R_1 + R_2 + R_3} \tag{2.22}$$

The fraction at the end of Equation (2.22) can be described as: the ratio of the thermal resistance 'gone through' from the 'start temperature' T_y up to the 'target temperature' T_2, and the total thermal resistance between 'start and end temperatures' T_y and T_z. Those considerations work for all types of problems: for single-layer wall between different environments with known temperatures, for multi-layer walls with known surface or interface temperatures, and all combinations of these cases.

Generalisation: multi-layer wall

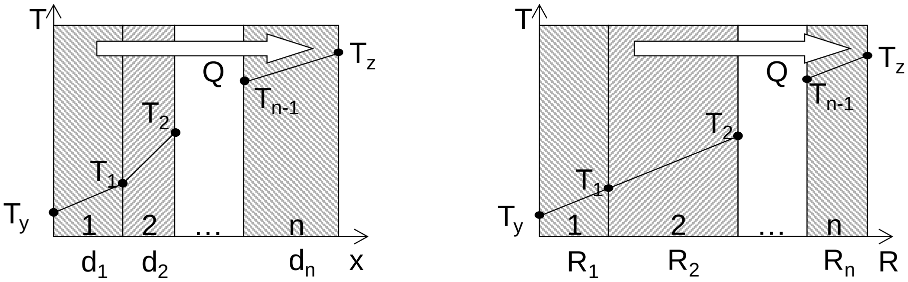

Figure 2.5 temperature profile through a multi-layer wall, in function of the coordinate (left) and the resistance (right).

Equations (2.20) and (2.22) can be generalized to multi-layer walls:

$$Q = A\left(T_y - T_z\right)/R_{y-z} \tag{2.23}$$

$$T_x = T_y + \left(T_z - T_y\right)R_{y-x}/R_{y-z} \tag{2.24}$$

in which R_{y-x} and R_{y-z} [m^2·K/W] are respectively the sum of resistances between interface y and x and the total resistance of the wall (between y and z thus).

At this point, looking to the analogy between Equations (2.23) and (2.24) and the equations for an electrical circuit with a series of electric resistances, is rather instructive. In fact, temperature replaces electric tension, conductive heat flow the electric current and thermal resistance the electrical resistance. This allows converting a thermal problem to an electrical analogous problem.

Environment to environment: U-value

For the specific case of heat transfer through a component from one environment temperature T_e to another environment temperature T_i, Equations (2.23) and (2.24) can explicitly be written as:

$$Q = \frac{A\left(T_e - T_i\right)}{R_{se} + \sum^{all} d/\lambda + R_{si}} = AU\left(T_e - T_i\right) \tag{2.25}$$

$$U = \frac{1}{R_{se} + \sum^{all} d/\lambda + R_{si}}$$

$$T_x = T_e + \left(T_i - T_e\right)\frac{R_{se} + \sum^{x} d/\lambda}{R_{se} + \sum^{all} d/\lambda + R_{si}} \tag{2.26}$$

in which U [W/m^2·K] is the “thermal transmittance”, or U-value, of the considered component. A large U-value thus indicates a badly insulated component, with a high heat loss, while low U-values characterise well insulated components, with resultantly lower heat losses.

3 AIR, MOISTURE AND MATERIALS

This chapter serves as an introduction to mass transfer part of the heat and mass transfer theory. The focus is on the moisture storage in air and materials and setting up mass balance for building zones.

There are three forms of moisture: vapor, liquid and ice.

In building applications, vapor is stored in air and liquid is stored in materials. The mass transfer takes place either as vapor or as liquid. Ice is not considered transferable.

Moisture is found everywhere. In building physics applications the sources for moisture – i.e. moisture loads – are typically grouped as

- Built-in moisture: New buildings, especially ones with in-situ- casted concrete, contain large amounts of moisture, which must be dried out before finalizing the constructions e.g. with paint or floor covering.
- Internal sources: Human activity in buildings makes an important share of the moisture loads, especially in residential buildings. A typical family produces about 10 kg/day as a result of domestic activities like laundry drying, showering,

  cooking, breathing and evaporation from plants
- External sources: Wind driven rain and vapor exchange with external weather is another main contributor for moisture loads. These depend highly on the local environment and climate, and on the type of construction.
- Water leakages: Leaky pipes and other accidents involving moisture, including rising damp, can be significant sources of moisture

One of the purposes of building physics engineering is to avoid too high – or too low – moisture loads on indoor air and building materials and constructions.

3.1 Conservation of mass

Analogous to theory of conservation of energy, there is a theory of conservation of mass (*Mikhail Lomonosov, 1748*). For moisture in an open system this means that the amount of moisture stored in the system $M_{m,stored}$ [kg] must be equal to the difference between the moisture amount added to the system $M_{m,in}$ [kg] and the moisture amount taken from the system $M_{m,out}$ [kg].

$$M_{m,stored} = \sum M_{m,in} - \sum M_{m,out} \tag{3.1}$$

M_m moisture mass [kg]

in/out	entering/leaving

The rate of moisture mass transfer is given by

$$dM_{m,stored}/dt = \sum G_{m,in} - \sum G_{m,out} \tag{3.2}$$

G_m	moisture flow [kg/s]
t	time [s]

This expression forms the basis of all moisture transfer analysis. Porous building materials and air contain moisture and can therefore store moisture. Moisture transfer can take place in air, between zones, through materials, constructions and components. In addition, building materials interact with the moisture in air. By relating storage and flow to moisture contents in air and materials, we can assess moisture response of whole buildings and building components

In many cases, we can limit ourselves to a stationary – or 'time-independent' – situation, in which all amounts of stored and transported moisture remain constant. In that case, the time derivative in Equation (3.2) becomes zero, and the standard moisture balance equation is obtained:

$$dM_{m,stored}/dt = 0 \tag{3.3}$$

$$\sum G_{m,in} - \sum G_{m,out} = 0 \quad \Rightarrow \quad \boxed{\sum G_{m,in} = \sum G_{m,out}} \tag{3.4}$$

3.2 Moisture storage in air

Moisture in air is moisture in gas phase, i.e. water vapor, in the following text simply: *vapor*. Vapor content in air, vapor mass M_v [kg], in given volume V [m^3], is given by the vapor density ρ_v [kg/m^3] that again is a function of vapor pressure p_v [Pa] and temperature T [K]. Due to ideal gas law, vapor pressure is the thermodynamic equivalent for vapor mass. This relation is analogous to temperature that is thermodynamic equivalent for heat.

$$M_v = V_a \rho_v(p_v, T) \quad \text{where} \quad \rho_v = p_v / R_v T \quad \text{and} \quad R_v = 462 \text{ J/(kg}\cdot\text{K)} \tag{3.5}$$

M	mass [kg]
V	volume [m^3]
ρ	density [kg/m^3]
p	pressure [Pa]
R	gas constant [J/(kg·K)]

T temperature [K]

$_{a/v}$ for air/vapor

An alternative expression for vapor density is the water vapor ratio x [-]: Ratio of vapor density to air density ρ_a [kg/m^3]

$$x_v = \rho_v / \rho_a \tag{3.6}$$

Different from heat, i.e. temperature, vapor pressure has an upper limit. This upper limit is called saturation vapor pressure $p_{v,s}$ [Pa] and it is strongly a function of temperature. For a given temperature, air can only contain certain amount of vapor and this amount determines the saturation vapor pressure.

Saturation is a state where there is an equilibrium for evaporation and condensation. Figure 3.1 illustrates an example on saturation: A closed vessel is partially filled with water and initially there is no vapor present. Water molecules start to escape from water surface. This leads to higher vapor pressure above the water. This can continue until number of escape molecules and return molecules is the same – and this is saturation.

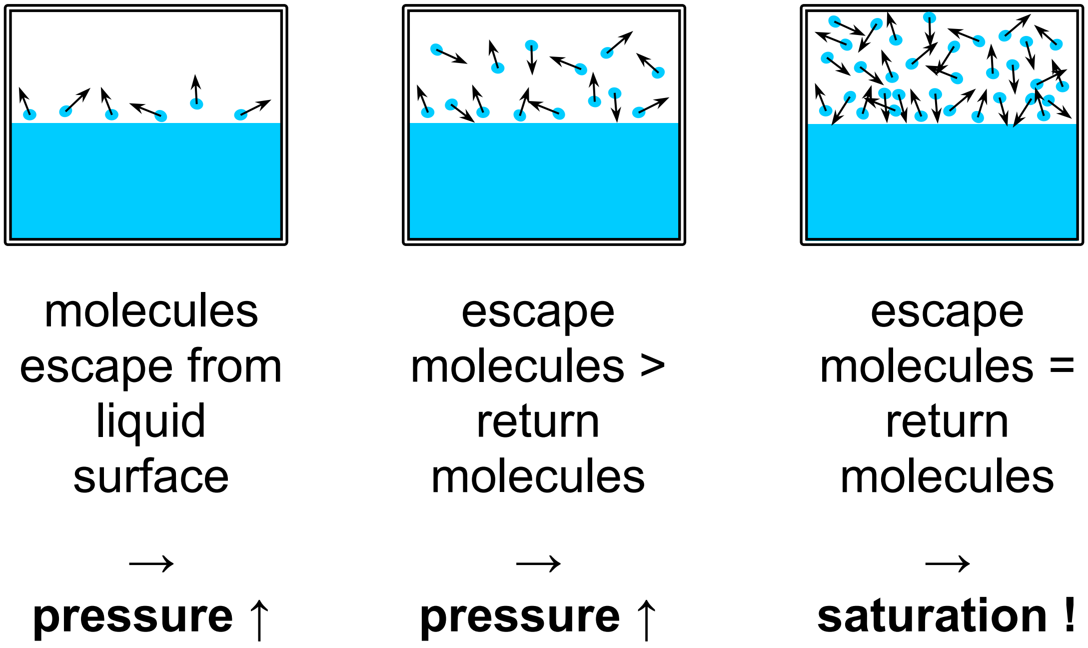

Figure 3.1 Saturation process in a closed vessel partially filled with water and initially no vapor present.

For increasing temperatures, there is more atomic vibration, which leads to more 'escapes'. This means higher saturation vapor pressure for higher temperatures. There are several expressions for this temperature dependence, and the below one is a common expression in hygrothermal building physics. Table values are found in the end of this chapter.

$$p_{vsat}(\theta) = 288.68(1.098 + \frac{\theta}{100})^{8.02}$$

(3.7)

where ϑ is temperature [ºC].

Relative humidity φ [-] describes the ratio of actual vapor pressure p_v [Pa] and the saturation vapor pressure p_{vsat} [Pa], for given temperature.

$$\varphi = p_v \,/\, p_{vsat} \tag{3.8}$$

p	pressure [Pa]
φ	relative humidity [-],[%]
v/sat	vapor/saturation

Temperature dependence of both saturation vapor pressure and relative humidity is illustrated in Figure 3.2.

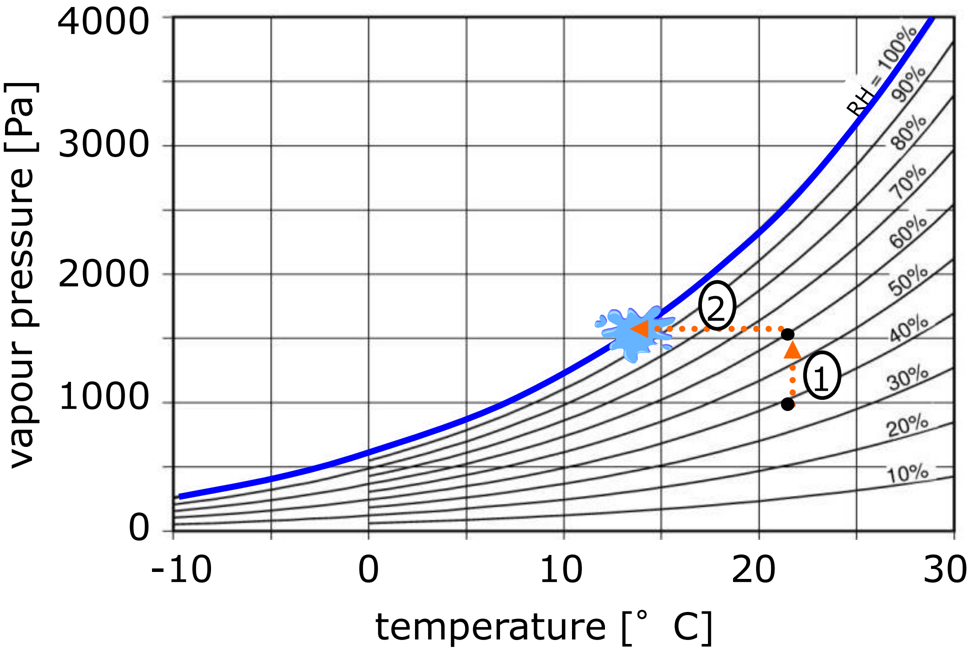

Figure 3.2 Water vapor pressure as a function of temperature. Also 2 typical processes are shown.

Two typical processes in buildings are shown in Figure 3.2:

1. Vapor is added to air without change of temperature. This is called an isothermal change of state. An example is vapor production in a room, e.g. cooking, that adds on vapor in the air and results to a higher relative humidity (for example from 40% to 60%) of the indoor air.

2. Temperature is changed without adding vapor. This is an isobaric change of state. An example is humid air (here 60%) meeting a cold surface, e.g. a window glass. If the temperature of the cold surface is lower than dew point of the humid air, condensation occurs.

3.3 Moisture storage in materials

Porous building materials contain moisture. Moisture in the pores of a porous material can exist either adsorbed to the surface, or physically fixed in pores, or as free water, see Figure 3.3b, which also illustrates the moisture content for increasing relative humidity. Some water can also be chemically bound with the material itself. The amount of hygroscopic moisture depends on relative humidity of the pore air and on the porosity of the material. Also type of pores – open or closed, see Figure 3.3a –b and the pore size distribution are governing the moisture content of the material. Fine-porous materials have larger inner pore surface area and can therefore contain larger amounts of hygroscopic moisture than large-porous materials.

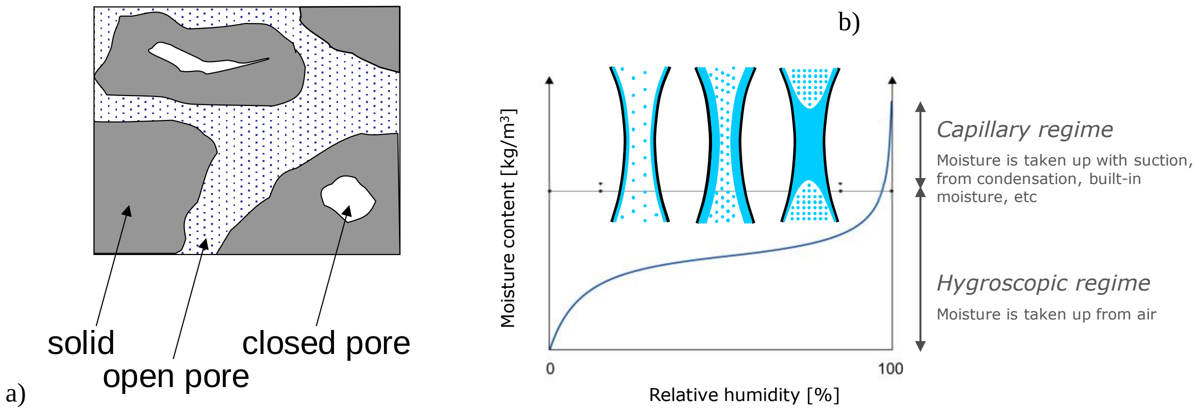

Figure 3.3 Different pore types in a porous material. b) Sorption isotherm with illustration of fixation of moisture as a function of relative humidity.

A material's ability to store moisture is experimentally determined by sorption and suction isotherms and mathematically described as the equation(s) of state. These isotherms together are called the retention curve. In this chapter only hygroscopic moisture (i.e. RH= 0 – 98%) and sorption isotherms are presented. More about liquid moisture and especially liquid moisture transport in porous materials in the later lecture in this course.

In the hygroscopic regime, the sorption isotherm represents the moisture content of the material u [kg/kg] or w [kg/m^3] as a function of relative humidity (Figure 3.3b). Different materials have very different sorption isotherms (see Figure 3.4).

Moisture content is determined from the weight of moist samples m_{moist} [kg] and from their dry weight m_{dry} [kg]. This difference gives mass of moisture m_{m} [kg]. Volumetric moisture content w is often most suitable for comparison of different materials.

$$u = \frac{m_m}{m_{dry}} = \frac{m_{moist} - m_{dry}}{m_{dry}} \tag{3.9}$$

$$w = u \cdot \rho_{dry} \tag{3.10}$$

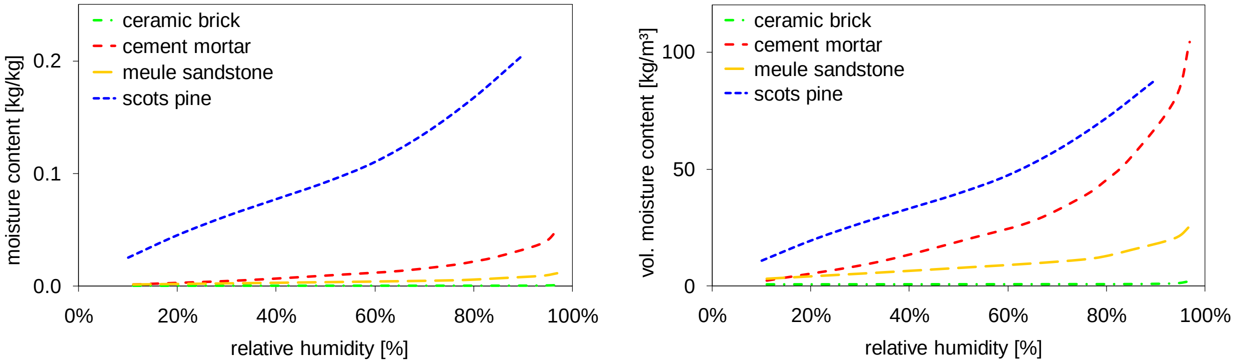

Figure 3.4 Sorption isotherm for some different building materials.

When determining sorption isotherms, different results are obtained for wetting a sample and drying a sample. This difference is called hysteresis and is explained by so called bottle neck effect. See illustration in Figure 3.5.

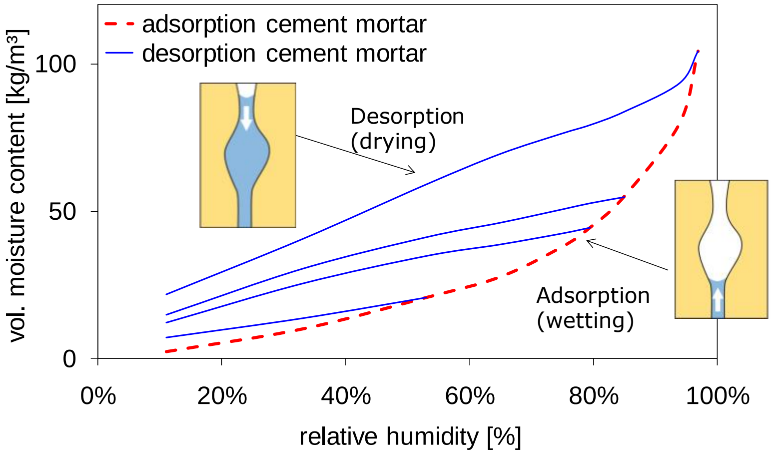

Figure 3.5 Adsorption and desorption isotherms for cement mortar. Illustration of hysteresis process.

3.4 Moisture transport in air (& materials)

There are different modes of moisture transport in air and materials and constructions. The modes of transport are depending on the medium itself and if the moisture is in vapor or in a liquid phase. There is no transfer of ice. Table 3.1 gives a summary of these transfer forms, their driving forces and in which cases they are relevant.

Vapor diffusion and capillary liquid transfer will be treated separately and more in depth later in this course and are not a subject in this chapter.

Table 3.1 Modes of moisture transfer.

	Transfer mode	**Medium**	**Driving force**
Vapor	ADVECTION	with fluid & solid	Transfer of mass
	DIFFUSION	through fluid & solid	Differences in vapor concentration
	CONVECTION	between surface and fluid	Local micro-diffusion and -advection between a surface and fluid
Liquid transfer	CAPILLARY	through porous solids	Capillary suction in material pores

3.4.1 ADVECTION

Advection is transfer of vapor with a fluid, e.g. with an air flow G_a [kg/s], where the stored vapor mass x_v [kg/kg] is transferred and results in vapor flow G_v [kg/s].

$$G_v = G_a x_v = \frac{G_a}{\rho_a}\rho_v = \frac{G_a}{\rho_a}\frac{p_v}{R_v T} \tag{3.11}$$

G_v	advective vapor flow [kg/s]
x_v	water vapor ratio [kg/kg]
$_{a/v}$	for air/for vapor

Typical example for advection in building physics is ventilation: Dry exterior air comes in and moist interior air goes out resulting in net loss of vapor mass. This is illustrated more in the next chapter about moisture balance for zones. Advection is also the transport form when moisture is transported through materials and components with an air flow. More about this in chapter 7. Air transfer.

3.4.2 CONVECTION

Convective vapor transfer is also transfer of moisture with fluid – as advection – but when talking about convection, we think about local micro-diffusion and -advection between a surface and fluid, see Figure 3.6. Typical examples for convection in buildings are vapor exchange between interior/exterior air and interior/exterior surfaces. The convective vapor flow G_v [kg/s] is given with equation, where β [kg/(m²·s·Pa)] is the convective vapor transfer coefficient and $p_{v,z}$ and $p_{v,y}$ are vapor pressures [Pa] for fluid and surface, respectively. A is the surface area [m²].

$$G_v = A\,\beta\left(p_{v,y} - p_{v,z}\right) \qquad (3.12)$$

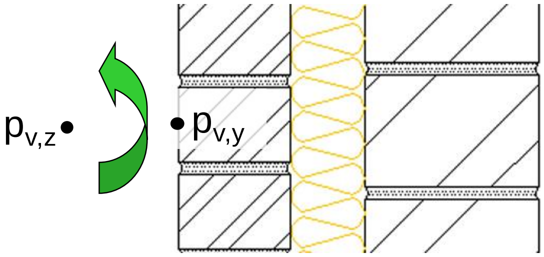

Figure 3.6 Convective moisture transfer between fluid and a surface.

The convective vapor transfer coefficient depends on the same parameters as convective heat transfer coefficient (see Lecture note 2. Heat transfer) and is related to it via Lewis relation:

$$\beta = \frac{h_c}{R_v \cdot T \cdot \rho \cdot c_p} \qquad (3.13)$$

where

h_c convective heat transfer coefficient [W/(m^{2}K)]

ρ air density [kg/m^3]

c_p specific heat capacity of air [J/(kg·K)]

Standard values for *β* can be used for most common building applications, for interior and exterior environments, respectively:

	β [kg/(m²·s·Pa)]
Interior environment: natural convection	*2·10-8*
Exterior environment: forced convection	*15·10-8*

3.5 Moisture balance for zones

In hygrothermal building physics, we often need to find the resulting state of air in a zone or in a component. In a real life, this state is ever changing and for solving it we need to apply transient methods which usually means applying numerical methods. This is a subject later in this course. However, many cases can be studied with simple steady state balances. In addition, learning to set up such heat and moisture balances is essential for understanding the concept of building physical diagnosis and design methods.

Given a space at constant temperature T_i [ºC] with a moisture production G_{vp} [kg/s] like in Figure 3.7, we can determine the resulting indoor relative humidity φ_i [%], if we know the ventilation rate G_a [kg/s] and the state of the outdoor air (T_e [ºC] and φ_e [%]). If not considering the moisture or heat capacity of the air or building materials and if only considering a steady state case, a moisture balance for a zone is given as

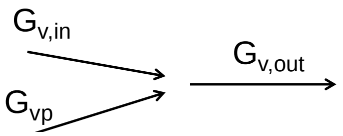

$$G_{v,in} + G_{vp} = G_{v,out} \tag{3.14}$$

Where G_a [kg/s] is the ventilation air flow rate and $x_{v,e}$ [-] and $x_{v,i}$ [-] are water vapor ratios for exterior air and interior air, respectively.

$$\begin{aligned} G_{v,in} &= x_{v,e} G_a \\ G_{v,out} &= x_{v,i} G_a \end{aligned} \tag{3.15}$$

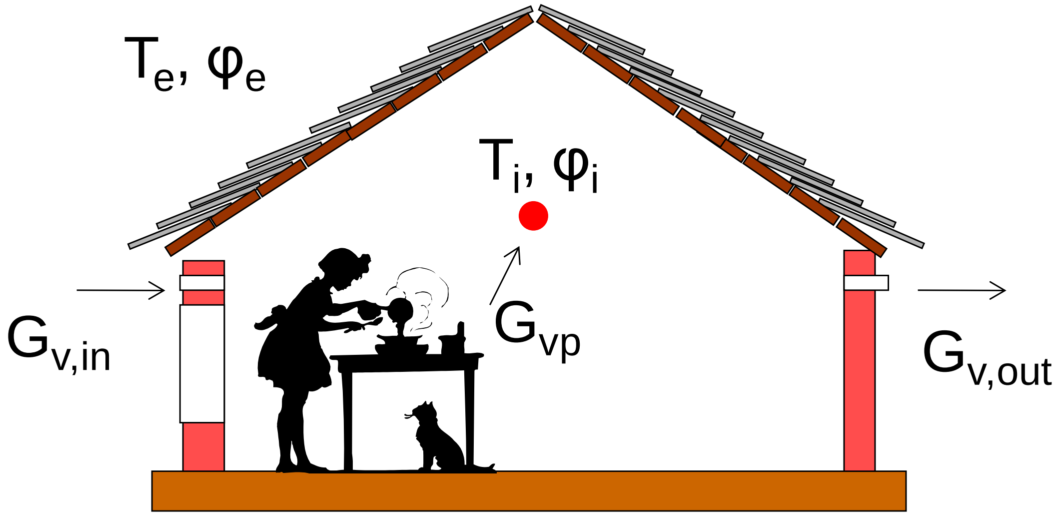

Figure 3.7 Moisture balance for a zone.

3.6 Tables for saturated vapor pressure

θ (°C)	0.0	0.1	0.2	0.3	0.4	0.5	0.6	0.7	0.8	0.9
0	611	615	620	624	629	634	638	643	647	652
1	657	662	666	671	676	681	686	691	696	701
2	706	711	716	721	726	731	736	742	747	752
3	758	763	768	774	779	785	790	796	802	807
4	813	819	824	830	836	842	848	854	860	866
5	872	878	884	890	896	903	909	915	922	928
6	935	941	948	954	961	967	974	981	987	994
7	1001	1008	1015	1022	1029	1036	1043	1050	1057	1065
8	1072	1079	1087	1094	1101	1109	1117	1124	1132	1139
9	1147	1155	1163	1171	1178	1186	1194	1203	1211	1219
10	1227	1235	1243	1252	1260	1269	1277	1286	1294	1303
11	1312	1320	1329	1338	1347	1356	1365	1374	1383	1392
12	1401	1411	1420	1429	1439	1448	1458	1467	1477	1487
13	1497	1506	1516	1526	1536	1546	1556	1566	1577	1587
14	1597	1608	1618	1629	1639	1650	1661	1671	1682	1693
15	1704	1715	1726	1737	1748	1760	1771	1782	1794	1805
16	1817	1829	1840	1852	1864	1876	1888	1900	1912	1924
17	1936	1949	1961	1973	1986	1999	2011	2024	2037	2050
18	2063	2076	2089	2102	2115	2128	2142	2155	2169	2182
19	2196	2210	2224	2237	2251	2265	2280	2294	2308	2322
20	2337	2351	2366	2381	2395	2410	2425	2440	2455	2470
21	2486	2501	2516	2532	2547	2563	2579	2595	2611	2627
22	2643	2659	2675	2691	2708	2724	2741	2758	2774	2791
23	2808	2825	2842	2859	2877	2894	2912	2929	2947	2965
24	2983	3001	3019	3037	3055	3073	3092	3110	3129	3148
25	3166	3185	3204	3224	3243	3262	3281	3301	3321	3340
26	3360	3380	3400	3420	3440	3461	3481	3502	3522	3543
27	3564	3585	3606	3627	3649	3670	3692	3713	3735	3757
28	3779	3801	3823	3845	3868	3890	3913	3935	3958	3981
29	4004	4028	4051	4074	4098	4122	4145	4169	4193	4218
30	4242	4266	4291	4315	4340	4365	4390	4415	4440	4466
31	4491	4517	4543	4569	4595	4621	4647	4673	4700	4727
32	4753	4780	4807	4835	4862	4889	4917	4945	4973	5001
33	5029	5057	5085	5114	5143	5171	5200	5229	5259	5288
34	5318	5347	5377	5407	5437	5467	5498	5528	5559	5590
35	5621	5652	5683	5715	5746	5778	5810	5842	5874	5907
36	5939	5972	6004	6037	6071	6104	6137	6171	6205	6239
37	6273	6307	6341	6376	6410	6445	6480	6516	6551	6587
38	6622	6658	6694	6730	6767	6803	6840	6877	6914	6951
39	6989	7026	7064	7102	7140	7178	7217	7255	7294	7333
40	7372	7412	7451	7491	7531	7571	7611	7652	7692	7733

4 VAPOR DIFFUSION

Moisture transfer in porous media involves a complex interaction of different transport mechanisms, their driving forces, and the effects of available capacity and possible temperature gradients. This chapter introduces one of them: water vapor diffusion.

Diffusive transport is proportional to the gradient of the driving force, the proportionality coefficient being a material parameter which is determined experimentally.

Typical examples for diffusion in buildings are:

- vapor transfer in and out from building materials, also called moisture buffering
- internal condensation caused by vapor diffusing in materials and condensing when reaching low temperature regions

In this lecture, we learn how to calculate moisture transfer as diffusion and how to evaluate if interstitial condensation in composite walls will be a problem.

4.1 Fick’s law

Figure 4.1 Liquid diffusion in water.

Theory on moisture transport in porous materials is originally based on Fick’s law of diffusion of ions in water (Fick, 1855), see Figure 4.1. In hygrothermal building physics, Fick’s law is adopted to describe diffusion of gas (water vapor) in air and in porous materials. Diffusion is driven by differences in vapor concentration and lead to net vapor transfer. Figure 4.2 illustrates diffusion process: molecules diffuse from high concentration to lower concentration. This process is active until equilibrium is reached.

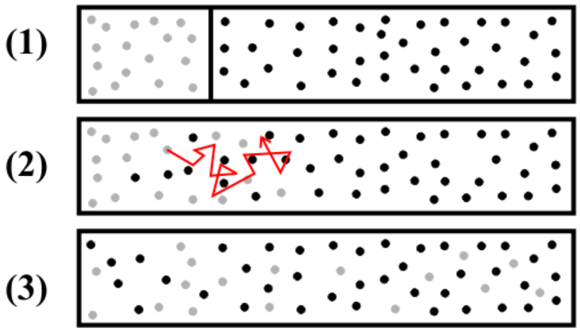

Figure 4.2: Illustration of the diffusion process. (1) Two different gasses are in a vessel separated by a wall. (2) The wall between the gasses is removed and for t>0 the gas molecule start to diffuse towards lower concentration until (3) there is equilibrium in a vessel with no concentration gradients.

Fick's law for diffusion in still air is generally given for the density of the water vapor ρ_v [kg/m³] as driving force

$$g_v = -a_a \frac{\partial \rho_v}{\partial x} \tag{4.1}$$

Where g_v [kg/(m²s)] is the density of vapor transport in air and a_a [m²/s] the diffusivity of water vapor in stagnant air.

By applying the ideal gas law and assuming isothermal conditions, the vapor diffusion can be expressed with the vapor pressure as driving force, see below both the differential form and the discretized form. For the latter see also Figure 4.3. In this course and in many practical applications this is the form we know as Fick's law.

$$g_v = -\delta \frac{\partial p_v}{\partial x} \tag{4.2}$$

$$G_v = A\delta \frac{p_v - (p_v + dp_v)}{dx} = -A\delta \frac{dp_v}{dx} \tag{4.3}$$

Where

G_v:	vapor flow [kg/s]
δ:	vapor permeability [kg/(m·s·Pa)]
p_v:	vapor pressure [Pa]
x:	coordinate [m]
A:	surface area [m²]

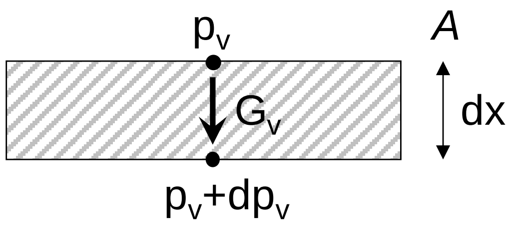

Figure 4.3: Illustration of Fick's law

The density of water vapor ρ_v [kg/m³] and water vapor pressure p_v [Pa] have the following relationship

$$\rho_v = \frac{p}{R_v \cdot T} \tag{4.3}$$

Vapor permeability in air δ_a [kg/(m·s·Pa)] is depending on the temperature T [K] and total gas pressure P [Pa] and increases for increasing temperature and decreases for increasing total gas pressure and has the below expression. At 20 °C and at sea level pressure a standard value can be used: $1.9 \cdot 10^{-10}$ kg/(m·s·Pa). R_v is the gas constant for vapor [J/(kg·K)].

$$\delta_a = \frac{2.262}{R_v T \cdot p}\left(\frac{T}{273.15}\right)^{1.81} \tag{4.4}$$

4.2 Vapor permeability of materials

The diffusion of water vapor in a porous material can be regarded as diffusion in air, but with reductions because of the pore system, and is therefore a function of parameters like 'porosity' and 'tortuousity' as explained below. Water vapor diffusion through some fibrous insulation materials with very low density is practically equal to diffusion in still air.

Diffusion of water vapor in porous materials takes place in the pore volume. If a material has very narrow pores, the vapor molecules collide with the pore walls. This process is called Knudsen diffusion. See Figure 4.4 for an illustration.

porosity:	vapor can only flow in open pores of materials, high porosity gives normally high permeability
tortuousity:	in a pore system with high turtuousity, vapor has to take tortuous path, decreasing the permeability

Practical average values of some typical building materials are given in Table 4.1.

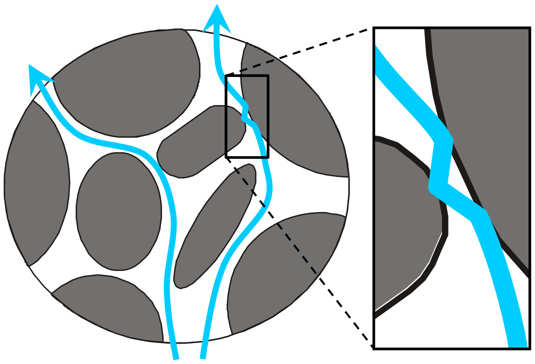

Figure 4.4: Illustration of vapor diffusion through a porous material. The longer (tortuous) path a vapor molecule needs to take, the lower the permeability. The enlargement shows a path of a vapor molecule in a very narrow pore, where it collides with the pore walls. This process is so called Knudsen diffusion.

Table 4.1 Vapor permeability of some typical building materials.

Material	**Vapor permeability δ** $[10^{-10}$ kg/(m·s·Pa)]
still air	1.9
mineral wool	0.7-1.9
cellular concrete	0.3
gypsum board	0.2
ceramic brick	0.1
exp. polystyrene	0.1
High dens. Concrete	0.02
wood	0.02

Fick's law can also be expressed for a material layer (see Figure 4.5) with a thickness of *d* [m] and vapor permeability δ [kg/(m·s·Pa)]. By introducing a vapor diffusion resistance *Z* [m²sPa/kg] and vapor pressures on each surface of the layer – $p_{v,y}$ and $p_{v,z}$ respectively –the following equation for diffusion flow G_v [kg/s] is obtained.

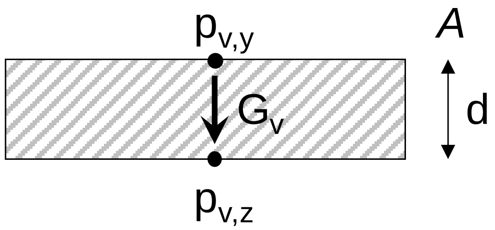

Figure 4.5: Illustration of vapor diffusion through a material layer with thickness d.

$$G_v = A\delta \frac{p_{v,y} - p_{v,z}}{d} = A \frac{p_{v,y} - p_{v,z}}{Z}; \quad Z = \frac{d}{\delta} \qquad (4.5)$$

Where

Z: diffusion resistance [m²sPa/kg]
d: thickness [m]

The above relations and expressions are valid with following conditions:

- stationary: no changes of $p_{v,y/z}$,d with time
- one-dimensional: vapor transfer normal to surface
- constant properties: no changes of d with thickness
- no mass generation: no internal moisture source or sink

When assuming constant parameters the above equation results in linear p_v profiles through a material layer.

It is worthwhile mentioning that Fick's law for vapor diffusion is analogous to Fourier's law for heat conduction:

$Q \rightarrow G_v$ for flow
$T \rightarrow p_v$ for driving force
$\lambda \rightarrow \delta$ for material parameter
$R \rightarrow Z$ for resistance

Vapor permeability or diffusion resistance of a material layer can also be given with other notations. The most common are:

Table 4.2 Also used notations for vapor permeability and diffusion resistance.

Vapor resistance factor	μ [-]	Material is μ times more vapor tight than air
Equivalent air layer thickness	s_d [m]	Gives a thickness of stagnant air that has the same Z

They are defined as:

$$\mu = \frac{\delta_a}{\delta_{mat}} \qquad s_d = \mu d_{mat} \tag{4.6}$$

Even though diffusion is pure diffusion of water vapor molecules in air, we also talk about diffusion when there is small amount of liquid transfer involved in the vapor transfer process. The fact is that for increasing relative humidity, the moisture content of a porous material increases and in the smallest pores capillary condensation starts to take place. Figure 4.6 illustrates how water vapor permeability increases for increasing relative humidity and how this is explained with increasing moisture content for increasing relative humidity. The higher permeability at higher moisture content is due to combination of vapor and liquid transfer, which speeds the transfer up. This is called equivalent diffusion.

For experimentally determined vapor permeabilities (the values in Table 4.1) it is not possible to distinguish between vapor and liquid transfer. Correctly these values should be called *equivalent vapor permeability* but they are just called *vapor permeability*.

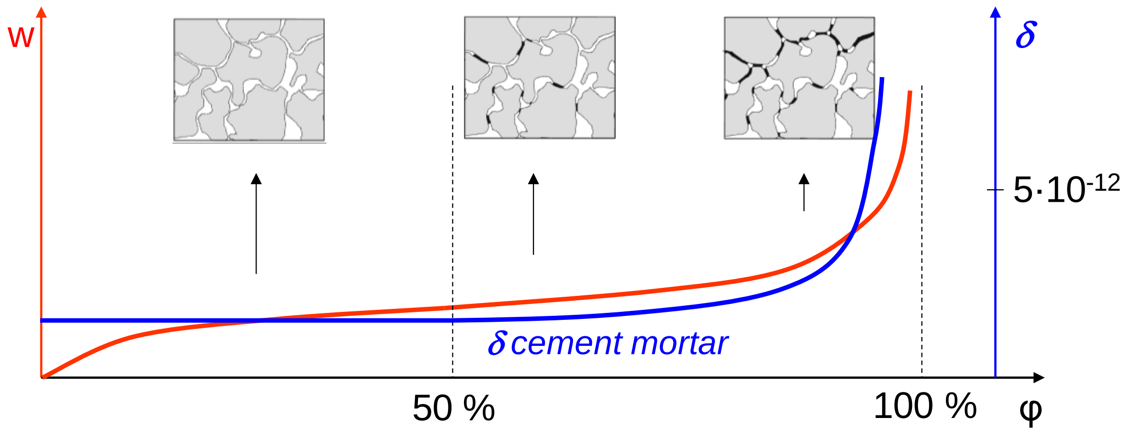

Figure 4.6: Water vapor permeability and moisture content of cement mortar as a function of relative humidity.

Note: The first few molecular layers of water, which are absorbed to the pore walls (low *RH*), are so tightly attracted to the solid material that they behave more like a 'solid' than as a 'liquid'!

4.3 Vapor diffusion through multilayer constructions

For practical applications in hygrothermal building physics, we often need to study vapor transfer in multilayer constructions, also called composite walls. The following description is analogous to heat transfer through a composite wall described in lecture note 2. Heat transfer.

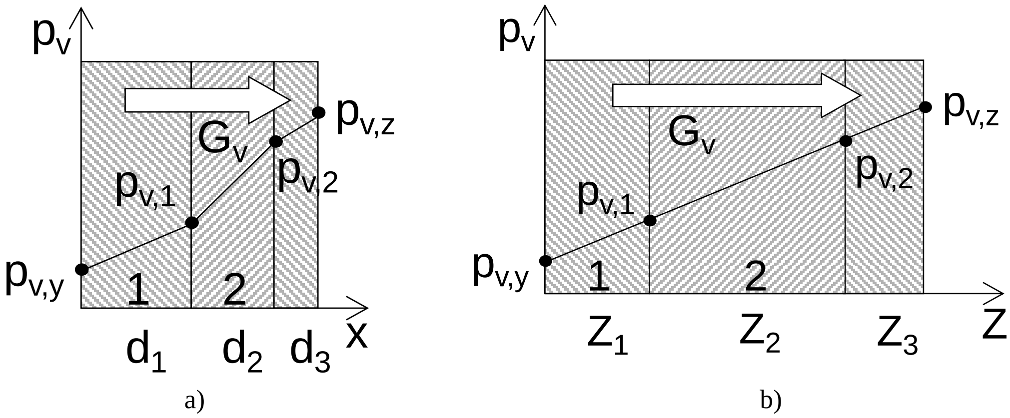

Figure 4.7: Composite wall with 3 material layers. Figure shows vapor flow Gv and vapor pressure profile as a function of a) thickness of the layers and b) vapor resistance.

Given layer 1 in Figure 4.7 with diffusion resistance *Z_1*, vapor flow *G_v* and vapor pressures *$p_{v,y}$* and *$p_{v,1}$*, the Fick's law can be expressed as:

$$G_v Z_1 = A(p_{v,y} - p_{v,1}) \tag{4.7}$$

Setting up similar balances for all 3 layers and summing them up, the following expression is found that describes vapor flow through a multilayered construction.

$$G_v = \frac{A(p_{v,y} - p_{v,z})}{Z_1 + Z_2 + Z_3} \tag{4.8}$$

Assuming linearity of the vapor pressure profile as in Figure 4.7b, vapor pressure e.g. in the intersection of layer 2 and 3 can be found with

$$p_{v,2} = p_{v,y} + (p_{v,z} - p_{v,y})\frac{Z_1 + Z_2}{Z_1 + Z_2 + Z_3} \tag{4.9}$$

Vapor pressure in any intersection can be found with

$$p_{v,x} = p_{v,y} + (p_{v,z} - p_{v,y})\sum_{j=1}^{x} Z_j \,/\, \sum_{n} Z_j \tag{4.10}$$

When analyzing vapor diffusion through a composite wall with given conditions of both interior and exterior environment, one must keep in mind whether the conditions are for the ambient air or for the surface. If the conditions are given for the air ($p_{v,y}$ and $p_{v,z}$), surface transfer coefficients Z_{sy} and Z_{si} must be included and the resulting vapor diffusion flow becomes:

$$G_v = \frac{A(p_{v,y} - p_{v,z})}{Z_{sy} + \sum^{all} d / \delta + Z_{sz}} \tag{4.11}$$

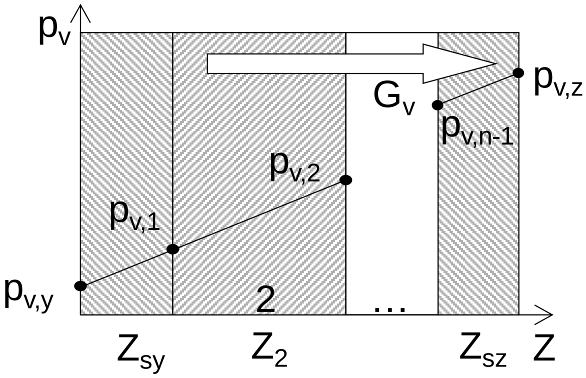

Figure 4.8: Composite wall with n material layers.

Surface resistances Z_s:

$$Z_{sy} = \frac{1}{\beta_y} \qquad Z_{sz} = \frac{1}{\beta_z} \tag{4.12}$$

Where β is surface transfer coefficient for vapor [kg/(m^{2}sPa)]

4.4 Glaser method

Calculation of moisture diffusion through a multi-layered construction under steady-state conditions (see previous chapter) has been widely used as a design method to assess and avoid internal condensation in real life engineering tasks. This method is called the ‘Glaser method’ and was originally introduced by H. Glaser in 1950’s for assessment of walls in contact with cold storage rooms.

The Glaser method is described in **EN ISO 13788** and contains these calculation steps:

1. calculate the temperature profile in construction
2. calculate the profile of saturated vapor pressure (based on temperature profile)
3. calculate the profile of actual vapor pressure in construction
4. check whether vapor pressures < saturated vapor pressures
   → YES: no interstitial condensation
   → NO: interstitial condensation will occur
5. insert condensation planes and correct vapor pressure profile
6. calculate condensation flows and/or dimension vapor barriers

The purpose of the method is to find out if and where there exists a condensation risk under typical worst case climatic conditions during winter, and if yes, then also to find out if the construction has a necessary drying potential during summer.

In a design phase, the Glaser method can be used to improve a construction, i.e. to find a solution where no interstitial condensation will occur. Furthermore, the Glaser methods can also be used to assess if there is risk for mold growth somewhere in the construction, i.e. RH > 80% and when temperature > 0º C.

4.4.1 LIMITATIONS OF METHOD

The Glaser method is rather simplified since it is a steady state method. Therefore, when calculating the condensation risk of a construction it is assumed that the construction for "infinite" time has been subjected to the same climatic conditions. The moisture capacity of the building materials is not considered. Also, only vapor diffusion is considered as moisture flow mechanism, and constant values for the material's vapor permeability are assumed.

These issues causes the Glaser method to give a conservative estimate of condensation risk. And therefore more advanced analysis with transient numerical simulation is normally required.

4.4.2 BOUNDARY CONDITIONS

According to the standard **EN ISO 13788** monthly averaged air temperatures and vapor pressures are used as internal and external boundary conditions. Monthly values for normative Danish outdoor and indoor conditions are given in Table 4.3. Indoor conditions are divided in the actual moisture load classes. Other values may be used if the conditions are expected to differ significantly from the given description.

Table 4.3: Monthly values for Danish outdoor and indoor climate. Indoor relative humidity is given as limits between indoor moisture load classes 1-5 (SBI Anvisning 224)

	Outdoor		**Indoor**				
Month	Temperature	Relative humidity	Temperature	Relative humidity			
	[ºC]	[%]	[ºC]	1-2 [%]	2-3 [%]	3-4 [%]	4-5 [%]
January	-0,6	94	20	35	46	58	69
February	-1,1	91	20	35	46	58	69
March	2,6	91	20	39	49	58	69
April	6,6	82	20	45	53	58	69
May	10,6	78	20	50	56	60	69
June	15,7	67	22	55	59	64	69
July	16,4	74	23	59	62	66	69
August	16,7	71	23	61	64	66	69
September	13,7	85	22	58	62	65	69
October	9,2	87	20	51	57	63	69
November	5,0	91	20	45	53	61	69
December	1,6	88	20	38	49	59	69

Moisture load classes are defined according to the use of buildings, with respect to moisture production intensity indoors, see Figure 4.9 for amount of moisture supply to indoor air in g/m^3.

The low classes are the ones with no or very little moisture production compared to air volume of the building and the high classes have e.g. intensive and/or "moisture productive" use. The class descriptions are:

1. Dry warehouses, sports halls without audience, factories without moisture production
2. Dwellings with normal occupant rate, offices, shops
3. Dwellings with unknown occupant rate, sport halls with audience
4. Industrial kitchens, cantinas, bathrooms and dressing rooms
5. Special buildings, e.g. laundries, breweries, indoor swimming pools

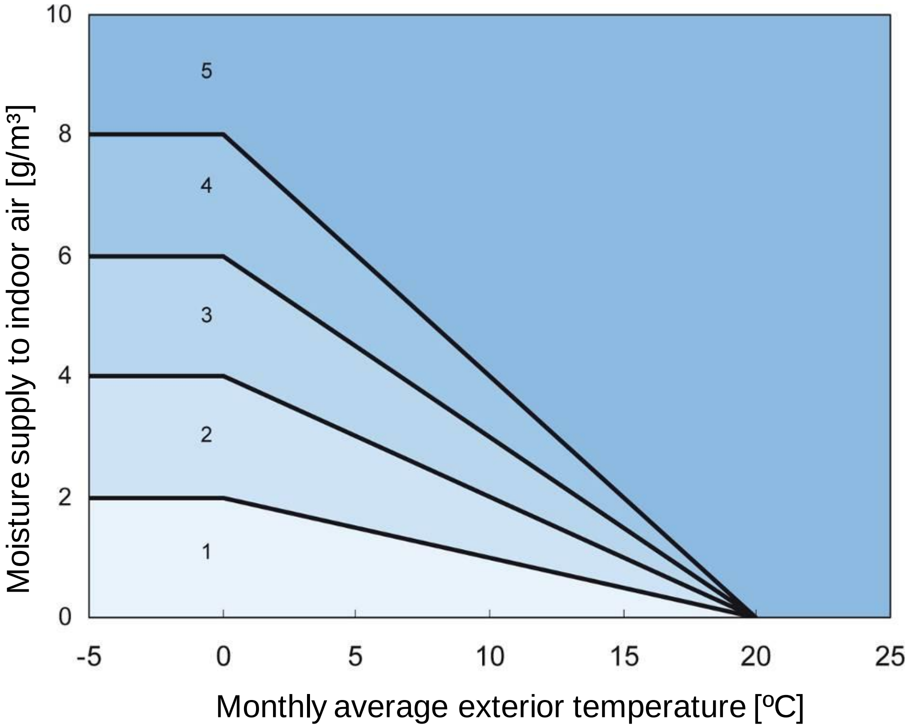

Figure 4.9: Illustration of moisture supply to indoor air as a function of exterior temperature for the different moisture load classes.

5 MOISTURE TRANSFER IN PORES

This lecture note introduces liquid moisture. So far, we have been dealing with heat, air and vapor. As already discussed, the pores size and the pore structure have a great influence on the storage and transport properties of materials. In order to be able to set up models for storage and transport we need to simplify the real materials:

1. First, we are looking at a single pore that is simplified to a capillary tube.
2. Secondly, these single pores are set together to a bundle of capillary tubes.
3. Finally, we are describing the materials on material level.

The focus in this chapter is on liquid moisture storage and liquid moisture transfer on **pore size level**. Both as a single pore and as a bundle-of-tubes.

The phenomena of capillarity and capillary pressure in pores and their effects on moisture transfer and storage in pores are introduced. Next chapter will deal with the liquid moisture storage and transfer on material level.

5.1 Introduction

In many cases, liquid transfer is the dominant mechanism for transport of moisture in materials and in building components. Phenomena like rising damp and driving rain can only be analyzed when involving the theory for liquid moisture. Specially, from the durability and health point of view, liquid moisture has a significant effect on the resulting HAM states in building components. For certain but very common building materials, like brick and wood, the liquid moisture storage and/or transfer can result in very high moisture contents and thus to malfunction of the constructions and buildings. Thus understanding these phenomena is essential.

In chapter 3 we learned about moisture storage in air and materials. These were explained based on vapor content and vapor pressure. Moisture storage in materials was expressed as a sorption isotherm and the moisture mass could be expressed like:

$$m_l = m_{mat} u\left(p_v, T\right) = V_{mat} \rho_{mat} u\left(p_v, T\right) \tag{5.1}$$

M: mass [kg]
V: volume [m³]
p: pressure [Pa]
T: temperature [K] or [ºC]
u: moisture content [kg/kg]
$_{mat}$: for material
$_{v}$: for vapor
$_{\ell}$: for liquid

Sorption isotherm is the description of the moisture storage in the hygroscopic range, typically up to 95% RH. The moisture in material is in both vapor and liquid phase, the vapor phase being nearly negligible. However, the moisture originates from vapor in air, which is the definition of the hygroscopic moisture.

Therefore, for *RH* > 95% and even for lower *RH*, depending on the material pore structure, there is a dominant part of the moisture mass that is stored due to a liquid phenomenon: capillarity. When looking at the full material porosity, the sorption isotherm describes only a limited part of the porosity and needs extension.

5.2 Capillarity and capillary pressure

You can observe capillary rise, when you see water "climbing up" in the drinking glass, water rising up in paper towel and rise of water in capillary tubes (see Figure 5.1).

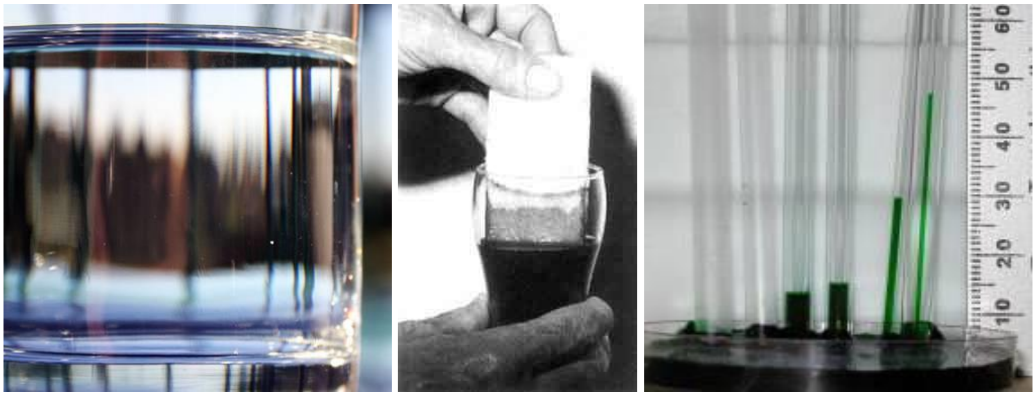

Figure 5.1 examples on capillary rise.

To explain this, we look at the forces between water, air and material surface, see Figure 2. Water molecules are polar molecules. Deep in the water they attract each other – this is internal cohesion – and there is no resultant force. If a water molecule is at the liquid surface to air, the cohesion to water is higher than the attraction to air. To separate a surface water molecule from the liquid work is needed. The water surface behaves as an elastic sheet. This energy difference per surface unit is called surface energy, but it is normally in this context given as surface tension σ [N/m].

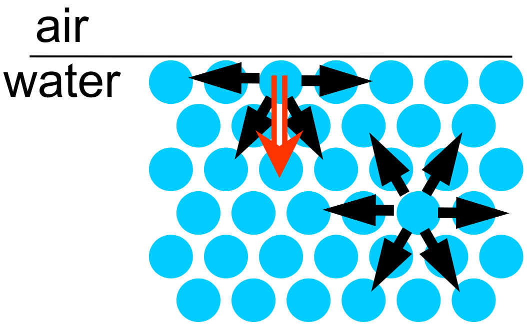

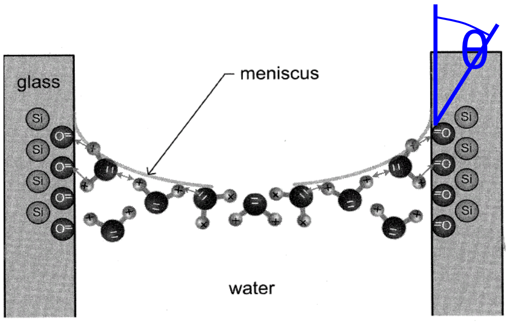

Figure 5.2 left: Cohesion forces near the surface and in the water. - right: Forces around a meniscus in an ideal capillary pore convection over a flat surface, with the velocity and thermal boundary layers.

Surface tension is a function of temperature. For 20°C it has a value $\sigma = 72.5 \cdot 10^{-3}$ N/m.

$$\boxed{\sigma = \left(122.3 - 0.17T\right) \cdot 10^{-3}\ N/m} \tag{5.2}$$

σ: surface tension [N/m]
ϑ: contact angle [-]
T: temperature [K]

When the water in a material pore is in contact with the pore wall, a meniscus is created (See Figure 2 right). If the adhesion to the wall is higher than the attraction to air, the water "creeps" up the wall, creating a meniscus with a contact angle $\vartheta < 90$ ° and a pore wall is called hydrophilic. If the adhesion to the wall is lower than the attraction to air, a contact angle $\vartheta > 90$ ° is created and a pore wall is called hydrophobic.

For open water surface, liquid pressure p_l and gas pressure p_g are equal, see below table, left. For liquid in a capillary pore, the capillary action gives under or over pressure in the liquid, see below table, right. This pressure difference, capillary pressure p_c, is called suction. This capillary pressure increases for decreasing pore radius.

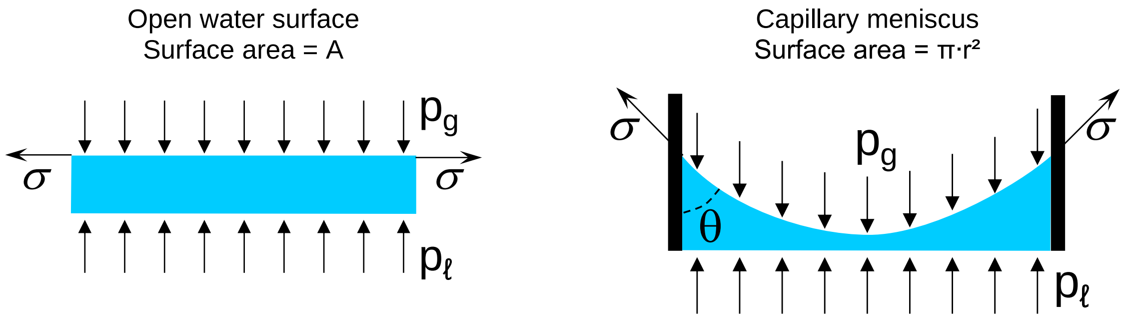

$$Ap_l - Ap_g = 0 \tag{5.3}$$

$$\pi r^2 p_l + 2\pi r \sigma \cos\left(\theta\right) - \pi r^2 p_g = 0 \tag{5.4}$$

$$\boxed{p_l - p_g = 0} \tag{5.5}$$

$$\boxed{p_l - p_g = p_c = \frac{-2\sigma\cos\theta}{r}} \tag{5.6}$$

Figure 5.3 capillary principals described mathematically.

r: pore radius [m]
p_ℓ: liquid pressure [Pa]
p_g: gas pressure [Pa]
p_c: capillary pressure [Pa]

The acting forces for liquid transfer in a capillary are given in Figure 5.4:

- Capillary pressure difference
- Friction to pore wall
- Gravity

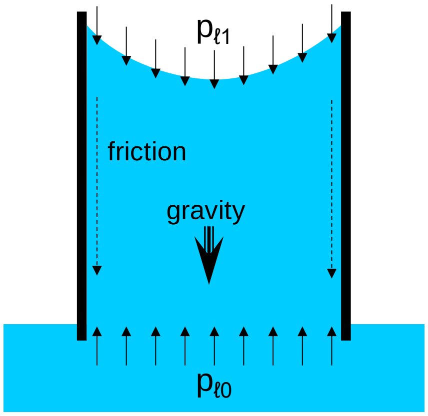

Figure 5.4 forces involved in a water filled capillary.

5.3 Single pore

Analysis of the liquid transfer is started with transfer in a single pore. Two cases are studied: a horizontal pore and a vertical pore. For practical applications, rain absorption by a capillary active exterior finish, like brick wall, is described by transfer in horizontal pore, while rising damp in a foundation is described by a transfer in a vertical pore.

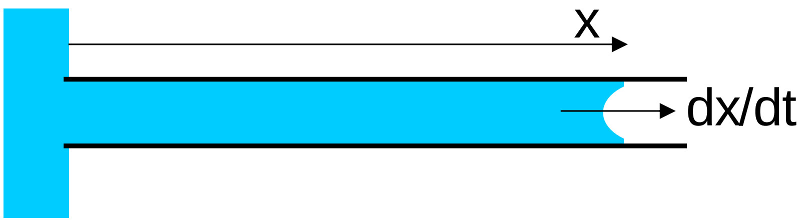

Figure 5.5 transfer in a horizontal pore.

The forces involved in water absorption in a capillary in absence of gravity are capillary pressure and friction. The resulting balance is

$$\boxed{-p_{c1} = \frac{friction}{\pi r^2}} \tag{5.7}$$

To quantify the friction, the Hagen-Poiseuille law is applied for a fully filled pore, see figure and equations below:

$$G_l = \frac{\rho_l \pi r^4}{8\mu_l L}\left(p_{l,y} - p_{l,z}\right) \tag{6.8}$$

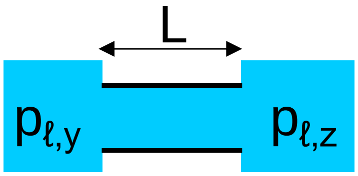

$$friction = \pi r^2\left(p_{l,y} - p_{l,z}\right) = \pi r^2 \frac{G_l 8\mu_l L}{\pi r^4 \rho_l} \tag{6.9}$$

$$friction = 8\pi\mu_l L \frac{G_l}{\pi r^2 \rho_l} = 8\pi\mu_l x\, \partial x/\partial t \tag{5.10}$$

Figure 5.6 the Hagen-Poiseuille law is applied for a fully filled pore to quantify the friction.

Where:

x:	coordinate [m]
t:	time [s]
p_c:	capillary pressure [Pa]
r:	pore radius [m]
p_ℓ:	liquid pressure [Pa]
G_ℓ:	liquid flow [kg/s]
ρ_ℓ:	liquid density [kg/m³]
$\mu_{\ell l}$:	liq. dynamic viscosity [Pa/s]
L:	pore length [m]

By inserting expressions for p_c and friction, we get:

$$\boxed{\frac{2\sigma\cos\theta}{r} = \frac{8\pi\mu_l x\, \partial x/\partial t}{\pi r^2}} \tag{5.11}$$

Resulting equation for the development of the water front dx/dt and solution of it for time t is given below, where B [m/s$^{0.5}$] is the water penetration coefficient.

$$\frac{dx}{dt} = \frac{2r\sigma\cos\theta}{8\mu_l x} \tag{5.12}$$

$$x = \sqrt{\frac{r\sigma\cos\theta}{2\mu_l}}\sqrt{t} = B\sqrt{t} \tag{5.13}$$

B:	water penetration coefficient [m/s$^{0.5}$]

By multiplying both sides of the last equation with the water density, we get the absorbed water m_w [kg/m²]:

$$m_w = \rho_w B\sqrt{t} = A\sqrt{t} \tag{5.14}$$

A:	capillary water absorption coefficient [kg/(m²s$^{0.5}$)]

The horizontal capillary water absorption goes on until the pore ends. In practical applications this means e.g. absorbed rain water on a brick to the inner side of the brick. Once the meniscus reaches the other end of the pore, the meniscus surface straightens outs and suction becomes zero. Capillary absorption is therefore not the reason for water running down in cavity of the cavity wall, but external forces like wind pressure are.

While friction is independent of the pore radius, the pore diameter has an influence on the penetration speed: For increasing r, the driving force grows. Thus the quickest filling takes place for the largest pore.

Transfer in a vertical pore

Capillary transport in a vertical pore is under influence of gravity. There is a maximal height for vertical capillary rise x_{max} [m], given by equations 9.10-11. This height is inversely proportional to the pore radius: Materials with small pores have higher capillary rise than materials with large pores.

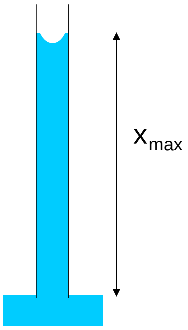

$$-p_{c1} = \frac{2\sigma\cos\theta}{r} = \frac{gravity}{\pi r^2} = \frac{\pi r^2 x_{max} \rho_l g}{\pi r^2} \tag{5.15}$$

$$x_{max} = \frac{2\sigma\cos\theta}{\rho_l \, g \, r} \tag{5.16}$$

$$\boxed{\rightarrow \quad x_{max} \sim \frac{1}{r}} \tag{5.17}$$

Figure 5.7 capillary transport in a vertical pore.

Where:

ρ_ℓ: liquid density [kg/m³]
g: gravity acceleration [m/s²]
x_{max}: height capillary rise in pore [m]

5.4 Bundle of tubes

Porous materials are in this chapter idealised with the bundle-of-tubes representation: We go from single pore representation to bundle-of-tubes. Number of pores with a given radius r_i are proportional to volume of r_i pores in material, see 错误!未找到引用源。. Length of the pores is dx and pores are assumed to be fully filled with air or water.

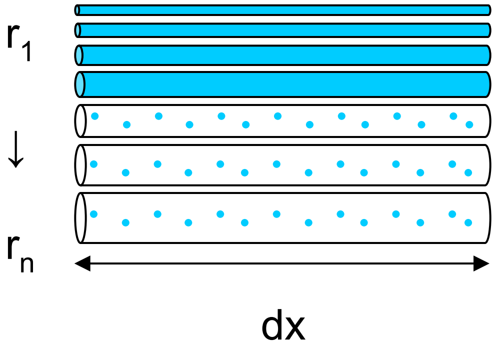

Figure 5.8 bundle-of-tubes representation of a porous material with pores with radius r_i – r_n.

An example of representation of a “porous material” as bundle-of-tubes is given below. Only 2 different pore radii are used to describe 3 different materials with all 20 % porosity. These “materials” are used later in this chapter to illustrate liquid moisture in pores.

Table 5.1 representation of different "porous material".

A		Mortar	20 % porosity with r = 10^{-8} m
B		Brick	20 % porosity with r = 10^{-6} m
C		“Mortar & brick”	10 % porosity with r = 10^{-8} m 10 % porosity with r = 10^{-6} m

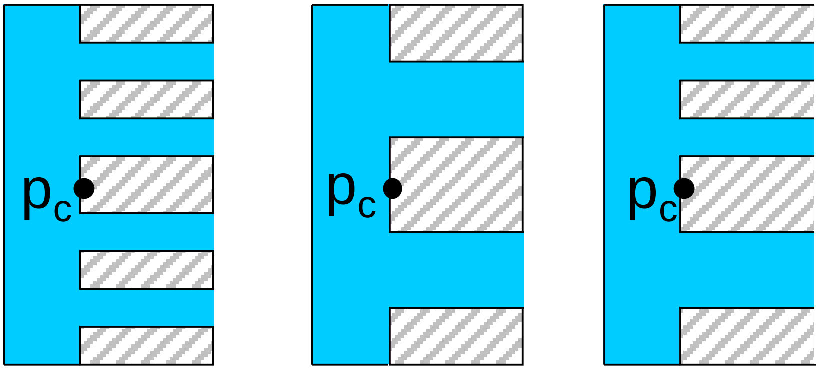

Figure 5.9 3 different “materials”: A is fine porous, B has coarse pores and C has a mix.

Pore filling

Pores can be filled by contact with liquid water (= Direct pore filling, as described earlier in this chapter) or/and by contact with humid air (= Indirect pore filling, which is the topic in this subsection). The air in pores is in equilibrium with the liquid water and the resulting vapor pressure in pore air is determined by temperature and pore radius. While the vapor pressure above a regular water surface is equal or lower than the saturation vapor pressure (see Chapter 3), the vapor pressure above a meniscus is always saturated. However, the relative humidity of the pore air is reduced and given by equation 6.20, which is also known as Kelvin equation.

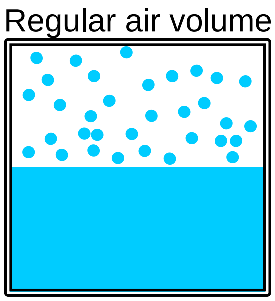

Figure 5.10 Vapor pressure determined by 'escape rate' that is function of temperature only. Vapor pressure is usually below saturation

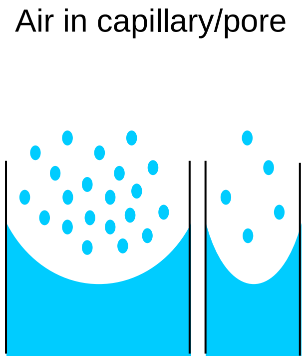

Figure 5.11 Vapor pressure determined by 'escape rate' that is reduced for smaller pore radius. Vapor pressure assumed always saturated

$$\boxed{p_v = \phi p_{v,sat} \le p_{v,sat}} \tag{5.18}$$

$$p_v^* = p_{vsat}^* = p_{vsat}(T)\exp\left(\frac{-2\sigma\cos\theta}{r\,\rho_l R_v T}\right) \tag{5.19}$$

$$\boxed{\phi^* = p_{vsat}^* / p_{vsat} = \exp\left(p_c / \rho_l R_v T\right)} \tag{5.20}$$

Where:

p_v: vapor pressure [Pa]

Φ: relative humidity [-]

$p_{v,sat}$: satur. vapor pressure [Pa]

T: temperature [K]

σ: surface tension [N/m]

ϑ: contact angle [-]

r: pore radius [m]

ρ_ℓ: liquid density [kg/m³]

R_v: gas constant vapor [J/(kg·K)]

*: for one pore

Pore filling due to saturated air above a water meniscus is called capillary condensation. 错误!未找到引用源。 Pores with relative humidities equal to capillary pressure pc below "critical" capillary pressure for a given pore radius (see equation 5.15) build up mono- and multilayer adsorption of water molecules. First after $\Phi > \Phi * p_c(r)$ capillary condensation onto meniscus starts. p_c is given in equation 5.15.

$$\boxed{p_l - p_g = p_c = \frac{-2\sigma\cos\theta}{r}} \tag{5.21}$$

Table 5.2 pore filling with capillary condensation. An example with different size pores.

φ	10.0 %	34.3 %	89.8 %	99.9 %
p_c	$-3.12\cdot10^{8}$	$-1.45\cdot10^{8}$	$-1.45\cdot10^{7}$	$-1.45\cdot10^{5}$
$r_{meniscus}$	$4.7\cdot10^{-10}$	$1.0\cdot10^{-9}$	$1.0\cdot10^{-8}$	$1.0\cdot10^{-6}$
$r = 10^{-9}$ m $p_{c,pore}$ $= -1.45\ 10^{8}$ Pa	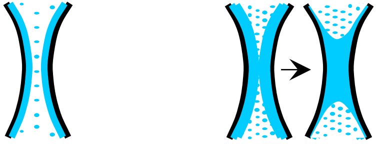			
$r = 10^{-8}$ m $p_{c,pore}$ $= -1.45\ 10^{7}$ Pa	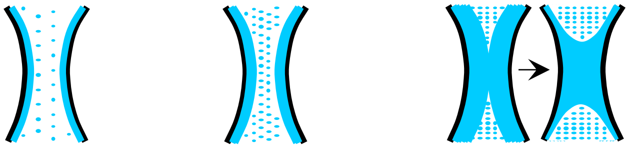			
$r = 10^{-6}$ m $p_{c,pore}$ $= -1.45\ 10^{5}$ Pa	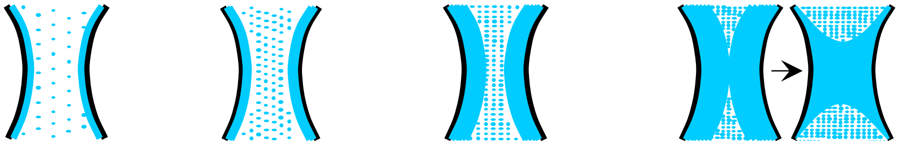			

Pore transfer

In the following, we are looking at moisture transfer in pores as transfer of liquid water and as transfer of vapor.

Liquid transfer G_l [kg/s] is given with Hagen-Poisseuille law for a fully filled pore. Liquid transfer is driven by the capillary pressure difference (equation6.22). A liquid transfer coefficient is derived (equation 5.24) and called liquid permeability k^*_l [kg/(m·s·Pa)].

Finite length pore

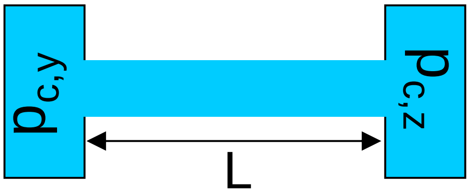

Infinitesimal length:

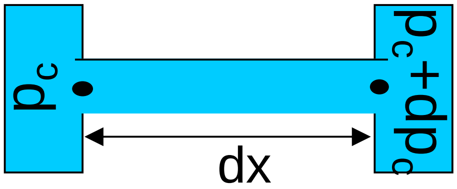

$$G_l^* = \frac{\rho_l \pi r^4}{8\mu_l L}\left(p_{c,y} - p_{c,z}\right) \tag{5.22}$$

$$\begin{aligned} G_l^* &= \frac{\rho_l \pi r^4}{8\mu_l}\frac{\partial p_c}{\partial x} \\ &= \pi r^2 \frac{\rho_l r^2}{8\mu_l}\frac{\partial p_c}{\partial x} \\ &= A^* k_l^* \frac{\partial p_c}{\partial x} \end{aligned} \tag{5.23}$$

$$\boxed{k_l^* = \frac{\rho_l r^2}{8\mu_l}} \tag{5.24}$$

Where:

G_ℓ: liquid flow [kg/s]
ρ_ℓ: liquid density [kg/m³]
r: pore radius [m]
μ_ℓ: liq. dynamic viscosity [Pa/s]
L: pore length [m]
p_c: capillary pressure [Pa]
x: coordinate [m]
A^*: pore flow area [m²]
k_ℓ: liquid permeability [kg/(m·s·Pa)]

Vapor transfer takes place in air filled parts of pores and is illustrated. Vapor is assumed to be transferred with vapor diffusion. Vapor is assumed to be transferred with vapor diffusion.

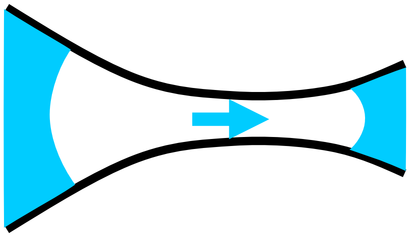

Figure 5.11 illustration of vapor transfer in pore air between 2 different menisci with liquid water.

According to Fick's law, vapor transfer goes from higher vapor pressure to lower vapor pressure. In a pore, the vapor pressure is affected by the pore size and the resulting capillary pressure. As a consequence, the vapor transfer takes place from high to low capillary pressure and larger radius to smaller radius.

Vapor transfer in a pore G_v [kg/s] can be determined from the "normal" Fick's law to be driven by the capillary pressure difference as in equation -6.25. Vapor permeability of empty (= air filled) pores k_v* is determined in equation -6.26.

$$G_v^* = -A^* \delta_a \frac{\partial p_v}{\partial x} = -A^* \delta_a \frac{\partial p_v}{\partial p_c} \frac{\partial p_c}{\partial x} = -A^* k_v^* \frac{\partial p_c}{\partial x} \tag{5.25}$$

$$k_v^* = \delta_a \frac{\partial p_v}{\partial p_c} = \delta_a \frac{p_v{}^*}{\rho_l R_v T} \tag{5.26}$$

r: pore radius [m]
p_v: vapor pressure [Pa]

p_c: capillary pressure [Pa]
G_v: vapor flow [kg/s]
A^*: pore flow area [m²]
δ_a: vapor permeability in air [kg/(m·s·Pa)]
k_v: vapor permeability [kg/(m·s·Pa)]
R_v: gas constant vapor [J/(kg·K)]
ρ_ℓ: liquid density [kg/m³]
T: temperature [K]

Liquid moisture content

Moisture storage in pores is equal to the liquid water content in pores and is a function of the capillary pressure (equation 9.20). Moisture storage in vapor phase is negligible.

$$m_{m,stored} = m_{mat} u(p_c) = V_{mat} \rho_{mat} u(p_c) \tag{5.27}$$

$$\frac{\partial m_{m,stored}}{\partial t} = m_{mat} \frac{\partial u(p_c)}{\partial t} = m_{mat} \frac{\partial u}{\partial p_c}(p_c) \frac{\partial p_c}{\partial t} \tag{5.28}$$

M_m: moisture mass [kg]
V_{mat}: material volume [m³]
u: moisture content [kg/kg]

Above equations illustrate the relation of liquid moisture content, pore radius and capillary pressure and relative humidity for the exemplary "materials" idealized as bundles-of-tubes.

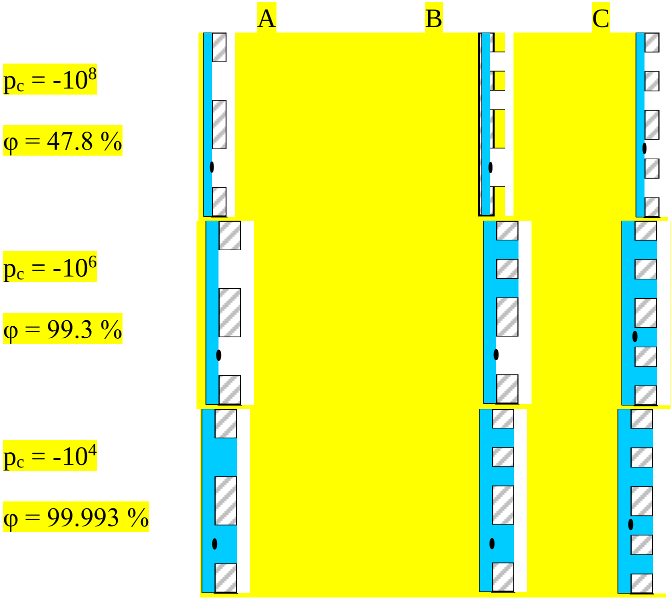

Figure 5.12 illustration of liquid moisture content by pore filling of the 3 exemplary "materials".

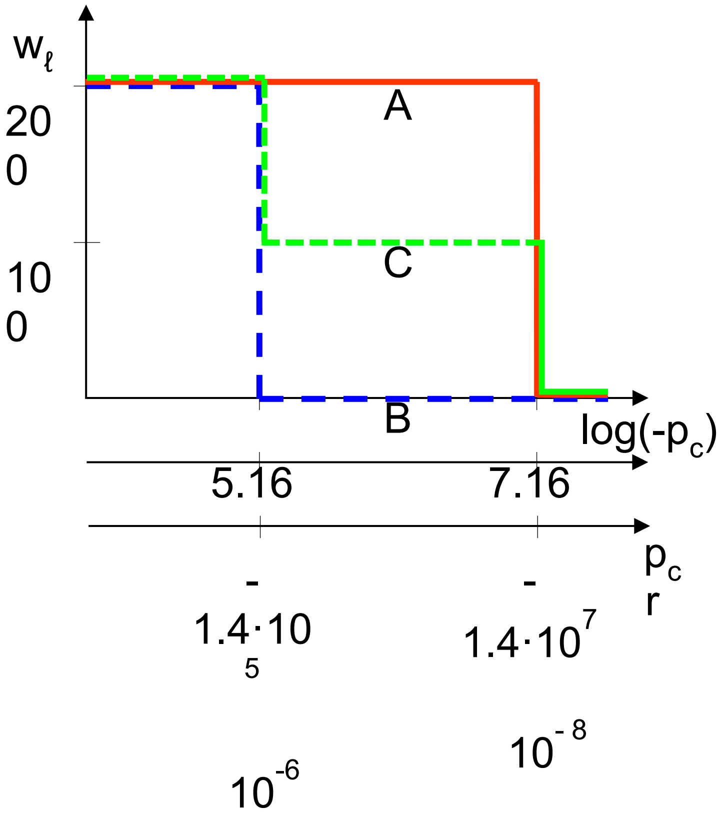

Figure 5.13 liquid moisture permeability as a function of capillary pressure for the 3 exemplary “materials”.

6 MOISTURE TRANSFER IN MATERIALS

Liquid moisture storage and transfer in porous materials were introduced in Chapter 9 in a very idealized form at a pore size level. In this chapter, the description of liquid moisture storage and transfer is extended to material level.

6.1 Relating porosity of materials to their moisture properties

Porous materials were idealized as bundles-of-tubes in the previous chapter. In real materials, there is a wide and continuous range of pore sizes, see for example pore size distribution for aerated concrete in Figure 8.1. There are mostly large pores ($r = 10^{-3}$ m), but also some small pores ($r = 10^{-7}$ m) and pores of size in between.

Different materials can have quite different pore size distributions and consequently, they may have rather different properties for moisture storage and transport. The pore size distribution has a direct influence on where and how moisture is stored and which conduits are available for transporting the moisture, and thus the moisture properties of materials.

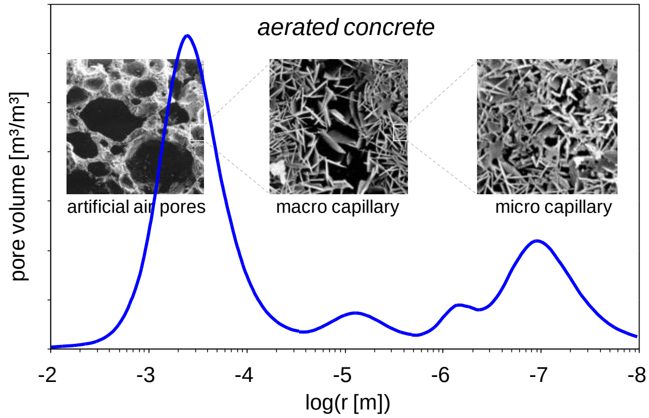

Figure 6.1 distribution of pore volume over different pore size ranges. Aerated concrete as an example.

The link between pore size distribution and material properties is given by the capillary pressure p_c (equation 8.1)

$$\boxed{p_l - p_g = p_c = \frac{-2\sigma\cos\theta}{r}} \tag{6.1}$$

p_ℓ: liquid pressure [Pa]
p_g: gas pressure [Pa]
p_c: capillary pressure [Pa]
σ: surface tension [N/m]
ϑ: contact angle [-]

r: pore radius [m]

The above equation illustrates volumetric moisture content *w* [kg/m³](or u (kg/kg)) of our example material as a function of capillary pressure – and as a function of pore size *r* [m]. For small pore radii, the negative capillary pressure is high and the moisture content low. For increasing pore radii, and decreasing negative capillary pressure, the moisture content increases as well, and the increase for larger pores is high.

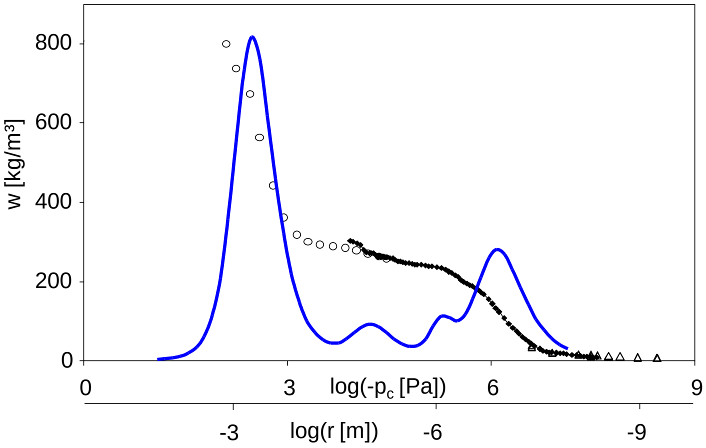

Figure 6.2 equilibrium between capillary pressure and moisture content.

When relating the porosity of a material to its moisture storage capacity, some characteristic values are important to note. These are illustrated in Figure 6.3, where also the “dry” and “wet” material regimes are given.

- $p_{c,critical}$ is the capillary pressure where there exists a continuous liquid phase in the pores of the material. $w_{critical}$ (or $u_{critical}$)is the corresponding moisture content at that point. For lower moisture contents, the liquid water exists as single molecular layers and liquid islands.
- For decreasing negative capillary pressure, larger and larger pores get filled with liquid until the free water uptake stops. This point is given as capillary moisture content $w_{capillary}$(or $u_{cappilary}$). At this moisture content, not all the pores of the material are filled with water.
- To fill all the open pores of the material, normally external work – pressure - is needed. This moisture content is saturated moisture content $w_{saturated}$(or $u_{satuated}$).

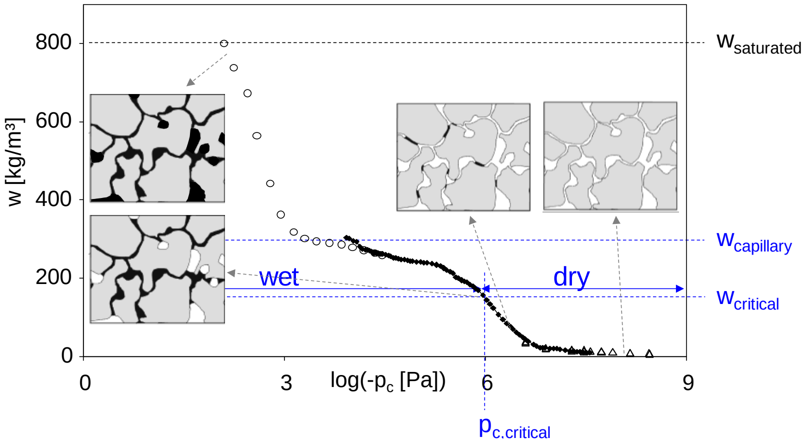

Figure 6.3 definition of saturated, capillary and critical moisture content.

Also the moisture transfer property, moisture permeability k_m, has a relation with capillary pressure, moisture content and permeability, such as illustrated in Figure 6.4. For low moisture contents, when there is no continuous liquid phase, the vapor diffusion is the dominating moisture transfer form. It increases for increasing pore radius, but not only due to higher vapor diffusion area but also due to increasing liquid transport in filled smallest pores and in liquid islands. Once the liquid phase is continuous, at $p_{c,critical}$, the permeability increases until all pores are filled with liquid water. For increasing pore radius, the moisture permeability is assumed the same, as increasing the moisture content above $w_{capillary}$(or $u_{cappilary}$) would involve external work (see $w_{saturated}$(or $u_{satuated}$) above).

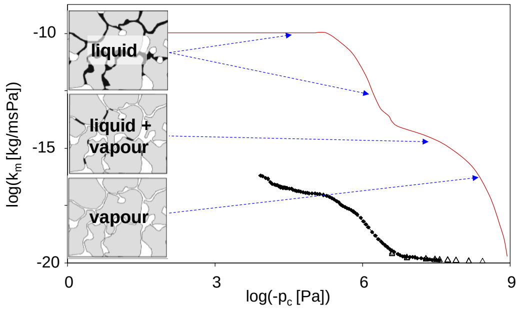

Figure 6.4 moisture permeability depends on moisture content of material.

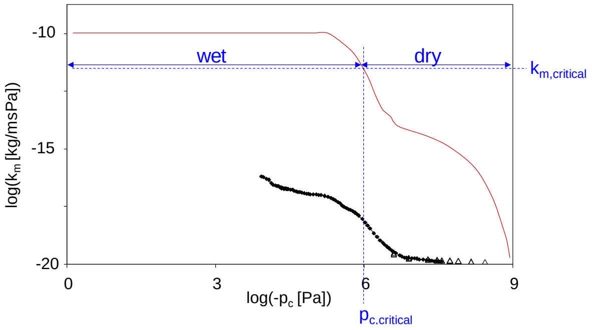

Figure 6.5 definition of critical capillary pressure and moisture permeability.

As a result of the link between porosity and moisture properties, moisture storage and moisture transfer in materials can be expressed as a function of capillary pressure p_c

$$\boxed{\frac{\partial m_{m,stored}}{\partial t} = V_{mat}\rho_{mat}\frac{\partial u}{\partial p_c}(p_c)\frac{\partial p_c}{\partial t}} \tag{6.2}$$

$$G_m = -k_m(p_c)\frac{\partial p_c}{\partial x}A \tag{6.3}$$

M_m: moisture mass [kg]

V_{mat}: material volume [m³]

u: moisture content [kg/kg]

G_m: moisture flow [kg/s]

k_m: moisture permeability [kg/(m·s·Pa)]

A: surface area [m²]

6.2 Simplified moisture transfer models

Moisture transfer and storage, especially in liquid phase and the combination of vapor and liquid transfer, is a complex problem and usually also involves combined heat and air transfer. Solutions are therefore found only by using numerical tools such as Delphin. Simplified analytical solutions can be found, however, for some simple cases. In the following, some simplified models for capillary absorption and isothermal drying are shown. Also, a model with transport equations applicable for both cases is set-up.

For calculation of isothermal drying – which is an important parameter in e.g. material production industry – there exits also some more advanced chart methods for solution of drying for different basic geometries. One of them is presented in the Appendix.

Capillary absorption

Capillary absorption is illustrated with a classical water uptake experiment. A dry sample is placed in contact with water. The capillary rise starts. The moisture mass increase as a function of time is registered by repeated weighing.

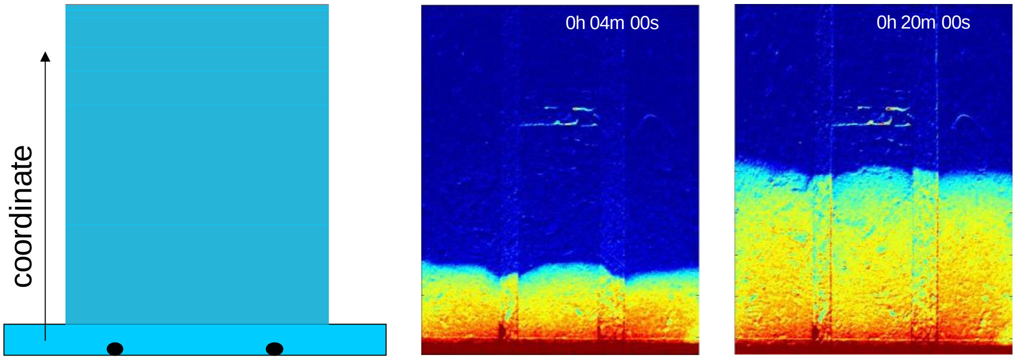

Figure 6.6 the capillary absorption experiment. Set-up (left) and measured moisture content after 4 minutes (middle) and after 20 mins (right).

To be able to set-up the model for moisture transfer, it is important to know the progression of the wet front in the material. The moisture content profiles are as a function of time and location.

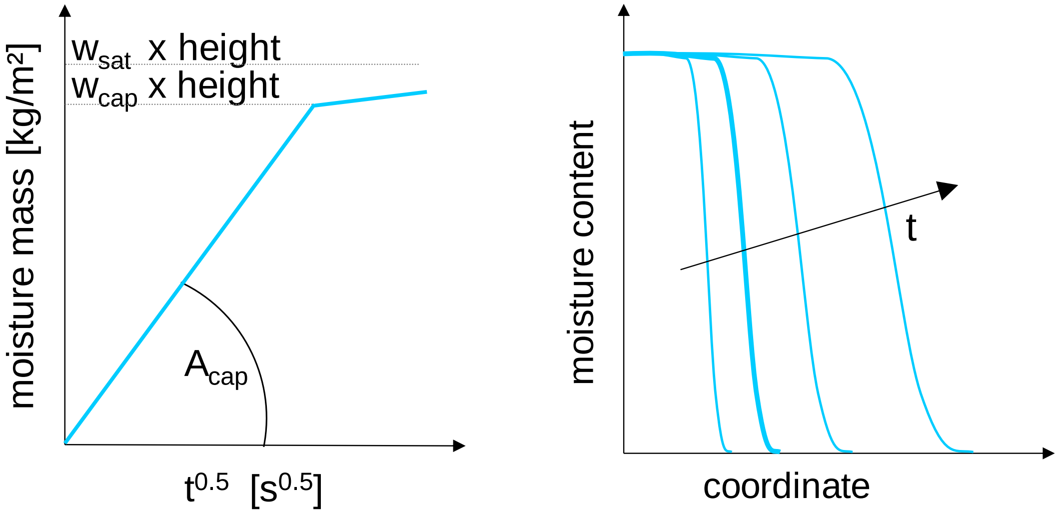

Figure 6.7 typical behavior for capillary absorption. Capillary water uptake (left) and moisture content profiles (right).

A simplified calculation of the progression of the water front *dx*/*dt* and the absorbed water *m*(*t*) is shown below. It also illustrates the square root of time behavior of capillary absorption. Figure 6.8 shows the moisture content profile in material, originally in equilibrium with *RH* = 50%, $w_{50\%}$. The moisture content at the water front is assumed equal to $p_{c,\ critical}$ and the moisture content above the water front (in illustration to the right) is $w_{50\%}$. At the surface from which water absorption takes place, the moisture content is equal to the capillary saturation moisture content $w_{capillary}$(or $u_{cappilary}$).

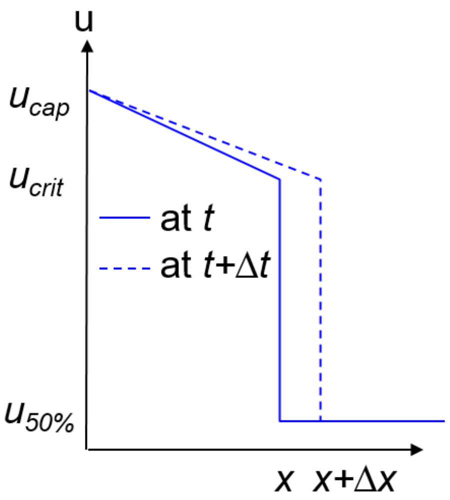

Figure 6.8 capillary absorption. Penetration of moisture front into material.

The equation for capillary moisture uptake into the material can be written as equation 6.4, with a liquid and a vapor transfer part.

$$\frac{\partial m}{\partial t} = \Delta w \frac{dx}{dt} = \rho_{mat} \Delta u \frac{dx}{dt} = k_{m,crit} \frac{p_{c,0} - p_{c,crit}}{x} - \delta \frac{p_{v,crit} - p_{v,RH=50\%}}{L - x} \tag{6.4}$$

x: coordinate [m]
t: time [t]
p_c: capillary pressure [Pa]
k_m: moisture permeability [kg/(m·s·Pa)]
w: moisture content [kg/ m^3]
u: moisture content [kg/kg]
ρ_{mat}: density of dry material [kg/ m^3]
m: moisture mass density [kg/m^2]
δ: vapor permeability [kg/(m·s·Pa)]
L: material total thickness [m]
$_{crit}$: critical
$_v$: vapor

Neglecting vapor transfer and assuming $p_{c,0} = 0$ Pa (at the water reservoir), we get the resulting equation for penetration of moisture front into material:

$$\frac{\partial x}{\partial t} = \frac{-k_{m,crit}\, p_{c,crit}}{x\, \rho_{mat} \Delta u}$$

$$\Delta u = \frac{\left(u_{cap} + u_{crit}\right)}{2} - u_{50\%} \tag{6.5}$$

The simplified "wet" moisture content is the average value of $u_{capillary}$ and $u_{critical}$. Solutions for wet front *x(t)* and absorbed moisture *m(t)* is given with equation 6.6.

$$x(t) = \sqrt{\frac{-2k_{m,crit}\, p_{c,crit}}{\rho_{mat} \Delta u}}\sqrt{t} = B\sqrt{t} \tag{6.6}$$

$$m(t) = \sqrt{-2k_{m,crit}\, p_{c,crit}\, \rho_{mat} \Delta u}\,\sqrt{t} = A\sqrt{t} \tag{6.7}$$

$$A: absorption\ coefficient\ \left[kg/(m^2 \cdot s^{0.5})\right]$$

$$B: water\ penetration\ coefficient\ [m/s^{0.5}]$$

Isothermal drying

In an isothermal drying experiment, a wet sample ($u > u_{critical}$) is exposed to air with a given RH_e. The sample is sealed on all surfaces but one. The moisture content decreases as a function of time. Everything is at the same temperature, and we are neglecting the heat of evaporation.

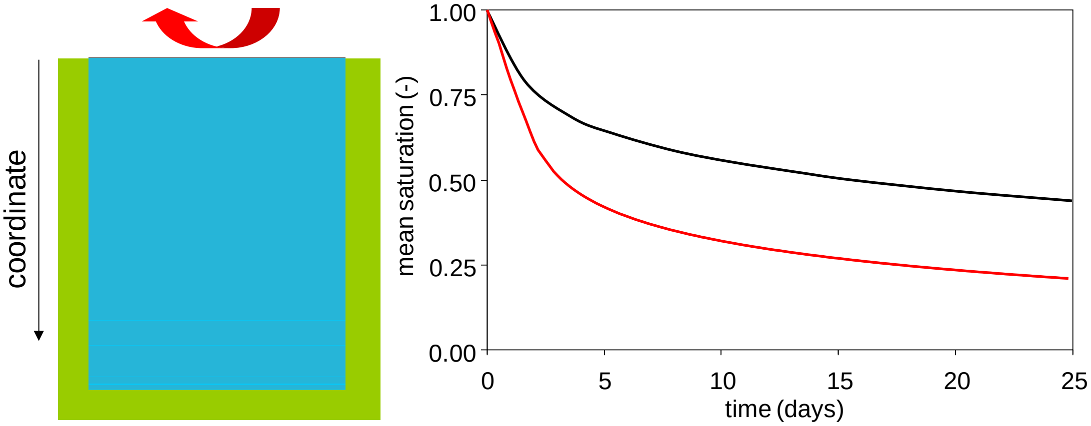

Figure 6.9 isothermal drying. Left: The set-up. Right: Drying of moisture mass as a function of time for 2 different materials: Ceramic brick (red) and calcium silicate (black).

The isothermal drying is characterized with a 3 stage process.

During the first drying period, the drying rate is rapid and constant. The drying is determined by the rate of evaporation from the surface (see Equation 6.7). The material surface is assumed saturated ($p_v = p_{v,sat}$) and the moisture content gradient inside the materiel is negligible. Furthermore, it is assumed that all moisture transfer inside the material is in liquid form. The first drying phase ends when the moisture content at the surface comes below $w < w_{critical.}$(or $u < u_{critical.}$)

$$\frac{\partial m}{\partial t} = \beta(p_{v,sat} - p_{v,RHe}) \tag{6.8}$$

β: surface vapor transfer coefficient [kg/(m²·s·Pa)]

The second drying period starts when the moisture content on and near the surface comes below $w_{critical.}$(or $u_{critical.}$). A “dry” zone develops near the surface, and the wet front moves into the material. Moisture transfer in the form of vapor diffusion in the dry zone is now determining the drying rate. The relative humidity at the surface comes below 100 % and will at some stage reach RH_e. The drying rate is therefore declining, and is no longer kept constant such as in Phase 1. Equation 6.8 gives the drying rate at the end of Phase 2. The moisture content profile in the wet zone is still practically constant. The second drying phase ends when the moisture content of the whole sample has come below $w_{critical.}$(or $u_{critical.}$).

$$\frac{\partial m}{\partial t} = -\delta \frac{p_{v,sat} - p_{v,RHe}}{x} \tag{6.9}$$

$p_{v,sat}$: saturation vapor pressure [Pa]

During the third and last drying phase, the moisture content everywhere in the material is below $w_{critical.}$(or $u_{critical.}$) and approaching the equilibrium with RH_e. This stage can take a long time, sometimes years. The moisture transfer is dominated by vapor diffusion.

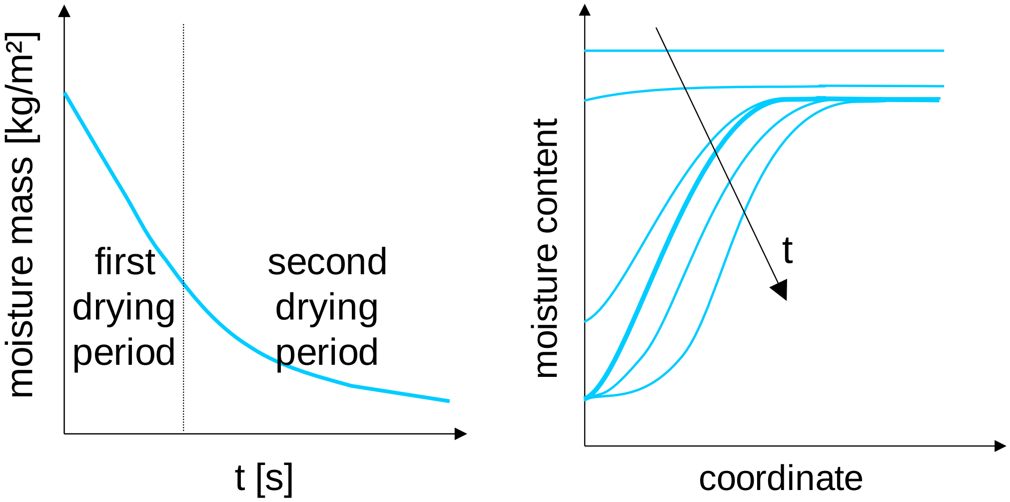

Figure 6.10 typical behaviour for isothermal drying. First and second phases of drying (left) and moisture content profiles (right).

Simplified model for capillary absorption and isothermal drying

Both these examples were characterised by sharp moisture fronts. In our simplified model, the front is absolutely sharp: the material is either wet or dry, see the illustration in Figure 6.11 错误!未找到引用源。. In real life, the front is not so sharp. However, the assumption of the sharp front is not bad as an approximation. The reason why the front is sharp is that the dry zone has only little capability for moisture transfer due to low moisture content and low permeability, while the wet zone has high moisture transfer capability due to the high moisture content and high permeability.

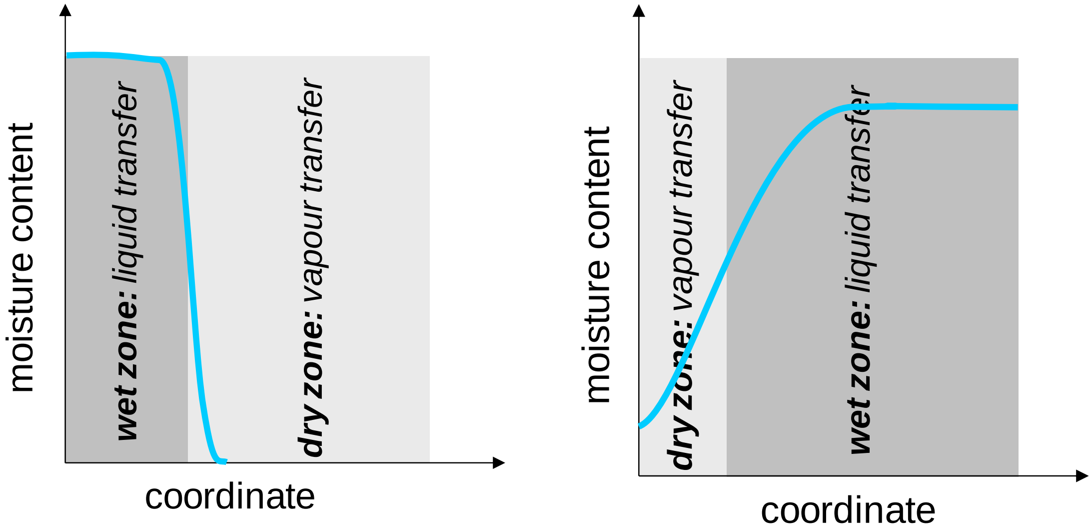

Figure 6.11 distinct separation between wet zone for liquid transfer (dark grey) and dry zone for vapor transfer (light grey).

Transfer mechanisms in the wet zone (liquid) and the dry zone (vapor) can be summarised as below. $P_{c,0}$ means that capillary pressure is zero (= the capillaries are in contact with free water). It is important to note that the coupling between the wet and dry zones is described by $p_{c,critical}$ and $w_{critical}$.(or $u_{critical}$).

$$p_c = p_{c\_0} \quad \text{and} \quad u = u(p_{c\_0}) \quad \text{and} \quad w = w(p_{c\_0}) \tag{6.10}$$

Wet zone:
Liquid
transfer

$$G = G_l = -k_{m,crit}\frac{\partial p_c}{\partial x}A = \frac{k_{m,crit}}{d_{wet}(p_{c0} - p_{c,crit})}A$$

$$G = G_l = -k_{m,crit}\frac{\partial p_c}{\partial x}A = \frac{k_{m,crit}(p_{c0} - p_{c,crit})}{d_{wet}}A \tag{6.11}$$

$$p_c = p_{c,crit} \quad \text{and} \quad u = u_{crit} \quad \text{and} \quad w = w_{crit} \quad \text{and} \quad p_v = p_v(p_{c,crit})$$

Dry zone:
Vapor
transfer

$$G = G_v = -\delta_v\frac{\partial p_v}{\partial x}A = \frac{\delta_v}{d_{dry}(p_{v,crit} - p_{v1})}A$$

$$G = G_v = -\delta_v\frac{\partial p_v}{\partial x}A = \frac{\delta_v(p_{v,crit} - p_{v1})}{d_{dry}}A \tag{6.12}$$

$$p_v = p_{v1} \quad and \quad u = u(p_{v1}) \quad and \quad w = w(p_{v1})$$

G: mass flux [kg/s]
p: pressure [Pa]
x: coordinate [m]
k_m: moisture permeability [kg/(m·s·Pa)]
w: vol. moisture content [kg/m^3]
u: moisture content [kg/kg]
δ: vapor permeability [kg/(m·s·Pa)]
$_{crit}$: critical
$_v$: vapor
$_c$: capillary
d: thickness [m]
$_{wet}$: wet section
$_{dry}$: dry section

6.3 Hydrophobation

An example of application of the moisture transfer theory is hydrophobation: By application of water-repellent polymers as a “nano”-layer on the material surface, it is possible to change the capillary activity of the material. The idea is to avoid water penetration for instance in a brick wall and thereby also avoiding moisture damage.

At first, the treated material will reject water droplets that impinge on its surface, which can be seen on the droplets’ contact angle with the surface. The contact angle is larger than 90°, meaning that the droplets tend to roll over the surface. After a while, the droplets smear out, the contact angel become less than 90°, and the surface is generally wetted.

If the water-repellent is of a “penetrating” nature (as opposed to “film forming” repellents which only work by coating the surface), the polymers are deposited on surfaces inside the porous material. Examples of film forming repellents are acrylics, mineral gum waxes and urethanes, and they typically can last a few yerars. Examples of penetrating repellents are siloxanes and silanes, which can last for more than 10 years (Brick industry Foundation, 2008).

The depth of entry into the material of a penetrating repellent can be expected to be some 4-9 mm (Carmeliet, 2001, and Brick industry Foundation, 2008). As illustrated in Figure 6.12 (right), the large pores are partly filled with the polymer, and the polymer partly or fully clogs the entry into the smallest capillaries of the material.

Several types of penetrating polymers can be used, for example polysiloxanes, which have a chain length of 10^{-8} to 10^{-7} m (Carmeliet, 2001).

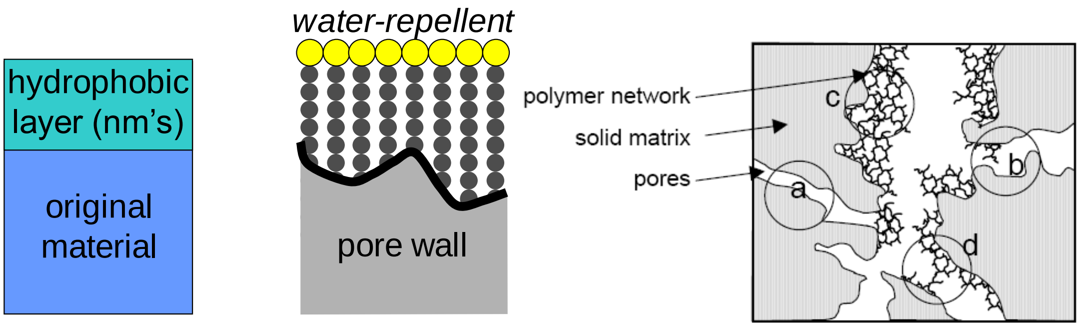

Figure 6.12 the idea of hydrophobation (illustration to the right from Carmeliet, 2001).

The effect of hydrophobation is to block pores with certain pore radius for capillary transport, such that the small pores (a), which normally have the strongest liquid tension for capillary suction, become largely passivated. Furthermore, the polymer reduces the open space of the large pores (c), as well as the connectivity between them (b & d), and since these pores normally are the ones that contribute most to the liquid permeability of the material, the water transporting capability is significantly reduced. The effect of hydrophobation on liquid moisture permeability is illustrated in the following figure.

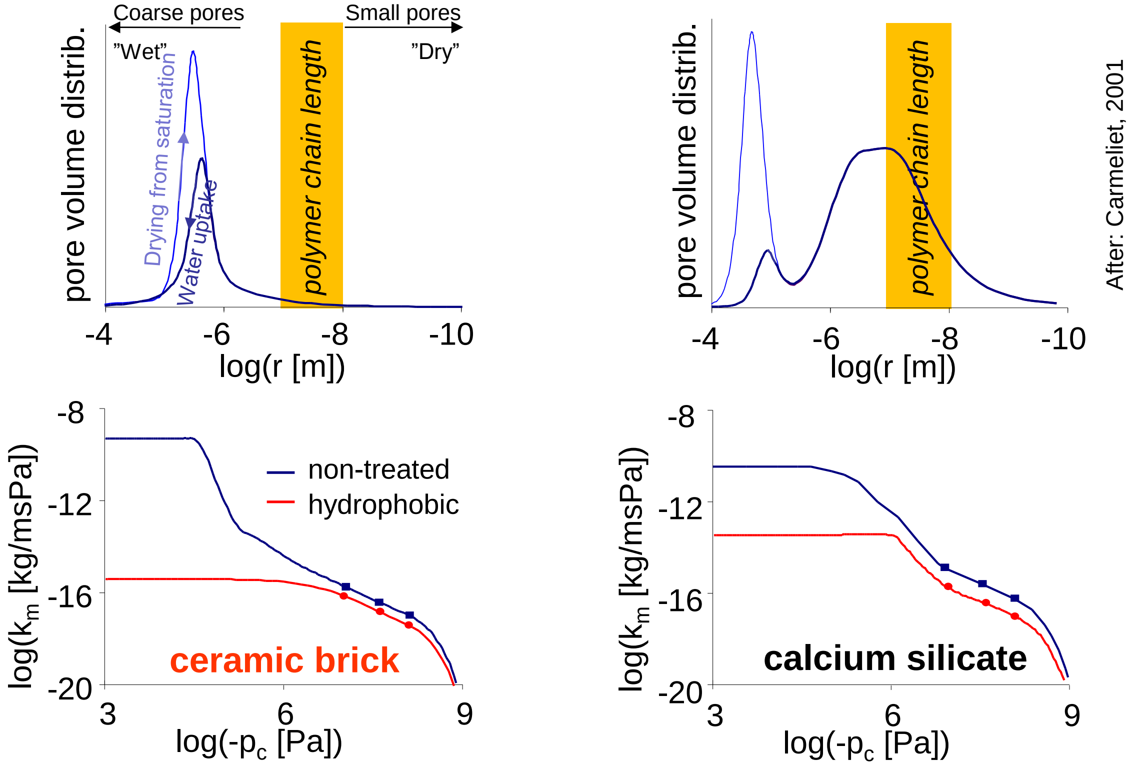

Figure 6.13 illustration of the polymer size of a penetrating water repellent in comparison with the pore sizes of brick and calcium silicate (top graphs), and the effect of hydrophobation on liquid moisture permeablity (below).

The effect of hydrophobation on capillary absorption is shown in the above figures. As desired, hydrophobation reduces the capillary absorption significantly as seen by the below numbers for the absorption coefficient *A*.

Table 6.1 properties of two different building materials non-treated and treated.

Absorption coefficient	Ceramic brick	Calcium silicate
$A_{\text{non-treated}}$	0.18 kg/ $(\text{m}^2 \cdot \text{s}^{0.5})$	0.048 kg/ $(\text{m}^2 \cdot \text{s}^{0.5})$
$A_{\text{hydrophobic}}$	0.0006 kg/ $(\text{m}^2 \cdot \text{s}^{0.5})$	0.0012 kg/ $(\text{m}^2 \cdot \text{s}^{0.5})$

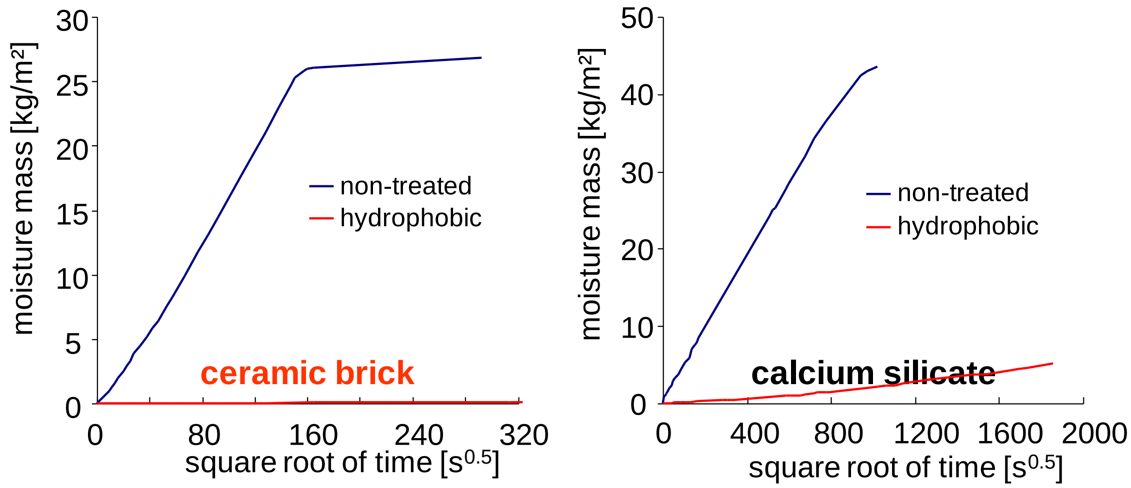

Figure 6.14 effect of hydrophobation on capillary absorption.

Hydrophobation also influences vapor transfer to some degree. The film forming water repellents, which coat the surface, are generally made of products with larger molecular sizes than the penetrating repellents. Thus, they can act as vapor retarders on the surface and hinder the evaporation of moisture that may come from inside the material, and this may for instance lead to freeze-thaw damage during winter.

The penetrating water repellents will reduce the vapor permeability between a factor 2 (for brick) and 6 (for calcium silicate). However, since also the capillary transport capability is reduced by the presence of the polymer in the pores, hydrophobation has a significant effect on possible drying time.

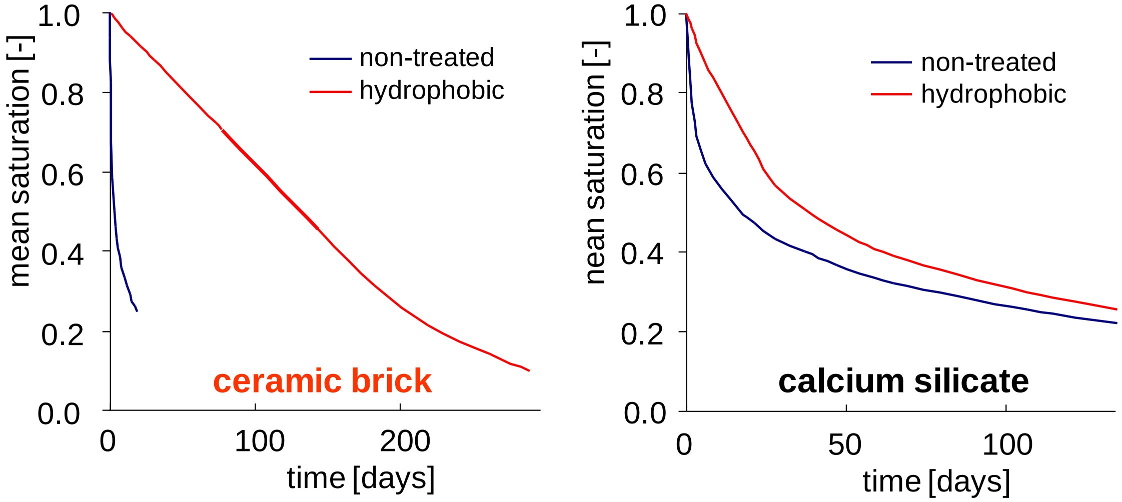

Figure 6.15 effect of hydrophobation on isothermal drying.

6.4 Literature

The Brick Industry Association. 2008. Colorless Coatings for Brick Masonry, TECHNICAL NOTES on Brick Construction, 6A. www.gobrick.com

Carmeliet, J. 2001. Water Transport—Liquid and Vapor—in Porous Materials: Understanding Physical Mechanisms and Effects from Hydrophobic Treatments. Hydrophobe III - 3rd International Conference on Surface Technology with Water Repellent Agents, Aedificatio Publishers, 171–178 (2001)

6.5 Appendix: Chart method for isothermal drying

The following method is Pihlajavaara's method for drying, and is applied here from the lecture note "Moisture II" by Anker F Nielsen.

For more accurate determination of the drying rate, the transient moisture transport equation can be used, where moisture content *w* [kg/m³] is the driving force. Moisture content is not continuous over material boundaries, so this method is valid for objects made of one material only with a given geometry.

$$\frac{\partial w}{\partial t} = D_w \cdot \frac{\partial^2 w}{\partial x^2}, \quad \text{or} \quad \frac{\partial u}{\partial t} = D_w \cdot \frac{\partial^2 u}{\partial x^2} \tag{6.13}$$

Where:

D_w moisture diffusivity [m^2/s]

A solution to this equation can be found for different geometric shapes of bodies with the initial condition being the same moisture content everywhere in the body, followed by a sudden change, so the surface moisture content immediately shifts to the equilibrium value.

For a slab:

$$U = \frac{u - u_\infty}{u_o - u_\infty} = f(Fo), \qquad Fo = \frac{D_w \cdot t}{1^2} \tag{6.14}$$

Where:

u	moisture content at time t
u_∞	equilibrium moisture content
u_o	intial moisture content
Fo	Fourier number
t	time
l	a characteristic length, see Figure 14.
U	dimensionless moisture content

The moisture content in a plate can be determined at a certain point in time when D_w and l are known. The time it takes to reach a certain mean moisture content can be found. In the figures, $U(t)$ and U_∞ indicate dimensionless moisture content at a given position in a plate or as a mean value, respectively.

$$U(t) = \frac{u(t) - u_\infty}{u_0 - u_\infty} \qquad U_m = \frac{u - u_\infty}{u_0 - u_\infty} \tag{6.15}$$

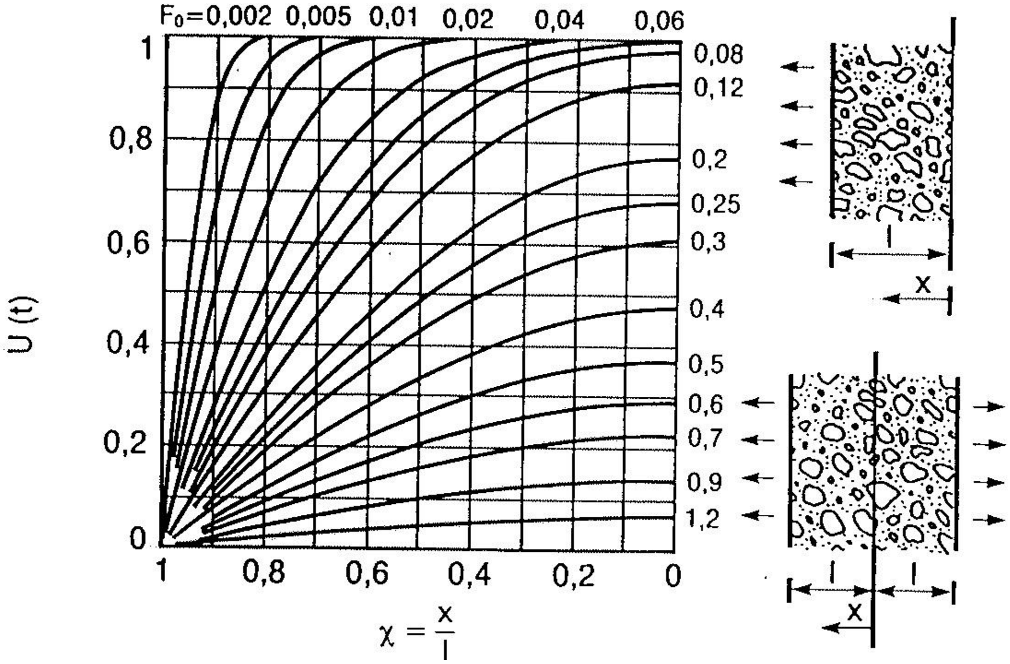

Figure 6.16 moisture content distributions at various times for a slab. The curves correspond to different values of the Fourier number (Fo).

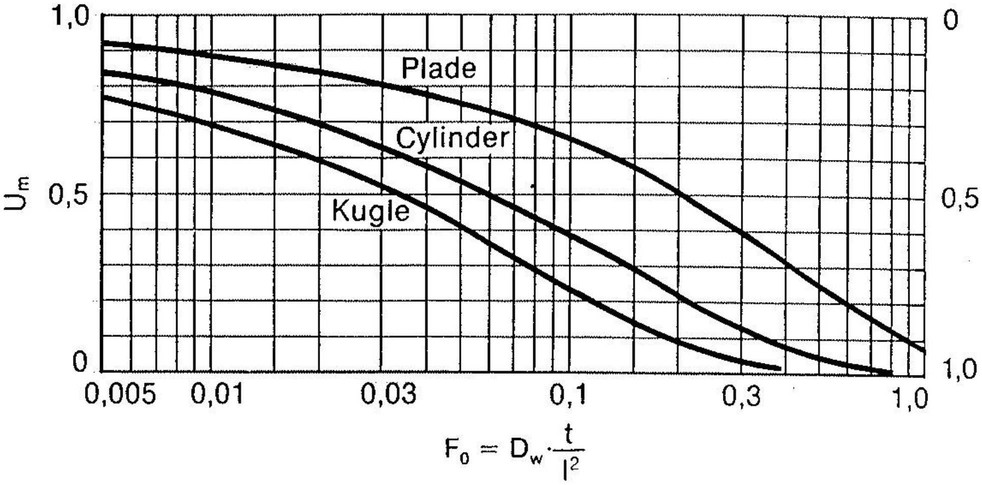

Figure 6.17 Drying of a plate (plade), a cylinder, or a sphere (kugle) as a function of the Fourier number (Fo).

7 AIR TRANSFER

Air transfer in buildings can be both intentional and unintentional. When we open windows or use kitchen hood or mechanical ventilation system, we have a desire to get some fresh air supply and/or pollutants exhaust. In order to perform as expected, the window openings and mechanical systems including the ducts must be correctly designed and dimensioned in order to provide the designed airflow.

On the other hand, there exist also unintentional airflows in buildings. These can be leaks between window & frame, leaks between gypsum boards, cracked render, unfilled joints, air permeable building components, etc. Unintentional air transfer can cause extra heat losses, interstitial condensation in building constructions and transfer of pollutants, and should be normally avoided.

In this lecture note, you will learn how to set-up and solve air balances for a zone in a building and in/across building materials and constructions. In addition, you will be able to formulate and apply the airflow descriptions for permeable media and for openings, and to formulate and apply the wind pressure and stack pressure boundary conditions for airflow.

7.1 Air conservation and storage

Conservation of mass was defined in 1748 by Mikhail Lomonosov, and has been defined for moisture in a previous chapter. For air in an open system conservation of mass means that the amount of air stored in the system $m_{a,stored}$ [kg] must be equal to the difference be-tween the mass of air added to the system $m_{a,in}$ [kg] and the mass of air taken from the system $m_{a,out}$ [kg]:

Base formulation:

$$m_{a,stored} = \sum m_{a,in} - \sum m_{a,out} \tag{7.1}$$

Rate of air transfer

$$dm_{a,stored}/dt = \sum G_{a,in} - \sum G_{a,out} \tag{7.2}$$

$$dm_{a,stored}/dt = 0$$

$$\sum G_{a,in} - \sum G_{a,out} = 0 \tag{7.3}$$

Where

G_a is the flow of air, kg/s
m_a is the mass of air, kg
in/out : entering/leaving

t: time [s]

If we can relate storage and flow to air pressures then we can assess air response of buildings and building components.

For considerations on air flow conditions, two types of objects are considered: Spaces and porous materials – each with their variables that will be kept track of as it appears in the following relations.

For rooms/spaces:

$$m_a = V_a \rho_a = \frac{V_a p_a}{R_a T} \tag{7.4}$$

Porous materials:

$$m_a = V_{mat} \psi \rho_a = \frac{V_{mat} \psi p_a}{R_a T} \tag{7.5}$$

Where

V_a is the volume of air, m3
ρ_a is the density of air, kg/m3
P_a is the air pressure, p_0 = 101,325 Pa
R_a is the gas constant for atmospheric air = 287.1 J/(kg·K)
T is absolute temperature, K
V_{mat} is the volume of material, m3
Ψ is the open porosity, -

7.2 Pressure driven flows

Flows are driven by air pressure differences, where the pressures arise from the wind, stack effect (“chimney effect”), and from mechanical systems (fans).

7.2.1 WIND PRESSURE

First of all, we have to note the metrics, which are used to represent wind velocity. The meteorological wind velocity v_{met} is the wind speed, which is measured in 10 m’s height in an open field, i.e. over an undisturbed landscape. The wind velocity has a profile which develops with the height over the ground, and the profile also depends on the type of landscape, i.e. if we are not in the open field, but for instance in a built up area. We have to determine the profile of local wind velocity v_{loc}, which derives from the profile from the undisturbed landscape, v_{wind}

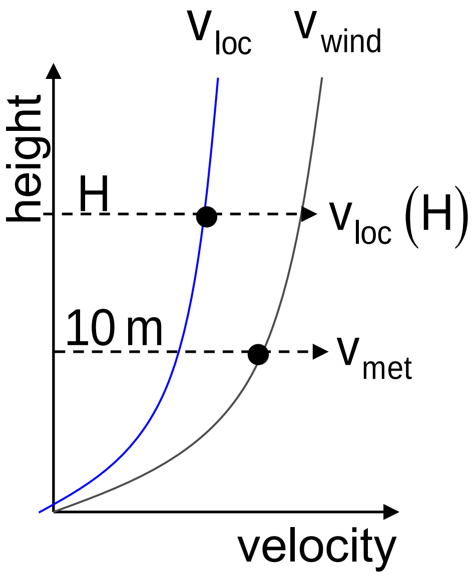

Figure 7.1 profiles of wind velocity in a particular local site of interest and the reference wind velocity profile location in an undisturbed field.

Local wind speed v_{loc} can be calculated at different surface (landscape) roughness, and at different height according to the equation:

$$v_{loc}(H) = v_{met}\,\kappa\,H^{\alpha} \tag{7.6}$$

Where the following coefficients from Table 7.1 pertain to the different types of landscape.

Table 7.1 coefficients to be inserted in Eq. (7.6) to determine local wind velocity (after ASHRAE Handbook of Fundamentals, 2012).

Terrain category	κ	α
Large city centers, in which at least 50% of buildings are higher than 25 m, over a distance of at least 0.8 km or 10 times the height of the structure upwind, whichever is greater	0.21	0.33
Urban and suburban areas, wooded areas, or other terrain with numerous closely spaced obstructions having the size of single-family dwellings or larger, over a distance of at least 460 m or 10 times the height of the structure upwind, whichever is greater	0.43	0.22
Open terrain with scattered obstructions having heights generally less than 9 m, including flat open country typical of meteorological station surroundings	0.72	0.14
Flat, unobstructed areas exposed to wind flowing over water for at least 1.6 km, over a distance of 460 m or 10 times the height of the structure inland, whichever is greater	0.93	0.10

Next, we should determine the pressure loads on building surfaces that arise from the local wind velocities. This follows from Bernouilly's equation which states that the total of the dynamic pressure (or velocity pressure), hydrostatic pressure, and static pressure (or atmospheric pressure) is constant:

$$\begin{aligned} p_{a,total} &= p_{a,\text{atmospheric}} + p_{a,\text{hydrostatic}} + p_{a,dynamic} = \\ &\quad p_{a,\text{atmospheric}} + \rho_a \cdot g \cdot h + \frac{\rho_a v^2}{2} = \quad constant \end{aligned} \tag{7.7}$$

The wind pressure, that arises from the wind speed, and would be felt by total blocking of the wind, is:

$$p_{a,wind} = \frac{\rho_a v_{loc}^2}{2} \tag{7.8}$$

Where

$p_{a,wind}$ is the wind pressure at a surface where the air is brought to complete stop, Pa

However, since the wind is still flowing with some velocity around a building, i.e. it is not brought to a complete stop, the wind pressure that is exerted on the building is only some fraction of dynamic pressure from the free flow field. In some places, the air speed is even higher than in the free flow field (e.g. over the roof), so the wind pressure becomes a negative value, and there may also be under-pressures on the leeward side of the building. Thus, the actual wind pressures in different locations of a building's exterior surfaces facade are modified by the local wind pressure coefficient, C_p.

$$p_{a,wind,local} = C_p \frac{\rho_a v_{loc}^2}{2} \tag{7.9}$$

Where

C_p is the local wind pressure coefficient, -

Local wind pressures at exterior building surfaces and "maps" and tables of local wind pressure coefficients are shown in the following figures and table.

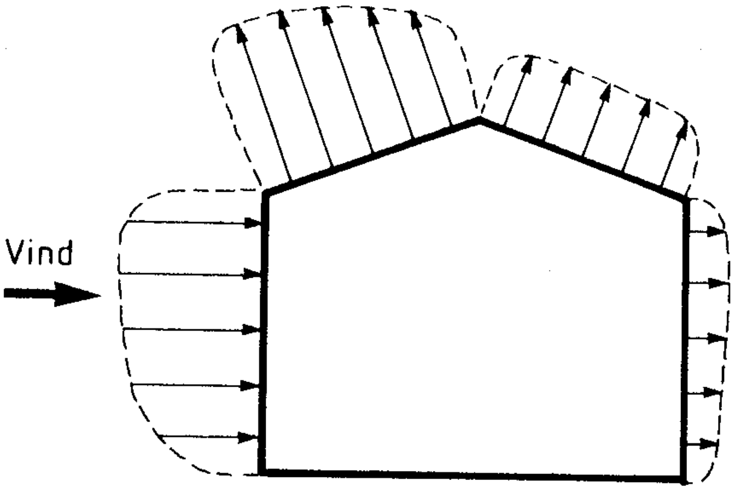

Figure 7.2 pressure profiles around a building (Byggforsk, Norwegian Building Research Institute).

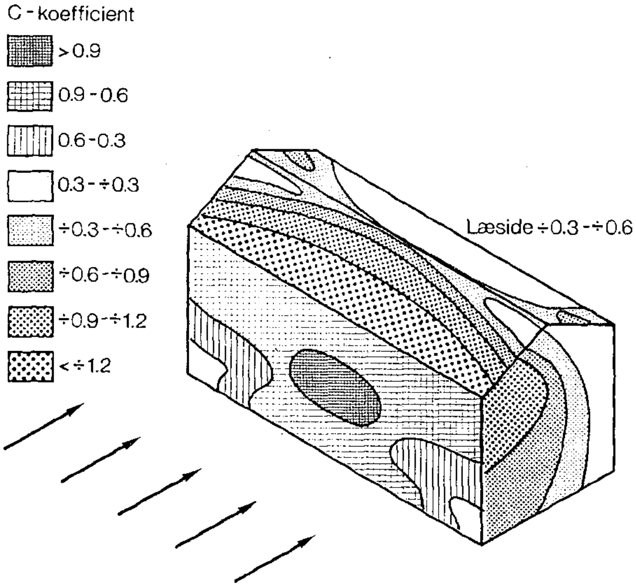

Figure 7.3 map of local wind pressure coefficients around a building. It should be noted that most of them are negative. (Danish Building Research Institute).

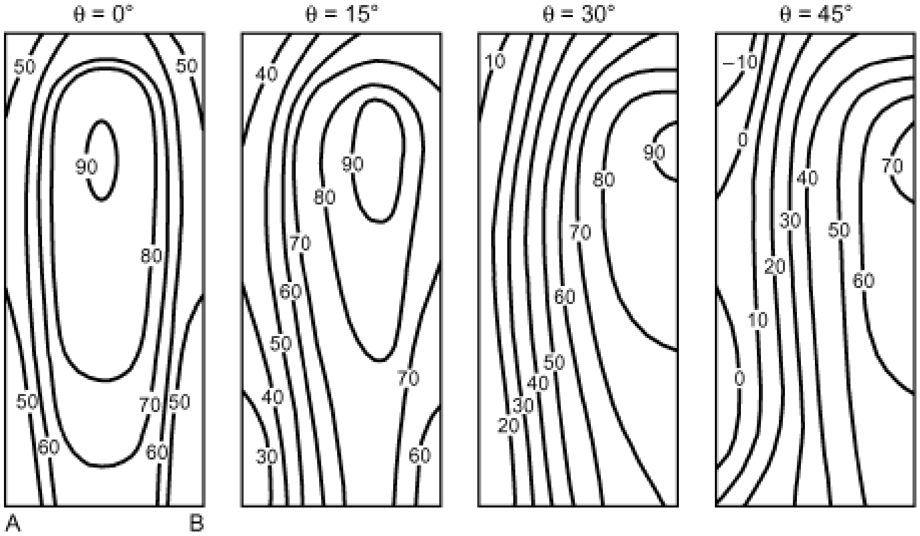

Figure 7.4 distribution of the local wind pressure coefficient over the surface of a tall façade that faces the wind directly (0°), or at various oblique angles (ASHRAE Handbook of Fundamentals 2012).

Low-rise building – plan:

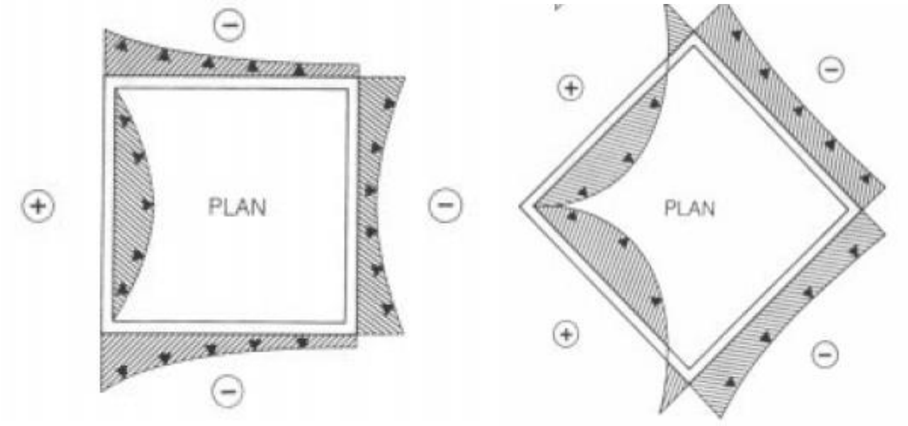

Figure 7.5 plan of a low-rise building showing the lateral distribution of the local wind pressure coefficient over the façades when either one of the facades of the building faces the wind directly (left), or one of the corners of the building faces the wind (right). (ASHRAE Handbook of Fundamentals 2012).

Table 7.2 unshielded low-rise buildings. Local wind pressure coefficients for four facades and two roof surfaces at different slopes. Wind from different angles as indicted in table's top bar. From the AIVC (Air Infiltration and Ventilation Centre):

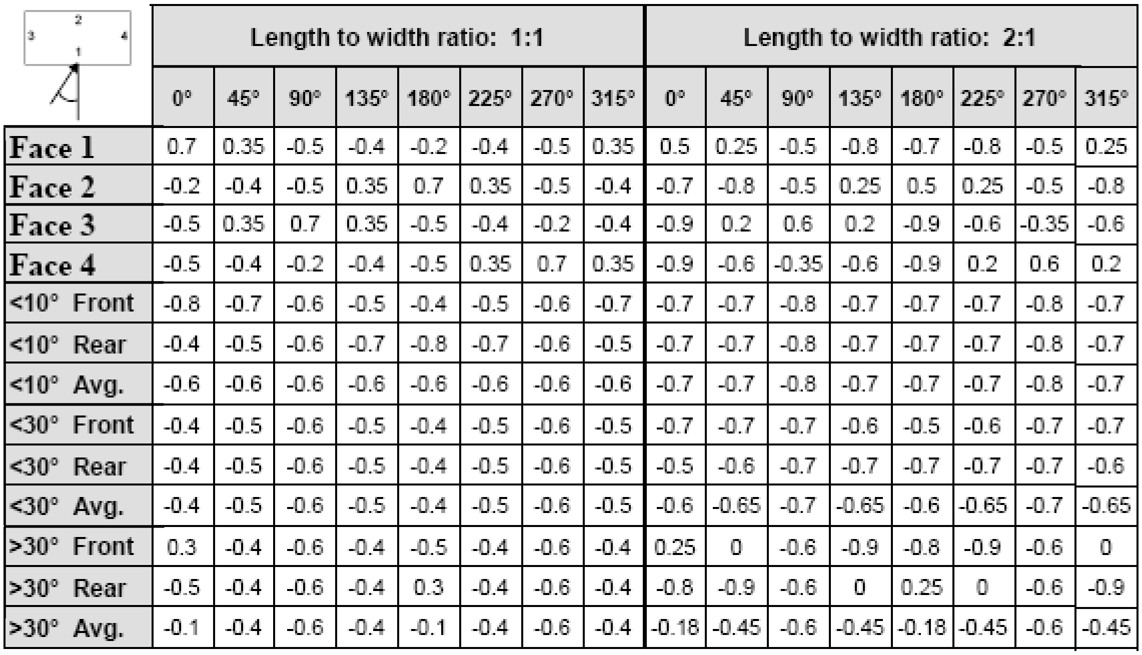

2 3 4 1	Length to width ratio: 1:1								Length to width ratio: 2:1							
	0°	45°	90°	135°	180°	225°	270°	315°	0°	45°	90°	135°	180°	225°	270°	315°
Face 1	0.7	0.35	-0.5	-0.4	-0.2	-0.4	-0.5	0.35	0.5	0.25	-0.5	-0.8	-0.7	-0.8	-0.5	0.25
Face 2	-0.2	-0.4	-0.5	0.35	0.7	0.35	-0.5	-0.4	-0.7	-0.8	-0.5	0.25	0.5	0.25	-0.5	-0.8
Face 3	-0.5	0.35	0.7	0.35	-0.5	-0.4	-0.2	-0.4	-0.9	0.2	0.6	0.2	-0.9	-0.6	-0.35	-0.6
Face 4	-0.5	-0.4	-0.2	-0.4	-0.5	0.35	0.7	0.35	-0.9	-0.6	-0.35	-0.6	-0.9	0.2	0.6	0.2
<10° Front	-0.8	-0.7	-0.6	-0.5	-0.4	-0.5	-0.6	-0.7	-0.7	-0.7	-0.8	-0.7	-0.7	-0.7	-0.8	-0.7
<10° Rear	-0.4	-0.5	-0.6	-0.7	-0.8	-0.7	-0.6	-0.5	-0.7	-0.7	-0.8	-0.7	-0.7	-0.7	-0.8	-0.7
<10° Avg.	-0.6	-0.6	-0.6	-0.6	-0.6	-0.6	-0.6	-0.6	-0.7	-0.7	-0.8	-0.7	-0.7	-0.7	-0.8	-0.7
<30° Front	-0.4	-0.5	-0.6	-0.5	-0.4	-0.5	-0.6	-0.5	-0.7	-0.7	-0.7	-0.6	-0.5	-0.6	-0.7	-0.7
<30° Rear	-0.4	-0.5	-0.6	-0.5	-0.4	-0.5	-0.6	-0.5	-0.5	-0.6	-0.7	-0.7	-0.7	-0.7	-0.7	-0.6
<30° Avg.	-0.4	-0.5	-0.6	-0.5	-0.4	-0.5	-0.6	-0.5	-0.6	-0.65	-0.7	-0.65	-0.6	-0.65	-0.7	-0.65
>30° Front	0.3	-0.4	-0.6	-0.4	-0.5	-0.4	-0.6	-0.4	0.25	0	-0.6	-0.9	-0.8	-0.9	-0.6	0
>30° Rear	-0.5	-0.4	-0.6	-0.4	0.3	-0.4	-0.6	-0.4	-0.8	-0.9	-0.6	0	0.25	0	-0.6	-0.9
>30° Avg.	-0.1	-0.4	-0.6	-0.4	-0.1	-0.4	-0.6	-0.4	-0.18	-0.45	-0.6	-0.45	-0.18	-0.45	-0.6	-0.45

7.2.2 STACK EFFECT

The pressure effect due to density difference of air is called a stack effect or chimney effect. Characteristic for the stack effect is that it creates an under pressure in the lower parts of a building and overpressure in the upper parts of a buildings, see figure below.

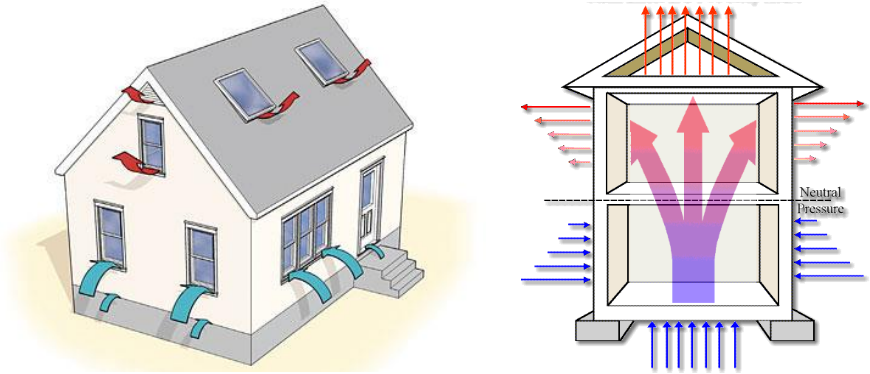

Figure 7. 6 illustration of pressure distribution in dependency of height (right) and ensuing direction of air flow through leaks in the building envelope of a house (left).

The atmospheric pressure we have at ground level is the result of the hydrostatic pressure of the air layers in the atmosphere above. The pressure is highest at ground level and be-comes less with height according to Eq. 7.10! Reference source not found.

$$p_a\left(h\right)=p_{a,0}-\rho_a gh=p_{a,0}-\frac{p_{a,0}}{R_a T}gh=p_{a,0}\left(1-\frac{g}{R_a T}h\right) \tag{7.10}$$

Where

P_a(h)	is the air pressure as a function of height over ground level, Pa
$P_{a,0}$	is the air pressure at ground level, Pa
ρ_a	is the density of air, kg/m^3
g	is the acceleration of gravity, m/s^2
h	is height over ground level, m
R_a	is the gas constant for atmospheric air = 287.1 J/(kg·K)
T	is absolute temperature, K

Under conditions when the temperature is different between the air inside and outside of a building, also the density will be different, as it appears from the influence of temperature in either of the last two terms of Eq.7.10. Under the assumption of same air pressures at ground level inside and outside of a building, this will lead to the different developments of the air pressure vs. height distributions between in-side and outside the building as illustrated in the left-hand part of Figure 7.7. Consequently, there will be a difference in air pressure between inside and outside for all height above ground level. The development with height of this air pressure difference is illustrated in the right-hand part of Figure 7.7.

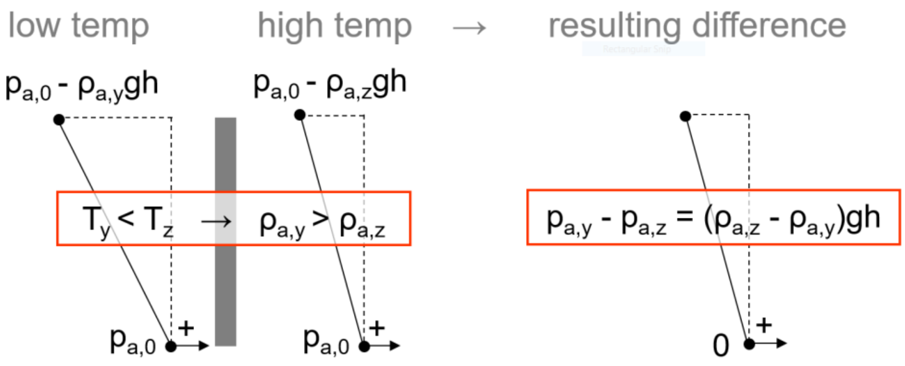

Figure 7.7 left-hand part of figure: Theoretical development of pressure vs. height in-side (e.g. high temp.) and outside (low temp) of a building. Right-hand part: Difference in air pressure between inside and outside as it develops with height.

However, the pressure development shown in the figures can be regarded as valid only under the theoretical assumption of same air pressure at height 0 m. This would require a very open building envelope down at ground level (i.e. a unhindered air exchange through the walls at their bottom/near the foundation). In real buildings, the leakiness between in-side and outside may be distributed over various heights of the building envelope structure, so the height in which the air pressures are the same inside and outside of the building may be at some higher level over the ground, depending on where the building has its dominating leaks. This height is called the neutral plane.

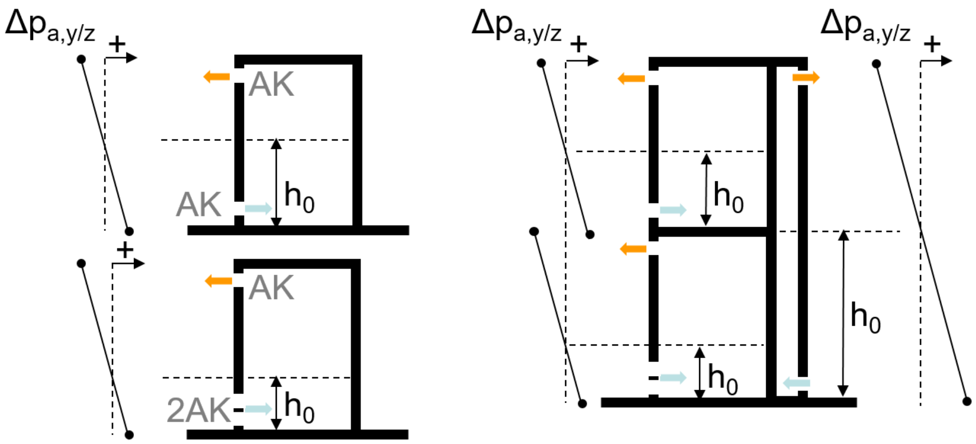

Figure 7.8 illustration of inside and outside pressure distributions for two different cases of where in the height a building has its dominating leaks.
Top left: The lower and upper parts of the building envelope are equally leaky, so the neutral plane is in the middle of the height of building.
Lower left: The lower part of the building envelope is more leaky than the up-per, so the neutral plane is closer to the ground level than to the ceiling.
The right-hand part of the figure illustrates how stair cases, elevator shafts or chimneys that span several floors may have other pressure vs. height devel-opments than the rooms on the individual floors.

For a heated building located in a cold climate, the stack effect will cause air pressures to be higher inside than outside of the building for the upper parts of the buildings, whereas the inside pressure is lower than the outside pressure in the lower parts of the building. If stack effect is the only mechanism to cause air pressure differences between inside and outside of a building, it would lead to exfiltration of air through possible cracks, leaks in the building envelope or through ventilation openings in the upper parts of the building, whereas the air would infiltrate into the building through such openings in the parts of the building which are below the neutral plane. This is illustrated in Figure 7.9. For a cooled building located in a warm climate, the pressure differences and directions of potential airflows would be opposite.

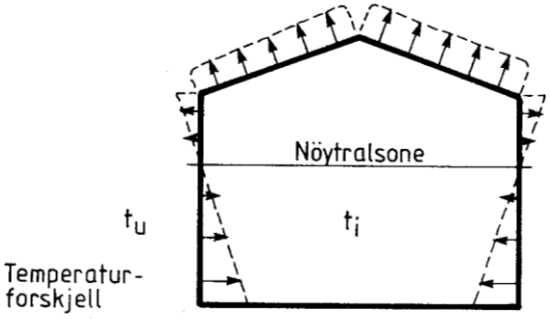

Figure 7.9 illustration of pressure differences between inside and outside as caused by the stack effect, and demarcation of the neutral plane for a building located in a climate which is colder than the temperature inside of the building (Byggforsk, Norwegian Building Research Institute).

For a vertical shaft or cavity (e.g. behind a ventilated cladding at the exterior side of a building envelope) we could have the condition which is illustrated in the rightmost part of Figure 7. 9. If the shaft contains warmer air than outside of the building, the development with height of the pressure differences between inside and outside is such that air in the shaft will be sued upwards. This is the effect that is used in a chimney over a fire place or a boiler to drive the warm fumes upwards in the chimney (and by the way: for the room in which the fireplace is located, this will cause relatively cold replacement air to be drawn in-to the room, and this air is then come to the fireplace to sustain the continued fire).

Cooling of the vertical shaft, e.g. by long-wave radiation to the sky if the shaft is a cavity below the roofing / over the insulation in a sloped roof, may in some periods cause the air in the shaft to be colder than the outside air, in which case the air will be driven down-wards by the stack effect.

7.2.3 MECHANICAL SYSTEMS

In buildings where fans (“mechanical systems”) are operated there will either be an over- or under-pressure of the inside air compared to the outside. This may potentially cause ex-filtration or infiltration of air through leaks in the building envelope or through ventilation openings. Figure 38 illustrates the situation for a building with an exhaust fan that causes an under-pressure in the building.

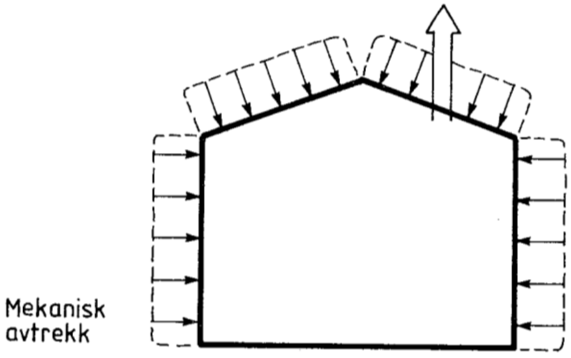

Figure 7.10 illustration of pressure differences between inside and outside as caused by an exhaust fan that extracts the air from inside of the building causing an under-pressure in the indoor space compared to the outdoor air (Byggforsk, Norwe-gian Building Research Institute).

Exhaust fans will typically sit in kitchen or bathrooms, or in rooms where other polluting processes take place, e.g. in a commercial buildings. Since the air to be exhausted has to come as fresh air to these rooms, the air may either be draw from the outside through ventilation openings or from other rooms which will then have to have some conduits for fresh air supply. In this way, the under-pressure caused by one room’s exhaust fan may propagate to several or all rooms of a building. It is noteworthy to mention that air that is exhaust by a device in one room of a building must somehow be replenished by a similar volume of supply air. It will not be possible to cause ventilation with an exhaust fan if the building envelope is perfectly airtight, and there are no provisions for fresh air supply.

A mechanical ventilation system may also be installed which is supplied with both an exhaust and a supply fan. With such a so-called balanced ventilation system it may be possible to maintain an almost neutral pressure difference between inside and outside of a building.

7.2.4 COMBINED PRESSURE EFFECTS

In reality a building and its constructions will be exposed to air pressures that arise both from the wind and the stack effect (when temperature differences exist). These two causes of pressure differences are categorized as natural forces. Since most buildings have either one or several exhaust fans or a dedicated ventilation system, the air pressures will in addition be influenced by the mechanical system. Consequently, the air pressure condition in a building is determined as the summation of these individual reasons for build-up of pressure differences, and they all have to be assessed. In certain situations some may be significantly more important than others, but it will be important to consider an operating conditions that may likely occur – and their duration.

7.3 FLOW THAT RESULTS FROM THE PRESSURES

Two types of air flow are described: Air flow through porous materials and air flow in ducts. These two types have fundamentally different characteristics and therefore need to be treated in different ways:

Table 7.3 flow through types and characteristiscs.

Flow through air permeable materials	Flow through ducts (vents, orifices, leaks, channels cracks, …)
flow through fine porous system	flow through large openings
large resistance (by wall friction)	far smaller flow resistances
low air velocities inside the pore	high air velocities in orifices
laminar flow	turbulent flow
linear relation between air flow & pressure difference	nonlinear relation between air flow & pressure difference

7.3.1 FLOW THROUGH POROUS MATERIALS

Following figures illustrate the nature of some typical porous materials. Air flow these materials can be described with Darcy's law (Henry Darcy, 1856).

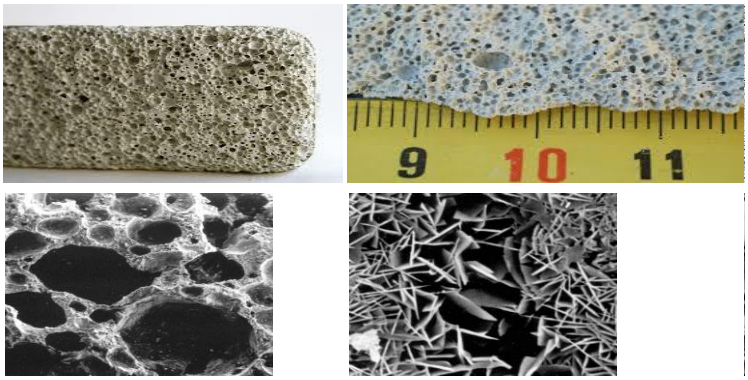

Figure 7.11 cellular concrete.

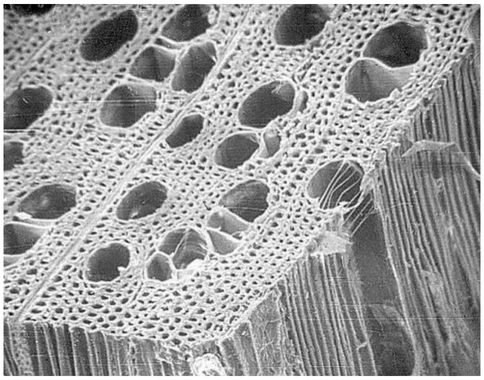

Figure 7.12 wood.

Typical for these air permeable materials is that the air flows with low air velocities through the fine porous system and with a large resistance by wall friction. This results in laminar flow (see figure on the right) and a linear relation between air flow Ga and pressure difference:

$$p_{a,y} - p_{a,z} = G_a/(AK) \quad \sim \quad G_a/A \qquad (7.11)$$

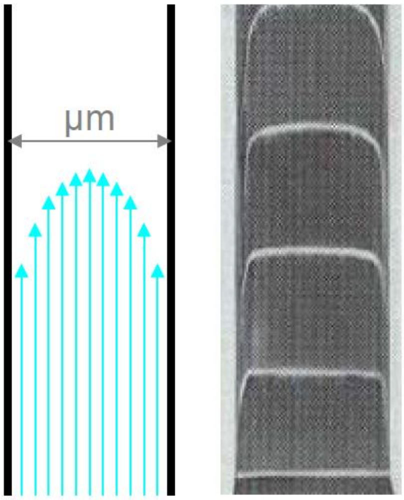

Darcy's law is analogous to Fourier's law for heat conduction and Fick's law for vapor diffusion. When assuming steady state conditions, one-dimensional transfer, constant material parameters and no mass generation Eq 7. 11 is valid. Furthermore, due to low air velocities in the pores, the air flow is assumed to be laminar. Illustration of air flow G_a through a material layer with thickness d over a pressure difference is below.

$$G_a = A k_a \frac{p_{a,y} - p_{a,z}}{d} = A \frac{p_{a,y} - p_{a,z}}{W} \quad W = \frac{d}{k_a} \tag{7.12}$$

Where:

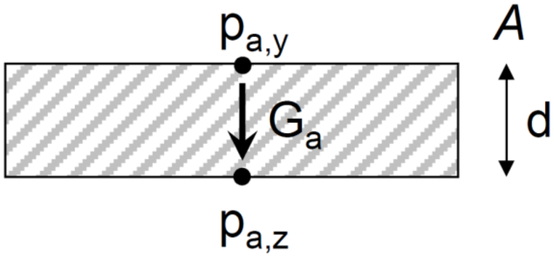

G_a: air flow [kg/s]
k_a: air permeability [kg/(m·s·Pa)]
p_a: air pressure [Pa]
W: air flow resistance [m²·s·Pa/kg]
d: thickness [m]
A: surface area [m²]

Idealized the porous materials can be assumed as a bundle of cylindrical tubes, see Figure 7. 13.

Figure 7.13 porous material idealized as a collection of cylindrical tubes.

The air flow in cylindrical tubes can be described with the Hagen-Poiseuille equation:

$$G_a = A \frac{\rho_a \sum r^2}{8 \mu_a L} \left(p_{a,y} - p_{a,z} \right) \tag{7.13}$$

Where the blue part represents the "permeability of the tubes" and:

G_a: air flow [kg/s]
ρ: density [kg/m³]
r: tube radius/gap width [m]
p_a: air pressure [Pa]
μ_a: dynamic viscosity [kg/(m·s)] (18 10-6 kg/(m·s) at 20 °C)
L: tube/gap length [m]
A: surface area [m²]

Permeability of materials can normally be assumed proportional to their porosity and tortuosity, and to the pore diameter squared. Air permeability, k_a [kg/(m·s·Pa)] of some common building materials are given in Table 3.

Table 5.4 air permeability

Material	k_a[kg/(m·s·Pa)]	Material	k_a [kg/(m·s·Pa)]
wood wool cement board	$5.0\cdot10^{-4}$	particle board	$6.9\cdot10^{-9}$
mineral wool	$5.0\cdot10^{-5}$	aerated concrete	$5.0\cdot10^{-9}$
cellullose insulation	$5.0\cdot10^{-5}$	gypsum board	$2.0\cdot10^{-9}$
expanded polystyrene	$5.0\cdot10^{-7}$	cement mortar	$1.0\cdot10^{-9}$
cement board	$3.0\cdot10^{-9}$	Plywood	$8.0\cdot10^{-10}$
extruded polystyrene	$9.3\cdot10^{-9}$	ceramic brick	$3.0\cdot10^{-10}$
fibre cement	$9.0\cdot10^{-9}$	oriented strand board	$1.0\cdot10^{-10}$

For composite walls, the general formula of Darcy's law for air flow results in:

Transfer:
$$G_a = A\,k_a\,\frac{p_{a,y}-p_{a,z}}{d} = -A\,k_a\,\frac{\partial p_a}{\partial x} \qquad (7.14)$$

Resistance:
$$W_j = d_j \big/ k_{a,j} \qquad (7.15)$$

Profile:
$$p_{a,x} = p_{a,y} + (p_{a,z}-p_{a,y})\sum_{j=1}^{x} W_j \Big/ \sum_{n} W_j \qquad (7.16)$$

For air transfer from environment to environment we define:

Permeance:
$$K = 1 \Big/ \left(\sum_{n} d_j / k_{a,j}\right) \qquad (7.17)$$

Transfer:
$$G_a = AK\left(p_{a,y}-p_{a,z}\right) \qquad (7.18)$$

7.3.2 FLOW THROUGH DUCTS, ORIFICES AND CHANNELS

Air flow through ventilation openings, ducts and unintentional leakages in building envelope (e.g. leaks between different building constructions like window and wall or cracks in masonry wall) is fundamentally of different nature than air flow through air permeable materials described in the previous section: The openings are larger and result in far smaller flow resistances. The low resistance gives some higher air velocities in these conduits, which again gives turbulent flow (see illustration on the right) and nonlinear relations be-tween airflow and pressure difference:

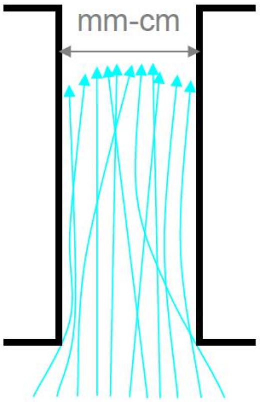

$$p_{a,y} - p_{a,z} \sim (G_a/A)^2 \qquad (7.\ 19)$$

The total pressure loss through a duct is the sum of local losses at the entry and outlet, and friction loss along the length of the duct. See the illustration on the right, and the expression below:

$$p_{a,y} - p_{a,z} = \Delta p_{a,loc,1} + \Delta p_{a,fric} + \Delta p_{a,loc,2} \qquad (7.20)$$

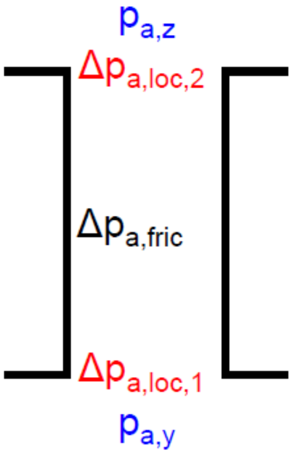

Local and friction losses are calculated differently:

Local pressure loss is created due to contraction or widening of the duct, or passing the sharp angles at the entrance to and outlet from a duct and through an orifice. Some simple values exist for local loss factors ξ [-] for common cases:

Table 7.5 common case factors describing local losses.

	Local loss factor ξ [-]
Entering an opening	0.50
Leaving an opening	1.00
Flow through orifice	2.85

The resulting expression for the local pressure loss is given

$$\Delta p_{a,loc} = \frac{\xi}{2\rho_a}\left(\frac{G_a}{A}\right)^2 \qquad (7.21)$$

Friction pressure loss is caused by friction internally in the fluid and between the fluid and the duct walls. The friction factor f depends on the nature of the flow, geometry of cross section and Reynolds number:

$$\mathrm{Re} = \frac{G_a d_H}{A\mu_a} \tag{7.22}$$

Where:

G_a: airflow [kg/s]

d_H hydraulic diameter [m] = 4 A/P

A: surface area [m²]

μ_a: dynamic viscosity [kg/(m·s)] (18·10-6 kg/(m·s) at 20 °C)

Depending on the magnitude of the Reynolds number and roughness of the duct walls, the friction factor can be read from the so-called Moody diagram, see next page. From the diagram follows these main observations about the friction factor's dependencies:

$Re >> 3500$ → f = constant

For a cylindrical tube:

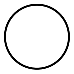: $Re < 2500$ → $f = 64 / \mathrm{Re} \Rightarrow$ $$\Delta p_{a,fric} = \frac{32\mu_a L}{\rho_a d_H^2}\left(\frac{G_a}{A}\right)$$

For a crack/cavity represented as two parallel surfaces, which are close and infinitely wide:

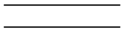: $Re < 2500$ → $\boldsymbol{f = 96 /} Re \Rightarrow$ $$\Delta p_{a,fric} = \frac{48\mu_a L}{\rho_a d_H^2}\left(\frac{G_a}{A}\right)$$

Solutions also exist for ducts of rectangular cross section leading to other factors than "64" or "96" (Kronvall, 1980).

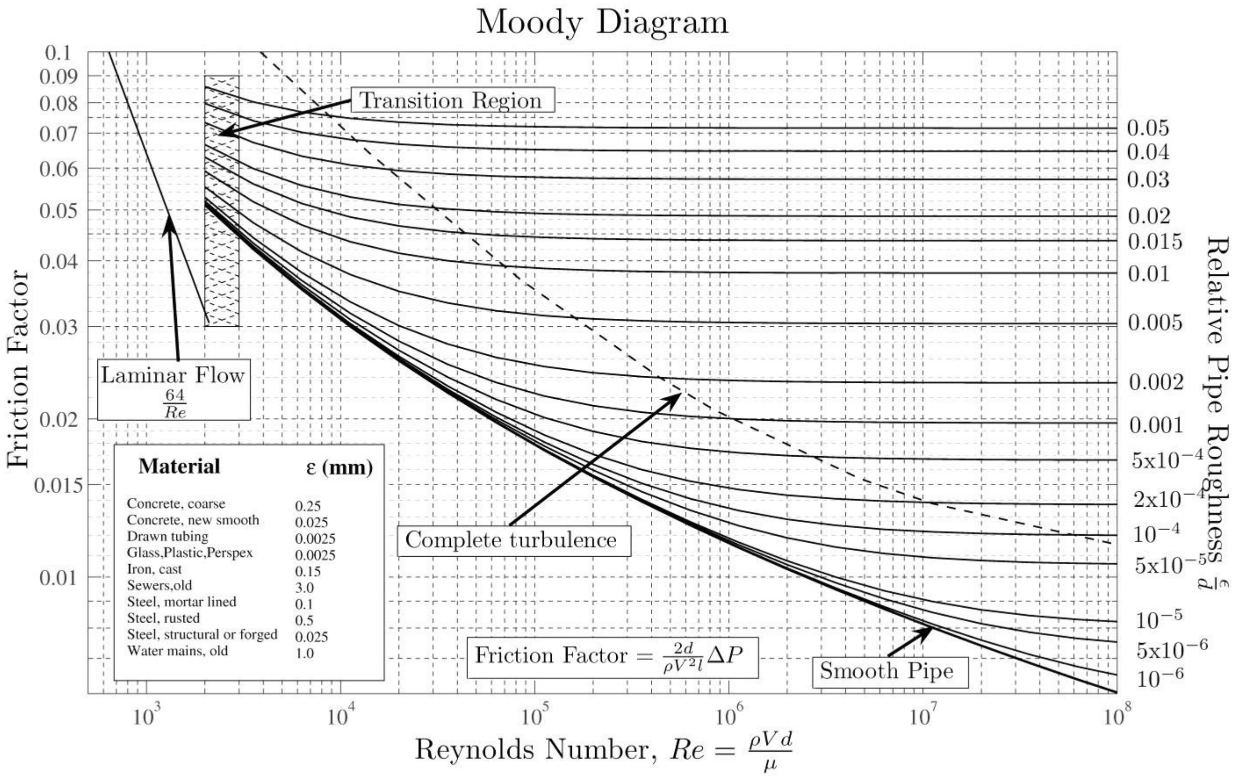

Figure 7. 14 lockup Moody diagram.

The total pressure losses can now be calculated as follows in dependency of the airflow:

$$p_{a,y} - p_{a,z} = \Delta p_{a,loc,1} + \Delta p_{a,fric} + \Delta p_{a,loc,2}$$

$$= X\left(\frac{G_a}{A}\right)^2 + Y\left(\frac{G_a}{A}\right)^a + Z\left(\frac{G_a}{A}\right)^2, \quad 1 \le a \le 2 \tag{7.23}$$

where *X*, *Y* and *Z* are coefficients as per the above descriptions, and the exponent of the middle term should have a value between 1 (for laminar flow) and 2 (for fully developed turbulent flow).

The following approximate expressions can be derived to give the airflow as function of the pressure difference:

$$G_a = (AK)_{ref}\left(p_{a,y} - p_{a,z}\right)^b \tag{7.24}$$

b = 1: laminar flow;

b = 0.5: turbulent flow

For calculation purposes it can be advisable to split it up in a part that depends linearly on the pressure difference, and the rest:

$$G_a = (AK)_{ref}\left(p_{a,y} - p_{a,z}\right)^{b-1}\left(p_{a,y} - p_{a,z}\right) \tag{7.25}$$

8 TRANSIENT (HEAT &) MOISTURE TRANSFER

Previous chapters have dealt with heat, air and moisture transport under the assumption of steady state conditions. This was analyzed by setting up equations for conservation of heat and mass within a volume, e.g. a room or a lump of material, by assuming conditions were constant so there was no accumulation of heat or mass within the volume. The amount of heat or mass going into the volume should always be balanced by the amount going out.

Heat:

$$\sum Q_{in} - \sum Q_{out} = \frac{dE}{dt} = 0 \tag{8.1}$$

Water vapor:

$$\sum G_{v,in} - \sum G_{v,out} = \frac{dm_v}{dt} = 0 \tag{8.2}$$

Air:

$$\sum G_{a,in} - \sum G_{a,out} = \frac{dm_a}{dt} = 0 \tag{8.3}$$

Where

Q	is the flow of heat, J/s = W
E	is the enthalpy (heat) content, J
t	is time, s
G_v	is the flow of water vapor, kg/s
m_v	is the water vapor content by mass, kg
G_a	is the flow of air, kg/s
m_a	is the mas of air, kg

However, most processes in real buildings are transient, i.e. time varying, so the steady state assumption does not always give a good representation of the real conditions. We consider the transient conditions by using the same conservation equation as above but without the assumption that the time derivatives of the energy or mass contents are zero.

Heat:

$$\sum Q_{in} - \sum Q_{out} = \frac{dE}{dt} \tag{8.4}$$

Water vapor: $$\sum G_{v,in} - \sum G_{v,out} = \frac{dm_v}{dt} \tag{8.5}$$

Air: $$\sum G_{a,in} - \sum G_{a,out} = \frac{dm_a}{dt} \tag{8.6}$$

The flows of heat are determined based on temperature or temperature gradients, e.g. as in the transport law for heat flow by advection and in Fourier's law. The flows of water vapor are determined based on the water vapor pressure and gradients thereof, and while air flow is determined by air pressures.

So the conservation equations keep track of the balance of heat, and the masses of water vapor and air, while temperature, water vapor pressure and air pressure constitute the driving potentials for the flows. For Q, G_v and G_a in the above equations, we can insert the transport equations, which depend on those driving potentials.

In order to solve the equations we should know how the driving potentials are linked to the parameters which are kept track of in the conservation equation. This we can do for each of the three parameters from the conservation equations both in cases when the balance is set up for a volume of air, like in a room, or for a volume of material.

For a volume of air, the energy (heat) content in dependency of the temperature can be written as:

$$E = V_a \rho_a c_a T \tag{8.7}$$

The mass of water vapor can be written as:

$$m_v = V_a p_v / R_v T \tag{8.8}$$

And the mass of air can be written as:

$$m_a = V_a p_a / R_a T \tag{8.9}$$

Where

V_a	is the volume of air, m^3
ρ_a	is the density of air, kg/m^3
c_a	is the specific heat (heat capacity) of air, J/(kg·K)
T	is temperature, K
p_v	is the water vapor pressure, Pa
R_v	is the gas constant for water vapor = 461.5 J/(kg·K)
p_a	is the air pressure, Pa

R_a is the gas constant for atmospheric air = 287.1 J/(kg·K)

The gas constant for water vapor is equal to the universal gas constant R = 8.314 J/(mole·K) divided by the molar mass of water, M_{H20} = 18.02 g/mole, and likewise for the gas constant for atmospheric air with molar mass M_a = 28.96 g/mole.

For a volume of material, the energy content in dependency of the temperature can be written as:

$$E = V_{mat}\rho_{mat}c_{mat}T \tag{8.10}$$

The mass of moisture in the material can be written as.

$$m_{H_2O} = V_{mat}\rho u(p_v, T) = V_{mat}w(p_v, T) \tag{8.11}$$

And the mass of air in the material can be written as:

$$m_a = V_{mat}\Psi p_a / R_a T \tag{8.12}$$

Where

V_{mat} is the volume of the material, m^3

ρ_{mat} is the density of the material, kg/m^3

c_{mat} is the specific heat (heat capacity) of the material, J/(kg·K)

m_{H20} is the mass of water in the material, of which most will be in an absorbed or condensed phase, i.e. the mass of vapor in the material's pores can most often be seen as negligible, kg

u is the moisture content by mass of the material, kg/kg

w is the moisture content by volume of the material, kg/m^3 (1)

Ψ is the porosity of the material, -

The above conservation equations can also be expressed in a rate formulation, i.e. by looking to how the same conservation parameters and the associated potentials vary pr. unit of time in a transient situation.

For a zone of air:

$$\frac{dE}{dt} = V_a\rho_a c_a \frac{dT}{dt} \tag{8.13}$$

---

[1] Moisture content in a material can be given either by mass (*u)* or by volume (*w*) of the material. We prefer to use the mass based moisture content, but will occasionally also refer to the use of the volume based value, which in that case will be put in gray text.

$$\frac{dm_v}{dt} = \frac{V_a}{R_v T}\frac{dp_v}{dt} \tag{8.14}$$

$$\frac{dm_a}{dt} = \frac{V_a}{R_a T}\frac{p_a}{dt} \tag{8.15}$$

For a lump of material:

$$\frac{dE}{dt} = V_{mat}\rho_{mat}c_{mat}\frac{dT}{dt} \tag{8.16}$$

$$\frac{dm_{H_2O}}{dt} = V_{mat}\rho_{mat}\frac{du}{dp_v}\frac{dp_v}{dt} = V_{mat}\frac{dw}{dp_v}\frac{dp_v}{dt} \tag{8.17}$$

$$\frac{dm_a}{dt} = \frac{V_{mat}\psi}{R_a T}\frac{dp_a}{dt} \tag{8.18}$$

Where

$\frac{du}{dp_v}$ (or $\frac{dw}{dp_v}$) can be derived from the slope of the sorption curve and denotes moisture capacity of the material.

From each of the above six equations (8.13) -- (8.18) we can introduce six capacity coefficients as the proportionality coefficients between driving potential and the associated parameter being kept track of in the conservation equation:

For a zone of air:

Capacity coefficient for energy content of an air zone $= V_a\rho_a c_a$ (8.19)

Capacity coefficient for vapour content of an air zone $= \frac{V_a}{R_v T}$ (8.20)

Capacity coefficient for mass of air of an air zone $= \frac{V_a}{R_a T}$ (8.21)

For a lump of material:

Capacity coefficient foe energy content of a lump of material $= V_{mat}\rho_{mat}c_{mat}$ (8.22)

Capacity coefficient for moisture content of a lump of material $= V_{mat}\rho_{mat}\frac{du}{dp_v}$ (8.23)

$$\text{Capacity coefficient for mass of air of a lump of material} \quad = \frac{V_{mat}\psi}{R_a T} \tag{8.24}$$

There are two approaches to solving for the time evolution of the potentials from the above equations: Lumped analyses and distributed solutions.

Lumped analysis assumes the object being studied to be under fully mixed conditions, i.e. for a room, that all temperatures or vapor pressure are the same anywhere in the room. Or for a material, that it is so small or the transport processes within the material are so easy or fast that all internal points of the material can be assumed to have the same temperature, vapor pressure and moisture content.

Distributed solutions, in contrast, do consider the distributions of temperature or vapor pressure that exist within the rooms or materials. However, in this course we will not consider the distributions that ay exists with rooms or other air spaces, since that will require a complex fluid dynamics analysis (e.g. as solved numerically with CFD – Computational Fluid Dynamics methods).

8.1 Biot number

To determine whether a lumped or distributed approach should be used, we can use the *Biot* number. The *Biot* number compares the internal resistance to flow inside of a material to the resistance to flow of transport from the surface of a material to its ambient. For thermal processes, this is done by comparing the resistance to heat conductance of a piece of material of certain dimension, namely the so-called characteristic length, to the convective surface heat transfer resistance, R_s.

$$Bi = \frac{\text{internal resistance}}{\text{external resistance}} = \frac{R_{conduction}}{R_s} = \frac{\frac{L}{\lambda}}{\frac{1}{h_s}} \tag{8.25}$$

Where

R is thermal resistance, m^{2}K/W

L is the characteristic length of the material, m

λ thermal conductivity of the material, W/(m·K)

h_s surface heat transfer coefficient, W/(m^2·K)

The characteristic length of a material can be calculated as its volume divided by its surface area: $L = V/A_s$.

A *Biot* number also exists for the associated moisture (vapor) transport processes. In a similar definition, the Bi-number for water vapor transport can be found by comparing the water vapor diffusion resistance of a piece of material of dimension as the characteristic length, to the convective moisture transfer resistance.

$$Bi_v = \frac{\text{internal resistance}}{\text{external resistance}} = \frac{Z_{p,diffusion}}{Z_{p,convection}} = \frac{\dfrac{L}{\delta_p}}{\dfrac{1}{\beta_p}} \tag{8.26}$$

Where

Z_p is resistance to moisture transfer, $m^2 \cdot s \cdot Pa/kg$
L is the characteristic length of the material, m
δ_p water vapor permeability of the material, $kg/(m \cdot s \cdot Pa)$
β_p surface coefficient for convective moisture transport, $kg/(m^2 \cdot s \cdot Pa)$

If the *Biot* number is less than one 0.1, it indicates that the internal resistance to transport is rather negligible compared to the resistance between the ambient air and the surface of the material. The implication would be that there are hardly any internal gradients in the driving potential compared to those over the surface of the material, i.e. for heat transport, that all internal temperatures can be assumed practically identical, or for moisture, that vapor pressure is everywhere the same within the material. We can then adopt lumped analysis, whereas we would otherwise have to use distributed solutions

8.2 Lumped analysis (Bi < 0.1)

As an example of lumped analysis we will consider the vapor pressure of a room assuming fully mixed conditions. The room is initially at the same vapor pressure as the vapor pressure of the outside air that surrounds the room:

$$p_{v,i}(t=0) = p_{v,e} \tag{8.27}$$

Where

$p_{v,i}$ indoor vapor pressure, Pa
$p_{v,e}$ vapor pressure of the outdoor surrounding air (at all times, *t*), Pa

Until time *t*=0 there is no water vapor release in the room, but at *t*=0 starts a constant vapor production G_{vp}, kg/s.

The differential equation that governs the differential increment of the room's vapor pressure after water vapor begins to be released into the room:

$$\frac{V_a}{R_v T_i} \frac{dp_{v,i}(t)}{dt} = G_{vp} + G_{a,vol} / (R_v T_i)(p_{v,e} - p_{v,i}(t)) \tag{8.28}$$

A little more generic form of this equation can be put as:

$$Cap\frac{dp_{v,i}(t)}{dt}=G_{vp}+Con\left(p_{v,e}-p_{v,i}(t)\right) \quad (8.29)$$

Where

Cap can be understood as a Capacity coefficient cf. Equations (8.19)- (8.24).

Con can be understood as a Contact coefficient, which in this case represents the transmittance between the indoor and outdoor vapor pressures.

Typical Contact coefficients between spaces and their exterior environment:

For heat transfer by thermal transmittance and ventilation:

$\sum U\cdot A + c_a\cdot G_a$ [W/K]

For vapor transfer by ventilation:

$G_{a,vol}/(R_v.T_i)$ [kg/(s·Pa)]

For air transfer by ventilation:

$\rho_a\cdot C$ [kg/(s·Pa)]

Where

U Thermal transmittance, [W/(m^2·K)]

A Area, m^2

$G_{a,vol}$ Volumetric flow of air, [m^3/s (= G_a/ρ_α)]

C air flow coefficient, [m^3/(s·Pa)]

Typical Contact coefficients which are relevant for materials and their surroundings:

For heat transfer by surface heat transfer or conduction within the material:

$A\cdot h_s$ or $A\cdot\lambda/\mathrm{d}$ or A/R [W/K]

For vapor transfer by surface moisture transfer or diffusion within the material:

$A\cdot\beta_p$ or $A\cdot\delta_p/\mathrm{d}$ *or* A/Z_p [kg/(s·Pa)]

For air transfer by ventilation:

$A\cdot\rho_a\cdot K$ or $A\cdot k/\mathrm{d}$ *or* A/W [kg/(s·Pa)]

Where

d Transmission distance within the material, [m]

K	Air permeance, [m^3/(m^2·s·Pa)]
k:	Air permeability, [m^2]
W	Air flow resistance, [m^2·s·Pa/kg]

The solution to Equation (8.29) is:

$$p_{v,i}(t) = p_{v,e} + \frac{G_{vp}}{Con}\left(1 - \exp\left(\frac{-Con}{Cap}t\right)\right) \tag{8.30}$$

This is the typical equation for an exponential decline, e.g. of an RC-network, see Figure 8.1.

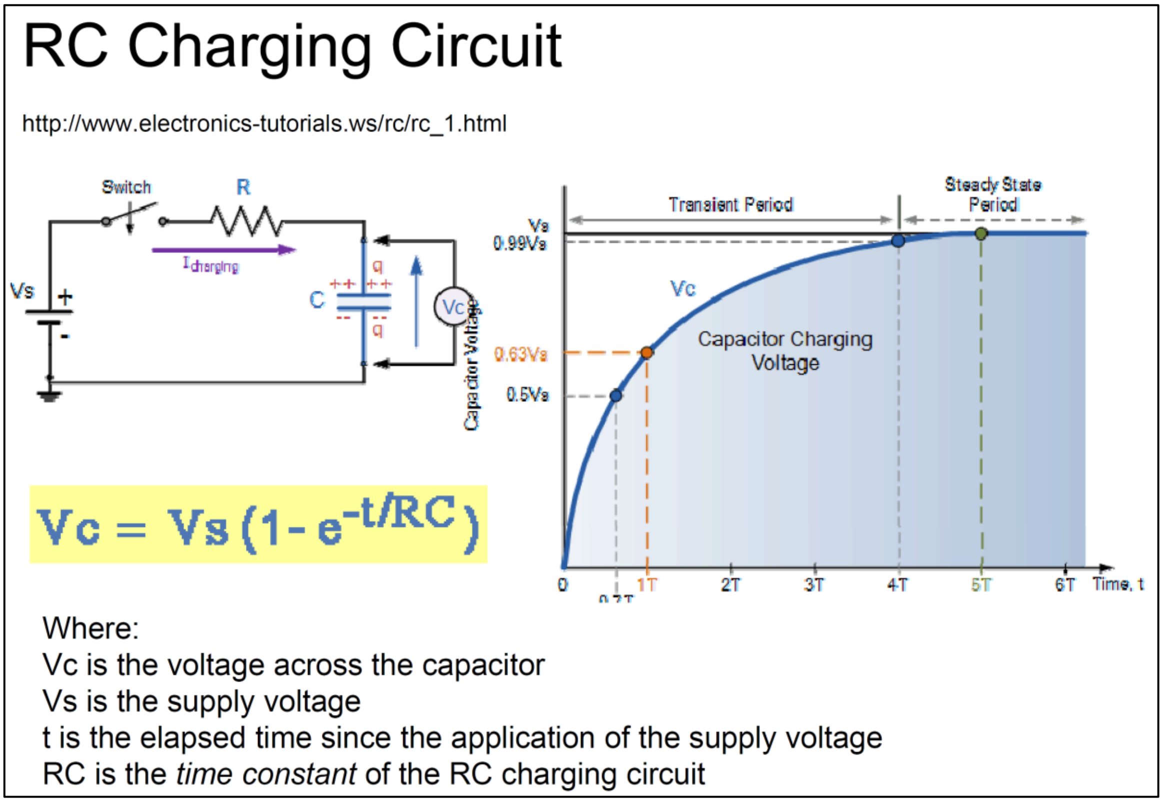

RC Charging Circuit

http://www.electronics-tutorials.ws/rc/rc_1.html

$$Vc = Vs\,(1 - e^{-t/RC})$$

Where:
Vc is the voltage across the capacitor
Vs is the supply voltage
t is the elapsed time since the application of the supply voltage
RC is the *time constant* of the RC charging circuit

Figure 8.1 convection over a flat surface, with the velocity and thermal boundary layers.

The time constant is:

$$\tau = \frac{Cap}{Con} \tag{8.31}$$

The time constant is the time after which 63% of the change has happened of what will be the new equilibrium after a long time. E.g. for the case from before, the final equilibrium will be:

$$p_{v,i}(\infty) = p_{v,e} + \frac{G_{vp}}{Con} = p_{v,e} + \frac{G_{vp}}{G_{a,vol}}R_vT \tag{8.32}$$

8.3 Distributed solutions, step change of surface vapor pressure

We start the discussion of distributed solutions by illustrating transient moisture distribution in a so-called semi-infinite slab of material. Being semi-infinite means that the material has one surface that is exposed to the ambient, and that the material extends infinitely in the depth behind the surface. Initially, the uniformly distributed vapor pressure in the slab is $p_{v,0.}$. At time, $t = 0$, the vapor pressure at the surface of the material is suddenly changed to a new value, $p_{v,1}$ and remains at that level. The vapor pressure at a depth x within the material at time t, can be calculated as (see also Figure 8.2):

$$p_v(\mathrm{x},\mathrm{t}) = p_{v,0} + \left(p_{v,1} - p_{v,0}\right) \operatorname{erfc}\left(\frac{\mathrm{x}}{2\sqrt{\mathrm{a}_v \mathrm{t}}}\right) \tag{8.33}$$

Where

erfc is the complementary “error function” – a well-known mathematical function.

aa_v is the moisture diffusivity $$a_v = \frac{\delta}{\rho_{mat} \dfrac{\partial u}{\partial p_v}} = \frac{\delta}{\dfrac{\partial w}{\partial p_v}}$$

The total mass of accumulated moisture in the slab can be calculated as (see also Figure 8.3):

$$m(t) = A_{mat} \frac{2\, b_v \left(p_{v,1} - p_{v,0}\right)}{\sqrt{\pi}} \sqrt{t} \tag{8.34}$$

Where

b_v is the moisture effusivity $$b_v = \sqrt{\delta\, \rho_{mat} \frac{\partial u}{\partial p_v}} = \sqrt{\delta \frac{\partial w}{\partial p_v}}$$

The moisture effusivity indicates how much moisture the material takes up from the surroundings when the environment changes, i.e. its capacity to work as a moisture buffer.

The notion of a moisture penetration depth can be introduced as a measure of how deep the moisture profile has penetrated into the material after a certain time. For instance the depth at which the vapor pressure has increased by half of $p_{v,1} - p_{v,0}$ is:

$$d_{p,50\%,step} = \sqrt{a_v \cdot t} \tag{8.35}$$

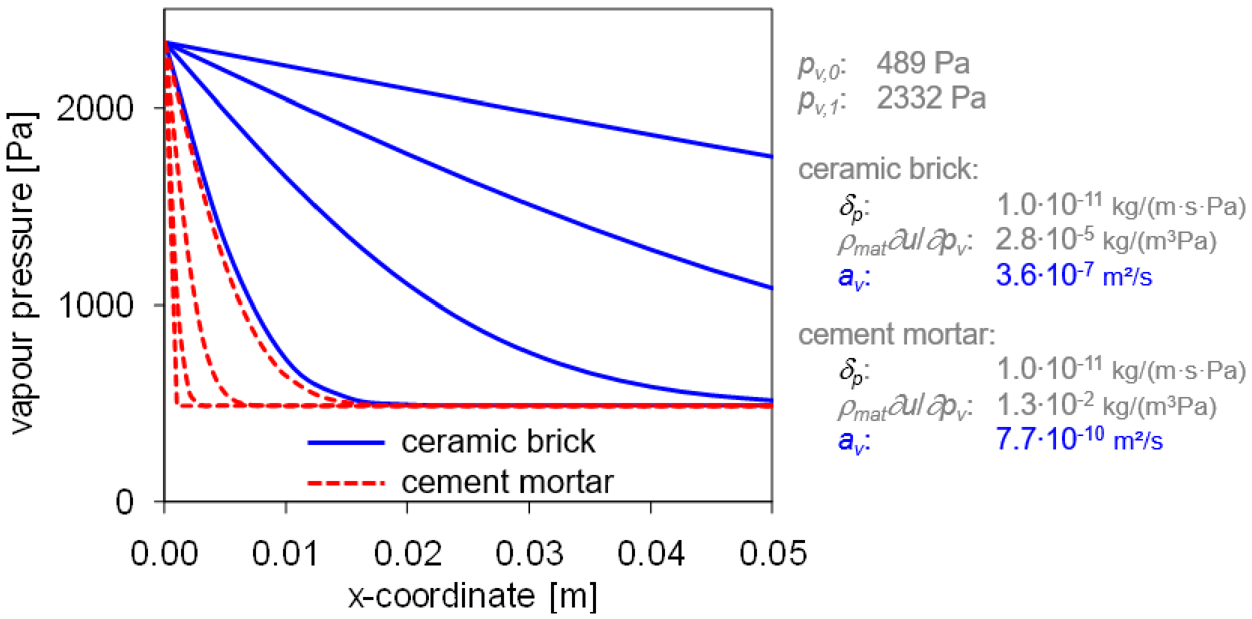

Figure 8.2 Vapor pressure profiles 1 min, 10 min, 1 hour, 6 hours after the vapor pressure at the surface increases fom $p_{v,0}$ to $p_{v,1}$.

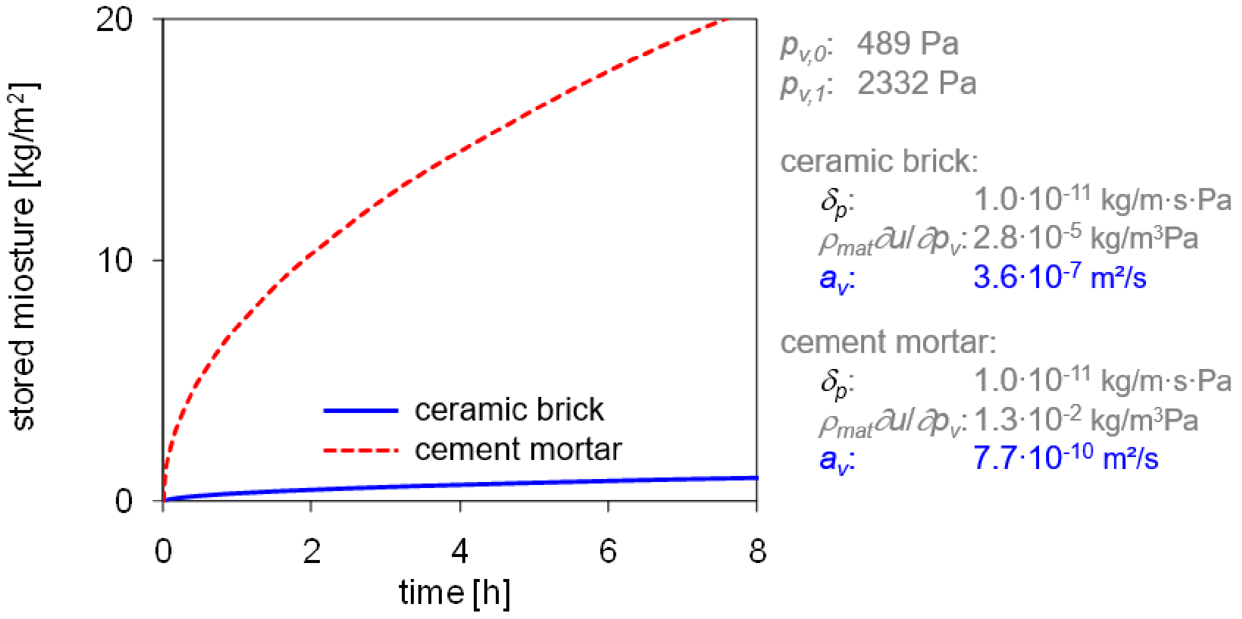

Figure 8.3 Total mass of accumulated moisture in the materials from Figure 8.2 over time.

8.4 Distributed solutions, harmonic change of surface vapor pressure

A similar story can be told, also for the semi-infinite slab, in the case that the surface vapor pressure does not change in a step from one level to another but continues to vary in a harmonic (e.g. sinusoidal) evolution with time. $p_{v,0}$ is the base level of the surface vapor pressure (at $x = 0$), and $p_{v,1}$ now indicates the amplitude of the periodic variation, which has period t_p

$$p_v(0,\ t) = p_{v,0} + p_{v,1} sin(2\pi t / t_p) \tag{8.36}$$

The vapor pressure at a depth *x* within the material at time *t*, can be calculated as (see Figure 8.4):

$$p_v(\mathrm{x}, \mathrm{t}) = p_{v,0} + p_{v,1} \cdot \exp\left(\frac{-\mathrm{x}}{d_{p,v}}\right) \cdot \sin\left(\frac{2\pi t}{t_p} - \frac{\mathrm{x}}{d_{p,v}}\right) \tag{8.37}$$

Where

$d_{p,v}$ is the moisture penetration depth for harmonic exposure as explained below, m

At a certain time, the accumulated mass of moisture taken up by the slab can be calculated as (see Figure 8.5):

$$m(t) = A_{mat}\ b_v \sqrt{\frac{t_p}{2\pi}}\, p_{v,1} \cos\left(\frac{2\pi t}{t_p} + \frac{\pi}{4}\right) \tag{8.38}$$

The moisture penetration depth in this case indicates the depth at which the amplitude the vapor pressure variations has been reduced to certain fraction of the amplitude at the surface. If the fraction is 36.7 %, we have the depth which is most often referred to as the moisture penetration depth for periodic variation, and which was referred to in Equation 8..39 as $d_{p,v}$:

$$d_{p,v} = d_{p,36.7\%,harmonic} = \sqrt{\frac{\delta_p t_p}{\pi\, \rho \frac{\partial u}{\partial p_v}}} \tag{8.39}$$

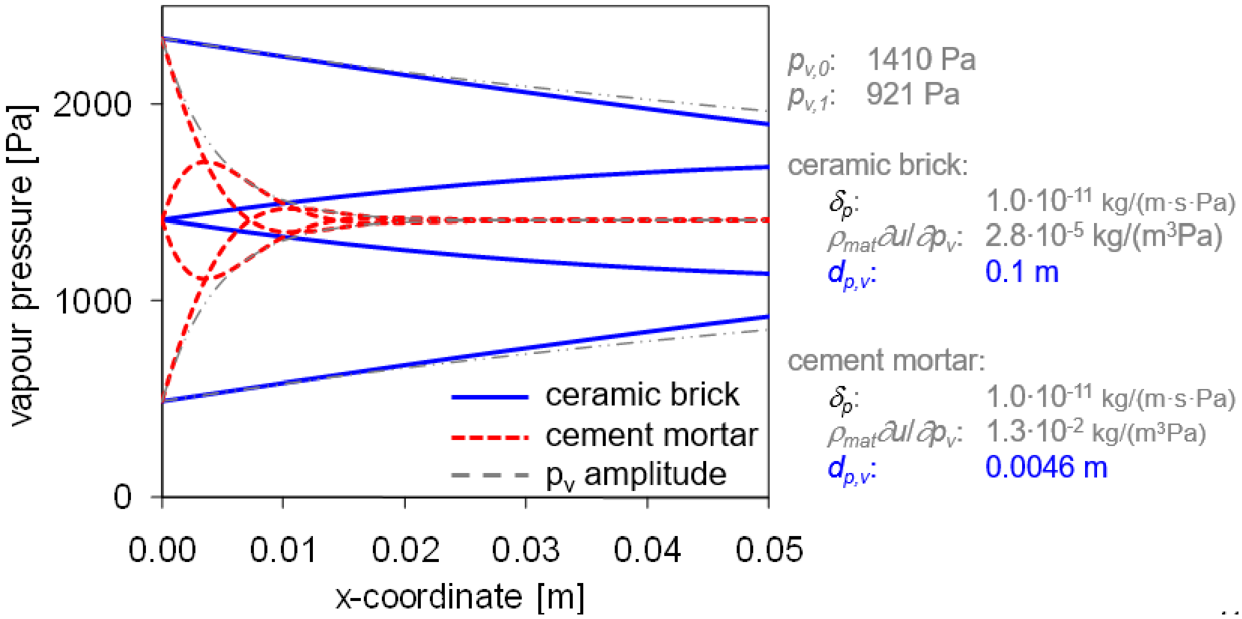

Figure 8.4 Vapor pressure profiles at 6, 12, 18 and 24 hours for harmonic daily variation of the surface vapor pressure with mean value $p_{v,0}$ and amplitude $p_{v,1}$.

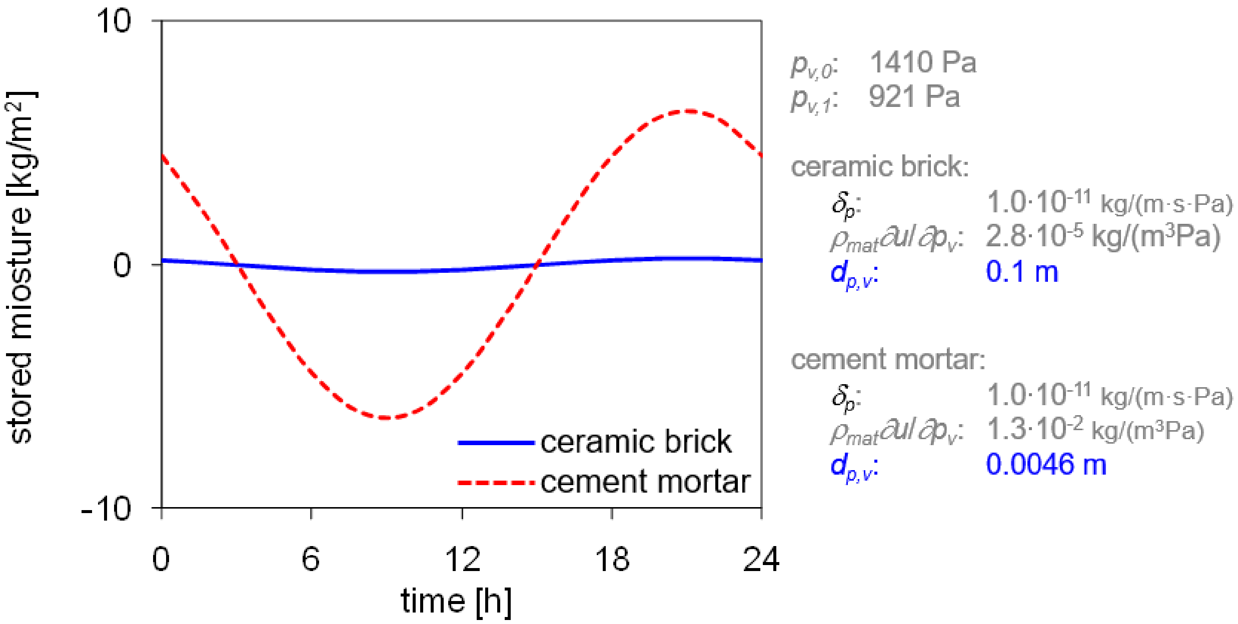

Figure 8.5 Total mass of accumulated moisture in the materials from Figure 8.4 as it varies with time.

8.5 Room with moisture buffer in the walls:

It is now possible to consider the humidity variation in a room when also considering the transient moisture uptake and release from the materials that are in contact with the room air. Two common types of models exist, which are referred to as:

- Effective Moisture Penetration Depth model (EMPD)
- Effective Capacitance model (EC)

8.5.1 EMPD-MODEL

Response of materials is approximated with a single-layer lumped model, with a thickness equal to the penetration depth $d_{p,v}$:

$$A_{mat} d_{p,v} \rho_{mat} \frac{\partial u}{\partial p_v} \frac{dp_{v,mat}(t)}{dt} = A_{mat} \frac{p_{v,i}(t) - p_{v,mat}(t)}{1/\beta_p + d_{p,v}/(2\delta_p)} \qquad (8.40)$$

Where

$p_{v,i}$	vapor pressure of room air [Pa]
$p_{v,mat}$	vapor pressure in the material at depth $d_{p,v}$, from the exposed surface [Pa]
β_p	convective surface transfer coefficient for vapor [kg/(m^2·s·Pa)]
δ_p	vapor permeability of the material [kg/(m·s·Pa)]

Term to be added to the vapor balance for the interior environment is here the blue one:

$$\frac{V_a}{R_v T_i} \frac{dp_{v,i}(t)}{dt} = \mathrm{K} - A_{mat} \frac{p_{v,i}(t) - p_{v,mat}(t)}{1/\beta_p + d_{p,v}/(2\delta_p)} \qquad (8.41)$$

Figure 8.6 illustrates the effect of this moisture buffering on the room vapor pressure.

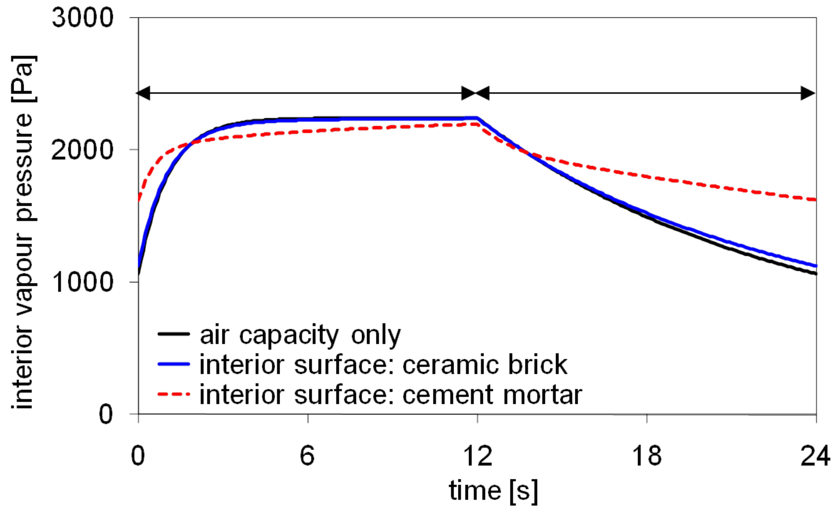

Figure 8.6 Response of interior vapor pressure, coupled to mortar/brick walls.

8.5.2 EC-MODEL

Another simple way of taking into account for the moisture capacity of material layers in contact with the indoor air is to add their capacity to capacity of zone air:

$$\left(\frac{V_a}{R_v T_i} + A_{mat} d_{p,v} \rho_{mat} \frac{\partial u}{\partial p_v}\right)\frac{dp_{v,i}}{dt} = G_{vp} + \frac{G_{a,vol}}{R_v T_i}\left(p_{v,e} - p_{v,i}\right) \tag{8.42}$$

The EC-model thus assumes that the vapor pressure in the zone air and in the material layers (up to $d_{p,v}$ from the material surface) is always the same (walls always in equilibrium with air)

9 WHOLE BUILDING HEAT, AIR AND MOISTURE (HAM) TRANSFER

9.1 Introduction

The heat and moisture behavior of building envelopes is an important aspect of the overall performance of a building. Today building design criteria are: (a) energy efficiency, (b) minimization of environmental impact and (c) protection of the health and safety of the inhabitants. While critical information can be obtained by investigating the one to one relationships of a building envelope to interior and exterior environments, the total behavior of the actual whole building is not accounted for. Simultaneous heat and mass transfer between building envelopes and indoor air is complicated and expensive to measure in laboratory or field experiments. Numerical modeling becomes an attractive alternative as it is important in understanding and extrapolating experimental results, as well extending and optimizing building performance. During the past ten years, a number of computer codes/models have been developed and validated worldwide for analysis the hygrothermal transport phenomena through a building enclosure exposed to the exterior environment (Trechsel, 2001). However, few models incorporate the critical hygrothermal interactions between the indoor air and the building envelope.

Furthermore, in most applications, building envelope designers attempt to predict the hygrothermal performance of an individual building envelope, for example a wall, roof or basement by uncoupling the system not only to the interior environment but the interactions of the other envelope components to both the exterior and interior environments. This one-to-one interaction of a small part (section of a wall system perhaps) of a building is termed today as state-of-the-art. The stand-alone analysis of specific envelope parts is important in understanding the influences of various controlling elements in terms of their effect on the hygrothermal performance of the envelope, but provides limited performance information on the overall heat and mass transfer of a building. An iterative open loop approach of complete hygrothermal analysis of a building is demonstrated which requires the direct coupling of all building envelope systems with the interior environment and mechanical systems (HVAC) and the exterior environmental loads

The objective of this chapter is to develop a model for predicting transient thermal and moisture transfer behavior in air-conditioned buildings including building envelopes and indoor air. The whole building heat and moisture transfer model takes into account the main hygrothermal effects: moisture sources and sinks inside a room, moisture input from the envelope, diffusion and vapor sorption-desorption at the exterior and interior wall surfaces, heat sources and sinks inside the room, heat input from the envelope, the solar energy input through walls and windows and hygrothermal sources and sinks due to air-conditioning systems etc. The coupled system model is implemented in MATLAB-Simulink, and is also validated by using a series of published testing tools. Fig. 12.1 depicts the concept of such an integrated model where balance equations for the interior space and the different envelope parts have to be solved simultaneously.

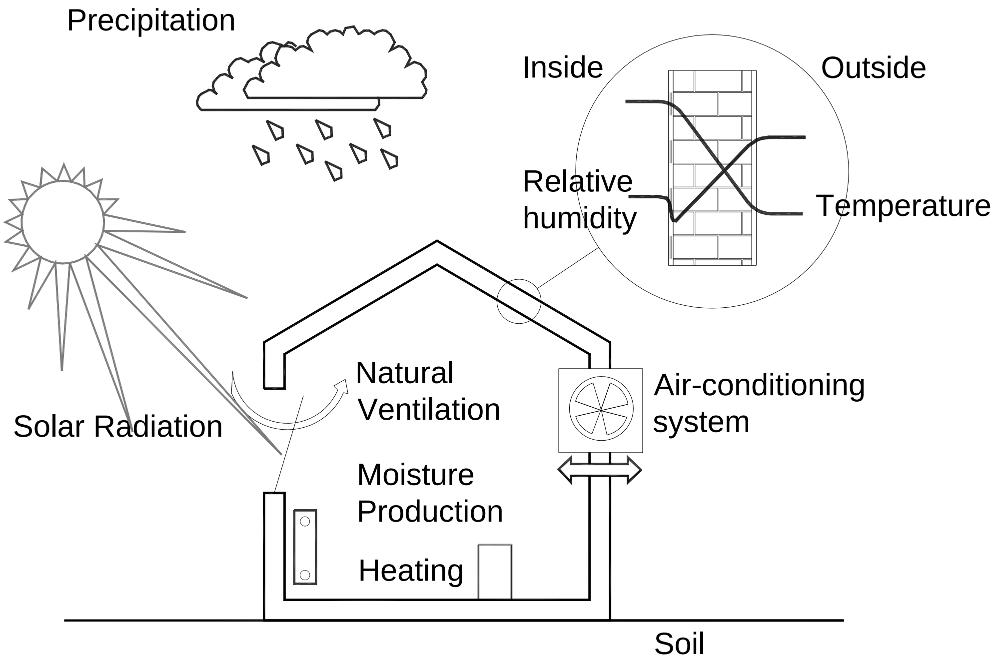

Figure 9.1 Whole building heat and moisture transfer conception (Künzel et al., 2005)

9.2 Mathematical modeling

9.2.1 HEAT AND MOISTURE BALANCE IN AIR-CONDITIONED SPACE

Heat balance

Thermal model of the room is based on the WAVO model described by de Wit (2000). The model is developed by these assumptions:

1. the room air has the uniform temperature,
2. the surface coefficients for convection and radiation are constant,
3. the view factors are approximated with the integrating sphere values (long wave radiation is equally distributed over the walls),
4. all radiative heat input (short wave and emitted long wave) is distributed in such a way that all surfaces except windows (glazing) absorb the same amount of that energy per unit of surface area.

(1) Heat flow to the room

Transmission heat losses:

$$Q_{construction} = \sum_{i=1}^{Snr} \frac{A_i \cdot \left(T_{a,in} - T_{surf,i}\right)}{R_i} \tag{9.1}$$

Where, S_{nr} is the number of attached construction blocks, R is the heat resistant ($m^2K^{-1}W^{-1}$).

Ventilation heat losses:

$$Q_{ventilation} = \rho_a \cdot c_p \cdot \sum_{i=1}^{Sysnr+Snr} g_{a,i} \left(T_{a,ext,k} - T_{a,in}\right) \tag{9.2}$$

Where, S_{ysnr} is the number of the attached system blocks. g_a are all positive air flows to the room ($m\ s^{-1}$).

(2) Heat sources in the room

Depending on the heating (cooling) plant type, the heat supply is split into convective and radiative part. This is also done for the casual and solar gains.

Solar heat gains coming through glazing areas:

$$Q_{solar} = \sum_{i=1}^{Snr} q_{sun,i} A_i \tag{9.3}$$

Where, $q_{sun,i}$ is the transmitted solar energy (J). A_i is the area of the surface number I (m^2).

Heat gains coming from the heating system or casual gains (they are already divided in a convective and a radiation part at the input to the zone 1):

$$Q_{gains} = \sum_{i=1}^{Gnr} \left(Q_{gains,conv} + Q_{gains,rad}\right) \tag{9.4}$$

Where, G_{nr} is the number of attached gain blocks.

The convective part of all heat sources Φ_c is:

$$\Phi_c = CF_{sol} \cdot Q_{solar} + Q_{gains,conv} \tag{9.5}$$

where CF_{sol} represents the convective fraction of solar heat gains.

The radiation part of all heat sources Φ_r is:

$$\Phi_r = (1 - CF_{sol}) \cdot Q_{solar} + Q_{gains,rad} \tag{9.6}$$

The total energy balance equation can be expressed as follows:

$$\rho_a c_p \frac{dT_{a,in}}{dt} = Q_{constructions} + Q_{ventilation} + \Phi_c \tag{9.7}$$

Where, c_p is the air volume heat capacity (J kg^{-1} K^{-1}).

Moisture balance

(1) Moisture flows in the room

Vapor diffusion from/to construction elements:

$$J_{construction} = \sum_{i=1}^{Snr} \frac{A_i \cdot \left(v_{a,in} - v_{surf,i}\right)}{R_{p,i}} \tag{9.8}$$

Where, $R_{p,i}$ is the vapor diffusion resistant (s m^{-1}). v_{surf} is the vapor content at the construction surface (kg m^{-3}). $v_{a,in}$ is the vapor content of the indoor air (kg m^{-3}).

Vapor infiltration through ventilation systems:

$$J_{ventilation} = \rho_a \cdot \sum_{i=1}^{Sysnr+Snr} g_{a,k} \cdot \left(v_{a,ext,k} - v_{a,in}\right) \tag{9.9}$$

Where g_a are all positive air flows to the room (m s^{-1}), $v_{a\,ext.}$ is the vapor content of the outdoor air (kg m^{-3}).

(2) Moisture gains (from people, appliances, etc.):

$$J_{gains} = \sum_{i=1}^{Gnr} \quad \text{constant or function defined by user} \tag{9.10}$$

(3) The moisture balance equation reads

$$V \frac{dv_{a,in}}{dt} = J_{constructions} + J_{ventilation} + J_{gains} \tag{9.11}$$

Where, *V* is the air volume (m^3).

The moisture content in the air is limited to saturation value $v_{a,sat}(T)$. In the case that this level is exceeded, it is assumed that the condensed amount of water is taken by some other sink, as well as released heat.

9.2.2 HEAT AND MOISTURE TRANSFER AT THE EXTERIOR SURFACE

The model assumes that the external wall surface is exposed to convective heat and moisture exchange with outdoor air, incident solar radiation, and long wave radiation, transfer of latent heat, air and rain. All outdoor influences are lumped into equivalent outdoor surface air temperature.

Moisture transfer

The total moisture flux (vapor flux) $j_{v.ext}$ (kg m^{-2} s^{-1}) at the exterior surface of buildings can be divided into two cases.

(1)when the air is flowing into the structure:

$$j_{v,ext1} = \beta_{ext}(v_{a,ext} - v_{surf.ext}) + g_a v_{a,ext} \tag{9.12}$$

(2)when the air is flowing out from the structure:

$$j_{v,ext2} = \beta_{ext}(v_{a,ext} - v_{surf.ext}) + g_a v_{surf,ext} \tag{9.13}$$

where, $v_{a,ext}$ is the outdoor ambient vapor content (kg m^{-3}), $v_{surf,ext}$ is the vapor content at the exterior surface of the wall (kg m^{-3}), β_{ext} is the convective moisture transfer coefficient at the exterior surface (m s^{-1}).

Suction of water from driving rain only takes place for capillary active surfaces. The moisture content at surface is limited to w_{cap}.

Heat transfer

The heat flux q_{ext} (W m^{-2} s^{-1}) at the exterior surface can be expressed as:

(1) when the air is flowing into the building envelope:

$$q_{ext1} = \alpha_{e,ext}(T_{ext}^{eq} - T_{surf,ext}) + g_a \rho_a c_p T_{a,ext} + j_{v,ext} h_{LV} \tag{9.14}$$

(2) when the air is flowing out from the building envelope:

$$q_{ext2} = \alpha_{e,ext}(T_{ext}^{\ \ eq} - T_{surf,ext}) + g_a \rho_a c_p T_{surf,ext} + j_{v,ext} h_{LV} \qquad (9.15)$$

where, an effective heat transfer coefficient $\alpha_{e,ext}$ has been introduced:

$$\alpha_{e,ext} = \alpha_{c,ext} + \alpha_r$$

The convective heat transfer coefficient $\alpha_{c,ext}$ depends on air flow velocities and temperature differences between the surface and the air. The radiative heat transfer coefficient α_r depends on the temperature of the surroundings (sky temperature) and the temperature of the surface as well as the emissivity of the surface. The equivalent temperature is:

$$T_{ext}^{\ \ eq} = T_{a,ext} + \frac{1}{\alpha_{e,ext}}\left(I_{sol} \cdot \alpha_{sol} + \left(T^r - T_{a,ext}\right) \cdot \alpha_r\right) \qquad (9.16)$$

where, the solar radiation component, parallel to the normal of the structure, including both diffuse and direct radiation (global radiation), is denoted by I_{sol} (W m^{-2}). The ambient air temperature is $T_{a,ext}$. The temperature T^r depends on the surrounding surfaces and the atmosphere that has a long wave radiation exchange with the outer surface. The solar radiation terms must be obtained from metrological registrations, taken into account possible shading due to local conditions. In a similar way the radiation temperature T^r, can be calculated using the cloudiness, the air temperature, the inclination of the building envelope component and the local surroundings.

9.2.3 HEAT AND MOISTURE TRANSFER AT THE INTERIOR SURFACE

The internal wall surface is exposed to convective heat and moisture exchange, long wave radiation with other surfaces, and transfer of latent heat with inner air. All these influences are lumped into equivalent indoor surface air temperature.

Moisture transfer

The total moisture flux (vapor flux) $j_{v,in}$ (kg m^{-2}s^{-1}) at the interior surface consists of two parts:

(1) when the air is flowing into the structure:

$$j_{v,in1} = \beta_{in}(v_{a,in} - v_{surf,in}) + g_a v_{a,in} \qquad (9.17)$$

(2)when the air is flowing out from the structure:

$$j_{v,in2} = \beta_{in}(v_{a,in} - v_{surf,in}) + g_a v_{surf,in} \qquad (9.18)$$

where, $v_{a,in}$ is the indoor ambient vapor content (kg m^{-3}), $v_{surf,in}$ is the vapor content at the interior surface of the wall (kg m^{-3}), β_{in} is the convective moisture transfer coefficient at the interior surface (m s^{-1}).

Heat transfer

The heat flux q (W m^{-2}s^{-1}) at the interior surface also consists of two cases:

(1) when the air is flowing into the building envelopes:

$$q_{in1} = \alpha_{e,in}(T_{in}^{eq} - T_{surf,in}) + g_a \rho_a c_p T_{a,in} + j_{v,in} h_{LV} \tag{9.19}$$

(2) when the air is flowing out from the building envelopes:

$$q_{in2} = \alpha_{e,in}(T_{in}^{eq} - T_{surf,in}) + g_a \rho_a c_p T_{surf,in} + j_{v,in} h_{LV} \tag{9.20}$$

In the current research, the indoor equivalent temperature T_{in}^{eq} equals to the indoor air temperature.

9.3 Model validations

9.3.1 OVERVIEW

The testing and validation of a new simulation model requires reliable test suites with well documented initial and boundary conditions, as well as accurate material properties. Generally, the validation methodology includes three different kinds of tests: (1) Analytical verification, in which the output from the program is compared to the result from a known analytical solution. (2) Comparative testing, in which a program is compared to itself or to other programs. (3) Empirical validation, in which calculated results from a program are compared to monitored data from a real structure, test cell, or laboratory experiment.

International Energy Agency (IEA) has published a series of test suites for whole building energy simulation, which mainly include: IEA BESTEST (1995), IEA HVAC-BESTEST (2000), and IEA ECBCS Annex 21 / SHC Task 12 etc. Recently, IEA Annex 41 has added many analysis of the indoor and building envelope moisture conditions for the BESTEST building used in IEA ECBCS Annex 21 / SHC Task 12. These published test suites are used to validate the present model. Comprehensive testing and validations are carried out. Three different test methods are presented in the chapter.

9.3.2 COMPARATIVE TESTS

In the past twenty years, many computer programs have been developed for coupled heat and moisture transfer in buildings. A critical review was carried out by Hens (1996), and a comprehensive list of studies and computer codes to quantify the hygrothermal transport in building was listed in their reports. However, most of these codes are not commercially available, and are only for internal use at a given research facility or university. In this section, we will first briefly discuss some recent computer codes that are available in public domain and validated by experiments.

The simulation tools used in this comparative test are EnergyPlus, TRNSYS, and HAM-VIE. EnergyPlus and TRNSYS are two of the most widely used building simulation codes. They have been validated and tested worldwide. HAM-VIE is also a computer code to predict the hygrothermal transfer in buildings, which was developed by the Vienna University of Technology (Technische Universität Wien, TUW). The IEA BESTEST building from IEA SHC Task 21 & ECBCS Annex 21 was used in the test. The geometry of the IEA BESTEST building is shown in Fig. 5.25. There is an internal moisture gain of 500 g h^{-1} from 9:00 - 17:00 every day. The air change rate is always 0.5 ach. The heating and cooling control keeps the indoor temperature between 20 and 27ºC with an infinite capacity. The system is a 100% convective air system and the thermostat is on air temperature. Table 1 shows the wall geometry of the lightweight case (Case600_open). Detailed material properties can be found in Annex A and also in the BESTEST report (IEA 2005). The room is supposed to be located in Denver. The weather file is provided.

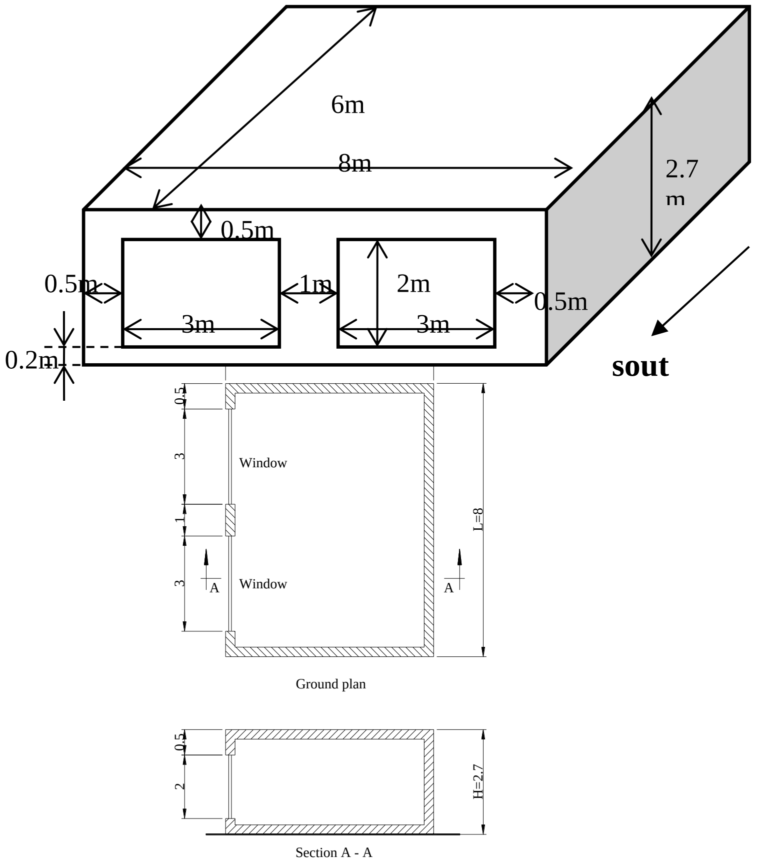

Figure 9.2 BESTEST base case building

Table 9.1 Wall geometry of Lightweight case (600-Open) (IEA 2005)

Component	Area (m^2)	Structure	Thickness (m)
Exterior wall (inside to outside)	63.600	Wood panels	0.012
		Cellulose insulation	0.066
		Wood siding	0.009
Floor (inside to outside)	48.000	Timber flooring	0.025
		Insulation	1.003
Roof (inside to outside)	48.000	Wood panels	0.010
		Cellulose insulation	0.1118
		Roof deck	0.019

It is a benchmark work. The simulated result of EnergyPlus is reported by the Oak Ridge National Laboratory, USA. The result of TRNSYS is reported by the Technische Universität Dresden, Germany. And the result of HAM-VIE is reported by the Vienna University of Technology, Austria. All these data are obtained from (IEA 2005). The calculations were run for as many years as it was necessary to achieve quasi-steady conditions. The results were reported for the last year of calculation. The calculated indoor relative humidity during one day (July 27th) from the present model and EnergyPlus, TRNSYS and HAM-VIE are presented in Fig. 9.3.

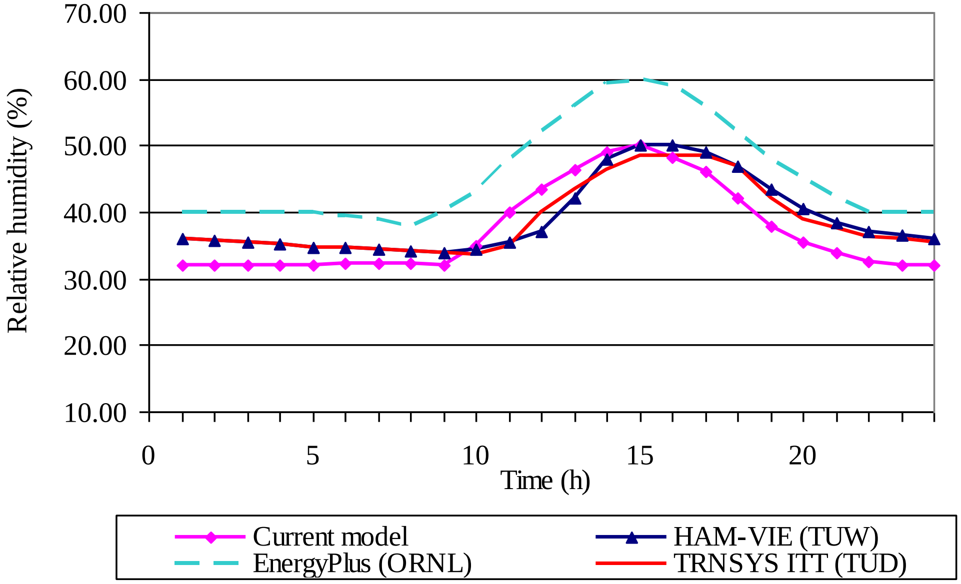

Figure 9.3 The comparison of simulated results from the present model and from other programs (July 27th)

To the current graph scale, it can be seen that there is a good agreement between the results from the present model, TRNSYS, and HAM-VIE. However, the indoor relative humidity calculated by EnergyPlus is a little bit larger than the results from other three codes. In order to well validate our model, the following analytical test and experimental tests are carried out.

9.3.3 ANALYTICAL VERIFICATION

IEA Annex 41- subtask1 (IEA 2005) also provides a collection of mathematical solutions for isothermal cases. For Case 0B, the building and its geometry is the same as that of the comparative test. Compared to the previous comparative test, the following changes are made for the analytical case:

1. The altitude is 0 m;
2. Constructions are made of monolithic aerated concrete with constant properties;
3. Tight membranes on the outside prevent loss of vapor from the building by transport all the way through the walls;
4. The exposure is completely isothermal, i.e. the same temperature outside as inside the building.
5. The building has no windows;
6. Outside and initial indoor conditions are Temperature 20°C and relative humidity is 30% RH. There are also initial conditions of materials in the constructions;
7. The environment below the building is outside air (i.e. no ground);
8. The building is shown in Fig. 9.2 (with windows that should be neglected).

A constant vapor convective surface resistance to vapor transfer of 5.0×10^7 Pa m^2 s kg^{-1} is given for the indoor boundaries. The material properties are constant and can be found in Annex B. The comparison of simulated results from the model for the periodic state of case 0B with the analytical solution provided by IEA report is presented. Perfect agreement is obtained.

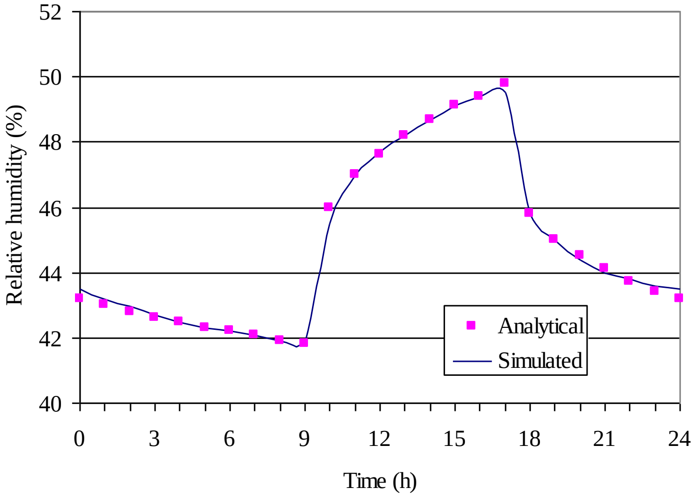

Figure 9.4 The comparison of simulated results from the model with the analytical solution

9.3.4 EMPIRICAL VALIDATION

Recently, IEA annex41-CE3 (Kristin et al. 2006) has published a series of experimental tests for the validation of the whole building hygrothermal performance. The measurements were carried out in Frauhofer-Institut Fur Bauphysik, Germany.

The test rooms have a floor area of 20 m^2 and a volume of 50 m^3. A vinyl covering was installed in order to avoid moisture flow to or from the ground. The exterior surfaces of the ceiling and partition walls are facing the conditioned space of the test building. The external walls consist of 240 mm thick brick masonry with 100 mm exterior insulation. Walls and ceiling of the rooms are coated with 12 mm standard interior plaster. The double-glazed windows are facing south. The rooms are equipped with calibrated heating, ventilation and moisture production systems. Temperature sensors and heat flux meters are also fixed to the interior surface of external walls. The tests are performed with a constant air change rate (ACH) of 0.5 h^{-1}. A basic production rate of 0.5 g m^{-3}h^{-1} is assumed with peaks in the morning and in the evening (8 g m^{-3} h^{-1} from 6:00 to 8:00 a.m. and 4 g m^{-3}h^{-1} from 4:00 to 10:00 p.m. every day). All information of the experimental set-up can be found in (Kristin et al. 2006).

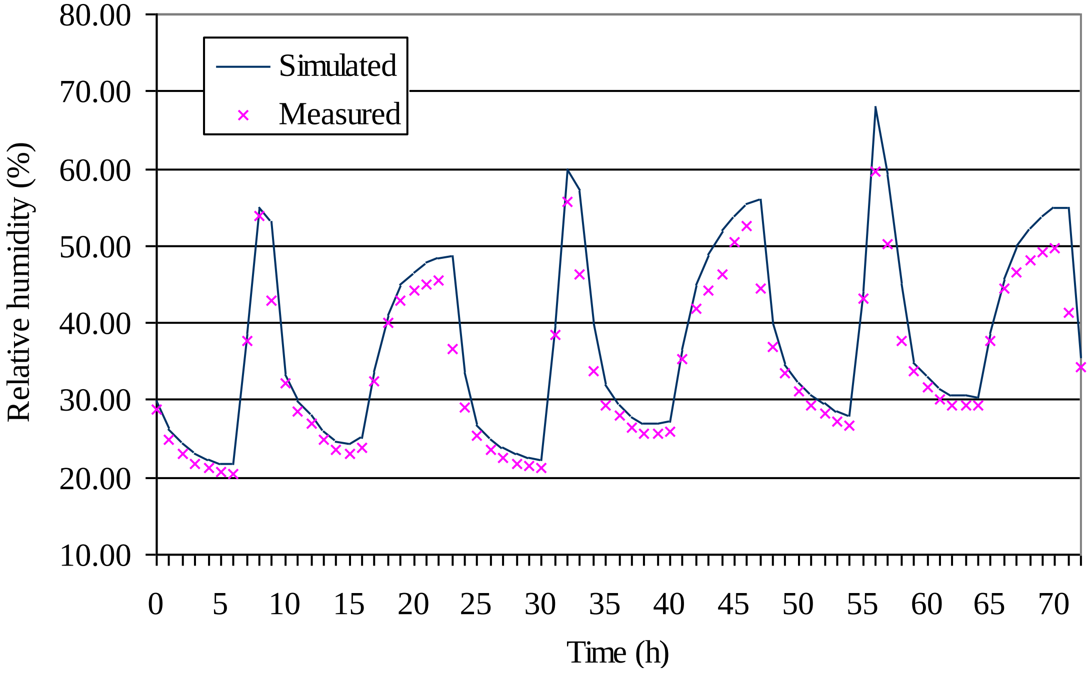

Figure 9.5 The comparison of simulated results with the measured data

(17 Jan. 2005 – 19 Jan. 2005)

Fig. 9.5 shows the comparison between experiment and simulation. The calculated indoor relative humidity is slightly larger than the measured data. It is assumed that the moisture buffering effect of the envelope retards the dynamic equilibrium in the experiment. Nevertheless, a considerably good agreement is found between the predicted results and the measures values. Consequently, it shows that the model presented above with a developed computer program is capable of simulating the whole building heat and moisture transfer.

9.4 Case study

After being validated, the model is applied to investigate the moisture transfer effect on indoor air humidity and building energy consumption under different climate. Two simulation cases are chosen. The BESTEST test room is assumed to be transferred to Hong Kong, China (hot and humid climate) and to Paris, France (Temperate climate) where it serves as a typical office room. The building geometry is presented in Fig. 9.2. The interior surfaces of the walls and ceiling are facing the conditioned space. There is no moisture flux from or to the ground. The room is occupied during the daytime from 9:00 a.m. to 5:00 p.m. and unoccupied the rest of the day. Detailed material properties can be found in the BESTEST report (IEA 2005).

In the following sections, eight different simulations will be carried out, and they are:

	Case I (Hong Kong Climate)
Case I.1	Simulation with taking into account the whole building heat and moisture transfer, and with air-conditioning system
Case I.2	Simulation without taking into account the whole building heat and moisture transfer, and with air-conditioning system
Case I.3	Simulation with taking into account the whole building heat and moisture transfer, but no air-conditioning system
Case I.4	Simulation without taking into account the whole building heat and moisture transfer, but no air-conditioning system

	Case II (Paris Climate)
Case II.1	Simulation with taking into account the whole building heat and moisture transfer, and with air-conditioning system
Case II.2	Simulation without taking into account the whole building heat and moisture transfer, and with air-conditioning system
Case II.3	Simulation with taking into account the whole building heat and moisture transfer, but no air-conditioning system
Case II.4	Simulation without taking into account the whole building heat and moisture transfer, but no air-conditioning system

In the cases of the “whole building heat and moisture transfer”, we takes into account the main hygrothermal effects: moisture sources and sinks inside a room, moisture input from the envelope, diffusion and vapor absorption-desorption at the exterior and interior wall surfaces, heat sources and sinks inside the room, heat input from the envelope, the solar energy input through windows and hygrothermal sources and sinks due to air-conditioning systems etc.

In the cases that do not take into account the whole building moisture transfer, we only include: moisture sources and sinks inside a room, heat sources and sinks inside the room, heat input from the envelope, the solar energy input through windows and hygrothermal sources and sinks due to air-conditioning systems etc. An aluminium covering was installed at the interior wall surfaces in order to avoid moisture flow to or from the room. Therefore, there is no moisture input from the envelope, no diffusion and vapor absorption-desorption at interior wall surfaces,

9.4.1 CASE I – HOT AND HUMID CLIMATE (HONG KONG, CHINA)

Hong Kong has a sub-tropical climate with hot, humid summers and warm winters. Winter lasts from January to March, the coldest month being February when the temperature averages 16°C in urban areas. Therefore, normally there is no heating system for most residential buildings in Hong Kong. In summer (May to October), the wind blows from the south, bringing in hot and humid air. Afternoon temperatures often exceed 33 °C whereas at night, temperatures generally remain around 26 °C with high humidity.

In this section, the test room used for the experimental validation is assumed to be transferred to Hong Kong, China where it serves as a typical office room. The room is occupied during the daytime from 9:00 a.m. to 5:00 p.m.; and unoccupied the rest of the day. When the room is occupied, there is an interior heat and moisture production rate of 500 W and 3 g $m^{-3}h^{-1}$ respectively. During the unoccupied period, the interior heat production decreases to 120 W and the moisture production decreases to 0.5 g $m^{-3}h^{-1}$. The set-points of working temperature and relative humidity for the air-conditioning system are 26 °C and 65% respectively. The AC system only works during the occupied period.

The simulated evolutions of the indoor temperature and relative humidity with or without taking into account the whole building moisture transfer are also presented in Figs. 9.6 – 9.9.

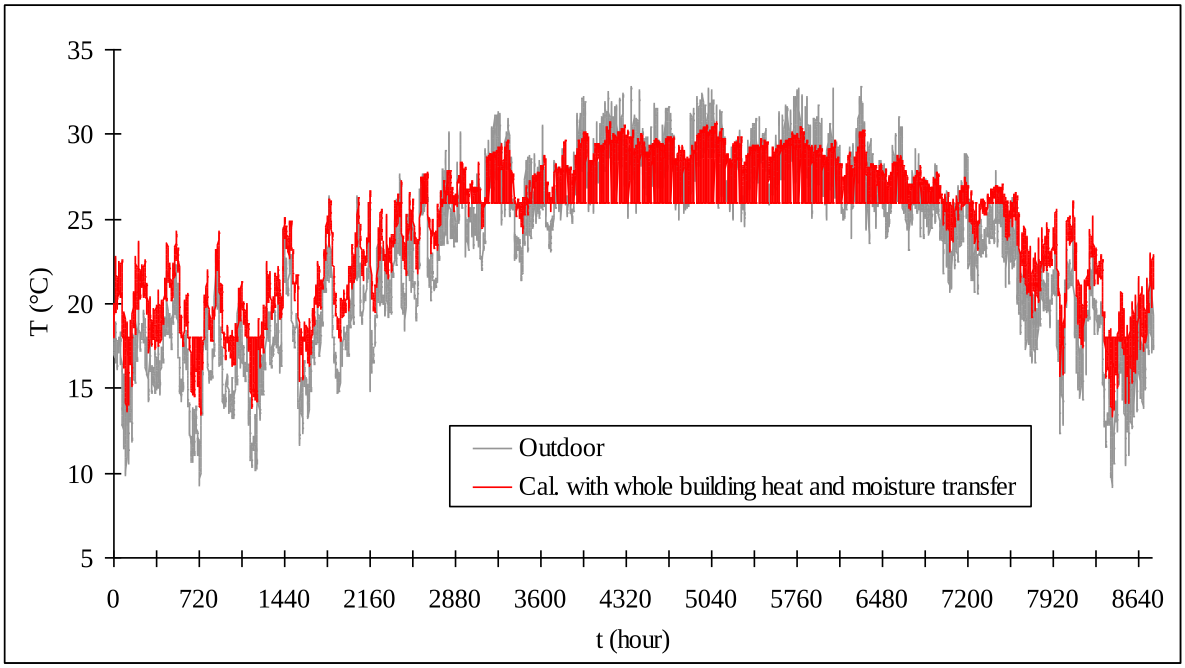

Figure 9.6 Simulated indoor temperature (Case I.1)

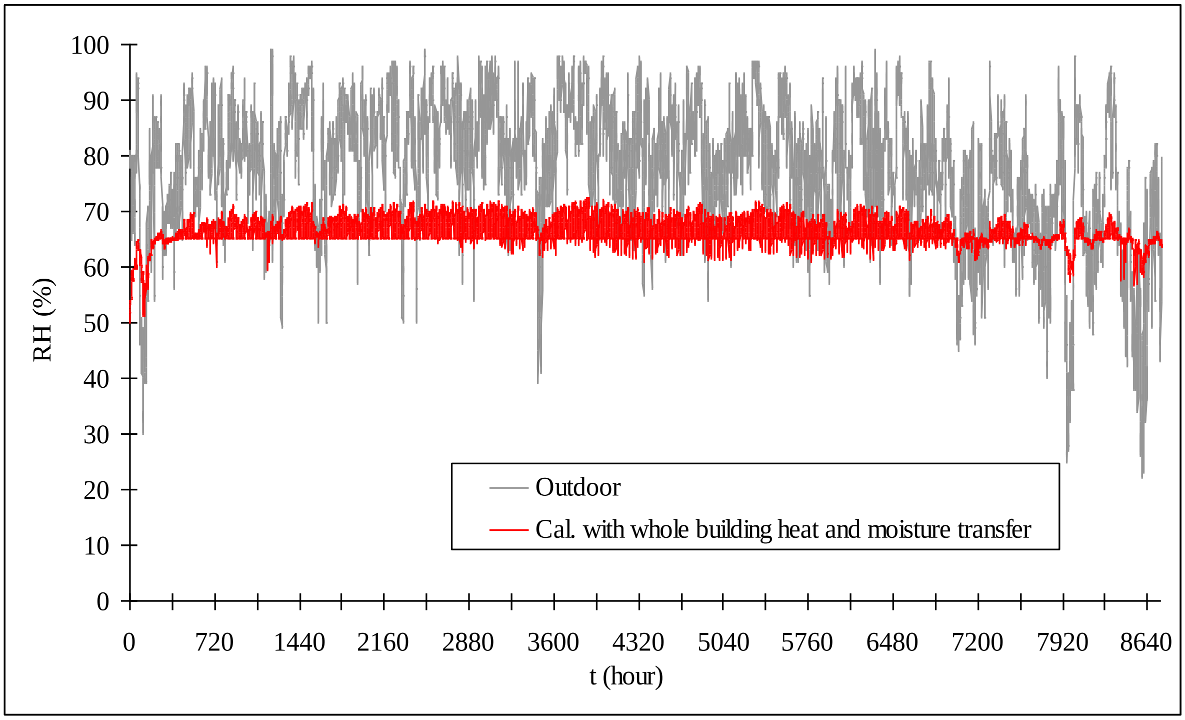

Figure 9.7 Simulated indoor relative humidity (Case I.1)

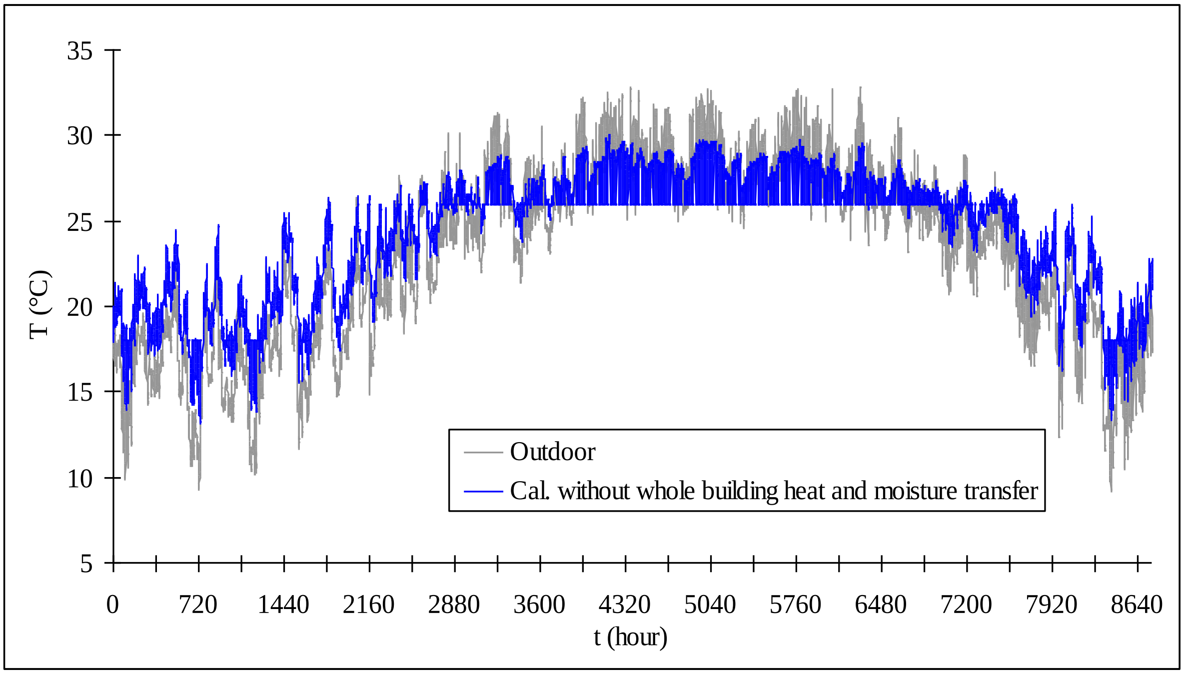

Figure 9.8 Simulated temperature (Case I.2)

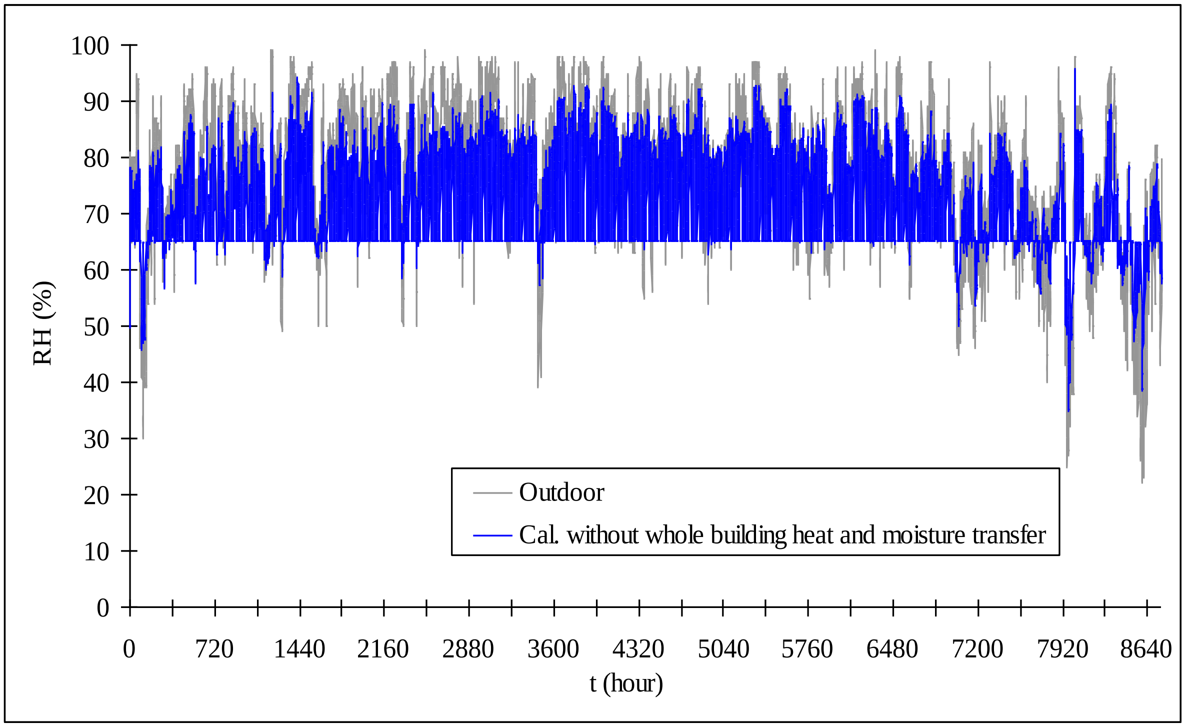

Figure 9.9 Simulated indoor relative humidity (Case I.2)

In order to clearly demonstrate the difference between the two cases, simulated indoor temperature and indoor relative humidity of one week in summer and one week in winter are presented in Figs. 9.10 – 9.13.

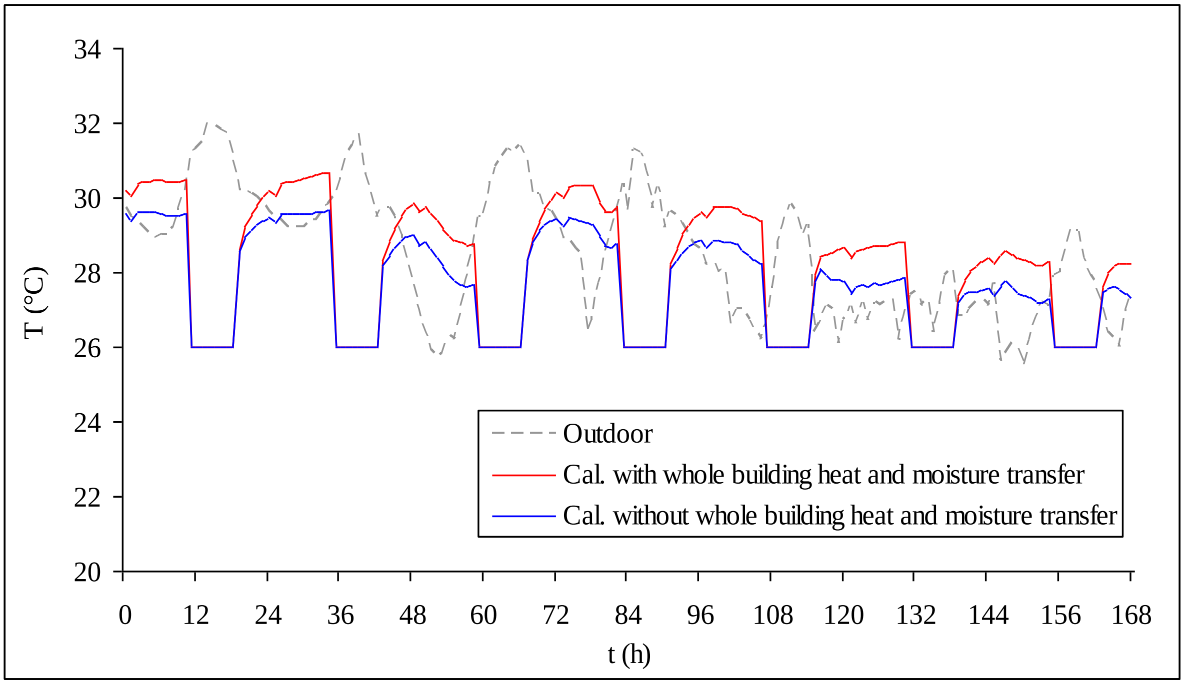

Figure 9.10 Simulated indoor temperature (August 1st -7th) in Hong Kong

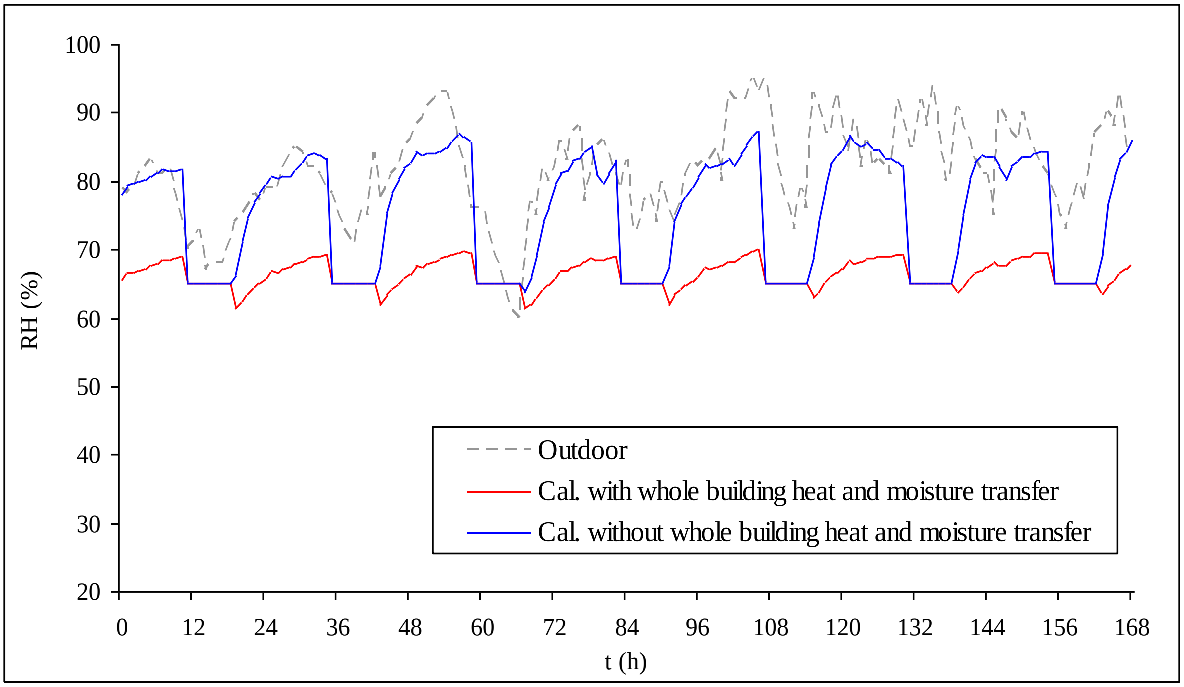

Figure 9.11 Simulated indoor relative humidity (August 1st -7th) in Hong Kong

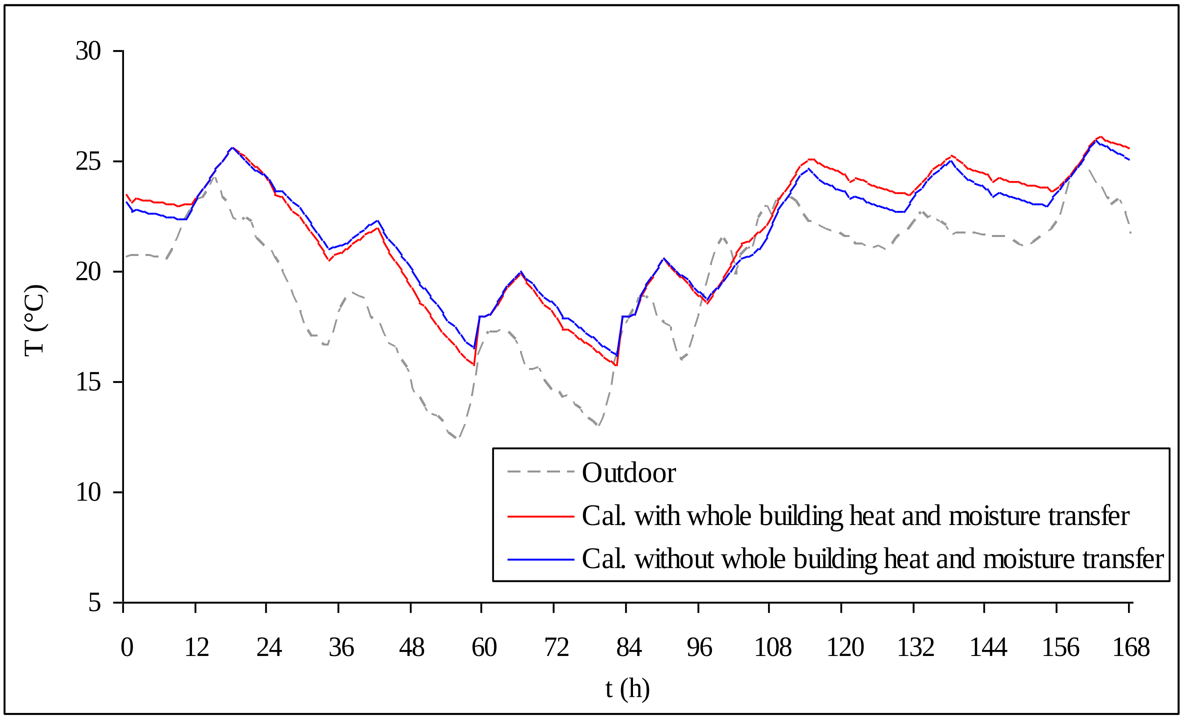

Figure 9.12 Simulated indoor temperature (December 1st -7th) in Hong Kong

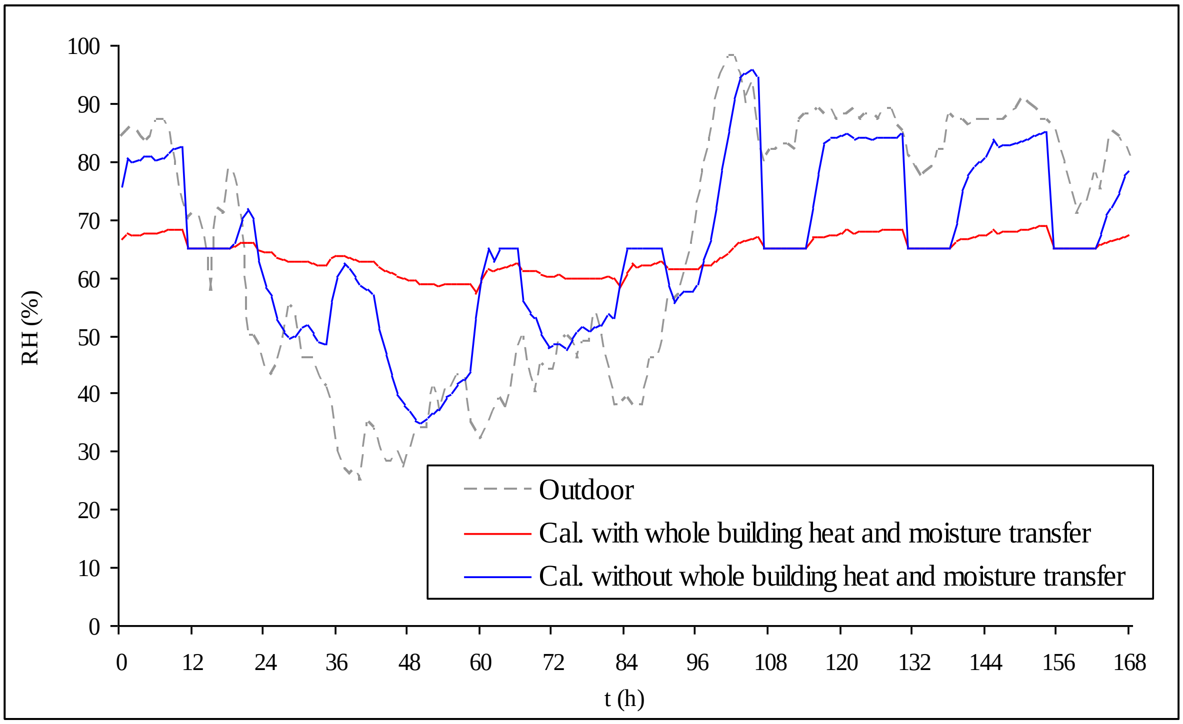

Figure 9.13 Simulated indoor relative humidity (December 1st -7th) in Hong Kong

The results reveal that moisture transfer through the building envelope and vapor sorption-desorption at the interior wall surface have a great effect on the indoor relative humidity. In the case that includes these phenomena, the indoor relative humidity stays below 70% during the shut-off period of air-conditioning system in summer. However, in the case without taking into account these phenomena, the maximum indoor relative humidity exceeds 80% during the shut-off period every day in summer. Even in winter, the indoor relative humidity exceeds 80% four times per week. According to Sedlbauer (2001), the risk of mold formation increases when the relative humidity in a room goes beyond 80% several times a week. An extra dehumidification procedure might be used.

Fig. 9.13 shows that the indoor air temperature is nearly the same for both cases. This means the moisture transfer in the building construction has a significant influence on the latent cooling load while does not affect the sensible cooling load too much. The similar results can also be found in (Künzel et al., 2005) and (Mendes et al., 2003).

As a reference, simulations of the same room without HVAC system were also carried out. The interior conditions and outdoor climate are the same as the case with HVAC system. The results are presented in Figs. 9.14 – 9.17.

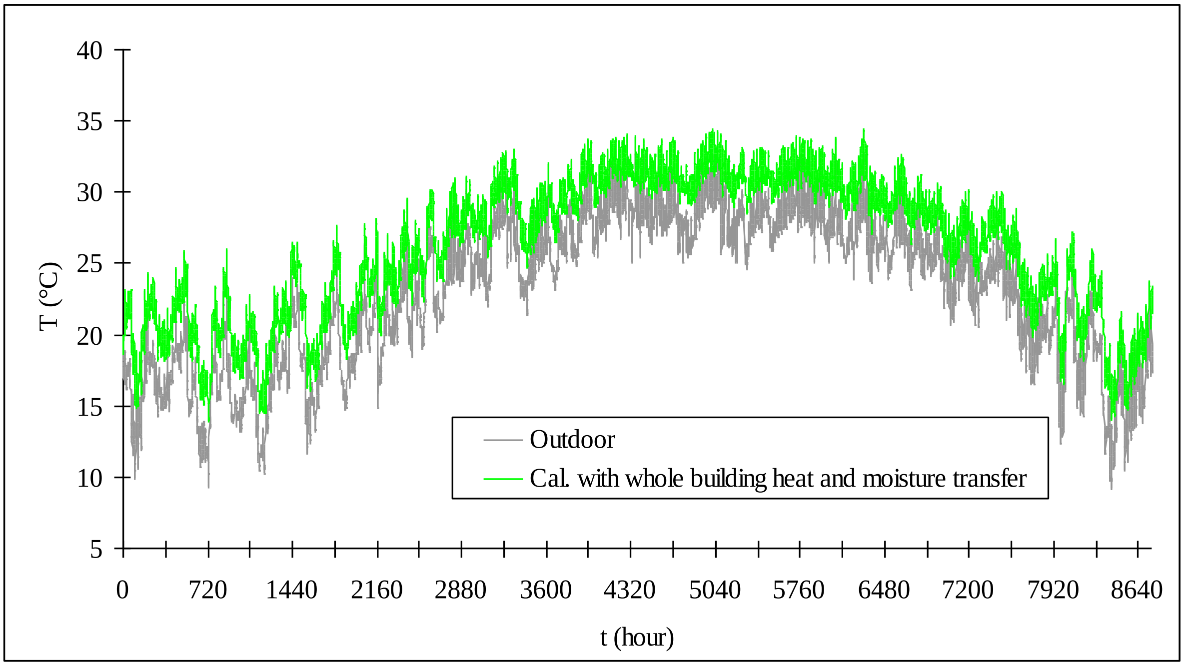

Figure 9.14 Simulated indoor temperature (Case I.3)

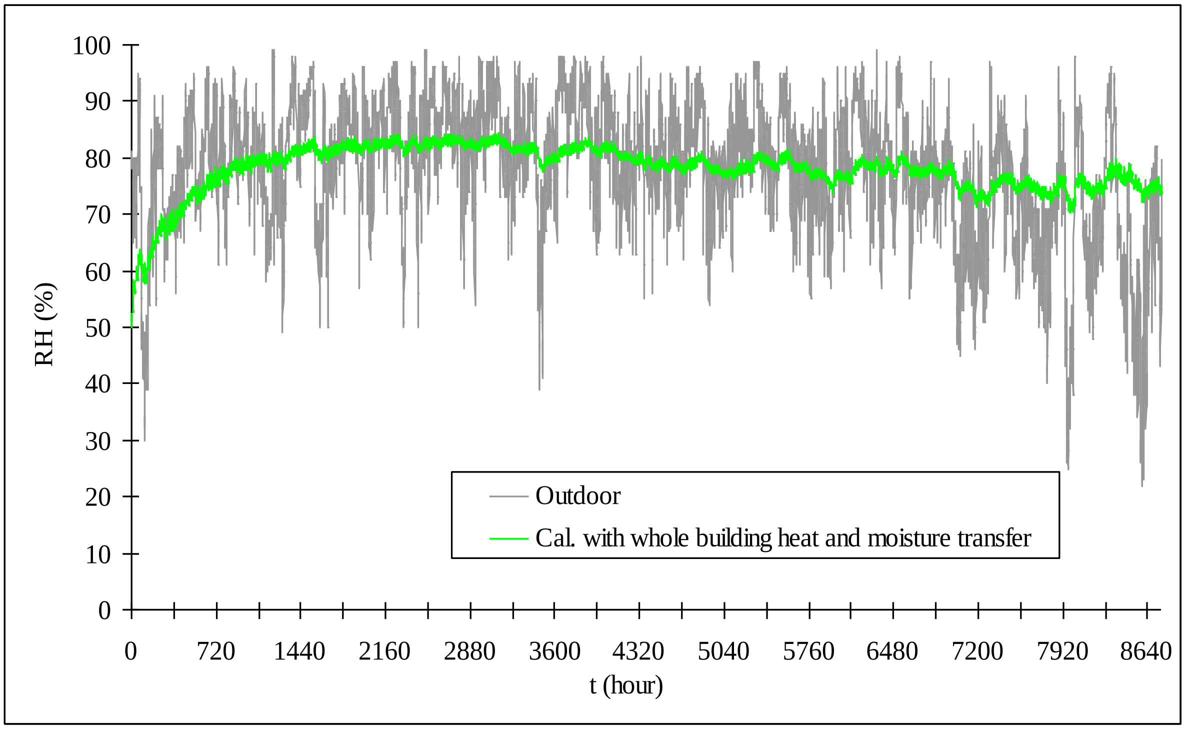

Figure 9.15 Simulated indoor relative humidity (Case I.3)

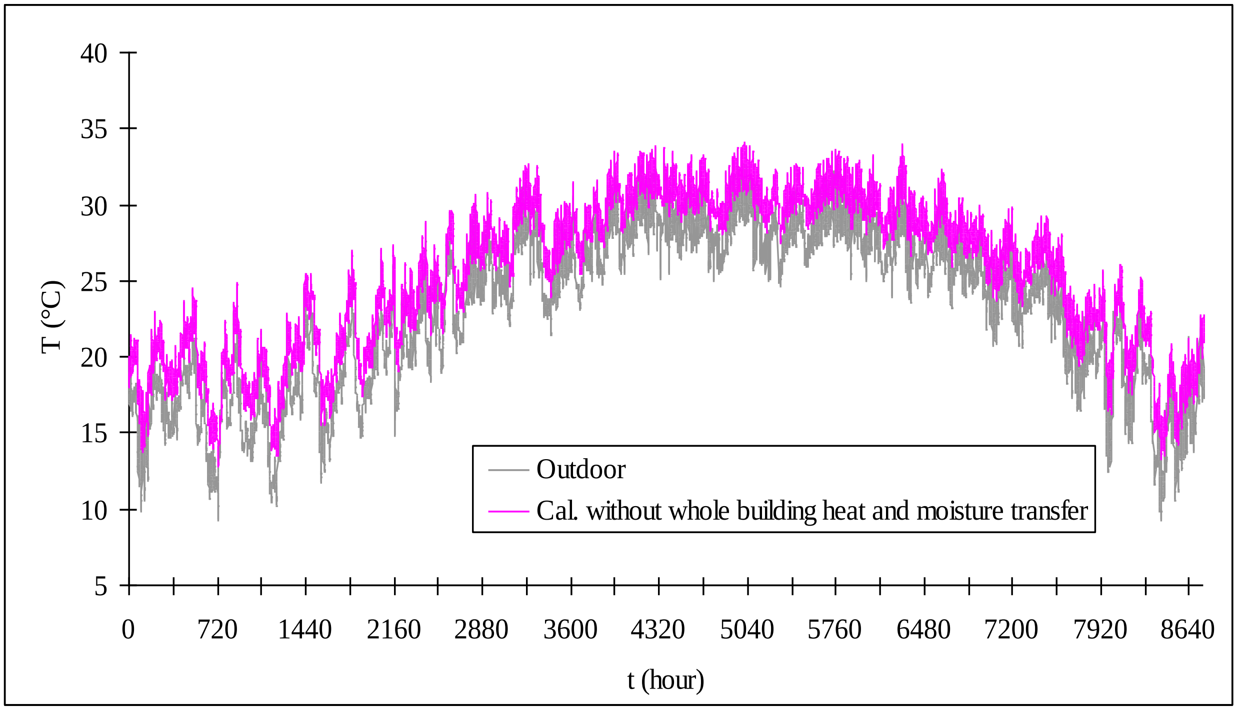

Figure 9.16 Simulated indoor temperature (Case I.4)

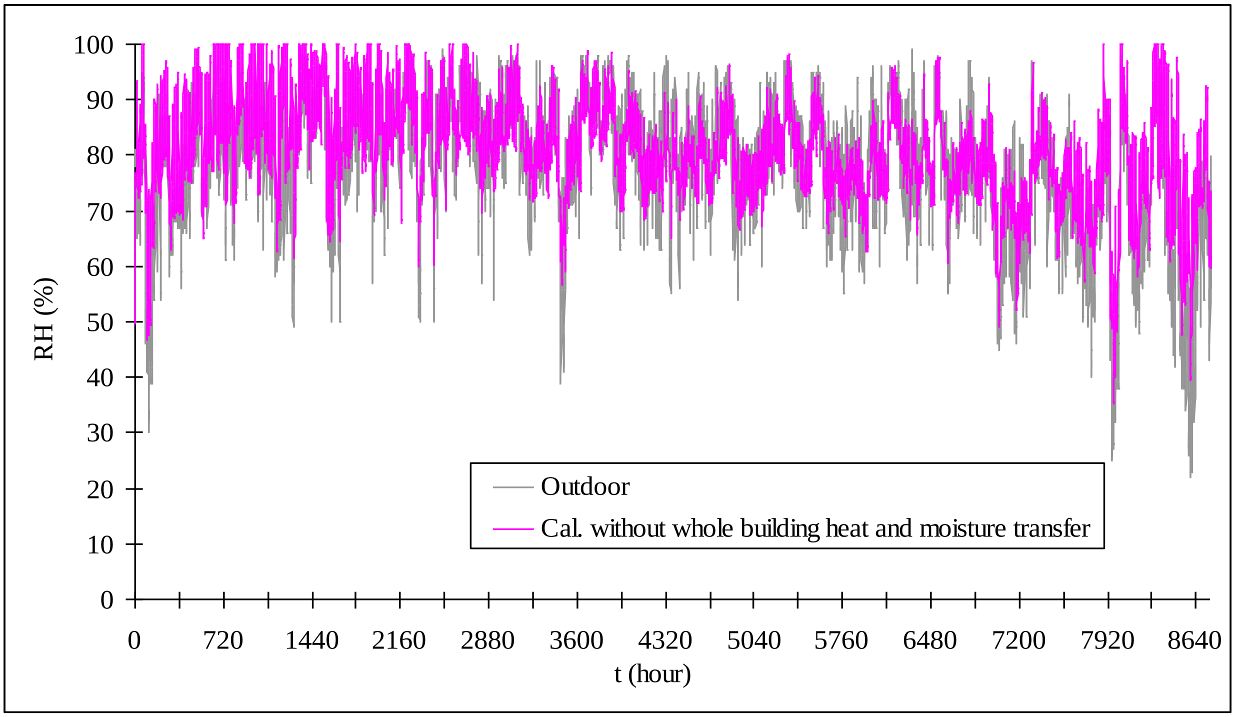

Figure 9.17 Simulated indoor relative humidity (Case I.4)

9.4.2 CASE II --TEMPERATE CLIMATE (PARIS, FRANCE)

The hot and humid climate of Hong Kong may not be representative for the temperate climate in Europe. Therefore, the hygrothermal simulation is repeated for Paris, France

Paris has a temperate climate. The daily average temperature during the summer doesn't exceed 20 °C. Therefore, most French residential buildings are only equipped with heating system and ventilation system. In this simulation case, the room is occupied during the daytime from 9:00 a.m. to 5:00 p.m.; and unoccupied the rest of the day. When the room is occupied, there is an interior heat and moisture production rate of 500 W and 3 g $m^{-3}h^{-1}$ respectively. During the unoccupied period, the interior heat production decreases to 120 W and the moisture production decreases to 0.5g $m^{-3}h^{-1}$. The ventilation system provides constantly 0.5 ACH. The set-points of heating temperature and cooling temperature for the air-conditioning system are 18°C and 26 °C respectively. The dehumidification system keeps the indoor relative humidity below 65%. The AC system only works during the occupied period.

The simulated evolutions of the indoor temperature and relative humidity with or without taking into account the whole building moisture transfer are also presented in Figs. 9.18 – 9.21.

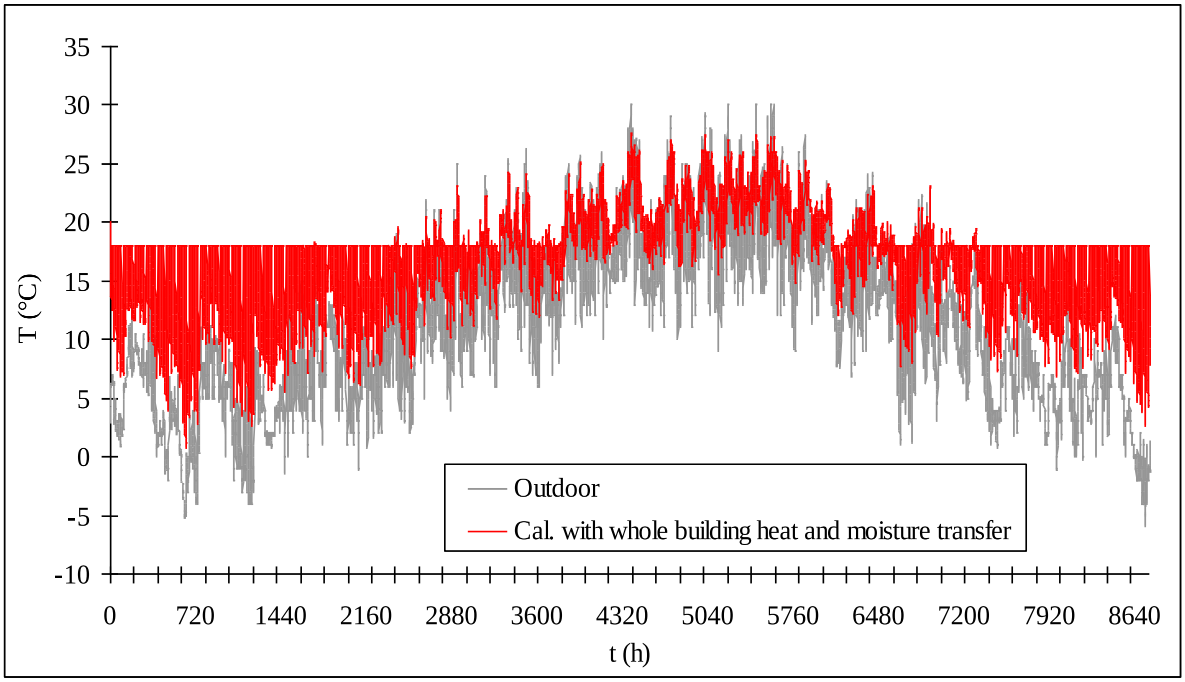

Figure 9.18 Simulated indoor temperature (Case II.1)

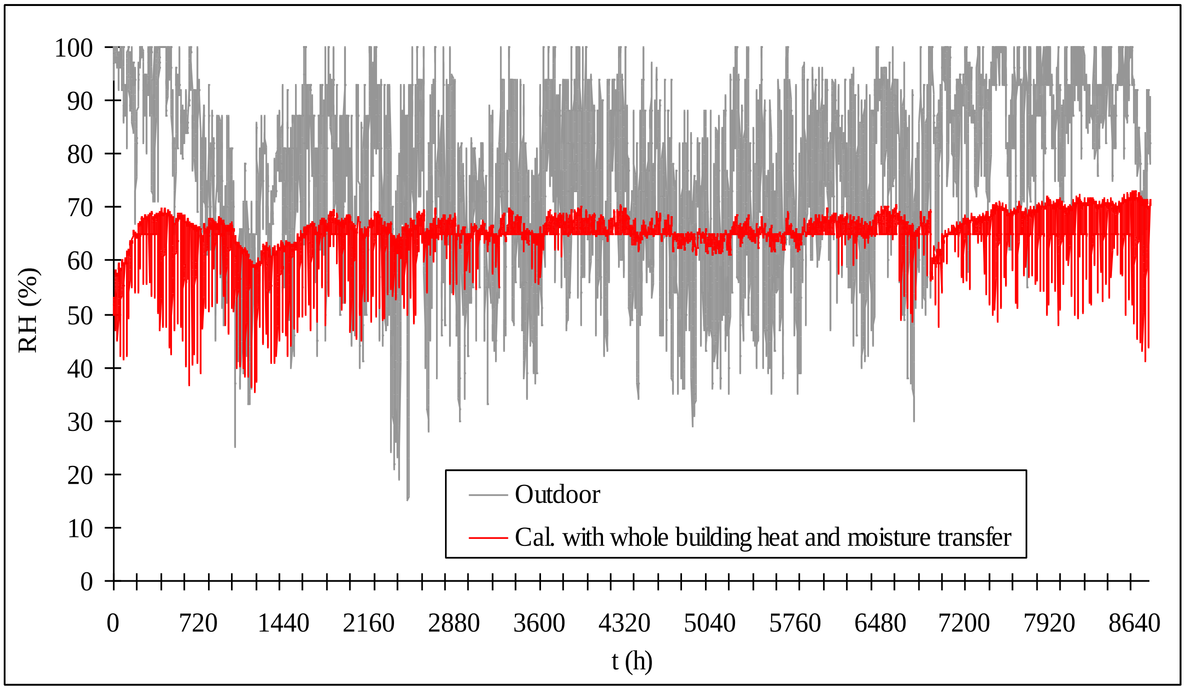

Figure 9.19 Simulated indoor relative humidity (Case II.1)

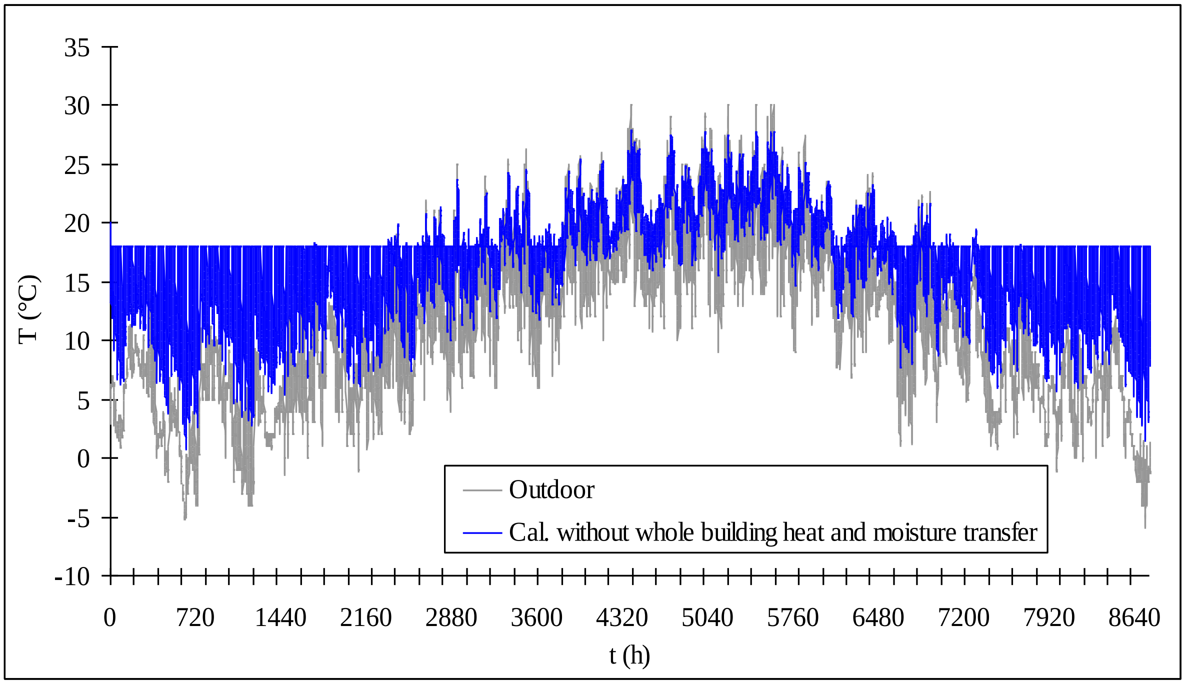

Figure 9.20 Simulated indoor temperature (Case II.2)

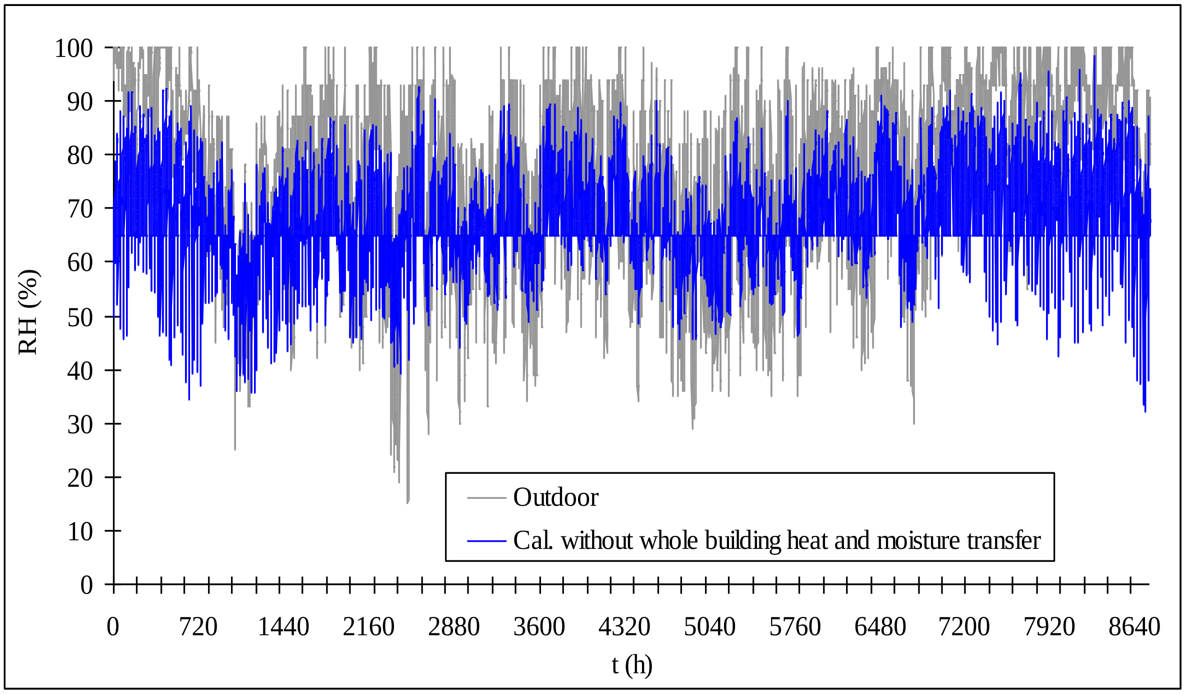

Figure 9.21 Simulated indoor relative humidity (Case II.2)

Simulated indoor temperature and indoor relative humidity of one week in summer and one week in winter are presented in Figs. 9.22 - 9.25.

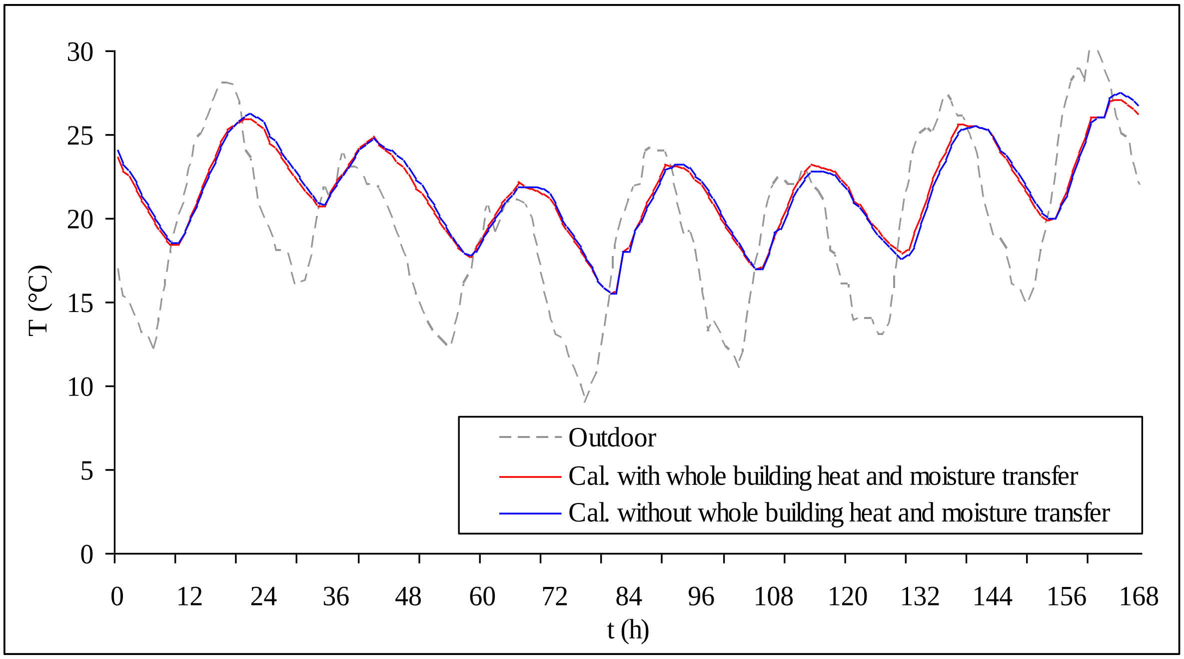

Figure 9.22 Simulated indoor temperature (August 1st -7th) in Paris

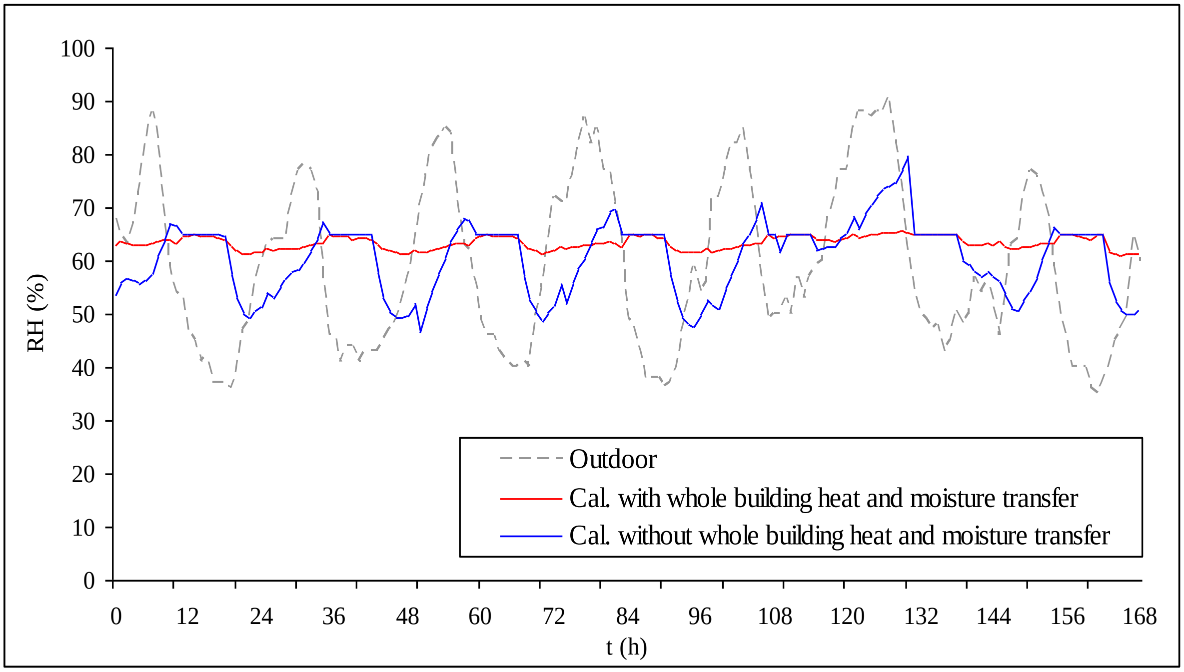

Figure 9.23 Simulated indoor relative humidity (August 1st -7th) in Paris

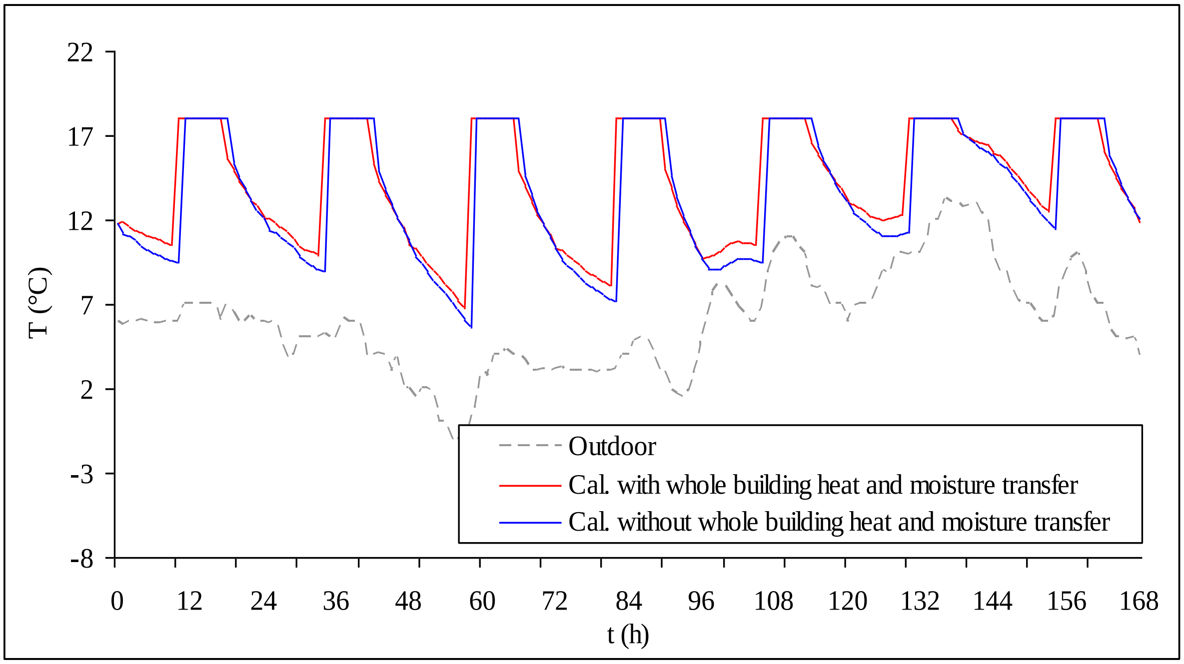

Figure 9.24 Simulated indoor temperature (December 1st -7th) in Paris

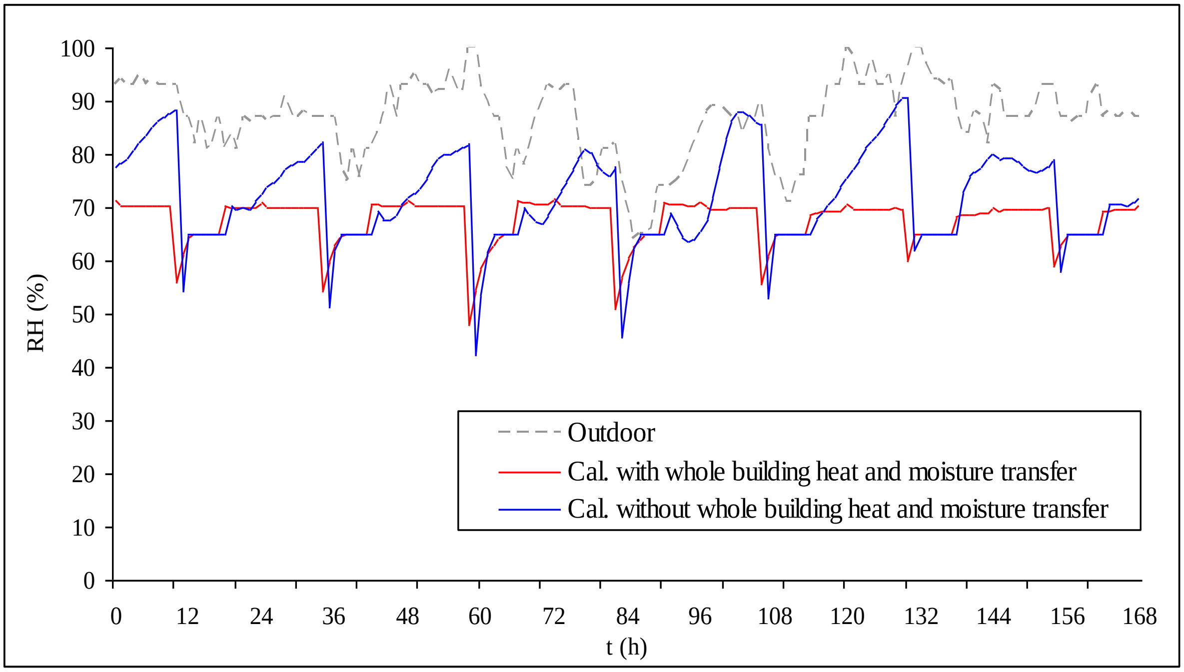

Figure 9.25 Simulated indoor relative humidity (December 1st -7th) in Paris

For temperate climate, the indoor relative humidity stays well low 80% in summer in both cases with and without these phenomena. No more extra dehumidification procedure is needed.

However, in winter, the indoor relative humidity exceeds 80% during the shut-off period of the air-conditioning system when we doesn't take into account the whole building heat and moisture transfer. In case II.3 that includes these phenomena, indoor relative humidity stays below 75%. It is important to note that relative humidity is not an important comfort parameter at low temperature, but has a strong effect on the risk of condensation and mold growth during the heating season (Sundell, 1996). An extra dehumidification procedure is required for case II.4 during the winter.

As a reference, the calculated indoor temperature and relative humidity for the same room without HVAC system (Case II.3 and Case II.4) are presented in Figs. 9.26 – 9. 29.

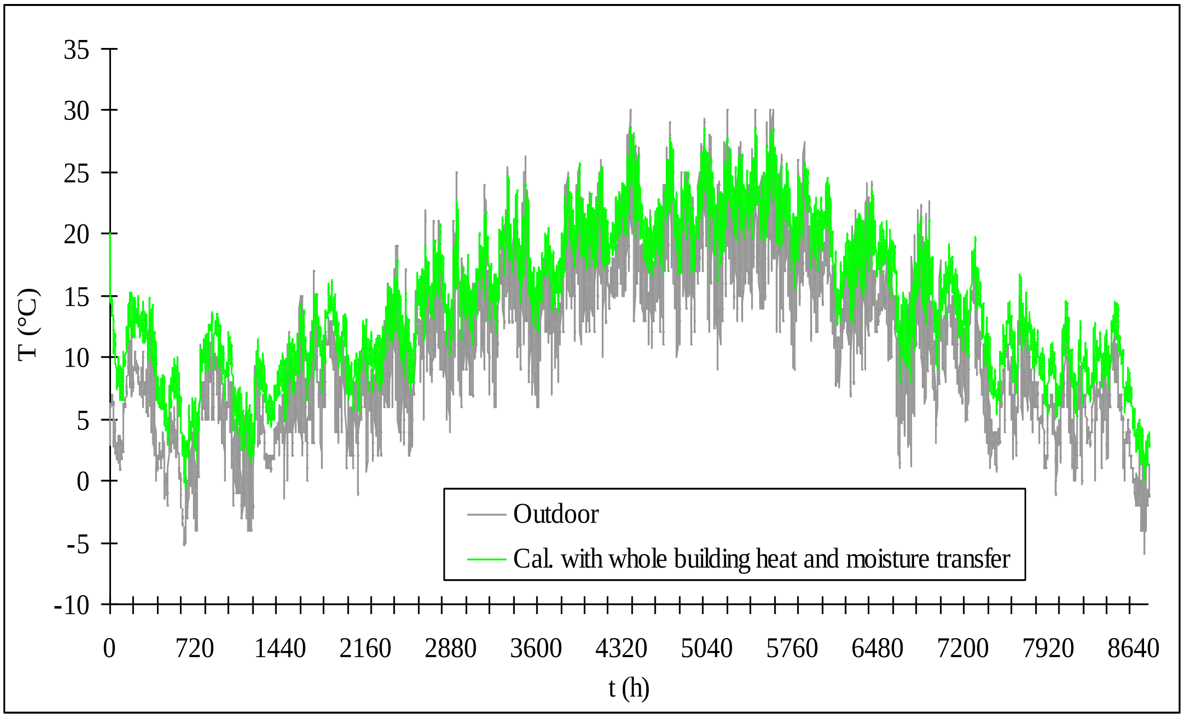

Figure 9.26 Simulated indoor temperature (Case II.3)

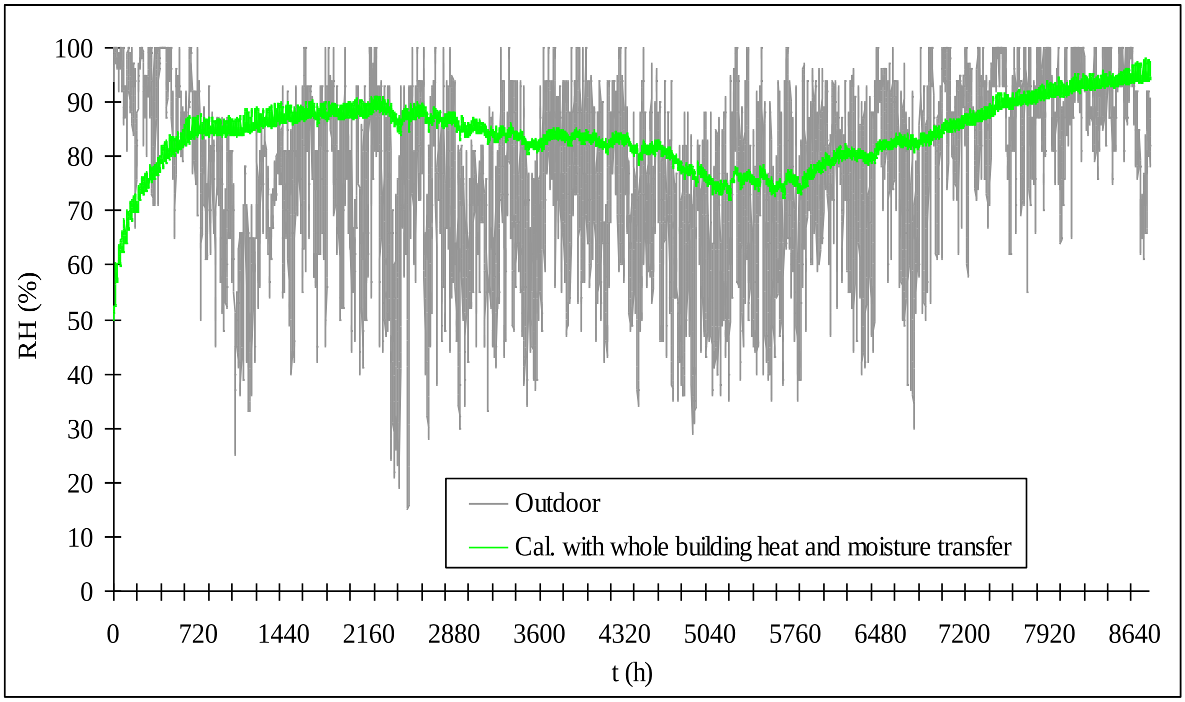

Figure 9.27 Simulated indoor relative humidity (Case II.3)

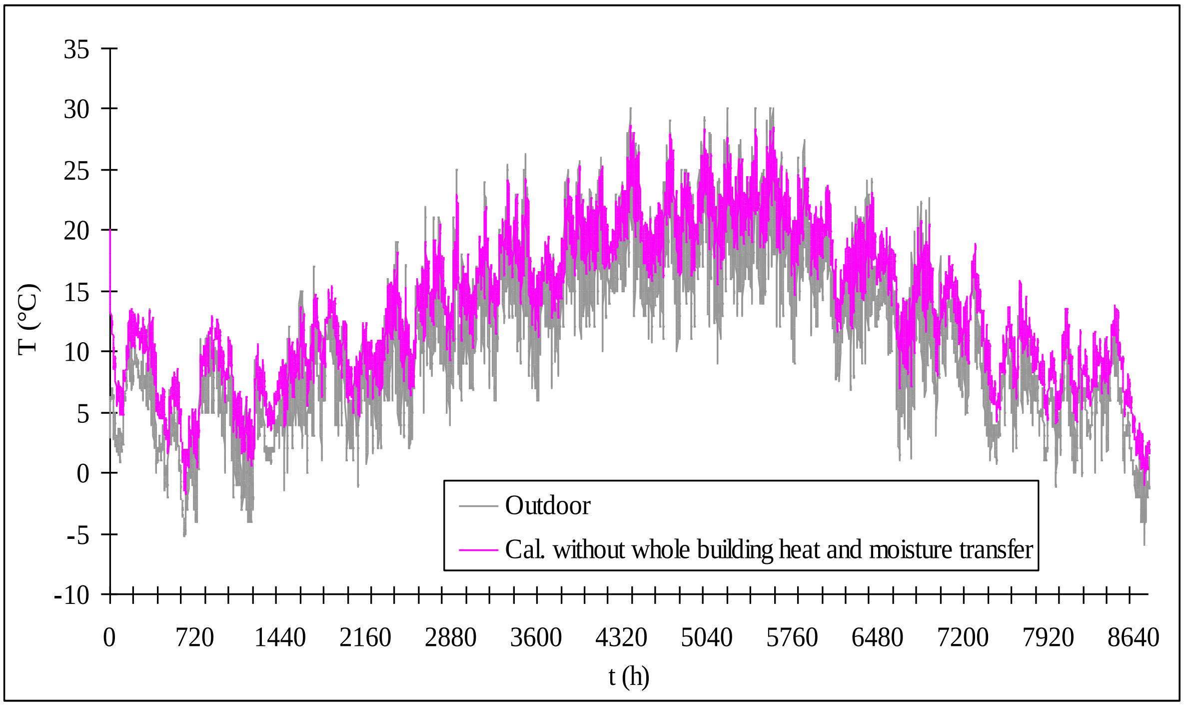

Figure 9.28 Simulated indoor temperature (Case II.4)

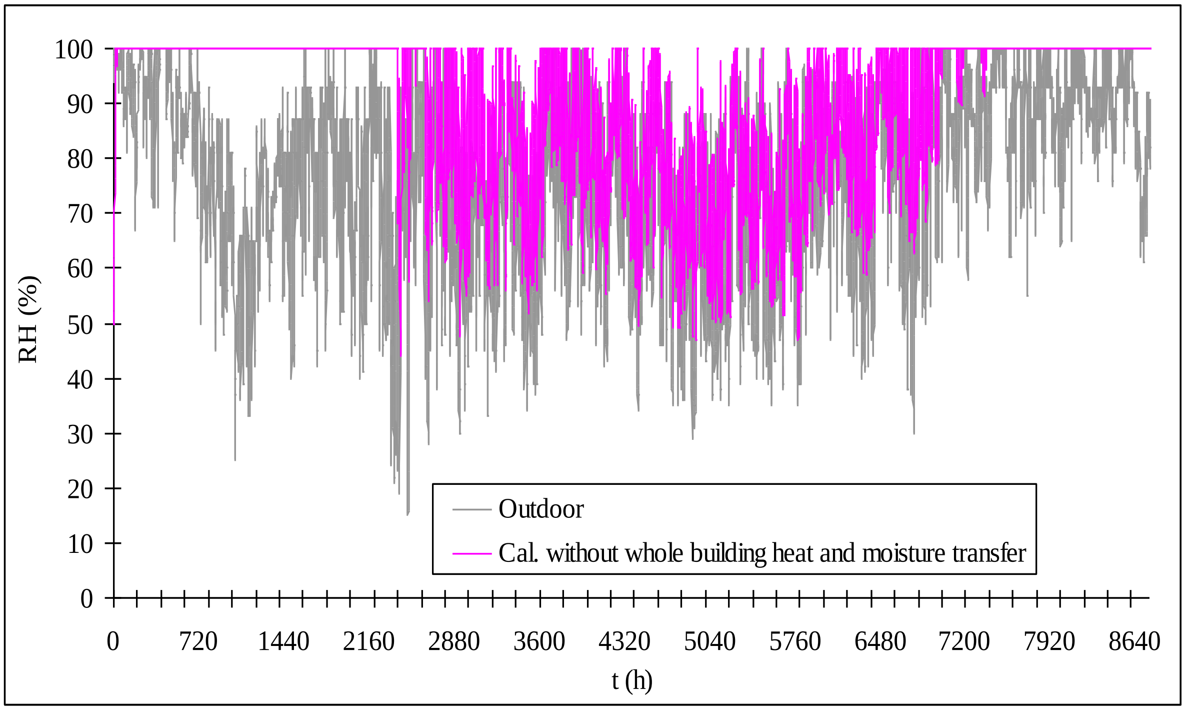

Figure 9.29 Simulated indoor relative humidity (Case II.4)

Furthermore, the simulations show that the indoor air temperature is nearly the same for both cases. This means the moisture transfer in the building construction has a significant influence on the latent cooling load while does not affect the sensible cooling load too much. The effect of hygrothermal transfer in building envelopes on energy consumption will be discussed in the following section.

9.4.3 ENERGY IMPACTS OF HYGROTHERMAL TRANSFER IN BUILDING ENVELOPES

Moisture migrating through building envelopes has effect on indoor climate, comfort and air quality, but the effect of hygrothermal transfer in building envelopes on energy consumption has not been studied to the same degree. In this section, we attempt to address the question of whether the hygrothermal transfer in building walls can reduce the energy needed to heat, cool and ventilate buildings. The main intent is to identify the magnitude of possible savings and suggest the most promising areas of future work.

To accomplish this, results from the simulation presented in the section, which are for a residential room in a wooden apartment building in Hong Kong and Paris, will be extrapolated to estimate the potential magnitude of energy savings. In this research, potential savings are savings in the required heating and cooling of a building.

Heating energy

In the heating season, direct energy savings are possible because moisture accumulation in hygroscopic materials releases 2.5 kJ kg^{-1} of moisture, which will decrease the required heating energy. Since humans are an important source of moisture in buildings, this moisture accumulation will occur during occupation. The energy required to heat the room in Paris during the occupied hours (9:00-17:00) for the cases with and without taking into account the whole building hygrothermal transfer is presented in Table 9.2. Normally, there is no heating season in Hong Kong. So we only discuss the heating energy of the case in Paris.

Table 9.2 Heating energy and energy saving (%) (Paris)

	heating energy (kWh m^{-2} a^{-1})		
	With whole building heat and moisture transfer (Case 1)	Without whole building heat and moisture transfer (Case 2)	Energy saving (%)
Paris	79.17	84.31	6.5

Table 9.2 shows that the energy consumption during occupation is about 6.5% lower in the case 1 (with whole building hygrothermal transfer) than in the case 2 (without whole building hygrothermal transfer), which means that moisture accumulation in the building materials during occupation can decrease the needed heating energy. On the other hand, energy is needed to dry the moisture from these materials during unoccupied periods if a building is continuously conditioned regardless of occupation. And the net result is that

the total energy saving of the case 1 (with whole building hygrothermal transfer) is about 4% lower than in the case 2 (without whole building hygrothermal transfer).

The results show that it may be possible to save heating energy with hygroscopic materials, but a control strategy is required to realize these savings. Such control strategies could be temperature and ventilation set back during unoccupied periods.

Cooling energy

During the cooling season, hygroscopic materials are able to reduce the indoor humidity and consequently reduce the indoor enthalpy. Decreasing the enthalpy of indoor air decreases the energy required to cool the building and also improves the indoor air quality. The potential for hygroscopic materials to reduce cooling energy consumption can be estimated from the calculated indoor enthalpy.

Table 9.3 Cooling energy and energy saving (%) (Paris and Hong Kong)

		With whole building heat and moisture transfer (Case 1)	Without whole building heat and moisture transfer (Case 2)	Energy saving (%)
Paris	Cooling energy (kWh m^{-2} a^{-1})	45.83	49.05	7
	peak cooling demand (kW)	0.97	1.067	10
Hong Kong	Cooling energy (kWh m^{-2} a^{-1})	204.23	234.86	15
	peak cooling demand (kW)	1.66	2.158	30

Table 9.3 shows that the required cooling energy during occupation is lower (from 7% in Paris to 11.2% in Hong Kong) with whole building hygrothermal transfer than without taking into account the moisture transfer. The peak cooling demand is also lower (from 10% in Paris to 30% in Hong Kong) with whole building hygrothermal transfer than without taking into account the moisture transfer. Similarly, as discussed before, a control strategy is needed to realize these savings because they represent the energy consumption and demand during occupied hours.

We also carried out the simulation for the case when a building is continuously conditioned regardless of occupation. The result shows that the savings in cooling energy consumption for all hours during the year are lower than during occupation which is similar to the findings of Fairey and Kerestecioglu (1985). Simulation results (Fairey et al., 1985) show that if a building is continuously conditioned (24 hours/day), the cooling energy savings due to hygrothermal transfer are in the order of 5% (for the month of July in Hong Kong), but if ventilation and cooling are controlled according to occupation greater savings can be realized. It is expected that a control strategy to optimize the benefits of hygroscopic mass would be similar to that recommended to optimize the benefits of thermal mass for the cooling of buildings (e.g. Keeney et al., 1996, Andresen et al., 1992, Braun, 1990).

Furthermore, peak cooling loads can be reduced by as much as 50% by precooling the building mass during unoccupied periods (Andresen et al., 1992), but such savings can be overestimated if the moisture adsorbed in the building structure during unoccupied periods is not included (Fairey et al., 1985). Nevertheless, it is not unreasonable to expect peak cooling load reductions of 10–30% when hygroscopic materials are applied. This could have a large impact on the size, cost and efficiency of cooling equipment in buildings.

Summary of potential energy savings

Table 5.4 summarizes the magnitude of the potential savings of heating and cooling energy considering the occupied hours. It is assumed that the HVAC control system is optimized to take advantage of the lower heating and cooling loads during occupation. As mentioned above, the total heating/cooling energy savings are relative to the total heating/cooling energy consumption (i.e., including both occupied and unoccupied hours) and are therefore lower than the relative savings presented in the table.

It is important to note that these values are estimates based on numerical simulation and must be used with caution. The similar research can be found in the literature (Fang et al., 1999, Fairey et al., 1985, Seppanen, 1999, Liu et al. 1999, and Woloszyn et al. 2000).

Table 9.4 Potential reduction in consumption (%) of heating and cooling energy when taking into account the whole building heat and moisture transfer

	Heating (%)	**Cooling (%)**
Optimized control of HVAC system	4-6.5	7-15
Reduction in energy demand	0-3.5	10-30

9.5 Conclusions

The coupled heat and moisture transfer in building envelopes has an important influence on the indoor air environment and the overall performance of air-conditioned buildings. In the chapter, a model for predicting the whole building heat moisture transfer was developed. The model was implemented in MATLAB-Simulink, and was validated by performing a series of testing and validation tools.

The model was applied to investigate the effect of moisture transfer on indoor air humidity and building energy consumption under different climate. Two simulation cases were chosen. The test room is assumed in hot and humid climates (e.g. Hong Kong, China) and in temperate climates (e.g. Paris, France) where it serves as a typical office room. The results confirm that moisture transfer through the building walls and vapor sorption-desorption at the interior wall surface have a great effect on the indoor relative humidity. In the case that includes these phenomena, the indoor relative humidity stays below 70% during the shut-off period of air-conditioning system. However, in the case without taking into account these phenomena, the maximum indoor relative humidity exceeds 80%. The high indoor humidity will dramatically increase the risk of mold formation and result in numerous health problems. An extra dehumidification demand is needed.

The research also indicates that moisture transfer has the potential to reduce the energy consumption of buildings, and the most promising energy savings are for buildings with mechanical cooling equipment located in hot and humid climates, but there are potential savings in all climates if the HVAC system can be optimally controlled to regulate the indoor climate, comfort and air quality. According to the current simulations, the potential energy savings are relatively small for heating (about 4% of the total heating energy), but significant for cooling (7–30% of the total cooling energy). The peak cooling demand is also lower (from 10% in Paris to 30% in Hong Kong) with whole building hygrothermal transfer than without taking into account the moisture transfer. However, these savings require the integration of hygroscopic materials and a well-controlled HVAC system.

10 HYGROTHERMAL ASSESSMENT METHODS

Based on "Guidelines for the use of building physical modelling methods and tools in the development of sustainable refurbishment technologies for external walls" report in a SUSREF project (Sustainable Refurbishment of Building Facades and External Walls), 7th framework programme, written in 2010-11 by Ruut Peuhkuri (that time at VTT Technical Research Centre of Finland) with contributions from Sverre Holøs (SINTEF; Norway), Stig Geving (SINTEF), Jonas Holme (SINTEF), Christopher Tweed (Cardiff University, Wales) and Kruti Gandhi (Cardiff University).

Introduction

This note is an introduction to assessment methods that use building physical modelling methods and tools and contains following main topics:

- A short description of some main methods and tools for building physical assessment
- Definition of some performance criteria for building physical assessment that can be used
- Guidelines for the building physical calculations - A procedure with an assessment example

The objective of this note is to give guidelines for how knowledge on building physics and modelling methods and tools can be used to assess and improve the hygrothermal performance of building constructions. The assessment can be seen as an iteration process where the best solution for any actual case is found by optimising, among others,

- thermal performance of the envelope: reduction of the heat losses through the envelope, minimising thermal bridges
- moisture performance of the envelope: ensuring drying capacity, avoiding condensation
- durability of the constructions: reduction of the risk for mold and decay
- indoor air quality and comfort: thermal symmetry, no draft, control of humidity

The building physics modelling is here understood as the analysis on the constructions only. The whole building analysis is another but related topic for impact on the space heating/cooling energy demand and on the resulting indoor climate.

10.1 Methods and tools for building physical assessment

Building physics is about understanding and analysing the heat, air and moisture (HAM) interactions - transport and storage - in and around building materials and constructions. This complicated theoretical analysis is typically implemented in more and more advanced simulation and modelling tools. The simulation algorithms solve the coupled heat, air and moisture (=hygrothermal) states throughout the control volumes to be studied as a function of time and place. Therefore, the dynamic simulations with hygrothermal simulation tools are an important and even necessary part of the assessment work. Some of the most used and verified simulation tools for hygrothermal analysis of building constructions are WUFI, DELPHIN and Match. In addition there are quite a few tools for pure thermal assessment, mostly two dimensional simulation tools for assessment of the thermal bridges. The coupled heat and moisture transport, however, is necessary to be analysed in order to assess almost any moisture related performance criteria. More about the tools later in this section.

The hygrothermal impacts on a building and the thermal envelope are illustrated in Figure 10.1.

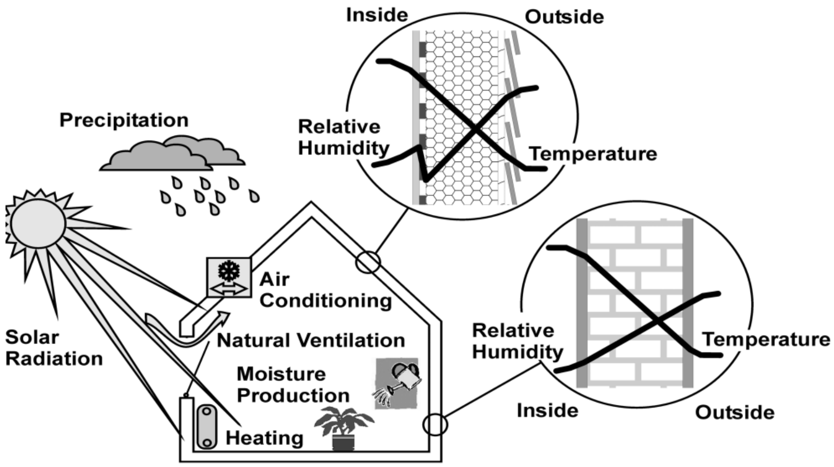

Figure 10.1 Illustration of the HAM impacts and mechanisms in and around an exterior wall (Sedlbauer, Künzel and Holm, 2004).

Moisture in a porous material can be transported either as water vapor or as liquid water, or as a combination of these two phases in the pores. The solid matrix is normally not active in the transport. Moisture transport can either be diffusive or convective. Diffusive transport is proportional to the gradient of the driving force(s), a proportionality coefficient being a material parameter which is determined experimentally, e.g. water vapor permeability. The convective flux is a product of the vehicle flux, e.g. air, and the transported density of moisture.

All the simulation tools for hygrothermal analysis consider usually water vapor diffusion that is transport of moisture in the air, typically in the pores of a material. This is the predominant transport mechanism in a very porous material (e.g. mineral wool). If the pores of the material are very microscopic (e.g. concrete) and/or the material is very wet (e.g. wet wood), the capillary transport will be dominating. This capillary transport is included at least in WUFI, DELPHIN and Match. In Figure 10.2 are shown some of the central moisture transport mechanisms within a porous material and some of the driving potentials. Beside the water vapor pressure, temperature is a driving force for coupled heat, air and moisture transport.

Convective moisture transfer takes place in air gaps of a construction and in very open porous materials like lightweight insulation materials. The driving force can be the air pressure difference due to the temperature gradient within the material that enables natural convection. Alternatively, the convection can be forced by air pressure through any air leakages in the envelope. Hygrothermal convection is normally modelled physically correct only in the most advanced 2D tools.

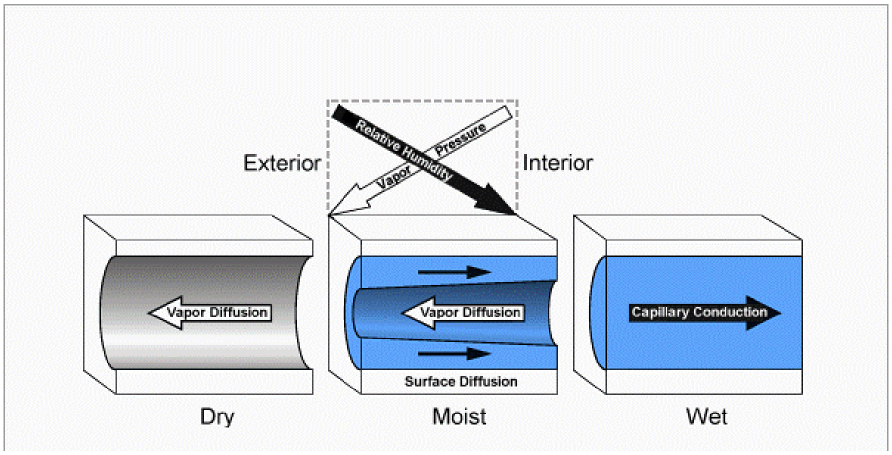

Figure 10.2 The different transport mechanisms of moisture within a porous building material. The transport mechanism is governed by the moisture content and the porosity of the material – source: http://www.wufi-pro.com/.

Depending on the construction type to be analyzed, the most suitable calculation and simulation tools should be chosen.

- 1D coupled heat and moisture calculations tools - 1D HAM -tools (e.g. WUFI-Pro (Fraunhofer IBP n.d.), DELPHIN (Bauklimatik Dresde n.d.), Match (Bygge- og Miljøteknik AS n.d.)) are the best choice for constructions and solutions consisting of just homogenous layers. Ventilated cavities can be studied simplified with these tools, too.
- 2D coupled heat and moisture calculations tools - 2D HAM -tools (e.g. 2D versions of WUFI and DELPHIN) should be used for constructions containing inhomogeneus layers, e.g. masonry walls, stud walls and ventilation cavities. 3D effects must be taken into account by qualified modification of the model, together with a possible 3D thermal calculation.
- Constructions with complicated cavities or elements with active fluids like air or water/brine should be modelled with multi-physics or CFD-tools (Computational Fluid Dynamics tools) (e.g. Comsol (COMSOL n.d.), Fluent (ANSYS n.d.)).

Generally, one-dimensional (1D) HAM-tools are sufficient for most of the analysis with skilled expert use. The computation of coupled heat and moisture transport in two dimensions (2D) is usually very time-consuming and the detailed information from a 2D or even 3D calculation may be overruled by other uncertainties. For instance, the thick stone wall constructions may prove a problem because many stone types are impervious to moisture penetration but the mortar in between stones is not. Strictly speaking, this should require a 2D model, but it may prove difficult to get reliable input data for all of the various material properties. Pure heat transmission tools (in 2D and 3D) are very usable for optimisation of the thermal bridges and assessment of the critical surface temperatures for e.g. mold risk.

Basically, advanced state-of-art building physics tools are recommended for research purposes in order to understand the phenomena as far as possible. Simpler tools and methods, engineering tools, are often the best way to analyse most of the cases and especially any real life problems.

The simulation output is typically the temperature, vapor pressure and moisture content states throughout the defined construction as a function of time. This output is then post-processed in order to give input for the assessment. The performance criteria used are described in the next section.

10.2 Performance criteria for building physical assessment

When assessing building envelope constructions from the viewpoint of building physics, following different sub-areas of performance, which form the overall performance, are included in this note:

- thermal performance of the envelope
- moisture performance and durability of the constructions
- indoor air quality and comfort

The assessment criteria for these subjects will be presented and shortly defined and motivated in this section.

10.2.1THERMAL PERFORMANCE OF THE ENVELOPE

The thermal performance of the envelope is basically evaluated on the basis of the heat losses through the envelope. An improvement is a goal, this requires typically action on two levels: increasing the thermal insulation of the envelope and minimising the thermal bridges:

- The overall U-value of the construction should be low in order to minimize the energy use for space heating and cooling.
- The effect of thermal bridges should be minimized in order to avoid additional heat losses and low local surface temperatures, which can cause local discomfort and unwanted micro-climate for biological growth.

10.2.2 INSULATION THICKNESS - OPTIMAL U-VALUES

The optimal and/or needed U-values for different construction types depend on the local climate and the building regulations, and on any additional energy or green labelling standard desired. As the energy use is typically a function of the whole building, the U-values cannot be optimised on the component level alone. However, different U-values can be taken as a parameter in the hygrothermal assessment.

10.2.3 THERMAL BRIDGE EFFECTS

Besides the U-values, which are motivated by environmental, economical and legislative reasons, the constructions should be designed such a way that the thermal bridges are minimised. Thermal bridges can occur in different ways:

- systemically throughout the construction, e.g. wooden studs
- due to the building geometry, e.g. corners
- connections between different building parts, e.g. window installations

Thermal bridges will influence the heat losses and indoor surface temperatures (more about this in 10.4 Indoor air quality and comfort).

The thermal performance and quality of constructions can also be expressed as a temperature factor (form factor for the thermal bridge effects) f_{Rsi} given in equation (10.1). This factor expresses the ratio of the temperature difference between indoor surface ϑ_{si} [◦C] and outdoor air ϑ_e [◦C] to the total temperature difference between outdoor air and indoor air temperature ϑ_i [◦C].

$$f_{Rsi} = \frac{\theta_{si} - \theta_e}{\theta_i - \theta_e} \tag{10.1}$$

In case of a pronounced thermal bridge, the indoor surface temperature is low and therefore the ratio small. Therefore, the higher f_{Rsi}, the smaller is the thermal bridge effect.

f_{Rsi} is determined for typical, dimensioning, winter conditions, for example ϑ_i = 20˚C and ϑ_e = -1.1˚C (ϑ_e = average temperature for the coldest month, which is -1.1˚C in February in Denmark). This temperature factor is recommended typically to have values over 0.7. Any value under this value and resulting moisture problems can be seen as a consequence of too poor thermal quality of the construction, thus the low indoor surface temperature, in combination with high relative humidity of the indoor air while for $f_{Rsi} > 0.7$ the moisture problems can mostly be allocated to the high relative humidity of the air. The resulting surface moisture conditions are a function of the indoor relative humidity and the average outdoor temperature in the coldest part of the year.

10.3 Moisture performance and durability of the constructions

The moisture performance of the envelope is central for the durability of the constructions: Moisture plays the main role in most of the decay and deterioration processes, e.g. growth of algae and mold, decay fungi, frost damage and corrosion. The conditions in the constructions should not exceed critical limits for moisture and temperature, which - if exceeded - will lead to these durability problems. Risk of condensation will typically lead to these other problems and, in addition, reduce the thermal insulation effect of the constructions.

Therefore, ensuring a good moisture performance of the constructions means

- keeping the construction dry (e.g. avoiding condensation, penetration of driving rain)
- choosing suitable materials (e.g. inorganic materials to exposed locations)
- ensuring drying capacity (e.g. with ventilation and right placement of materials)

An illustration of some of these critical limits is found in Figure 10.3 that gives some "safe" long term limits for mold growth in different building materials. The area above the curves expresses the critical conditions for mold growth. Inert substrates such as metals, foils, glass and tiles are usually not affected by mold, unless contaminated.

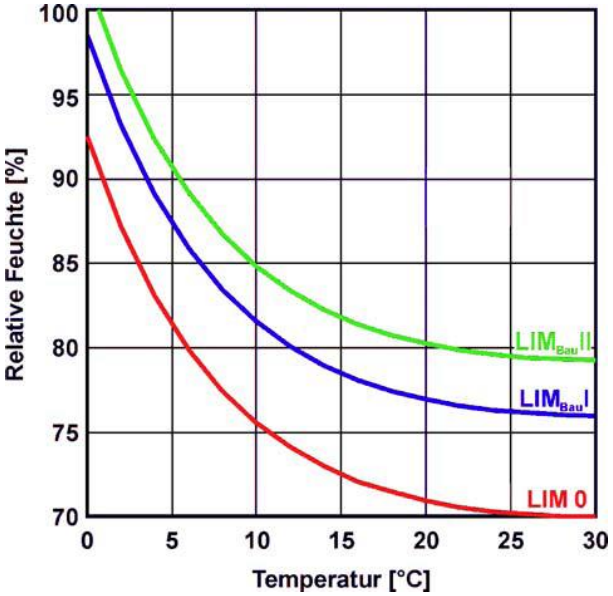

Figure 10.3 "Safe" limits for avoiding mold growth for different material classes.

- LIM 0: Optimal culture medium represents the maximum growth possible for any mold found in buildings.
- LIM I: Bio-utilizable substrates, such as wallpaper, plaster board, building products made of biologically degradable materials, strongly contaminated surfaces.
- LIM II: Less bio-utilizable substrates with porous structure, such as plasters, mineral building materials, certain woods, insulating materials not belonging to group I.
  From WufiBio manual (Sedlbauer 2001).

When performing building physical dynamic simulations, the resulting temperature and relative humidity hourly values on a material surface can for example be used for an evaluation of the risk for mold growth on this surface with so called TOW, time of wetness (= number of hours during a year when the given limits are exceeded.). Limits in Figure 10.3 can be used to calculate number of yearly hours, when these values are exceeded. When n_{hours} = 0, the construction can be evaluated as mold safe. TOW's can be used to compare different solutions: i.e. which solution gives the lowest TOW's.

Mold growth is one of the first signs of biological deterioration caused by excess of moisture, and therefore mold growth can be used as one of the best hygrothermal performance criteria of building structures. Mold does not deteriorate the material, but it is a sign of too high moisture content and it represents a risk for other moisture caused problems, like decay (see more about decay in next chapter). Mold affects the appearance of the surface and it can severely affect the indoor air quality when the growth is in contact with indoor air or with the leakage air flowing into the room space.

The time of wetness -method is a simple way of assessing the hygrothermal simulations. However, there exist also dynamic models for estimation of the risk for mold growth (Hukka & Viitanen 1999). The dynamic nature of these models result in results with much more information, which then requires even more expertise to assess. In the following, some of the central moisture related assessment factors are presented.

10.3.1 DRYING CAPACITY

The drying capacity is traditionally used as a security for the main strategy of keeping the construction dry. For example, in case of accidents, which involve water damage, the drying capacity will reduce the risk for mold growth. The drying mechanisms are also widely calculated in the construction process and time tables, and allow an effective building construction process.

Therefore one of the central criteria is the amount of accumulated water in the construction during a year Δw [kg/m^2/y], where w_{end} [kg/m^2] is the moisture content by the end of the year and w_{start} [kg/m^2] is the moisture content in the beginning of the year:

$$\Delta w = w_{end} - w_{start} \tag{10.2}$$

A well performing construction should not accumulate moisture at all and therefore the negative accumulation should be as high as possible to ensure large drying potential.

10.3.2 MOLD GROWTH

Mold growth is biological growth on almost any material surface. The mold growth is highly dependent on the temperature and especially of the moisture activity of the surface material. The time needed for the spores to germinate and the mold growth to start is a function of the hygrothermal conditions. In addition, the growth is dependent on the organic material available as nutrient. Figure 10.4 illustrates some threshold values for time, temperature and water activity (=relative humidity) for constant exposure for pine sap wood, which is one of the most sensible materials with respect to mold growth.

The mold growth is a general and common definition for the biological growth based on mold fungi that include several species. When talking about Mold Index etc, it includes all relevant fungi species. Mold spores are naturally everywhere and therefore hard to avoid especially on the exterior part of the building constructions. In addition, the conditions of the exterior parts of the building envelope are close to exterior weather conditions, which in many climate regions are favourable for mold growth (see e.g. Figure 10.4).

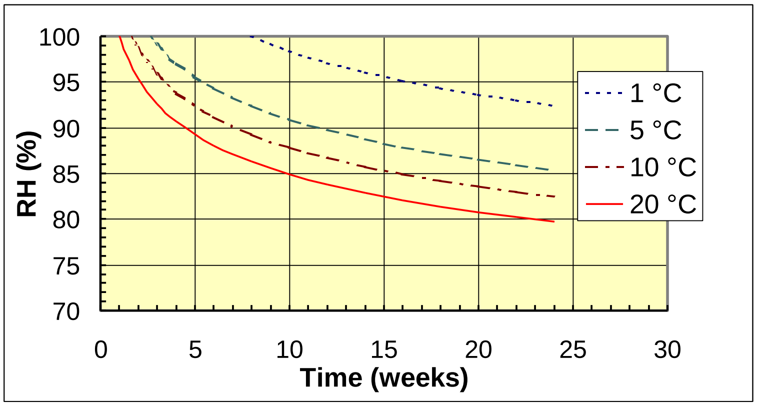

Figure 10.4 Critical conditions for mold growth in pine sap wood. Constant conditions (Viitanen, H. et al. 2010).

After the germination of the mold spores has taken place, the mold is growing in different intensities, depending on the conditions. There are several methods to assess the severity of the mold growth and one of them is the Mold index, which is defined as a scale from 0-6 (see below list). Figure 10.5 illustrates the mold index levels according to a model developed based on laboratory observations and Figure 47 shows these microscopic and visual observations.

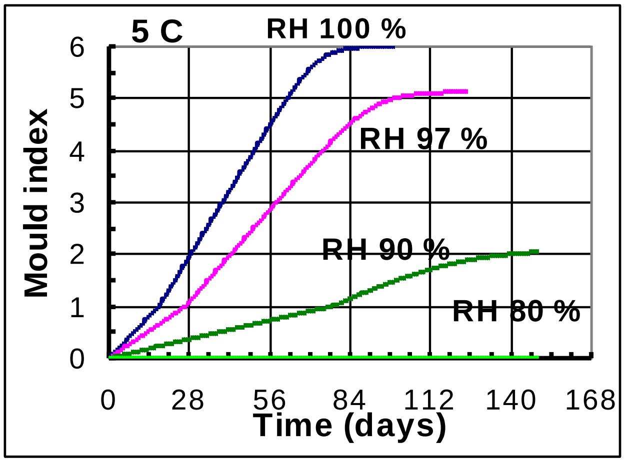

0 = no growth

1 = some initial growth (microscopy)

2 = moderate growth, local colonies,
coverage > 10 % (microscopy)

3 = some growth (visually detected, < 10%) or
< 50 % coverage (microscopy)

4 = mold growth coverage 10 - 50 % (visual) or
coverage > 50 (microscopy)

5 = plenty of growth, coverage > 50 (visual)

6 = heavy and tight growth, coverage 100 %

Figure 10.5 Development of the mold index as a function of time for different constant exposures at 5ºC. Pine sapwood. 8 The list gives the growth criteria for the different mold index levels (Ojanen 2010).

There have been some attempts to develop numerical models for the mold growth in order to evaluate the risks connected to overall performance, service life, interaction with indoor climate conditions or structural safety. (Hukka and Viitanen 1999 , Viitanen et al. 2000 , Sedlbauer 2001 , Clarke et al. 1998 , Hens 1999).

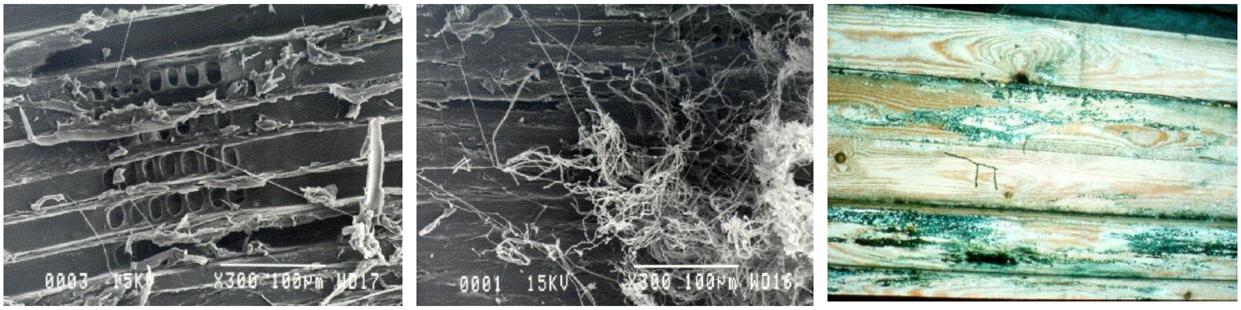

Mold index 1 (start of growth) Mold index 4 - 5 (plenty of growth) Mold index 6 (tight coverage)

Figure 10.6 illustration of the different mold index levels.

The model developed at VTT Technical Research Centre of Finland by Viitanen et al. is shortly presented in Appendix. Figure 48 illustrates the predicted mold growth given by this model with selected assumptions and a comparison with observed mold growth. This figure illustrates also that the mold growth simulation models do not guarantee any exact prediction of mold in different cases and conditions. The parameter sensitivity is high, estimation of a material sensitivity class is difficult without testing, the surface treatments may enhance or reduce growth potential, different mold species have different requirements for growth and the evaluation of the actual conditions in the critical material layers may include uncertainties. Nevertheless, the motivation to use and develop numerical mold growth models and application of them is to give tools for better prediction and evaluation of the risks for biological growth on structure surfaces and to find the best solutions to ensure safe performance for the building and the indoor climate.

The modelling results should not be taken as absolute values but used for comparison of the performance of different solutions.

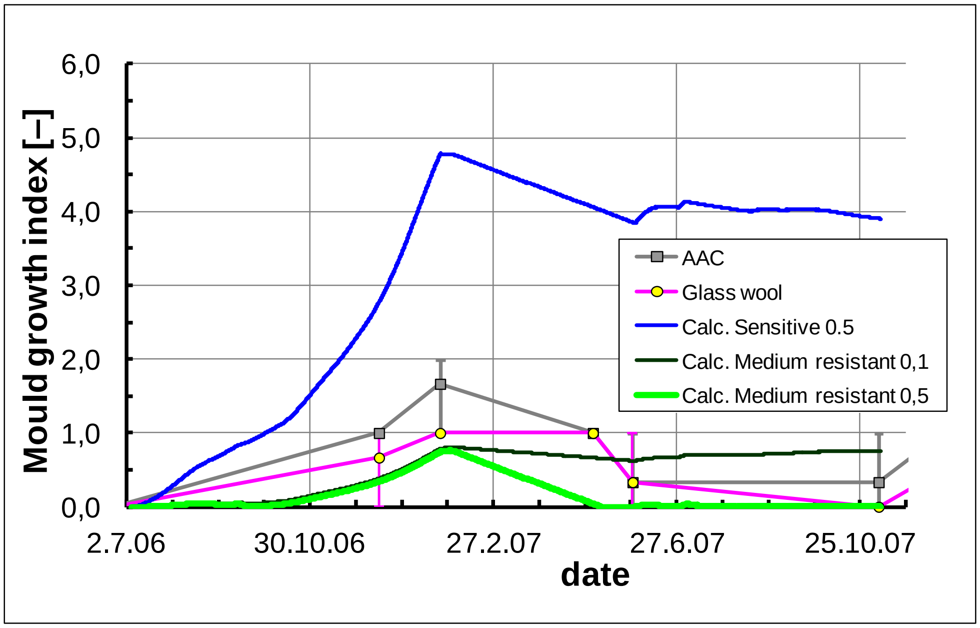

Figure 10.7 An example on the prediction of the mold growth with numerical, dynamic models and comparison with the measured (=observed) mold growth. Different material sensitivity classes and how the mold reacts on unfavorable conditions are calculated. (Ojanen et al, 2010)

Even though these numerical mold growth models are relatively easy to implement as post processing of hourly temperature and relative humidity results of the hygrothermal simulations, the correct interpretation of the results is often only possible with experience and expert knowledge. Therefore, there is a need for some far more simple evaluation methods that are suitable for comparison and the assessment of the risk.

One of the simplest post processing and evaluation methods is to determine time of wetness (TOW) for given threshold values of T and RH. (TOW is usually used for assessing the corrosion risks.). Figure 44 gives some "safe" limits for mold growth in different building materials.

ASHRAE has given a set of simple criteria for evaluating the moisture performance of constructions by using the threshold values determined by favourable conditions for mold growth, like in Figure 44. See Table 9.1.

Table 10.1 Performance criteria for evaluation of building constructions by ASHRAE standard method 160. The values give the favourable values for mold growth.

Criterion 1: 30-day running average	**RH > 80%**	**5°C < T < 40°C**
Criterion 2: 7-day running average	RH > 98%	5°C < T < 40°C
Criterion 3: 24-hour running average	RH = 100%	5°C < T < 40°C

10.3.3 GROWTH OF ALGAE ON EXTERIOR SURFACES

Another biological growth type unwanted in building constructions is the algae growth on the exterior surface of the building envelope. The problem with these typically blue and green algae, typically on north oriented surfaces, is mostly aesthetic but, nevertheless, unwanted.

The increasing problem with algae is partly a consequent of better insulation levels that reduces the exterior surface temperature. Algae need liquid water and this is available from driving rain and especially from condensed water on the facade during night under-cooling. Therefore, the performance criteria in order to avoid algae is to avoid liquid water and condensate on an exterior surface, i.e. RH < 100%.

Beside the U-value of the construction, the exterior surface temperature and relative humidity are function of the surface material properties: radiation properties (especially long wave emissivity) and heat and moisture absorption capacity. Experimental studies and simulation of the results show that darker and moisture absorbing surface materials reduce the algae access to condensate water. More about the biological growth on exterior surfaces can be found e.g. in (Møller 2003)

10.3.4 DECAY OF WOODEN CONSTRUCTIONS

The critical moisture levels for decay of wooden constructions are almost analogues to ones for mold growth. However, the funghi responsible for the decay of wooden materials needs clearly higher humidity than mold. Typically the relative humidity must be higher than 95% for long periods in order to give favourable conditions for decay fungi. Figure 49 shows some critical limits of temperature and relative humidity of pine sapwood under constant exposure.

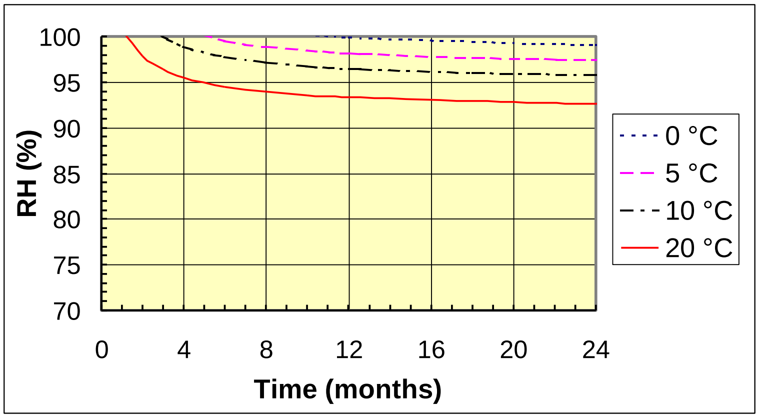

Figure 10.8 Critical conditions for decay development in pine sap wood. Constant conditions (Fagerlund, 1972).

Within a recent research project focusing on the durability of wooden exterior sheetings, a numerical model for the decay development was developed, based on a regression model of a general isoplet for decay development in untreated pine sapwood. This dynamic decay model can also be used to post process the results from the building physical simulations in order to assess the durability of the wooden constructions exposed to different conditions and the effects of e.g. insulation thickness and material choices.

10.3.5FROST DAMAGE

Frost damage occurs typically when a rigid porous material like masonry brick has very high water content and the temperature decreases below zero.

Performance criteria for constructions in order to avoid frost damages can be defined with the moisture content that should not exceed the critical value of saturation fraction, which theoretically is 0.917. The critical saturation fraction is very different for different materials and can/should be determined experimentally. Examples for e.g. reduction of the E-module of natural stone as a function of the water saturation degree, tested for 1, 19 and 110 freeze and thaw cycles is given in (Fagerlund 1972).

10.3.6CORROSION OF METALS

Metals and metal coatings in building constructions are exposed to atmospheric corrosion, when their surface is wetted. The ISO standard 9223 on classification of corrosion of metals defines the time of wetness as number of hour per year when the structure is exposed to *RH* > 80% and *T* > 0ºC at the same time, see Table 10.2. The metal used in the constructions should therefore fulfil the requirements for the given corrosion class according to the calculated time of wetness.

Table 10.2 Criteria for corrosivity classes of metals based on time of wetness according to ISO 9223.

Corrosion class	Typical condition for structures found in	Used categories for Time of wetness
τ1	-	< 10
τ2	-	10-250
τ3	Outdoors in cold and dry climates	250-2500
τ4	Outdoors in all other climates	2500-5500

T5	Outdoors in humid climates	> 5500

10.4 Indoor air quality and comfort

The indoor air quality and comfort are mainly the result of the whole building performance. Hence, there are couple of factors that are directly connected to the exterior envelope constructions: thermal symmetry and non-presence of mold growth on the interior surfaces. The inner surface temperature of the thermal envelope can be predicted with the (hygro)thermal simulations of constructions and the temperature difference can be calculated and evaluated.

In Table 10.3, there are gathered these relevant factors for the hygrothermal performance of the exterior constructions concerning indoor environment. The criteria regarding mold and dampness are closely connected to the assessment of moisture performance and durability described in the previous chapters.

Table 10.3 Indoor environment: Target values relevant for evaluation of the exterior walls.

Assessment/Factor	Thermal environment	Dampness and mold
Good	According to Class 1 or *PPD* < 6% (radiant asymmetry: cool wall ΔT < 10 ºC)	No detectable mold damage
Moderate	According to class 2 or *PPD* <10 % (radiant asymmetry: cool wall ΔT < 13 ºC)	Occasional condensation occurs. Minor areas of organic growth not exposed to indoor air of rooms for longer occupancy.
Bad	Not meeting criteria of class 2. *PPD* > 10% (radiant asymmetry: cool wall ΔT > 13 ºC)	Regular condensation, organic materials exposed to RH >80 % for extensive periods, visible mold growth exposed (directly indirectly to occupied spaces)
Reference	EN 15251 Annex A / CR 1752	WHO (2009)

10.5 THE GUIDELINES - Procedure for the calculation with an assessment example

The following instructions/guidelines are relevant when analysing the hygrothermal performance of building constructions and especially when finding a well performing refurbishment solutions for these. The simulations in these guidelines are assumed to be performed with a 1D or 2D hygrothermal simulation program, which solves the dynamic, coupled temperature and moisture conditions in a construction and can e.g. take into account the amount of water absorbed to construction due to the driving rain.

NOTE: These guidelines do not recommend use of any specific software. WUFI is just used as an example as it is a rather common tool and includes most of the features needed for the analysis.

If only thermal 2D/3D calculations are performed - e.g. with HEAT2 or Therm - (which are normally sufficient for studying effects of thermal bridges), a method described in EN ISO 13788 for calculation of critical temperatures of internal surfaces can be used for assessing the potential for mold growth.

10.6 Description of the construction

A sufficient description of the original and/or the refurbished construction is important for the documentation and understanding the performance of the analysed solutions. In this section, some examples are given, how to define and document a construction to be analysed.

10.6.1MATERIAL LAYERS

Typical material layers and material values for each construction type - also in 2D and 3D if relevant - should be given. These should be reported with a combination of a drawing and table, e.g. Figure 10.9 and Table 10.4 below. These should include at least following information:

- Material layers, with thicknesses
- List of some central material values e.g. density, thermal conductivity and water vapor diffusion coefficient or resistance factor.

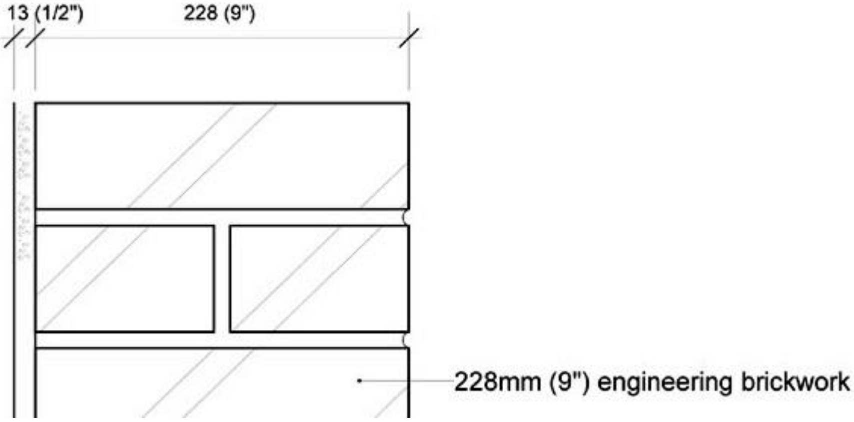

Figure 10.9 Example on description of a wall. The drawing should also include dimensions in vertical direction, if there are 2D effects.

It would be too laborious to list all the material parameters for all the materials in a table form, but including some of these basic material parameters already gives the reader of the report an idea of the material characteristics. A data sheet of all the relevant material parameters including also sorption isotherms and other material characteristics as a function of temperature and humidity (if available) should be included in an appendix.

If using the standard materials from the database of a common simulation software e.g. WUFI, it is sufficient to only refer to the material by exact name and then give the basic values in a table form as in Table 10.4.

Table 10.4 Example on presentation of the construction material layers with material thickness and some hygrothermal parameters.

	Thickness	Bulk density	Porosity	Specific Heat Capacity	Thermal conductivity	Vapor diffusion resistance
	d	ρ	p	c_p	λ	μ
	m	[kg/m³]	[m³/m³]	[J/(kg·K)]	[W/(m·K)]	[-]

brick	0.228	1900	0.24	850	0.6	10
interior plaster	0.013	850	0.65	850	0.2	8.3

The construction should be modelled as true to reality as possible with your software. Of course, simplifications cannot be totally avoided in any modelling, but these must be based on knowledge and experience in building physics. Figure 10 is the modelled version of Figure 10.9. Note the opposite placement of interior and exterior side in the model compared to the drawing in this example. Generally, the convention is adopted that the exterior of the construction is always shown on the left side of any cross-section.

Monitoring (=logging of state variables, typically temperature and relative humidity or moisture content, typically every hour during the simulation) of the hygrothermal conditions for further analysis should be done in any location assumed critical. This means monitoring at least on the both any material interface, cavity or surface that is assumed critical. Document this with a drawing or "screen dump". The model drawing in Figure 10 also indicates the used calculations mesh (= numerical cells where the state variables are solved for every time step), which should be defined as fine as necessary for a correct analysis. The software manuals typically give recommendations for the mesh size.

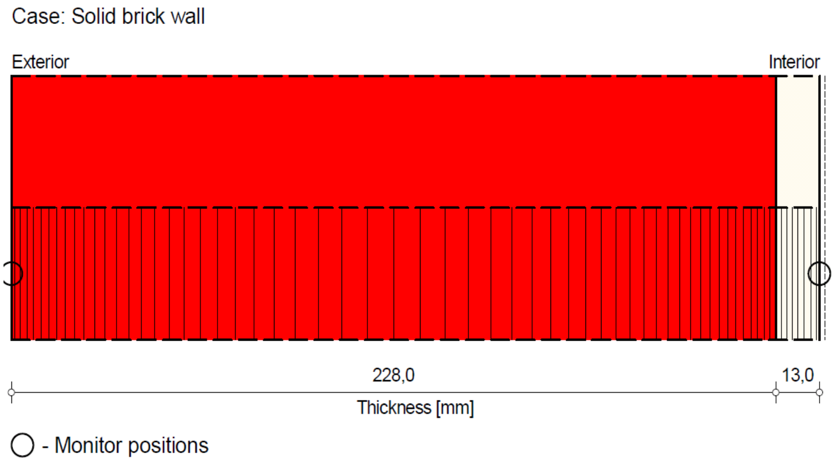

Figure 10.10 The modelled construction (Wufi Pro 5.0) with indication of the monitoring positions, where e.g. T and RH are logged as hourly values.

10.6.2 CONSTRUCTION MODELLED IN 2D

Most of the input parameters for a problem in 2 dimensions are the same as for a problem in 1 dimension. However, the physical model of the construction is different in 2D and below figures show an example on a model for a wall of solid granite stones.

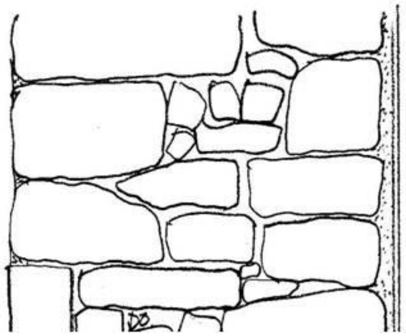

Figure 10.11 Cross section picture of the solid granite wall.

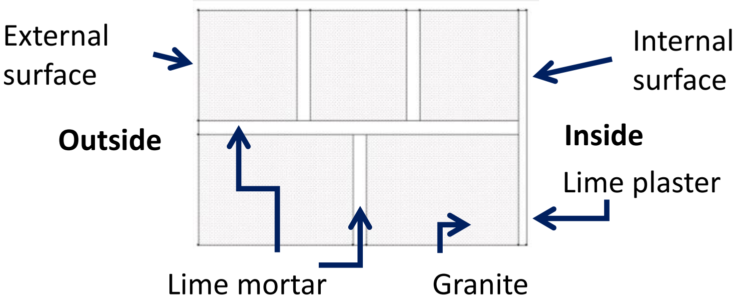

Figure 10.12 WUFI® 2D model of the solid granite wall

The presentation of the granite wall in Figure 10.12 shows a very simplified presentation of the stone/mortar matrix. The grade of simplification must be carefully planned and depends on the balance between computing capacity and time and the uncertainty of other parameters, including the material parameters.

NOTE: The assessment of the 2D simulation results is identical to the method described in this report for one-dimensional hygrothermal simulation.

10.6.3(VENTILATED) CAVITIES

If there is a ventilated cavity in the construction, the effect of the ventilation should be modelled as realistic as possible. However, a true description of the heat, air and mass flow in such a cavity would require a detailed CFD model, which is unnecessary for most of the cases.

A much simpler model can give, however, a qualified presentation of the drying potential or the opposite, of the cavity. E.g. 1D WUFI (Wufi Pro) uses a simple air change rate of the cavity, where the cavity is ventilated with outdoor air with a given rate.

The calculations should be performed for at least for a case with a "standard" ventilation rate of the cavity (e.g. 50 h^{-1}). A parameter study can cover cases with a very poor ventilation rate (e.g. 1 h^{-1}) and a good ventilation rate (e.g. 100 h^{-1}).

10.6.4SURFACE TRANSPORT COEFFICIENTS

The surface transport coefficients for heat and moisture should be estimated or the best standard values should be used. In some programs, these are determined dynamically as a function of wind, sun, facade color etc. Therefore, if possible, these factors should be taken into account for the most real representation of the construction and facade orientation to be studied. Typical colors, coatings etc. should be represented. These have an effect on the radiative heat transfer properties as well as on the transport of moisture. The effective water vapor resistance of e.g. interior painting should be estimated.

10.6.5 INITIAL MOISTURE CONTENT

Another important parameter for the description of the construction to be studied is the assumed initial moisture content of the material layers. According to the common standards, e.g. ASHRAE (TenWolde 2008) Guidelines, and practice, an equilibrium moisture content (EMC) corresponding to RH=80% should be used as a standard value (=EMC80).

A higher value. e.g. EMC90 or even 2 x EMC80, or any better estimate for the actual case, for the initial moisture content should be used

- If it is known that the construction to be studied has a higher moisture content, e.g. due to driving rain on unprotected facade
- If new concrete elements or other materials having high initial moisture content are included in the refurbished solution
- When studying the general drying potential of the facade.

10.7 Description of the boundary conditions

When assessing the hygrothermal performance of the constructions, the goal is to find as true a presentation as possible of the conditions the wall construction is exposed to. However, to reveal any potential risks of moisture related problems or damage, the simulated conditions should be chosen to present a worst, but also a probable case scenario. The calculation analysis should show that the construction is robust enough both regarding the durability and the indoor air quality and comfort. In the following, some guidelines are given for choice of the exterior and interior climates for simulations.

10.7.1 EXTERIOR CLIMATE

Data from a weather station representative to the analysed region and constructions should be chosen, because a great variety of the climatic effects can be possible within a relatively small geographical area. This concerns e.g. amount of driving rain and solar radiation. Therefore, depending on the actual or a probable location of the construction and the solution to be used, the necessary sensitivity analysis of the climate data should be considered.

10.7.2 LOCAL EXPOSURE AND COMPASS ORIENTATION OF THE FACADE

The performance of the vertical constructions should be analysed in the four main orientations: N-E-S-W. This kind of variation would reveal the impact of environmental factors as driving rain and solar radiation. Alternatively, the weather data can be analysed and the orientation with the biggest impact can be found (see Figure 10.13, where the worst orientation with regard to driving rain is SW-W). A calculation with the orientation with biggest impact of driving rain and/or solar radiation used as worst case and the opposite orientation as least worst case would often be enough.

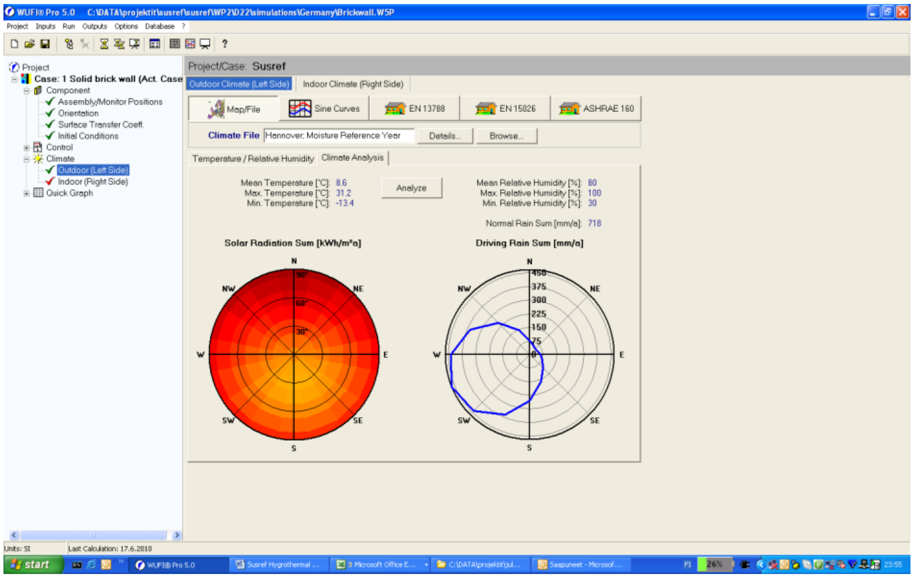

WUFI® Pro 5.0 C:\DATA\projektit\susref\susref\WP2\D22\simulations\Germany\Brickwall.W5P

Project/Case: Susref

Case: 1 Solid brick wall (Act. Case

Climate File: Hannover; Moisture Reference Year

Mean Temperature [°C]: 8.6
Max. Temperature [°C]: 31.2
Min. Temperature [°C]: -13.4

Mean Relative Humidity [%]: 80
Max. Relative Humidity [%]: 100
Min. Relative Humidity [%]: 30

Normal Rain Sum [mm/a]: 718

Units: SI
Last Calculation: 17.6.2010

Figure 10.13 Analysis of weather data in Wufi: Amount of solar radiation and driving rain as a function of orientation in Hannover.

If your software calculates the driving rain - combination of wind speed, wind direction and perception - make a sensitivity analysis of the impact of it. The worst case would be in the corners of a tall building and the least bad case in the middle of a low building facade.

10.7.3 INTERIOR CONDITIONS

For numerical simulations of the thermal envelope constructions, the typical temperature and relative humidity or additional moisture of the interior climate ranges should be used.

In general, EN ISO 13788, Annex A (CEN 2001) gives moisture loads for use in calculation of surface temperatures to avoid risk of condensation. But this model is intended for steady-state assessment of interstitial condensation using the Glaser method. EN 15026 (CEN 2007) describes numerical assessment of transient moisture transfer. This standard describes classes for high and low occupancy office buildings or dwellings.

User preferences and habits vary, affecting the way the users interact with the building and its technical systems. For building simulations it is often supposed that the indoor temperature will be kept somewhere between 20 ºC and 25 ºC (EN 15026) or in a narrower band (ASHRAE Standard 160), but some users may prefer higher or lower temperature than this, either for comfort or for trying to save energy. The moisture productive activities vary from the user to another. The ventilation system and rates have a huge impact on the resulting indoor air temperature and especially moisture concentrations. Thus, relative humidity may vary considerably between different buildings and even in different rooms in a single dwelling.

As a first choice for the analysis, moisture loads according to EN 15026 as a function of outdoor climate are therefore recommended to be used. A screen dump from WUFI program in Figure 10.14 shows the variation of both indoor temperature and indoor relative humidity as a function of the outdoor climate and internal moisture load. Use both standard and high moisture load for parameter analysis according to EN 15026.

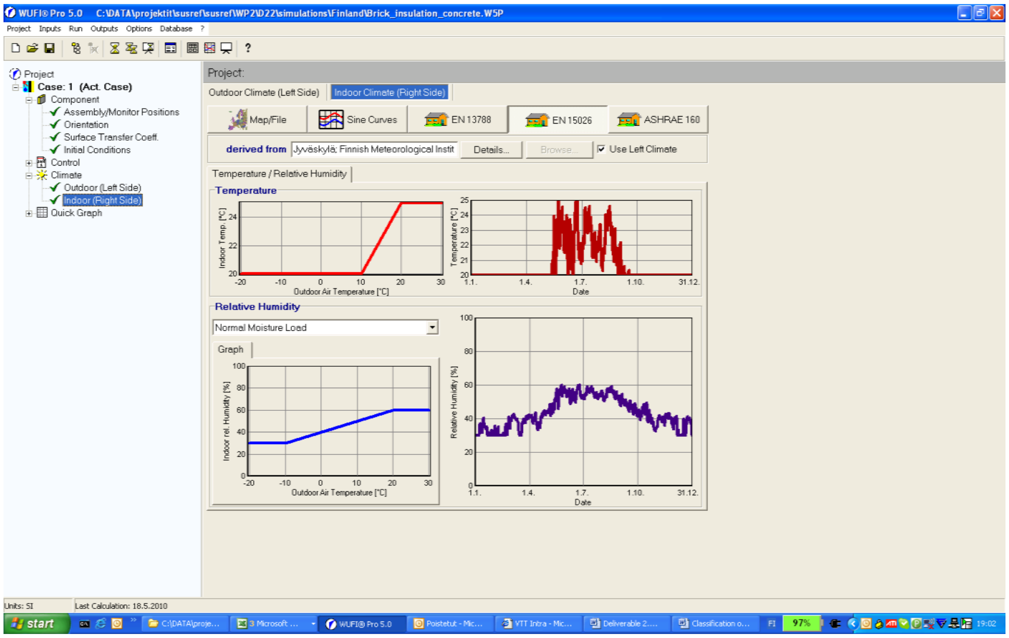

Figure 10.14 Definition of indoor climate as a function of outdoor climate according to EN15026.

This figure illustrates well why EN 15026 is more realistic than the EN13788 as the indoor temperature in EN 15026 floats up to 25 degrees as a function of outdoor temperature during the warm periods and is not fixed at 20 as in EN13788, which would require mechanical cooling.

The indoor climate will be (unrealistic) fixed when applying above standards. Therefore, in some software, there is a possibility to apply the resulting interior climate from a whole building simulation (e.g. EnergyPlus) as an indoor climate for a building physical simulation of the constructions: A kind of "indoor weather data file" can be created for any actual case, where the indoor boundary conditions are variables and a result of the outdoor conditions, the whole building design including HVAC systems and the performance of the building envelope. By using such a resulting indoor weather file, it is possible to apply e.g. the integrated effect of the solar radiation load and the thermal capacity of the whole building to a realistic temperature scale of the indoor air. This is, however, for the advanced use of the software.

10.8 Calculation and parameter variation

After selecting the suitable calculation tool, description of the construction and definition of the boundary conditions, the next step is the performing of the dynamic simulations. This section describes shortly some of the main parameters and assumptions for the calculations. Standard numerical setup of the calculations (accuracy, convergence, control of time steps etc.) depends on the software to be used and will therefore not be discussed here. The recommendations in the manual and professional experience should be followed.

10.8.1SIMULATION TIME PERIOD

The dynamic simulations of external constructions should typically run for 3-5 years and maybe more for the very massive constructions. Any construction involving soil as a semi-infinite medium will require a much longer simulation period and should be studied carefully.

The simulation period needed is based on the assumption of achieving so called quasi steady state for the analysed construction: The seasonal changes should be the same from year to year. The fulfilment of this criterion can be found with e.g. making the first calculation to take 10 years. Figure 10.15 illustrates the quasi steady state. Results for the first quasi steady state year are used for analysis.

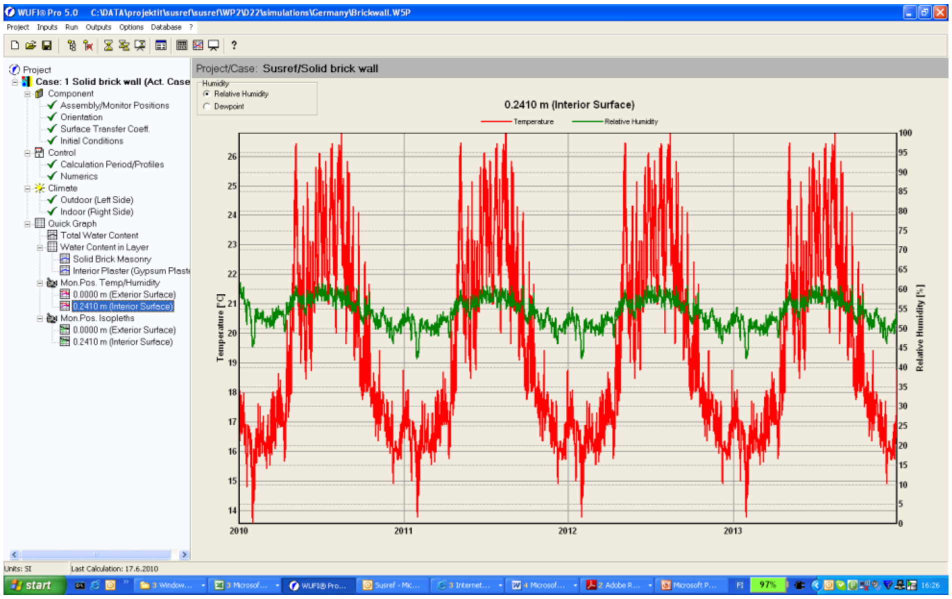

Figure 10.15 Illustration of the finding the quasi steady state for calculation. The simulation runs here for 4 years. In this case, the results for the 3. year fulfil the quasi-steady criterion and can be used for the further analysis.

During the calculation, the important variables at any critical locations/layers should be logged. These are listed in Table 10.5.

Table 10.5 Simulation output to be logged in every critical location.

Temperature	*T* [˚C]	Hourly values for last year of simulation
Relative humidity	*RH* [%]	Hourly values for last year of simulation
Moisture content	*w* [kg/m^3]	Water content of a material layer or whole construction in the start of the last year of simulation and in the end of the year.

Hourly information on T and RH can be used for different types of hygrothermal analysis and post processing of some key figures (indoor thermal comfort, condensation risk, TOW, Mold index, etc). The yearly change in water content shows an overview on the potential for moisture accumulation. Basically, the moisture content should not be increasing.

10.8.2 SENSITIVITY ANALYSIS OF PARAMETERS

Simulations should be run for a number of relevant parameters that may have an impact on the hygrothermal performance of the constructions. These are especially regarding:

- compass orientation
- outdoor climate type and loads (e.g.driving rain)
- any variation of surface properties relevant for the construction (e.g. colour for radiation, coatings for moisture diffusion resistance, etc)
- indoor moisture loads
- initial moisture content

Some examples on possible parameter values of these are given in Table 10.6.

When assessing the influence of the initial moisture content (built-in moisture), the assumption of using the results for a quasi-steady solution is not relevant. For this parameter, the simulation period needed has to be estimated and to be run for e.g. 5 years in order to reveal the robustness of the construction for the built-in moisture, e.g. wetting of the materials on the building site.

Table 10.6 Examples on parameters to be varied, and suggestions for the parameter values. The inclusion of the relevant parameters needs to be considered from case to case.

Parameter	**Suggested values for the parameters**			
Outdoor climate and type	Average year for the location		Extreme year (regarding moisture)	
Orientation	North	East	South	West
Driving rain	Less exposed		Very exposed	
Indoor moisture load	Normal		High	
Initial moisture content	Normal: EMC80		High: e.g.2 x EMC80	
Exterior surface diffusion resistance	None: S_d = 0 m		High: S_d = 10 m	
Interior surface diffusion resistance	None: S_d = 0 m		High: S_d = 100 m	
Colour of facade	Light: α = 0,4		Dark: α = 0,88	
Ventilation rate of ventilated cavities (if relevant)	Poor: e.g. n = 1 h^{-1}	Standard: e.g. n = 50 h^{-1}	Good: e.g. n = 100 h^{-1}	

Another and important group of parameters to be varied:

  - expected variation in the material data of the construction materials
  - choice and variation of materials (e.g. different types of insulation materials)

The sensitivity analysis of the expected variation in the material properties is recommended due to the great uncertainty around the material properties. Materials are presented in the simulation tools by a set of material parameters and there are typically quite a few simplifications and assumptions related to these parameters, even though they are based on measured data. Also, there might not exist material data for exactly the material in question.

It is difficult to give any clear recommendations for a systematic analysis of this uncertainty as the material values have a very large variation range - depending on the material and the exposure conditions, too. Therefore, the need for sensitivity analysis has to be evaluated from case to case. A study on the influence of uncertainty of input data on hygrothermal simulations shows that while probable variations in the indoor and outdoor climate have a great impact on the resulting hygrothermal behaviour of the construction, the influence of some material parameters like density, thermal conductivity and thermal capacity can often be neglected. But parameters related to the moisture storage capacity and the liquid moisture transport may have as big impact as the climate data (Holm 2004).

10.9 Analysis and assessment of the results

The purpose of performing a set of hygrothermal simulations with parameter variations is to create basis for presentation of the results in such way that a potential trend of solutions will be revealed. The result could be e.g. that the insulation thickness should not exceed a certain value with a specific insulation material or exterior finish or if a non-ventilated construction is used.

10.9.1TEMPERATURE AND RELATIVE HUMIDITY CONDITIONS

One of the basic outputs from the dynamic heat and moisture simulations are the hourly T and RH in a specific location of the construction. The number of these locations to be assessed depends strongly on the studied construction type. Figure 10.16 shows the temperature and relative humidity of the indoor surface of the non-insulated brick wall used as an example. This kind of result presentation illustrates easily, if there is a potential problem, like in this case: due to the non-insulated wall, the surface temperature of the wall in contact with indoor air varies strongly as a function of outdoor air. This combined with the relatively heavy load of driving rain - and no water protection of the facade - , which wets the construction from outside, the relative humidity of the interior surface is very high giving optimal conditions for mold growth (see Figure 10.17). This construction needs more insulation, and exterior insulation is normally the best solution when not dealing with listed buildings, etc. It is cost effective and results in no thermal bridging.

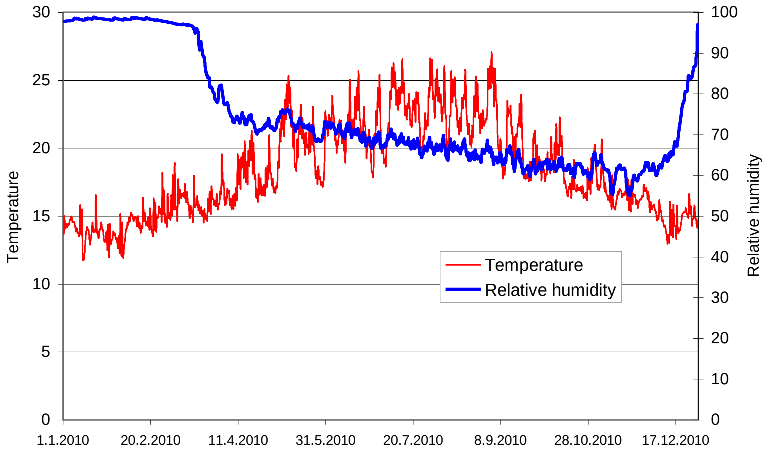

Figure 10.16 T and RH on the indoor surface of the massive brick wall facing south in Hannover.

In order to quantify the input to the assessment procedure, numerical data is needed as output from the hygrothermal calculations. There are 2 different methods: using a dynamic model for the post-processing or using some simple key figures.

10.9.2 ANALYSIS WITH DYNAMIC MODELS

One of the possibilities for post-processing the simulated temperature and relative humidity data is to perform the numerical mold growth calculations and get the predicted mold growth risk for critical parts of the construction. Figure 10.17 shows the calculated mold index during a three year period for the internal surface of the original example construction. The mold index is calculated on T and RH given in Figure 10.16.

The assumptions for the mold growth calculation are that the material of interior surface is relatively sensitive to biological growth, i.e. wall paper. The results from the used VTT model for prediction of mold growth must be seen in relation to other solutions and not as absolute values. The most important information from the Figure 58 is, however, that the modelled mold growth is increasing from year to year. This makes the hygrothermal conditions of this construction unacceptable.

The best way to use the predicted mold growth as an assessment tool is to compare different construction solutions with each others: The solution with the lowest risk for the mold growth would most probably also have least other moisture related problems.

For the example case, an obvious improvement is to add insulation. But how much, what type of materials, as an exterior or an interior insulation and whether there is a need for vapor barrier or not? These questions can be answered and the best solution found by comparing the resulting mold growth indexes.

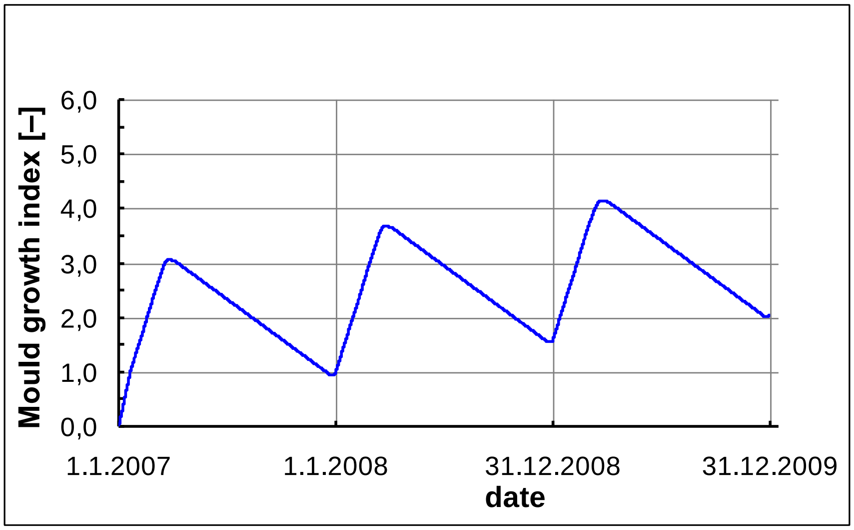

Figure 10.17 The mold growth index calculated from the data in Figure 57. The growth model is the modified VTT model and the growth index has been calculated for a sensitive class with the relatively strong decrease of the mold growth (0,5) outside the growth conditions.

10.9.3 ANALYSIS WITH SIMPLE KEY VALUES

Another approach for post-processing the simulated temperature and relative humidity data is to determine a set of simple key values from the hourly T and RH and assess the different solutions with them. The following list shows the parameters that could be determined for the different combinations of parameter variations (Table 10.6).

The graphical presentation of the results will often help to find any trends and the best solution (Figure 10.18).

- U-value of the construction
- Annual transmission heat loss
- Temperature factor f_{Rsi}
- Lowest indoor surface temperature, T_{min}
- Amount of accumulated water in the construction during a year, Δw
- Running averages of temperature and relative humidity according to the criteria given in Table 10.1 and resulting number of hours exceeding the criteria.
- or

TOW (time of wetness) according to the different criteria for different risks, as grouped together in

- Table 10.7.
- and eventually also
- Thermal bridge effects (if relevant) for use in whole building simulations = an addition to the U-value.

Table 10.7 Calculation criteria for time of wetness (TOW) to be used in the hygrothermal assessment.

	TOW for different performance criteria		
	Frost	Mold	Condensation, algae, decay
Temperature	<0˚C	> 0˚C	> 0˚C
Relative humidity	>95 %	>80 %	>95 %

Time of wetness (TOW), i.e number of hours above/below given threshold values depending on the risk in focus, is relatively simple to understand and implement in calculation work. Note that different risks are assessed with different threshold values.

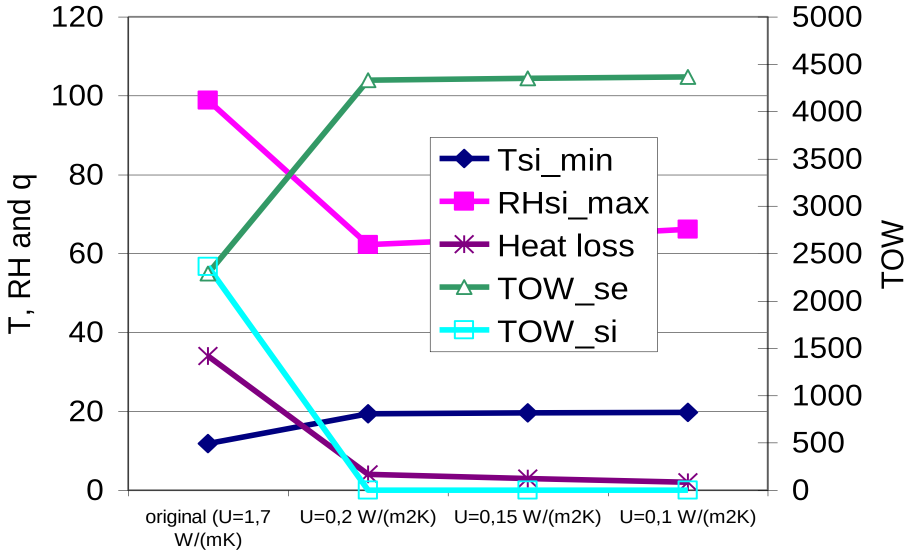

Figure 10.18 An example on the graphical presentation of the assessment results. The un-insulated original brick wall and three different exterior insulation solutions with different insulation thickness,

The different presented criteria for hygrothermal performance are typically determined by numerical HAM-simulations either in 1D or 2D. A very central issue in the simulation work is, however, the sensitivity analysis of any significant parameters. With such a sensitivity analysis, the expected range of any natural variation in material parameters and e.g. weather exposure and indoor loads can be found and can result in an expected risk.

Another approach is to make probabilistic analysis, where all input parameters can e.g. be varied randomly. The result will not be a numerical value of the risk but a probability function, which, however, will describe the risk more realistic.(Pietrzyk 2009)

Therefore, setting any numerical criteria for performance is difficult and risky, but a must for a proper assessment.

A central challenge in the assessment work is hereafter to evaluate these very different criteria as one number in order to find the best construction solutions: The purpose is, nevertheless, to

- minimise all risks:
    - no moisture accumulation, the better drying potential the better performance
    - TOW as low as possible for all the considered risks
    - T_{si} as high as possible in order to ensure excellent thermal indoor environment and good indoor air quality (e.g. no risk of mold growth due to the low surface temperatures)
- and maximise the benefits:
    - as low U-values as possible in order to save heating energy
    - no thermal bridges in order to save heating energy and improve the indoor environment

10.10 Appendix: Numerical model for estimation of risk for mold growth on different building materials

Numerical simulation of mold growth can be used as one of the hygrothermal performance criteria of building structures. Mold growth is one of the first signs of too high moisture content of materials and it may affect the indoor air quality and also the appearance of the visible surfaces. Mold growth potential can be predicted by solving a numerical value, mold growth index, by using the dynamic temperature and relative humidity histories of the subjected material surfaces.

The presented model was originally based on mold growth of wooden materials, but it has later been completed with several other building materials. The model can be used parallel with a heat, air and moisture simulation models or as a post processing tool. This presentation is a short description of the model equations. More information about the research work and the large experimental program behind the model is found in the given literature.

The Mold Growth Index

The mold growth is quantified by an index as given in Table 8.

Table 10.8 determination of Mold Growth Index for Experiments and Modeling.

	Description of the growth rate
0	No growth
1	Small amounts of mold on surface (microscope), initial stages of local growth
2	Several local mold growth colonies on surface (microscope)
3	Visual findings of mold on surface, < 10 % coverage Or < 50 % coverage of mold (microscope)
4	Visual findings of mold on surface, 10 - 50 % coverage Or >50 % coverage of mold (microscope)
5	Plenty of growth on surface, > 50 % coverage (visual)
6	Heavy and tight growth, coverage about 100 %

The critical conditions for mold growth

For very sensitive building materials, like wood, the relative humidity level of 80 % RH is typically considered to be the lowest possible to allow mold growth during long exposure time, usually months. Even lower levels of relative humidity has been seen (75 % RH), but mainly for other than building materials. The lowest RH level that starts the growth in wooden material corresponds to 17 – 19 % (by weight) moisture content. With more resistant materials the required growth condition is obviously higher or, at least, the required exposure time is much longer. Equation 1 gives the critical relative humidity RHcrit [%] in different temperatures T [ºC] and Table 9 presents the used material sensitivity classes together with observed and suggested RHmin [%].

$$RH_{crit} = \begin{cases} \max\left[-0.00267T^3 + 0.160T^2 - 3.13T + 100.0, RH_{min}\right], \text{ when } T \leq 20 \\ RH_{min}, \text{ when } T > 20 \end{cases} \tag{10.3}$$

Table 10.9 Mold sensitivity classes and some typical materials and suggested RH_{min} based on experimental observations.

Mold sensitivity class	Materials	RH_{min}
Very sensitive	Untreated wood, includes lots of nutrients for biological growth	80 %
Sensitive	Planed wood, paper coated products, wood based boards	80 %
Medium resistant	Cement or plastic based materials, mineral fibers	85 %
Resistant	Glass and metal products, materials with efficient protective compound treatments	85 %

The mold growth model

A differential equation presents the mold growth, equation 2

$$\frac{dM}{dt} = \frac{1}{7 \cdot \exp(-0.68 \ln T - 13.9 \ln RH + 0.14W - 0.33SQ + 66.02)} k_1 k_2 \tag{10.4}$$

where *M* is the Mold Growth Index [-], *t* is time [days], the factor k_1 represents the intensity of growth (Equation 3 and 4) and SQ is the term for surface quality (*SQ* = 0 for sawn surface, *SQ* = 1 for kiln dried quality). For other materials than wood the value *SQ* = 0 is used, which omits this factor. Numerical simulation is typically carried out using one hour time steps so this should be kept in mind when using the equation.

$$k_1 = \frac{t_{M=1,pine}}{t_{M=1}}; \quad when \quad M < 1 \tag{10.5}$$

$$k_1 = 2 \bullet \frac{t_{M=3,pine} - t_{M=1,pine}}{t_{M=3} - t_{M=1}}; \quad when \quad M \geq 1 \tag{10.6}$$

where t_M=1 is the time needed for the material to start the growth (Mold index reaches level *M* = 1), and t_M=3 the time needed for the material to reach level *M* =3. The subscript pine refers to the value with reference material pine.

The factor k_2 (Equation 5) represents the moderation of the growth intensity when the mold index (M) level approaches the maximum peak value.

$$k_2 = \max\left[1 - \exp\left[2.3 \cdot \left(M - M_{max}\right)\right], 0\right] \tag{10.7}$$

where the maximum mold index M_{max} level depends on the prevailing conditions and the material sensitivity class.

The mold growth intensity is the dominating factor in the simulation of growth when the mold index is not close to the maximum index values typical for the material under such conditions. The characteristic maximum values set restrictions for the growth and limit the index to realistic levels and can be written in form (Equation 6):

$$M_{\max} = A + B \cdot \frac{RH_{crit} - RH}{RH_{crit} - 100} - C \cdot \left(\frac{RH_{crit} - RH}{RH_{crit} - 100}\right)^2 \tag{10.8}$$

In this equation the coefficients A, B and C have values that depend on the material class. M_{max} has an effect on the factor k_2 (Equation 5). This classification is presented both for growth intensities and maximum mold index levels in Table 10.

Table 10.10 parameters for the different sensitivity class limits of the mold model.

	k_1		k_2 ($M_{\max}$)		
Sensitivity class	$M<1$	$M\geq1$	A	B	C
very sensitive	1	2	1	7	2
sensitive	0.578	0.386	0.3	6	1
medium resistant	0.072	0.097	0	5	1.5
resistant	0.033	0.014	0	3	1

Decline of mold index

The model takes into account also the change in the mold index level when the conditions are outside the favorable conditions for mold growth, i.e. the relative humidity is lower than the critical values solved in equation 1. This includes also the temperature limits: Mold does not grow below 0 °C . The warm end of the growth criteria have not been modeled as well as the area below typical indoor temperatures.

The degradation of mold on wooden surface has been modeled based on cyclic changes between two humidity conditions, equation 7:

$$\frac{dM}{dt}_{pine} = \begin{cases} -0.00133, \text{when } t \text{ - } t_1 \leq 6\,\text{h} \\ 0, when\ 6\,\text{h} \leq t - t_1 \leq 24\,\text{h} \\ -0.000667, \text{when } t \text{ - } t_1 > 24\,\text{h} \end{cases} \tag{10.9}$$

where M is the mold index and t is the time (h) from the moment t_1 when the conditions on the critical surface changed from growth to outside growth conditions. For longer periods (week, months) this gives practically linear decrease of mold index.

Decline of mold index for other materials is presented using a constant, relative coefficient for each material (Equation 8) so that the original decline model for wood could be applied using these additional factors.

$$\frac{dM}{dt}_{mat} = C_{mat} \cdot \frac{dM}{dt}_{pine} \qquad (10.10)$$

where $(dM/dt)_{mat}$ is the mold decline intensity for each material, $(dM/dt)_{pine}$ is that for pine and C_{mat} is the relative coefficient for mold index decline.

The decline of mold intensity on materials under unfavorable mold growth conditions could be presented as decline classes (Table 11). This classification is based on few measurements with relatively large scattering and it should be considered as the first approximation of these classes. By choosing a low value, a worst case scenario is presented: The mold growth risk potential stays on the level it reached under favourable conditions.

Table10.11 classification of relative mold index decline.

C_{mat}	Description
1.0	Strong decline (Pine in original model, short periods)
0.5	Moderate decline
0.25	Relatively low decline
0.1	Almost no decline

10.11 Literatures

Klaus Sedlbauer; Hartwig M Künzel; Andreas H Holm (2004) Predicting Indoor Temperature and Humidity Conditions Including Hygrothermal Interactions with the Building Envelope. ASHRAE Transactions Vol: 110 ISSN: 0001-2505 06/2004. Start Page: 820

Viitanen, H., Hanhijärvi, A., Hukka, A. and Koskela, K. Modelling mold growth and decay damages In: Seppänen, O. & Säteri, J. (ed). Healthy Buildings 2000. Vol. 4. FiSIAQ, s. 341 - 346.

Fagerlund, G. Kritiska vattenmättnadsgrader ved frysning av porøsa och spröda bygnadsmaterialer, Rapport 34, LTH-BML. Sverige,1972

Sedlbauer, K. 2001. Prediction of mold fungus formation on the surface of/and inside building components. University of Stuttgart, Fraunhofer Institute for building Physics, Thesis. Stuttgart. Germany.

Hukka, A, and Viitanen, H. 1999. A mathematical model of mold growth on wooden material. Wood Science and Technology. 33 (6) 475-485.

Ojanen, T, Viitanen, H, Peuhkuri, R, Lähdesmäki, K, Vinha, J, Salminen, K. (2010) Mold growth modeling of building structures using sensitivity classes of materials. Proceedings of Thermal Performance of the Exterior Envelopes of Whole Buildings XI. Clearwater Beach. December 2010 Florida.

Clarke, J.A. Johnstone, C.M. Kelly, N.J. Mclean, R.C. Anderson, J.A., Rowan N.J. and Smith, J.E. 1998. A technique for prediction of the conditions leading to mold growth in buildings. Building and Environment 34 pp 515-521.

Hens, H.L.S.C. 1999. Fungal defacement in buildings: A performance related approach. International Journal of Heating, Ventilation, Air-Conditioning and Refrigerating Research Vol 5 H 3, p. 256 – 280.

American Society of Heating, Refrigerating and Air-Conditioning Engineers. www.ashrae.com

ASHRAE Standard 160P-Criteria for Moisture Control Design Analysis in Buildings. Author: Anton TenWolde
ASHRAE Transactions 12/2008. Vol: 114 ISSN: 0001-2505.. Start Page: 167

Møller, E.B (2003) Hygrothermal performance and soiling of exterior building surfaces. PhD Thesis. Report R-068. Technical University of Denmark, Department of Civil Engineering.

Viitanen, H; Toratti, T; Makkonen, L; Peuhkuri, R; Ojanen, T.; Ruokolainen, L.; Räisänen, J. (2010) Towards modelling of decay risk of wooden materials. European Journal of Wood and Wood Products. Vol. 68 (2010) No: 3, 303 – 313

Viitanen, H. 1996. Factors affecting the development of mold and brown rot decay in wooden material and wooden structures. Effect of humidity, temperature and exposure time. Doctoral Thesis. Uppsala. The Swedish University of Agricultural Sciences, Department of Forest Products. 58 p

Holm, A. (2001). Drying of an AAC flat roof in different climates. Computational sensitivity analysis versus material property measurements. Paper to CIB-W40 Meeting, Wellington, New Zealand, April 2001

Pietrzyk, Krystyna (2010) Thermal Performance of a Building Envelope - A Probabilistic Approach. Journal of Building Physics Vol: 34 Issue: 1. ISSN: 1744-2591 Date: 07/2010 Pages: 77 - 96

Viitanen, Hannu; Ojanen, Tuomo (2007) Improved model to predict mold growth in building materials. Proceedings. Thermal Performance of the Exterior Envelopes of Whole Buildings X. Clearwater Beach, USA, 2 - 7 Dec. 2007. CD. ASHRAE, DOE, ORNL. Atlanta, USA

11 COUPLED HEAT-AIR & VAPOR-AIR TRANSFER IN BUILDING ENVELOPES

When air flows through a building component, it significantly affects the temperature and moisture distribution within the component. Moisture accumulation within the material of a building envelop can lead to poor thermal performance of the envelope, degradation of organic materials, metal corrosion and structure deterioration. In addition to the building's construction damage, moisture migrating through building envelopes can also lead to poor interior air quality as high ambient moisture levels result in microbial growth, which may seriously affect human health and be a cause of allergy and respiratory symptoms. Therefore, the investigation of heat and moisture transfer in porous building materials is important not only for the characterization of behavior in connection with durability, waterproofing and thermal performance but also for avoiding health risk due to the growth of microorganisms. This lecture note consists of two parts:

(1) Coupled heat and air transfer in building envelopes.
(2) Coupled vapor and air transfer in building envelopes.

The whole building heat, air and moisture transfer will be discussed in the next lecture.

11.1 Coupled heat and air transfer

Heat transfer and airflow through a building component exert an effect on each other. Coupled air advection and heat conduction leads to a completely different thermal regime in the component. The interaction between heat and air transfer in permeable conductive materials and components can be best explained by a case study of the dynamic insulation.

11.1.1 CONCEPT FOR DYNAMIC INSULATION APPROACH

Dynamic insulation is a form of insulation where cool outside air flowing through the thermal insulation in the envelope of a building will pick up heat from the insulation fibres. Buildings can be designed to exploit this to reduce the transmission heat loss and to provide pre-warmed, draft free air to interior spaces. This is known as dynamic insulation since the U-value is no longer constant for a given wall or roof construction but varies with the speed of the air flowing through the insulation. Dynamic insulation is different from breathing walls. The positive aspects of dynamic insulation need to be weighed against the more conventional approach to building design which is to create an airtight envelope and provide appropriate ventilation using either natural ventilation or mechanical ventilation with heat recovery. The airtight approach to building envelope design, unlike dynamic insulation, results in a building envelope that provides a consistent performance in terms of heat loss and risk of interstitial condensation that is independent of wind speed and direction. Under certain wind conditions a dynamically insulated building can have a higher heat transmission loss than an airtight building with the same thickness of insulation.

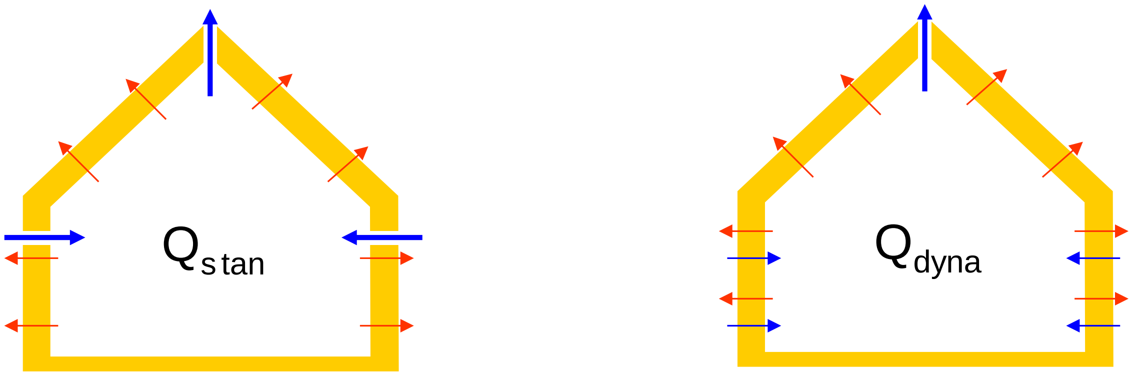

Standard insulation & ventilation

Dynamic insulation & ventilation

Figure 11.1 Comparison of Standard insulation and dynamic insulation

The heat balance for standard insulation & ventilation could be expressed as follow:

$$Q_{stan} = \left(\sum \underset{\rightarrow}{A_k U_k} + \underset{\rightarrow}{G_a c_a}\right)(T_i - T_e) \qquad (10.1)$$

Where:

Q: heat flow [W]
A: component area [m²]
U: component U-value [W/(m²·K)]
T: temperature [K]
G_a: air mass flow [kg/s]
c_a: air thermal capacity [J/(kg·K)]

11.1.2 SCIENCE OF DYNAMIC INSULATION

All the main features of dynamic insulation can be understood by considering the ideal case of one-dimensional steady state heat conduction and airflow through a uniform sample of air permeable insulation.

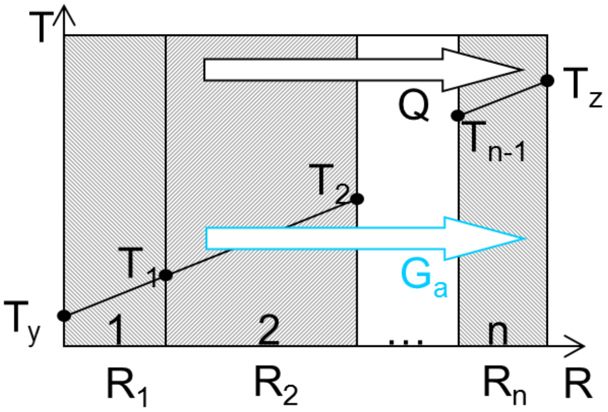

Figure 11.2 One-dimensional steady state heat conduction and airflow through a building component

The total heat flux could be expressed as follow:

$$Q_{tot} = Q_{adv} + Q_{cond} = constant \tag{10.2}$$

$$Q_{adv,y} = G_a c_a T_y \qquad \neq \qquad G_a c_a T_z = q_{adv,z} \tag{10.3}$$

$$Q_{cond,y} = -A\lambda \left.\frac{\partial T}{\partial x}\right|_y \qquad \neq \qquad -A\lambda \left.\frac{\partial T}{\partial x}\right|_z = Q_{cond,z} \tag{10.4}$$

Where

Q: heat flow [W]
G_a: air mass flow [kg/s]
c_a: air thermal capacity [J/(kg·K)]
T: temperature [K]
A: surface area [m^2]
λ: thermal conductivity [W/(m·K)]
adv: advection
cond: conduction
tot: total

At every point in the component, for steady state conditions, the energy balance equations are as follows:

$$Q_{tot} = Q_{adv} + Q_{cond} = constant$$

$$\left.\begin{aligned} Q_{adv} &= G_a c_a T \\ Q_{cond} &= -A\lambda \frac{\partial T}{\partial x} = -A \frac{\partial T}{\partial R} \end{aligned}\right\} \quad \begin{aligned} & G_a c_a T - A \frac{\partial T}{\partial R} = constant \\ & T_x = C_1 + C_2 \exp(g_a c_a R_{y-x}) \end{aligned}$$

$$\Rightarrow \boxed{T_x = T_y + \left(T_z - T_y\right) F_1\left(R_{y-x}\right)}$$

$$F_1\left(R_{y-x}\right) = \frac{\exp(g_a c_a R_{y-x}) - 1}{\exp(g_a c_a R_{y-z}) - 1}$$

$$\mathrm{Q_{tot} = Q_{adv} + Q_{cond} = constant}$$

$$\left.\begin{aligned} \mathrm{Q_{adv}} &= \mathrm{G_a c_a T} \\ \mathrm{Q_{cond}} &= -\mathrm{A}\lambda \frac{\partial \mathrm{T}}{\partial \mathrm{x}} = -\mathrm{A} \frac{\partial \mathrm{T}}{\partial \mathrm{R}} \end{aligned}\right\} \quad \begin{aligned} & \mathrm{G_a c_a T - A} \frac{\partial \mathrm{T}}{\partial \mathrm{R}} = \mathrm{constant} \\ & \mathrm{T_x = C_1 + C_2 \exp\left(g_a c_a R_{y-x}\right)} \end{aligned}$$

$$\boxed{\Rightarrow \mathrm{T_x = T_y + \left(T_z - T_y\right) F_1\left(R_{y-x}\right)}}$$

$$\mathrm{F_1\left(R_{y-x}\right)} = \frac{\exp\left(\mathrm{g_a c_a R_{y-x}}\right) - 1}{\exp\left(\mathrm{g_a c_a R_{y-z}}\right) - 1}$$

(10.5)

The Integration constants are

$$C_1 = T_y - \frac{T_z - T_y}{exp(g_a\, c_a R_{y-z}) - 1}$$

$$C_2 = \frac{T_z - T_y}{exp(g_a\, c_a R_{y-z}) - 1}$$

(10.6)

Where

Q:	heat flow [W]
G_a:	air mass flow [kg/s]
c_a:	air thermal capacity [J/(kg·K)]
T:	temperature [K]
A:	surface area [m²]
λ:	thermal conductivity [W/(m·K)]
g_a:	air mass flux [kg/(m²·s)]
R:	thermal resistance [m²K/W]
adv:	advection
cond:	conduction
tot:	total
y-x/z:	between faces y and x/z

The total heat flow through the building component can be expressed as follow:

$$
\begin{aligned}
Q_{tot} &= Q_{adv} + Q_{cond} = G_a c_a T_x + A F_2\left(R_{y-x}\right)\left(T_y - T_z\right) \\
&= A g_a c_a \left[T_y + \left(T_z - T_y\right) \frac{\exp\left(g_a c_a R_{y-x}\right) - 1}{\exp\left(g_a c_a R_{y-z}\right) - 1} \right] + A \frac{g_a c_a \exp\left(g_a c_a R_{y-x}\right)}{\exp\left(g_a c_a R_{y-z}\right) - 1} \left(T_y - T_z\right) \\
&= A g_a c_a \left[T_y + \left(T_y - T_z\right) \left(\frac{1 - \exp\left(g_a c_a R_{y-x}\right)}{\exp\left(g_a c_a R_{y-z}\right) - 1} + \frac{\exp\left(g_a c_a R_{y-x}\right)}{\exp\left(g_a c_a R_{y-z}\right) - 1} \right) \right] \\
&= A g_a c_a \left[T_y \frac{\exp\left(g_a c_a R_{y-z}\right) - 1}{\exp\left(g_a c_a R_{y-z}\right) - 1} + \left(T_y - T_z\right) \frac{1}{\exp\left(g_a c_a R_{y-z}\right) - 1} \right] \\
&= A g_a c_a \left[T_y \frac{\exp\left(g_a c_a R_{y-z}\right)}{\exp\left(g_a c_a R_{y-z}\right) - 1} - T_z \frac{1}{\exp\left(g_a c_a R_{y-z}\right) - 1} \right] \\
&= A \left[T_y \frac{g_a c_a \exp\left(g_a c_a R_{y-z}\right)}{\exp\left(g_a c_a R_{y-z}\right) - 1} - T_z \frac{g_a c_a}{\exp\left(g_a c_a R_{y-z}\right) - 1} \right] \\
&= A\left(T_y F_2\left(R_{y-z}\right) - T_z F_2(0)\right)
\end{aligned}
\tag{10.7}
$$

Where

$$
F_2\left(R_{y-x}\right) = \frac{g_a c_a \exp\left(g_a c_a R_{y-x}\right)}{\exp\left(g_a c_a R_{y-z}\right) - 1} \tag{10.8}
$$

Based on the above equations, we can calculate the temperature distribution within the building envelope for infiltration and exfiltration cases.

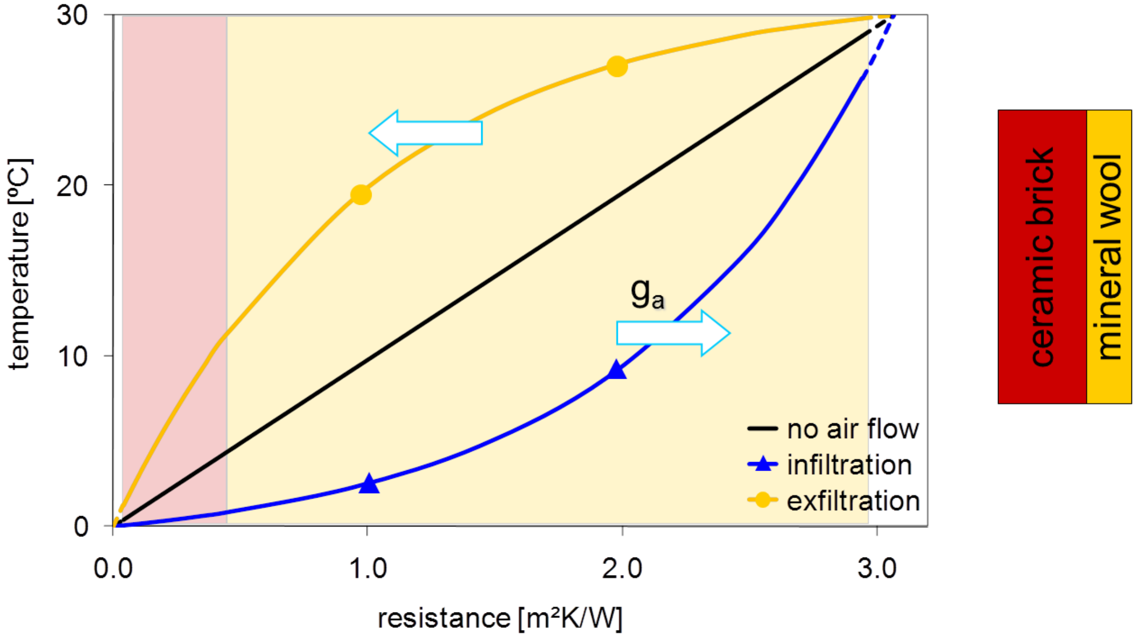

Figure 11.3 Temperature distribution within the building envelope

Temperature in insulated wall in function of R (|ga| = 1.0 10-3 kg/m²s)

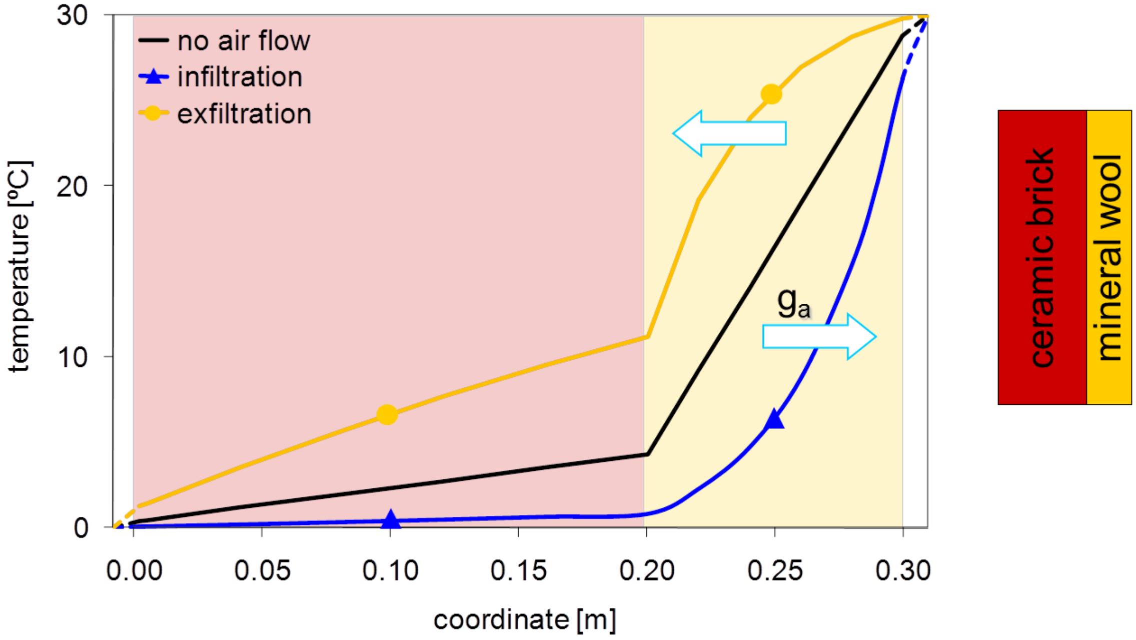

Figure 11.4 Temperature distribution within the building envelope

Temperature in insulated wall in function of x (|ga| = 1.0 10-3 kg/m²s)

Fig 11.4 shows the typical behaviour of the temperature profile through dynamic insulation where the air flows in the opposite direction to the heat flux. As the air flow increases from zero, the temperature profile becomes increasingly more curved. On the cold side of the insulation (x/L = 0) the temperature gradient becomes increasingly horizontal. As the conduction heat flow is proportional to the temperature gradient, the slope of the temperature profile on the cold side is a direct indication of the conduction heat loss through a wall or roof. On the cold side of the insulation the temperature gradient is close zero which is the basis for the claim often made that dynamic insulation can achieve a U-value of zero W/(m^2·K).

On the warm side of the insulation the temperature gradient gets steeper with increasing air flow. This implies heat is flowing into the wall at a greater rate than for conventional insulation (air speed = 0 mm/s). For the case shown of air flowing through the insulation at 1mm/s the temperature gradient on the warm side of the insulation *x/L* = 1) is 621 °C/m which compares with only 100 °C/m for the conventional insulation. This implies that with an air flow of 1mm/s the inner surface is absorbing 6 times as much heat as that for conventional insulation.

A consequence of this is that considerably more heat has to be put into the wall if there is air flowing through from outside. Specifically a space heating system six time larger than that for a conventionally insulated house would be needed. It is frequently stated that in dynamic insulation the outside air is being warmed up by heat that would be lost in any case.[5] The implication being that the outside air is being warmed by "free" heat. The fact that the heat flow into the wall increases with air speed is evidenced by the decreasing temperature of the inner surface. A dynamically insulated house requires also an air-to-air heat exchanger as does an airtight house. The latter has the further advantage that if it is well insulated it will require only a minimal space heating system.

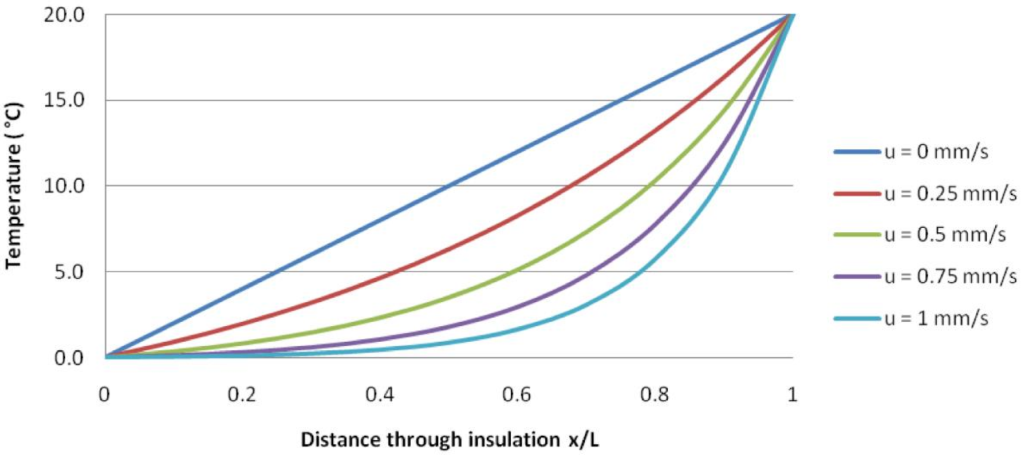

Figure 11.5 Air flowing through insulation from cold side to warm side

Fig 11.5 shows the typical behaviour of the dynamic insulation temperature profile when the air flows in the same direction to the conductive heat flow. As air at room temperature flows outwards with increasing speed the temperature profile becomes increasingly more curved. On the warm side of the insulation the temperature gradient becomes increasingly horizontal as the warm air prevents the insulation cooling down in the linear way that would occur with no airflow. The conductive heat loss into the wall is very much less than that for conventional insulation. This does not mean that the transmission heat loss for the insulation is very low.

On the cold side of the insulation the temperature gradient gets steeper with increasing air outward flow. This is because the air, having now cooled, is no longer able to transfer heat to the insulation fibers. In pro-flux mode, heat is flowing out of the wall at a greater rate than the case for conventional insulation. Warm moist air flowing out through the insulation and cooling rapidly increases the risk of condensation occurring within the insulation which will degrade the thermal performance of the wall and could, if prolonged, lead to mold growth and timber decay.

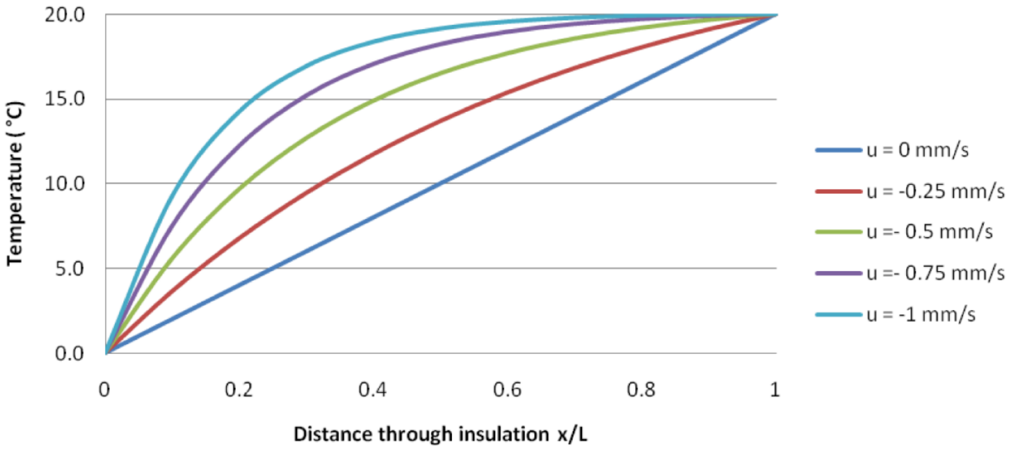

Figure 11.6 Air flowing through insulation from warm side to cold side

Fig 11.7 shows the interior surface temperature of insulated wall in function of infiltration rate.

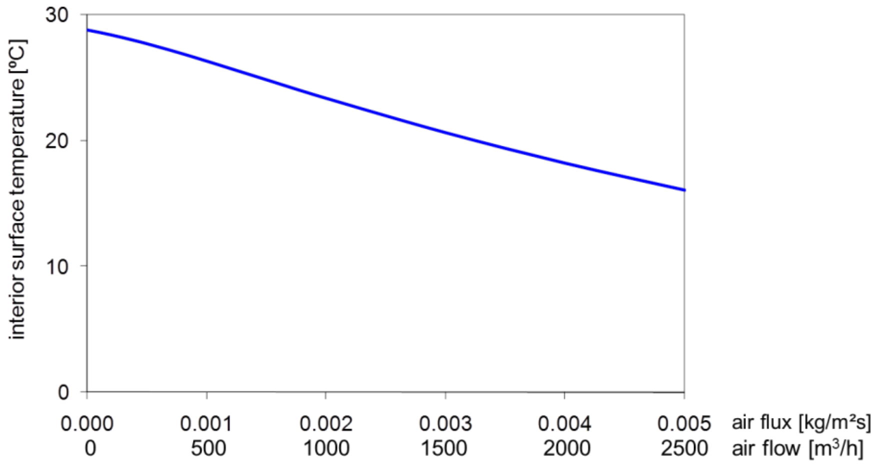

Figure 11.7 The interior surface temperature of insulated wall

11.1.3 U-VALUE OF THE DYNAMIC INSULATION

The conduction U-value of insulated wall in function of infiltration rate can be expressed by the following equation:

$$U = \frac{Q_{cond}(0)}{A(T_y - T_z)} = \frac{g_a c_a}{\exp(g_a c_a R_{y-z}) - 1} : \frac{\partial T}{\partial R}(0) \tag{10.9}$$

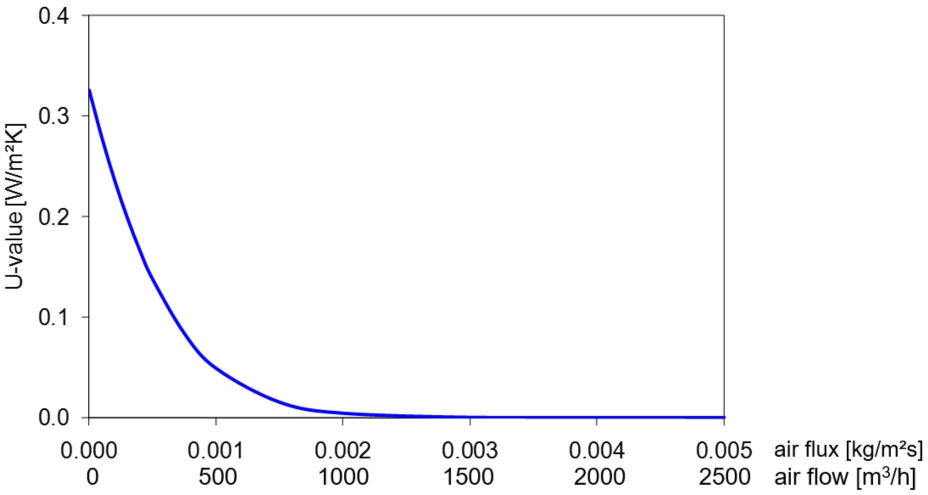

Figure 11.8 Conduction U-value of insulated wall in function of infiltration rate

With this definition, see shown in Fig. 10.9, the U-value of the dynamic wall decreases exponentially with increasing air flux.

11.1.4THE EFFECT OF INFILTRATION AIRFLOW ON OVERALL HEAT LOSSES

Needed heating for 'standard' case:

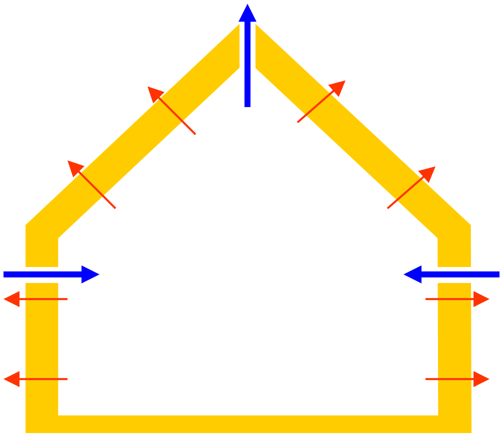

$$\begin{aligned}&\sum AU_{wall}\left(T_e-T_i\right)\\&\quad+\sum AU_{roof}\left(T_e-T_i\right)\\&\quad+G_a c_a\left(T_e-T_i\right)+Q_{\mathrm{stan}}=0\end{aligned} \qquad (10.10)$$

Needed heating for 'dynamic insulation' case:

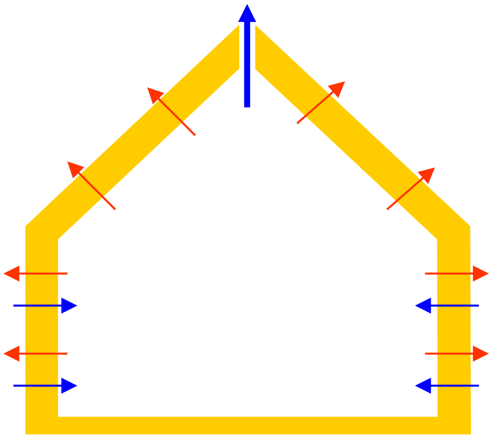

$$\begin{aligned}&\sum A\left(T_e F_2\left(R_{y-z}\right)-T_i F_2(0)\right)\\&\quad+\sum AU_{roof}\left(T_e-T_i\right)\\&\quad-G_a c_a T_i+Q_{dyna}=0\end{aligned} \qquad (10.11)$$

Fig 11.10 shows the Q_{stan} & Q_{dyna} of insulated wall in function of infiltration air flow.

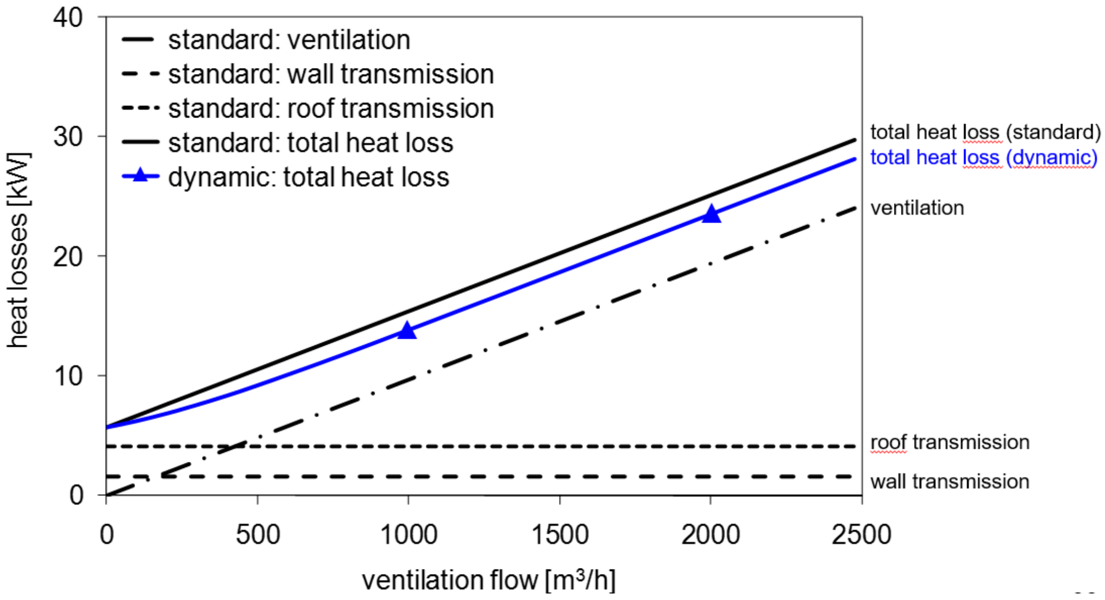

Figure 11.9 Total heat loss in function of infiltration rate

$\frac{Q_{dynamic} - Q_{standard}}{Q_{standard}}$ of insulated wall in function of infiltration air flow:

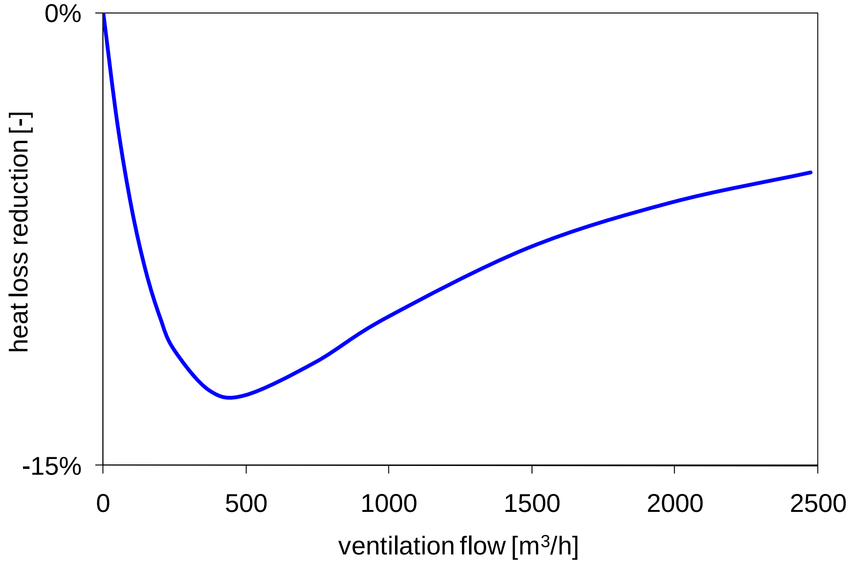

Figure 11.10 Dimensionless heat loss in function of infiltration rate

11.1.5 DESIGN OF A DYNAMIC INSULATED BUILDING

This is an example to explain the application of the theory of dynamic insulation. Assume a house of 100 m^2 floor area with a dynamically insulated ceiling. Putting dynamic insulation in the ceiling effectively limits the house to a single story.

The first step is to decide on an appropriate air change rate for good air quality. As this airflow rate will be supplied through the dynamically insulated ceiling and a mechanical ventilation and heat recovery system (MVHR), energy loss is not a major concern so 1 air change per hour (ach) will be assumed. If the floor to ceiling height is 2.4m, this implies an air flow rate of 240 m^3/h, part of which is supplied through the dynamically insulated ceiling and partly through the MVHR.

Next, the material for the air control layer is chosen to provide a suitable air flow rate at the chosen depressurization, taken as 10 Pa in this case. (The airflow rate could be determined from the desired U-value at the depressurization of 10 Pa.) In this case, fiberboard has an appropriate air permeability of $1.34 \text{x} 10^{-3}$ ($m^2/(h \cdot Pa)$).

For a 12mm thick sheet of fiberboard this gives, for the maximum pressure difference of 10 Pa, an airflow rate of 1.12 m^3/h per m2 of ceiling. This is equivalent to an air speed through the ceiling of 1.12 m/h or 0.31 mm/s. The 100m^2 ceiling will thus provide 112 m^3/h and therefore an air-to-air heat exchanger will provide the balance of 128 m^3/h

Dynamic insulation works best with a good thickness of insulation so taking 200 mm of cellulose insulation (k = 0.04 W/m °C) the dynamic U value for an air flow of 0.31 mm/s is calculated using equation above to be 0.066 W/m^2 °C. If a lower dynamic U-value is required then a material with lower air permeability than fiberboard would need to be selected for the air control layer, so that a higher air speed through the insulation at 10 Pa can be achieved.

The final step would be to select an air-to-air heat exchanger that had a good heat recovery efficiency with a supply airflow rate of 128 m^3/h and an extract air flow rate of 240 m^3/h.

11.2 Coupled vapor and air transfer

The interaction between vapor and air transfer in building envelopes is similar to that of heat and air transfer. In this section, we will discuss: (1) the coupled air advection and vapor diffusion in permeable diffusive materials and components; (2) the transfer equations for coupled advection & diffusion in permeable diffusive materials and components; (3) design and diagnose building components based on the hygric effects of air in/exfiltration.

11.2.1 ADVECTION & DIFFUSION: INTERACTION IN COMPONENT

One-dimensional steady state vapor diffusion and airflow through a uniform sample of air permeable insulation can be described as follows:

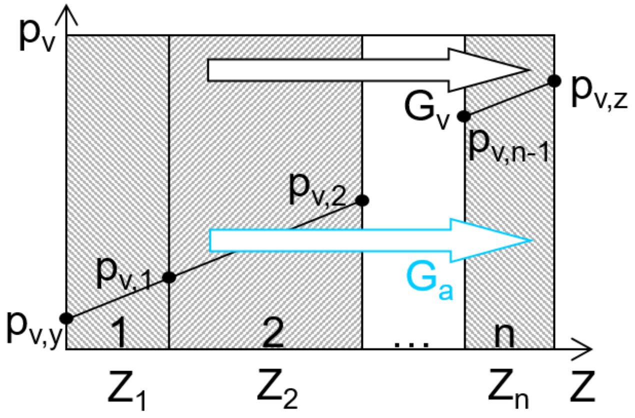

Figure 11.11 One-dimensional vapor diffusion and airflow through a wall

$$G_{v,tot} = G_{v,adv} + G_{v,diff} = constant$$

$$G_{v,adv,y} = G_a x_{v,y} \quad \boxed{\neq} \quad G_a x_{v,z} = G_{adv,z}$$

$$G_{v,diff,y} = -A\delta_v \left.\frac{\partial p_v}{\partial x}\right|_y \quad \boxed{\neq} \quad -A\delta_v \left.\frac{\partial p_v}{\partial x}\right|_z = G_{v,diff,z}$$

(10.11)

$$G_{v,adv,y} = G_a x_{v,y} \quad \boxed{\neq} \quad G_a x_{v,z} = G_{adv,z} \tag{10.12}$$

$$G_{v,diff,y} = -A\delta_v \left.\frac{\partial p_v}{\partial x}\right|_y \quad \boxed{\neq} \quad -A\delta_v \left.\frac{\partial p_v}{\partial x}\right|_z = G_{v,diff,z} \tag{10.13}$$

Where

G_v: vapor mass flow [kg/s]
G_a: air mass flow [kg/s]
x_v: vapor fraction [kg/kg]
p_v: vapor pressure [Pa]
A: surface area [m²]
δ: vapor permeability [kg/(m·s·Pa)]

adv: advection
diff: diffusion
tot: total

The coupled airflow and vapor diffusion can be expressed by the following equations:

Vapor pressure profile $$p_{v,x} = p_{v,y} + \left(p_{v,z} - p_{v,y}\right) F_1(Z_{y-x}) \tag{10.14}$$

$$F_1\left(Z_{y-x}\right) = \frac{exp\left(g_a b_a Z_{y-x}\right) - 1}{exp\left(g_a b_a Z_{y-z}\right) - 1} \tag{10.15}$$

Vapor flows

Advection: $$G_{v,adv}\left(Z_{y-x}\right) = G_a b_a p_v\left(Z_{y-x}\right) \tag{10.16}$$

Diffusion: $$G_{v,diff}\left(Z_{y-x}\right) = A F_2\left(Z_{y-x}\right)\left(p_{v,y} - p_{v,z}\right) \tag{10.17}$$

Total: $$G_{v,tot} = A\left(p_{v,y} F_2\left(Z_{y-z}\right) - p_{v,z} F_2\left(0\right)\right) \tag{10.18}$$

Where
G_v: vapor mass flow [kg/s]
G_a: air mass flow [kg/s]
b_a: air vapor capacity [kg/(kg·Pa)]
p_v: vapor pressure [Pa]
A: surface area [m²]
δ: vapor permeability [W/(m·K)]
g_a: air mass flux [kg/(m²·s)]
Z: diffusion resistance [m²·s·Pa/kg]
adv: advection
diff: diffusion
tot: total
y-x/z: between faces y and x/z

11.2.2 DEFINITION OF HYGRIC CAPACITY FACTOR B$_A$

Based on the analogy with heat transfer, define the hygric capacity factor b_a:

From the relation:

$$x = \frac{m_v}{m_a} = \frac{\dfrac{p_v \cdot V}{R_v \cdot T}}{\dfrac{p_a \cdot V}{R_a \cdot T}} = \frac{R_a \cdot p_v}{R_v \cdot p_a} \tag{10.19}$$

We get

$$b_a = \frac{R_a}{R_v \cdot p_a} = \frac{287.1}{461.5 \cdot 101{,}325} = 6.14 \cdot 10^{-6}\ Pa^{-1} \tag{10.20}$$

11.2.3 THE EFFECT OF INFILTRATION & EXFILTRATION ON VAPOR PRESSURE PROFILE

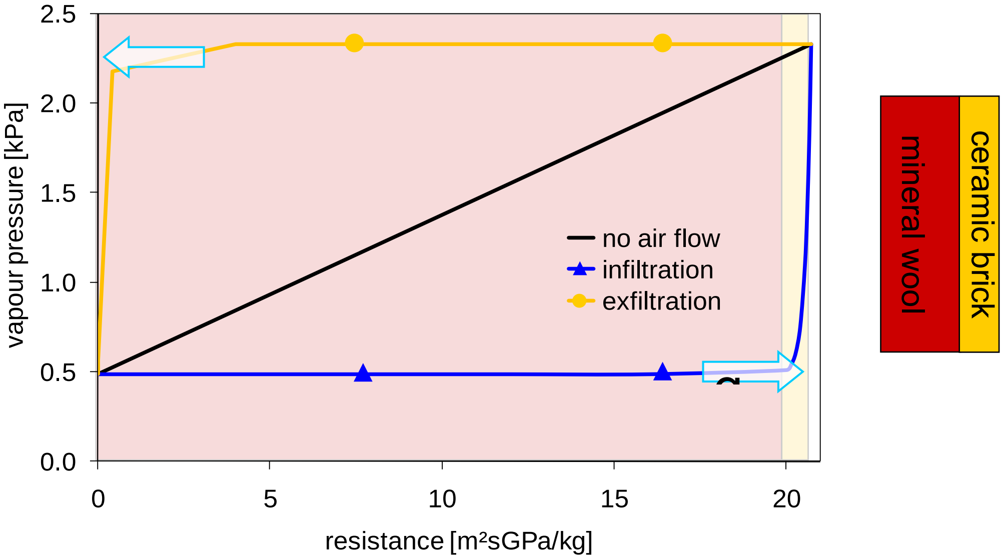

Figure 11.12 Vapor pressure in insulated wall in function of Z ($|g_a| = 1.0 \cdot 10^{-3}$ kg/(m^2s))

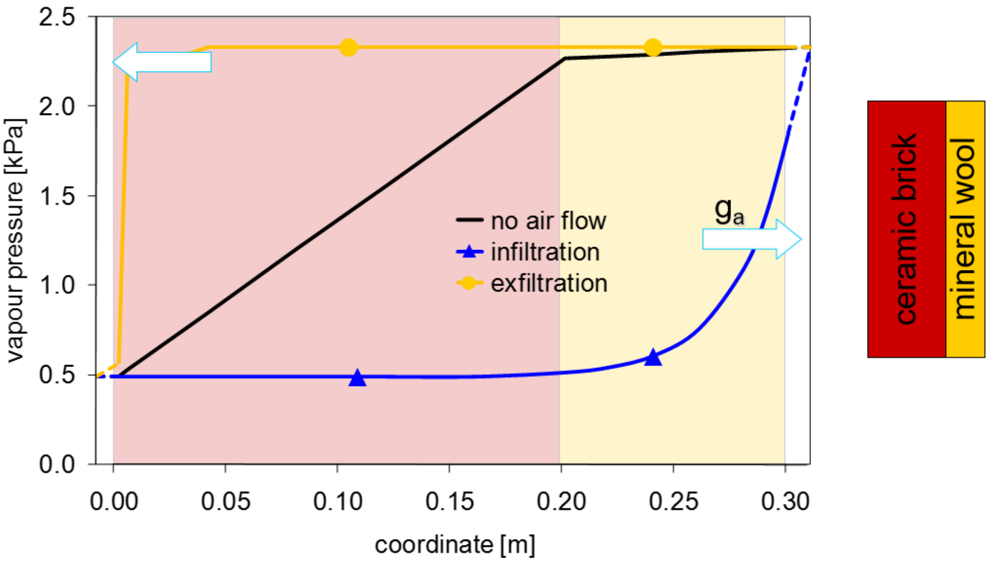

Figure 11.13 Vapor pressure in insulated wall in function of x ($|g_a| = 1.0\cdot10^{-3}$ kg/(m²·s))

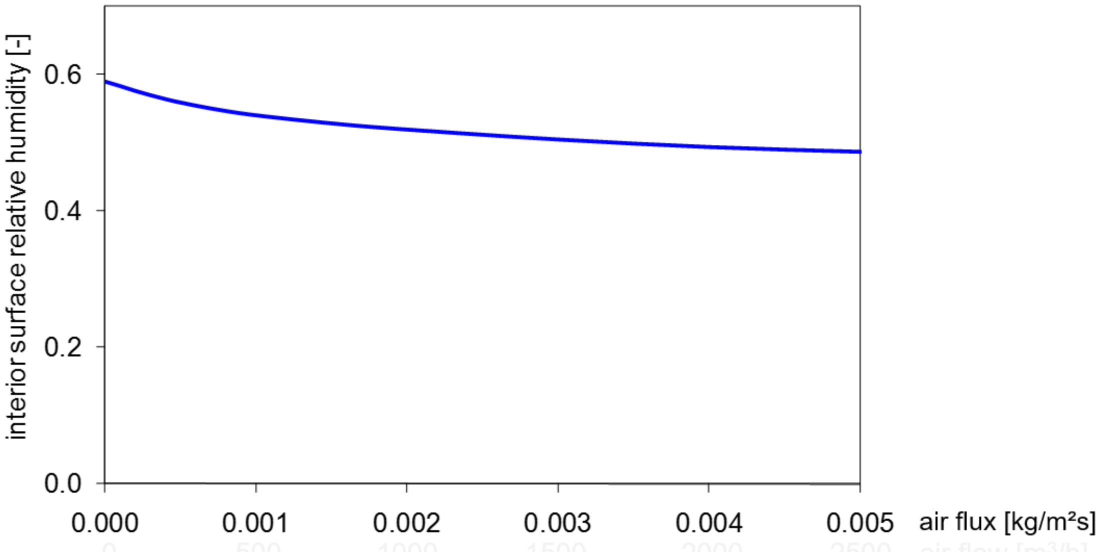

Figure 11.14 Interior surface RH of insulated wall in function of infiltration rate

11.2.4 THE EFFECT OF INFILTRATION AND EXFILTRATION ON INTERSTITIAL CONDENSATION

Figure 11.15 shows the effect of infiltration and exfiltration on the internal condensation.

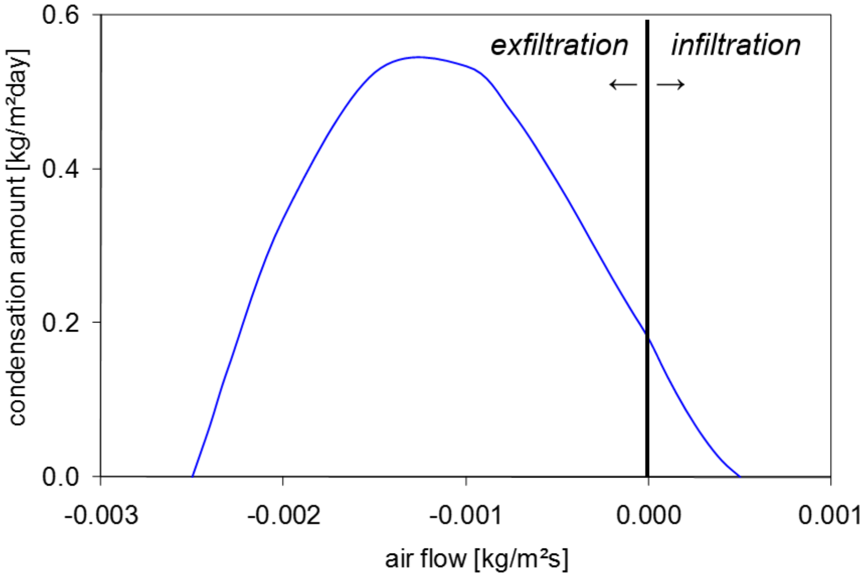

Figure 11.15 The effect of infiltration and exfiltration on the internal condensation

According to the above figures and analysis, we can get the following general conclusions for coupled heat, air and vapor transfer. Increasing infiltration rate will reduce temperature at inner surface; increasing exfiltration rate will result in higher risk of interstitial condensation; undesired increase in ventilation rate will increase the building energy consumption. Therefore, building components should be airtight.